MYCOSPHERE 16(2): 1–178 (2025) www.mycosphere.org ISSN 2077 7019
Doi 10.5943/mycosphere/16/2/1

ARTICLE

Mycosphere Notes 521–571: A special edition of fungal biodiversity to celebrate Kevin D. Hyde's 70th birthday and his exceptional contributions to Mycology

Hongsanan S[1], Khuna S[1*], Manawasinghe IS[2], Tibpromma S[3], Chethana KWT[4,5], Xie N[1], Bagacay JFE[6,7], Calabon MS[6,7], Chen C[4,8,9], Doilom M[8,10], Du HY[11], Gafforov Y[12,13], Huang SK[11], Li JX[11], Luangharn T[4], Luo ZL[14,15], Opiña LAD[6,7], Pem D[4], Sadaba RB[6,7], Singh R[16], Tan Q[8], Tang SM[14], Wang WP[14], Wen TC[17,18], Xia G[4,8], Zhao Q[19], Bhunjun CS[4,5], Cao B[20], Chen YP[21], de Silva NI[1], Dai DQ[3], Dong W[8,10], Du TY[3,4,5], Ferreira-Sá AS[22], Gao Y[4,5], Gui H[23], Han LS[3,24], Han MY[3], Han XX[4,5,20], Jayawardena RS[4,5], Khyaju S[4,5,25], Kumar S[26], Lei L[4,5,19], Leonardo-Silva L[22], Li H[4,5,8,10], Li YX[4,5,8,10], Liao CF[4,5,8,10], Liu JW[8,10], Liu XF[3,4,5], Lu L[3,4,5], Lu WH[3,24,27], Luo M[8,10], Maharachchikumbura SSN[21], Meng QF[4,5,28], Mi LX[4,5,29,30], Norphanphoun C[31], Peng XC[4,5,17,18], Su HL[4,5,19], Tennakoon DS[1], Thiyagaraja V[19], Tun ZL[4,5,25], Wijayawardene NN[3], Xavier-Santos S[22], Xiong YR[4,8], Xu RF[3,4,5], Yadav S[16], Yang T[31], Yang YH[4,5,8,10], Yarasheva M[32], Zeng XY[31,33], Zhang H[34], Zhang GQ[3], Zhang X[4,5,17,18], Zhao HJ[4,5,8,10], Zhao RL[20,35], Zheng DG[3], Wanasinghe DN[36], Karunarathna SC[3*]

[1] Shenzhen Key Laboratory of Microbial Genetic Engineering, College of Life Science and Oceanography, Shenzhen University, Shenzhen 518060, P.R. China
[2] Beijing Key Laboratory of Environment Friendly Management on Fruit Diseases and Pests in North China, Institute of Plant Protection, Beijing Academy of Agriculture and Forestry Sciences, Beijing 100097, P.R. China
[3] Center for Yunnan Plateau Biological Resources Protection and Utilization, College of Biology and Food Engineering, Qujing Normal University, Qujing, Yunnan 655011, P.R. China
[4] Center of Excellence in Fungal Research, Mae Fah Luang University, Chiang Rai 57100, Thailand
[5] School of Science, Mae Fah Luang University, Chiang Rai 57100, Thailand
[6] Division of Biological Sciences, College of Arts and Sciences, University of the Philippines Visayas, Miagao, Iloilo 5023, Philippines
[7] Graduate School, University of the Philippines Visayas, Iloilo 5000, Philippines
[8] Innovative Institute for Plant Health, College of Agriculture and Biology, Zhongkai University of Agriculture and Engineering, Guangzhou 510225, Guangdong, P.R. China
[9] Department of Entomology and Plant Pathology, Faculty of Agriculture, Chiang Mai University, Chiang Mai 50200, Thailand
[10] Key Laboratory of Green Prevention and Control on Fruits and Vegetables in South China, Ministry of Agriculture and Rural Affairs, Zhongkai University of Agriculture and Engineering, Guangzhou 510225, P.R. China
[11] College of Resources and Environment, Zunyi Normal University, Zunyi, Guizhou 563000, P.R. China
[12] Central Asian Center for Development Studies, New Uzbekistan University, Tashkent 100007, Uzbekistan
[13] Department of Ecology, Faculty of Biology and Ecology, National University of Uzbekistan, Tashkent 100174, Uzbekistan
[14] College of Agriculture and Biological Science, Dali University, Dali 671003, Yunnan, P.R. China
[15] Cangshan Forest Ecosystem Observation and Research Station of Yunnan Province, Dali University, Dali 671003, Yunnan, P.R. China
[16] Centre of Advanced Study in Botany, Institute of Science, Banaras Hindu University, Varanasi 221005, Uttar Pradesh, India
[17] State Key Laboratory of Green Pesticide, Key Laboratory of Green Pesticide and Agricultural Bioengineering, Ministry of Education, Guizhou University, Guiyang 550025, P.R. China
[18] Engineering Research Center of Southwest Bio-Pharmaceutical Resources, Ministry of Education, Guizhou University, Guiyang 550025, P.R. China
[19] State Key Laboratory of Phytochemistry and Natural Medicines, Kunming Institute of Botany, Chinese Academy of Sciences, Kunming, 650201, P.R. China

Submitted: 24 March 2025; **Accepted:** 03 May 2025; **Published:** 17 June 2025
***Corresponding Author:** S Khuna – e-mail – surapongway@gmail.com,
SC Karunarathna – email – samanthakarunarathna@gmail.com
Accepted by: Kasun M. Thambugala

[20] State Key Laboratory of Mycology, Institute of Microbiology, Chinese Academy of Sciences, Beijing 100101, P.R. China
[21] School of Life Science and Technology, Center for Informational Biology, University of Electronic Science and Technology of China, Chengdu 611731, P.R. China
[22] Laboratory of Basic and Applied Mycology and Scientific Dissemination (FungiLab), State University of Goiás, Anápolis, Goiás, Brazil
[23] Honghe Centre for Mountain Futures, Kunming Institute of Botany, Chinese Academy of Sciences, Honghe 654400, Yunnan, P.R. China
[24] Department of Biology, Faculty of Science, Chiang Mai University, Chiang Mai 50200, Thailand
[25] Mushroom Research Foundation, 128 M.3 Ban Pa Deng T. Pa Pae, A. Mae Taeng, Chiang Mai 50150, Thailand
[26] Forest Pathology Department, Forest Health Division, KSCSTE-Kerala Forest Research Institute, Peechi 680653, Thrissur, Kerala, India
[27] Excellence Center of Microbial Diversity and Sustainable Utilization, Chiang Mai University, Chiang Mai 50200, Thailand
[28] School of Public Health, Zunyi Medical University, Guizhou Province 563000, P.R. China
[29] Bioengineering and Technological Research Centre for Edible and Medicinal Fungi, Jiangxi Agricultural University, Nanchang 330045, P.R. China
[30] Nanchang Key Laboratory of Edible and Medicinal Fungi, Jiangxi Agricultural University, Nanchang 330045, P.R. China
[31] Department of Plant Pathology, College of Agriculture, Guizhou University, Guiyang, Guizhou 550025, P.R. China
[32] Microbiology Laboratory, Navruz International Corp. LLC, Salar settlement, 111219, Kibray, Uzbekistan
[33] Institute of Edible Mushrooms, Guizhou University, Guiyang 550025, P.R. China
[34] Shandong Provincial Key Laboratory of Water and Soil Conservation and Environmental Protection, College of Resources and Environment, Linyi University, West side of north section of Industrial Avenue, Linyi 276000, P.R. China
[35] College of Life Sciences, University of Chinese Academy of Sciences, Beijing 100049, P.R. China
[36] Department of Soil Science, College of Food and Agriculture Sciences, King Saud University, Riyadh 11362, Saudi Arabia

Citation – Hongsanan S, Khuna S, Manawasinghe IS, Tibpromma S, Chethana KWT, Xie N, Bagacay JFE, Calabon MS, Chen C, Doilom M, Du HY, Gafforov Y, Huang SK, Li JX, Luangharn T, Luo ZL, Opiña LAD, Pem D, Sadaba RB, Singh R, Tan Q, Tang SM, Wang WP, Wen TC, Xia G, Zhao Q, Bhunjun CS, Cao B, Chen YP, de Silva NI, Dai DQ, Dong W, Du TY, Ferreira-Sá AS, Gao Y, Gui H, Han LS, Han MY, Han XX, Jayawardena RS, Khyaju S, Kumar S, Lei L, Leonardo-Silva L, Li H, Li YX, Liao CF, Liu JW, Liu XF, Lu L, Lu WH, Luo M, Maharachchikumbura SSN, Meng QF, Mi LX, Norphanphoun C, Peng XC, Su HL, Tennakoon DS, Thiyagaraja V, Tun ZL, Wijayawardene NN, Xavier-Santos S, Xiong YR, Xu RF, Yadav S, Yang T, Yang YH, Yarasheva M, Zeng XY, Zhang H, Zhang GQ, Zhang X, Zhao HJ, Zhao RL, Zheng DG, Wanasinghe DN, Karunarathna SC. 2025 – Mycosphere Notes 521–571: A special edition of fungal biodiversity to celebrate Kevin D. Hyde's 70th birthday and his exceptional contributions to Mycology. Mycosphere 16(2): 1–178, Doi 10.5943/mycosphere/16/2/1

Abstract

This special edition of Mycosphere Notes commemorates the 70th birthday of Kevin D. Hyde, a seminal figure in fungal taxonomy whose work has profoundly influenced the study of fungal diversity and classification. In this paper, we provide entries on a new genus, 41 new species, five new geographical records, six new host records, and a new habitat record across 42 families, 22 orders, eight classes, and two phyla, continuing the invaluable work of Kevin D. Hyde in advancing our understanding of fungal biodiversity and distribution. The fungal species introduced in this paper were found as endophytes, epiphytes, pathogens, and saprobes on plant material and litter substrates across diverse ecosystems, including terrestrial, freshwater, and cave habitats in Brazil, China, India, the Philippines, Thailand, and Uzbekistan. Species boundaries were meticulously determined based on a rigorous process of morphological characteristics and molecular phylogenetic analysis, ensuring the accuracy of species delimitation. *Heterohelminthosporium* is introduced as the new genus in *Massarinaceae*, *Pleosporales* and the newly described 41 species are *Allocryptovalsa hydei*, *Amorocoelophoma hydei*, *Annulohypoxylon hydei*, *Brunnipila hydei*, *Candolleomyces aliensis*, *Candolleomyces hydei*, *Ceramothyrium hydei*, *Corynespora hydei*,

Coryneum hydei, *Crepidotus yunnanensis*, *Dacrymyces undulatomarginatus*, *Diaporthe hydei*, *Diorygma hydei*, *Distoseptispora monospora*, *Heterohelminthosporium hydei*, *Hevansia hydei*, *Hysterobrevium hydei*, *Keraliethelia hydei*, *Laccaria flavumbilicatus*, *Laccaria hydei*, *Lomaantha guizhouensis*, *Melomastia hydei*, *Microdochium guizhouensis*, *Muyocopron cavernae*, *Neoheleiosa hydei*, *Neottiosporina imperatae*, *Nigrospora guangdongense*, *Nigrosynnema hydei*, *Ophioceras hydei*, *Ophiocordyceps bannaensis*, *Orbilia longispora*, *Ostropomyces hydei*, *Periconia hydei*, *Phaeoseptum kunmingensis*, *Pseudosporidesmium hydei*, *Roussoella hydei*, *Stilbocrea hydei*, *Stilbocrea yunnanensis*, *Trichoderma hydei*, *Xylochrysis hydei*, and *Zasmidium hydei*. Notably, one species was discovered in the air within a cave habitat. In addition, *Favolaschia variistipitata* and *Hermatomyces indicus* are reported as a new geographical record, and *Comoclathris pimpinellae*, *Corynespora cassiicola*, *Dothiora sorbi*, and *Pseudocercospora snelliana* are reported as new host records. *Allodiatrype elaeidicola* and *Fusarium guangdongense* are reported as new host and geographical records, and *Leptobacillium coffeanum* is reported as a new geographical and habitat record. We provide new molecular data for all collected species and updated phylogenetic trees, spanning multiple phyla, classes, orders, and families. This study highlights the expanding diversity of fungi and represents Kevin D. Hyde's global collaborations in Mycology. We respectfully pay tribute to Kevin D. Hyde's invaluable contributions to mycology, which have significantly advanced our understanding of fungal diversity.

Keywords – 41 new species – Ascomycota – Basidiomycota – morphology – phylogeny

TABLE OF CONTENTS

Phylum Ascomycota Caval.-Sm.
Subphylum *Pezizomycotina* O.E. Erikss. & Winka
Class *Dothideomycetes* O.E. Erikss. & Winka
Subclass *Dothideomycetidae* P.M. Kirk, P.F. Cannon, J.C. David & Stalpers ex C.L. Schoch, Spatafora, Crous & Shoemaker
Dothideales Lindau
Dothideaceae Chevall.
521. ***Dothiora sorbi*** (Wahlenb.) Fuckel, Jb. nassau. Ver. Naturk. 23-24: 275 (1870), new host record (entry by Pem D, Yarasheva M, and Gafforov Y)

Mycosphaerellales (Nannf.) P.F. Cannon
Mycosphaerellaceae Lindau
522. ***Pseudocercospora snelliana*** (Reichert) U. Braun, H.D. Shin, C. Nakash. & Crous, Stud. Mycol. 75: 106 (2012), new host record (entry by Yadav S and Singh R)
523. ***Zasmidium hydei*** Khuna, Hongsanan & Xie N., sp. nov. (entry by Khuna S, Hongsanan S, and Xie N)

Subclass *Pleosporomycetidae* C.L. Schoch, Spatafora, Crous & Shoemaker
Hysteriales Lindau
Hysteriaceae Chevall.
524. ***Hysterobrevium hydei*** Hongsanan, Khuna & Xie N., sp. nov. (entry by Hongsanan S, Khuna S, and Xie N)

Pleosporales Luttr. ex M.E. Barr
Amorosiaceae Thambug. & K.D. Hyde
525. ***Amorocoelophoma hydei*** L. Lu & Tibpromma, sp. nov. (entry by Lu L, Karunarathna SC, and Tibpromma S)

Corynesporascaceae Sivan.

526. ***Corynespora cassiicola*** (Berk. & M.A. Curtis) C.T. Wei, Mycol. Pap. 34: 5 (1950), new host record (entry by Kumar S and Singh R)

527. ***Corynespora hydei*** C.F. Liao & Doilom, sp. nov. (entry by Liao CF and Doilom M)

Hermatomycetaceae Locq.

528. ***Hermatomyces indicus*** Prasher & Sushma, Nova Hedwigia 94(3-4): 552 (2014), new geographical record (entry by Li H and Manawasinghe IS)

Massarinaceae Munk

529. ***Heterohelminthosporium*** Khuna, Hongsanan & Xie N., gen. nov. (entry by Khuna S, Hongsanan S, and Xie N)

530. ***Heterohelminthosporium hydei*** Khuna, Hongsanan & Xie N., sp. nov. (entry by Khuna S, Hongsanan S, and Xie N)

Periconiaceae Nann.

531. ***Periconia hydei*** Y. H. Yang & Manawasinghe, sp. nov. (entry by Yang YH and Manawasinghe IS)

Phaeoseptaceae S. Boonmee, Thambugala & K.D. Hyde

532. ***Phaeoseptum kunmingensis*** Z. L.T, sp. nov. (entry by Tun ZL and Bhunjun CS)

Pleosporaceae Nitschke

533. ***Comoclathris pimpinellae*** S. Konta, Bulgakov & K.D. Hyde, Fungal Diversity 78: 50 (2016), new host record (entry by Pem D and Gafforov Y)

Roussoellaceae Jian K. Liu, Phook., D.Q. Dai & K.D. Hyde

534. ***Roussoella hydei*** L.S. Han & D.Q. Dai, sp. nov. (entry by Han LS and Dai DQ)

Subclass *Incertae sedis*
Dyfrolomycetales K.L. Pang, K.D. Hyde & E.B.G. Jones
Pleurotremataceae Walt. Watson

535. ***Melomastia hydei*** Hongsanan, Khuna & Xie N., sp. nov. (entry by Hongsanan S, Khuna S, and Xie N)

Monoblastiales Lücking, M.P. Nelsen & K.D. Hyde
Eriomycetaceae Huanraluek & K.D. Hyde

536. ***Neoheleiosa hydei*** Thiyagaraja, sp. nov. (entry by Thiyagaraja V)

Muyocopronales Mapook, Boonmee & K.D. Hyde
Muyocopronaceae K.D. Hyde

537. ***Muyocopron cavernae*** A.S. Ferreira-Sá, L. Leonardo-Silva & S. Xavier-Santos, sp. nov. (entry by Ferreira-Sá AS, Leonardo-Silva L, and Xavier-Santos S)

Dothideomycetes *genera incertae sedis*

538. ***Neottiosporina imperatae*** Y.P. Chen & Maharachch., sp. nov. (entry by Chen YP amd Maharachchikumbura SSN)

Class *Eurotiomycetes* O.E. Erikss. & Winka
Subclass *Chaetothyriomycetidae* Doweld
Chaetothyriales M.E. Barr
Chaetothyriaceae Hansf. ex M.E. Barr

539. ***Ceramothyrium hydei*** T. Yang & X.Y. Zeng, sp. nov. (entry by Yang T and Zeng XY)

Class *Lecanoromycetes* O.E. Erikss. & Winka
Subclass *Ostropomycetidae* V. Reeb, Lutzoni & Cl. Roux
Graphidales Bessey
Graphidaceae Dumort.
540. ***Diorygma hydei*** Meng & Wei Wu, sp. nov. (entry by Meng QF)

Ostropales Nannf
Stictidaceae Fr.
541. ***Ostropomyces hydei*** R.F. Xu, Tibpromma, sp. nov. (entry by Xu RF)

Class *Leotiomycetes* O.E. Erikss. & Winka
Subclass *Leotiomycetidae* P.M. Kirk, P. Cannon, Minter & Stalpers
Helotiales Nannf. ex Korf & Lizoň
Lachnaceae Raitv.
542. ***Brunnipila hydei*** H.L. Su & Q. Zhao, sp. nov. (entry by Su HL and Zhao Q)

Class *Orbiliomycetes* O.E. Erikss. & Baral
Subclass *Orbiliomycetidae* P.M. Kirk, P.F. Cannon, Minter & Stalpers
Orbiliales Baral, O.E. Erikss., G. Marson & E. Weber
Orbiliaceae Nannf.
543. ***Orbilia longispora*** R. Yang & H. Zhang, sp. nov. (entry by Zhang H)

Class *Sordariomycetes* O.E. Erikss. & Winka
Subclass Diaporthomycetidae Senan., Maharachch. & K.D. Hyde
Diaporthales Nannf.
Coryneaceae Corda
544. ***Coryneum hydei*** H.Y. Du & S.K. Huang, sp. nov. (entry by Du HY and Huang SK)

Diaporthaceae Höhn. ex Wehm.
545. ***Diaporthe hydei*** Y.R. Xiong & Manawas., sp. nov. (entry by Xiong YR and Manawasinghe IS)

Distoseptisporales Z.L. Luo, H.Y. Su & K.D. Hyde
Distoseptisporaceae K.D. Hyde & McKenzie
546. ***Distoseptispora monospora*** W.P. Wang & Z.L. Luo, sp. nov. (entry by Wang WP and Luo ZL)

Diaporthomycetidae families *incertae sedis*
Woswasiaceae H. Zhang, K.D. Hyde & Maharachch.
547. ***Xylochrysis hydei*** G.Q. Zhang & Wijayaw., sp. nov. (entry by Zhang GQ and Wijayawardene NN)

Subclass *Hypocreomycetidae* O.E. Erikss. & Winka
Hypocreales Lindau
Bionectriaceae Samuels & Rossman
548. ***Stilbocrea hydei*** X.C. Peng, & T.C. Wen, sp. nov. (entry by Peng XC and Wen TC)
549. ***Stilbocrea yunnanensis*** Y. Gao & H. Gui, sp. nov. (entry by Gao Y, Gui H, and Jayawardena RS)

Cordycipitaceae Kreisel ex G.H. Sung, J.M. Sung, Hywel-Jones & Spatafora
550. ***Hevansia hydei*** J. X. Li & S. K. Huang, sp. nov. (entry by Huang SK, Du HY, and Li JX)

551. ***Leptobacillium coffeanum*** (A.A.M. Gomes & O.L. Pereira) Okane, Nonaka, Kurihara, J.P. Abe & Yamaoka, Mycoscience 61(4): 169 (2020), new geographical and habitat records (entry by Calabon MS, Bagacay JFE, Opiña LAD, and Sadaba RB)

Hypocreaceae De Not.

552. ***Trichoderma hydei*** X.F. Liu, Karun. & Tibpromma, sp. nov. (entry by Liu XF, Tibpromma S, and Karunarathna SC)

Nectriaceae Tul. & C. Tul.

553. ***Fusarium guangdongense*** Y.X. Zhang, K.D. Hyde, L.T. Nie & Manawas., Mycosphere 15(1): 6674 (2024), new host and geographical record (entry by Liu JW and Luo M)

Ophiocordycipitaceae G.H. Sung, J.M. Sung, Hywel-Jones & Spatafora

554. ***Ophiocordyceps bannaensis*** X. Zhang & T. C. Wen, sp. nov. (entry by Zhang X and Wen TC)

Stachybotryaceae L. Lombard & Crous

555. ***Nigrosynnema hydei*** T.Y. Du, Tibpromma & Karun., sp. nov. (entry by Du TY and Tibpromma S)

Microascales Luttr. ex Benny & Kimbr.
Halosphaeriaceae E. Müll & Arx ex Kohlm.

556. ***Keraliethelia hydei*** Bagacay, Opiña, & M.S. Calabon, sp. nov. (entry by Calabon MS, Bagacay JFE, Opiña LAD, and Sadaba RB)

Subclass *Sordariomycetidae* O.E. Erikss. & Winka
Chaetosphaeriales Huhndorf, A.N. Mill. & F.A. Fernández
Chaetosphaeriaceae Réblová, M.E. Barr & Samuels

557. ***Lomaantha guizhouensis*** M.Y. Han. & Tibpromma, sp. nov. (entry by Han M and Tibpromma S)

Magnaporthales Thongk., Vijaykr. & K.D. Hyde
Ophioceraceae Klaubauf, E.G. LeBrun & Crous

558. ***Ophioceras hydei*** H.J. Zhao & W. Dong, sp. nov. (entry by Zhao HJ and Dong W)

Subclass *Xylariomycetidae* O.E. Erikss & Winka
Amphisphaeriales D. Hawksw. & O.E. Erikss.
Apiosporaceae K.D. Hyde, J. Fröhl., Joanne E. Taylor & M.E. Barr

559. ***Nigrospora guangdongense*** Y.X. Li & Doilom, sp. nov. (Li Y and Doilom M)

Pseudosporidesmiaceae Crous

560. ***Pseudosporidesmium hydei*** L.X. Mi & D.M. Hu, sp. nov. (entry by Mi L)

Xylariales Nannf.
Diatrypaceae Nitschke

561. ***Allocryptovalsa hydei*** Tennakoon & S. Hongsanan, sp. nov. (entry by Tennakoon DS and Hongsanan S)

562. ***Allodiatrype elaeidicola*** S. Konta & K.D. Hyde, Mycosphere 11(1): 251 (2020), new host and geographical record (entry by de Silva NI and Hongsanan S)

Hypoxylaceae DC.

563. ***Annulohypoxylon hydei*** Manawas., Q.L. Tan, Y.X. Zhang, sp. nov. (entry by Xia G, Chen C, Tan Q, and Manawasinghe IS)

Microdochiaceae Hern.-Restr., Crous & J.Z. Groenew.

564. ***Microdochium guizhouensis*** Norph. & S.Q. Guo, sp. nov. (entry by Norphanphoun C)

Phylum Basidiomycota R.T. Moore
Class *Agaricomycetes* Doweld
Subclass Agaricomycetidae
Agaricales Underw.
Agaricineae Fr.
Crepidotaceae (S. Imai) Singer

565. ***Crepidotus yunnanensis*** D.G. Zheng & Karun., sp. nov. (entry by Zheng D and Karunarathna SC)

Hydnangiaceae Gäum. & C.W. Dodge

566. ***Laccaria hydei*** S.M Tang & Z.L. Luo, sp. nov. (entry by Tang SM and Luo ZL)

567. ***Laccaria flavumbilicatus*** S.M Tang & Z.L. Luo, sp. nov. (entry by Tang SM and Luo ZL)

Psathyrellaceae Vilgalys, Moncalvo & Redhead

568. ***Candolleomyces aliensis*** R.L. Zhao & X.X. Han, sp. nov. (entry by Han XX, Cao B, and Zhao RL)

569. ***Candolleomyces hydei*** W.H. Lu, Karun. & Tibpromma, sp. nov. (entry by Lu WH, Tibpromma S, and Karunarathna SC)

Incertae sedis
Mycenaceae Overeem

570. ***Favolaschia variistipitata*** W.H. Lu, Tibpromma & Karun., Phytotaxa 694(2): 148 (2025), new geographical record (entry by Khyaju S and Luangharn T)

Class *Dacrymycetes* Doweld
Subclass *Incertae sedis*
Dacrymycetales Henn.
Dacrymycetaceae J. Schröt.

571. ***Dacrymyces undulatomarginatus*** L. Lei & Q. Zhao, sp. nov. (entry by Lei L, Zhao Q, and Luangharn T)

INTRODUCTION

Fungi, the unsung heroes of our ecosystem, are crucial to life on Earth. They perform various essential ecological functions and offer immense value to natural ecosystems and human society. They play a pivotal role in nutrient cycling by decomposing complex organic matter and releasing essential elements such as carbon, nitrogen, and phosphorus into the environment (Tedersoo et al. 2014, Treseder & Lennon 2015, Heng et al. 2016). However, their significance goes beyond this. Fungi engage in symbiotic relationships, including mycorrhizal associations, which enhance plant growth and resilience. These relationships, which we can learn from and be inspired by, improve nutrient and water uptake and increase resistance to pathogens. Fungi also contribute significantly to global carbon storage, particularly through their role in soil carbon sequestration. Moreover, in the world of biotechnology, fungi are true innovators. Their extensive exploitation has led to the production of antibiotics, enzymes, organic acids, and biofuels (Bills & Gloer 2016, Hyde et al. 2019a, Case et al. 2025). Their capacity to degrade pollutants and participate in bioremediation

further highlights their potential to address environmental challenges (Harms et al. 2011). These diverse contributions underscore fungi as indispensable components of environmental health and industrial innovation. Despite their profound importance, fungi remain vastly understudied, with an estimated 2.5 million species, of which only approximately 155,000 species are known (Niskanen et al. 2023). This leaves numerous species still waiting to be discovered and classified, highlighting the urgent need for further research. The potential for discovery in this field is immense, and understanding the ecological roles of these understudied species is crucial for ensuring the sustainability of our ecosystems. This mission is supported by Prof. Kevin D. Hyde, whose pioneering work has significantly shaped modern mycology.

Throughout his distinguished career, spanning over the decades, Prof. Kevin D. Hyde has revolutionized fungal taxonomy and ecology. His work has led to the discovery and description of numerous fungal species across diverse ecosystems, including tropical rainforests, freshwater habitats, and marine environments, enhancing our understanding of fungal biodiversity (Liu et al. 2021, Hyde et al. 2024a). Prof. Kevin D. Hyde has made a significant contribution to the growth of mycology in Asia. His efforts have fostered collaboration among Asian mycologists, leading to the establishment of journals, such as Fungal Diversity, Mycosphere, Asian Journal of Myology (AJOM), Plant Pathology and Quarantine (PPQ), Current Research in Applied and Environmental Mycology (CREAM) and Fungal Biotech, as well as platforms like coelomycetes.org, dothideomycetes.org, Facesoffungi, italianmicrofungi.org. He has also contributed to advancing fungal taxonomy, biodiversity studies, and applied mycology in the region (De Silva et al. 2013, Hyde et al. 2019a, Mapook et al. 2020). His leadership has inspired many researchers and elevated the global recognition of Asian mycology. Prof. Kevin D. Hyde has significantly advanced fungal taxonomy by integrating traditional morphological techniques with modern molecular phylogenetics, setting a new standard for species delimitation (Jeewon & Hyde 2016, Hongsanan et al. 2017, Hyde et al. 2017a, Liu et al. 2017a, Pem et al. 2021). Beyond his research contributions, Prof. Kevin D. Hyde has been a dedicated mentor, collaborator, and leader, fostering a global network of researchers committed to exploring fungal biodiversity. Most of his former students are recognized as the top 2% of highly cited mycologists worldwide from 2020 to 2024 (Stanford University, USA). With collaborative papers such as Fungal Diversity Notes (Ariyawansa et al. 2015a, Liu et al. 2015, Li et al. 2016, Hyde et al. 2017b, 2019, 2020a, Tibpromma et al. 2017, 2018a, Wanasinghe et al. 2018, Phookamsak et al. 2019, Boonmee et al. 2021, Jayawardena et al. 2022, Senanayake et al. 2023, Liu et al. 2024a, Manawasinghe et al. 2024), Mycosphere Notes (Boonmee et al. 2017, Thambugala et al. 2017, Doilom et al. 2018, Jayawardena et al. 2018, Hyde et al. 2018, 2021, 2023a, 2024a, Pem et al. 2019, Manawasinghe et al. 2022, Dong et al. 2023, Li et al. 2023), AJOM notes (Hyde et al. 2020b, Chethana et al. 2023) and CREAM Profiles (Hyde et al. 2024b), he continued to expand his global network of researchers and established "Global consortium for the classification of fungi and fungus-like taxa" (Hyde et al. 2023b).

In celebration of his 70th birthday, this special edition of *Mycosphere Notes* pays tribute to his extensive contributions by highlighting the ongoing research and discoveries in the field of mycology. We continue to explore fungal biodiversity across diverse ecosystems, ensuring that his legacy of rigorous and innovative research endures. In this edition, we describe a new genus and 41 new fungal species, bridging gaps in our knowledge of fungal distribution and ecology. These discoveries encompass Ascomycota and Basidiomycota, identified through integrative taxonomy (combining morphology and phylogeny) across diverse roles, including endophytes, epiphytes, pathogens, and saprobes, in terrestrial, freshwater, and cave ecosystems in Brazil, China, India, the Philippines, Thailand, and Uzbekistan. These insights are critical for applications in conservation, biotechnology, and understanding fungal evolution. While this edition celebrates Prof. Kevin D. Hyde's legacy and represents only a portion of his global impact, it stands as a testament to the profound influence he has had on mycology worldwide. His collaborative spirit continues to inspire mycologists worldwide.

MATERIALS AND METHODS

Fungal specimens were collected from woody substrates, leaves, and litter in terrestrial, freshwater, air, and coastal regions across Brazil, China, India, the Philippines, Thailand, and Uzbekistan between 2016 and 2024. Morphological observations, macro- and microscopic photography, and isolation were conducted using the methods described by Senanayake et al. (2020), with necessary adaptations. Fungal samples and isolates, including ex-type, living, and dried cultures, were deposited in the following herbaria and culture collections. CGMCC: China General Microbial Culture Collection Center, China; GACP: Guizhou Agricultural College, China; GZAAS: Guizhou Academy of Agriculture Sciences, China; GMB: Herbarium of Guizhou Medical University, China; GMBCC: Guizhou Medical University Culture Collection, China; GMB-W: Guizhou Medical University, China; GUCC: Culture Collection at the Department of Plant Pathology, Agriculture College, Guizhou University, China; GZCC: Guizhou Culture Collection, China; HFJAU: Herbarium of Fungi of Jiangxi Agricultural University, China; HGUP: Herbarium of the Department of Plant Pathology, Agricultural College, Guizhou University, China; HKAS: Herbarium of Cryptogams Kunming Institute of Botany Academia Sinica, China; HMAS: Herbarium of Mycology, Chinese Academy of Sciences, China; HUEG-Fungi: Herbarium of the State University of Goiás, Brazil; HUEST: Herbarium of the University of Electronic Science and Technology, China; JAUCC: Jiangxi Agricultural University Culture Collection, China; KFRIMCC: Kerala Forest Research Institute Mycological Culture collection, India; KFRIMH: Kerala Forest Research Institute Mycological Herbarium, India; KUMCC: Kunming Institute of Botany, Chinese Academy of Sciences, Kunming, China; KUNCC: Kunming Institute of Botany Culture Collection, China; KUN-L: Herbarium of Kunming Institute of Botany, China; MBSZU: Culture Collection of Microbial Shenzhen University, China; MFLU: Mae Fah Luang University, Thailand; MFLUCC: Mae Fah Luang University Culture Collection, Thailand; MHZU: Mycological Herbarium of Zhongkai University of Agriculture and Engineering, China; NFCCI: National Fungal Culture Collection of India, India; SZU: College of Life Science and Oceanography, Shenzhen University, China; TASM: Tashkent Mycological Herbarium of the Institute of Botany of Academy of Sciences of Uzbekistan, Uzbekistan; UESTCC: University of Electronic Science and Technology Culture Collection, China; ZHKU: Zhongkai University of Agriculture and Engineering, China; ZHKUCC: Zhongkai University of Agriculture and Engineering Culture Collection, China. DNA extraction was performed using both pure fungal cultures and fruiting bodies when cultures were not available. Procedures for DNA extraction, polymerase chain reaction (PCR), gel electrophoresis, and sequencing were conducted as outlined by Dissanayake et al. (2020). The sequence results generated in the study have been submitted to GenBank.

To delineate species boundaries, phylogenetic analyses were conducted using multiple methodologies. Maximum likelihood (ML) analyses were performed using RAxML via manual program (Silvestro & Michalak 2012, Stamatakis 2014) and the CIPRES Science Gateway portal (Miller et al. 2012), while Bayesian inference (BI) analyses were conducted using MrBayes v3.1.2 (Huelsenbeck & Ronquist 2001, Zhaxybayeva & Gogarten 2002), and via the same web portal as in ML. Maximum parsimony (MP) analysis was executed using PAUP* version 4.0b10 (Swofford & Sullivan 2003). Pairwise homoplasy index (PHI) tests were conducted using Split Tree software, as described by Quaedvlieg et al. (2014), to assess the level of recombination among closely related species when necessary. The identification of new fungal species adhered to the guidelines and criteria outlined by Chethana et al. (2021). Newly introduced fungal species were registered with Index Fungorum (www.indexfungorum.org) and the Faces of Fungi database (Jayasiri et al. 2015).

RESULTS

Taxonomy

For the updated taxonomic treatments, Hyde et al. (2024c) was followed.

Phylum Ascomycota Caval.-Sm.

Subphylum *Pezizomycotina* O.E. Erikss. & Winka
Class *Dothideomycetes* O.E. Erikss. & Winka
Subclass *Dothideomycetidae* P.M. Kirk, P.F. Cannon, J.C. David & Stalpers ex C.L. Schoch, Spatafora, Crous & Shoemaker
Dothideales Lindau
Dothideaceae Chevall.
Dothiora Fr., Summa veg. Scand., Sectio Post. (Stockholm): 418 (1849)

Index Fungorum number: IF1702; Facesoffungi number: FoF00078

Saccardo (1889) and Lindau (1897) classified *Dothiora* within discomycetes. Theissen & Sydow (1915) placed *Dothiora* in *Dothideales*. Later, Theissen & Sydow (1917) transferred *Dothiora* to *Dothioraceae*. Von Arx & Müller (1975) and Sivanesan (1984) classified *Dothiora* within *Dothideaceae*. Numerous authors, such as Hawksworth et al. (1995) and Lumbsch & Huhndorf (2010), have classified *Dothiora* within *Dothioraceae*, as they regarded *Dothideaceae* and *Dothioraceae* as distinct families in *Dothideales* (Thambugala et al. 2014). *Dothiora* is distinct from other genera in *Dothideaceae* in having hyaline, one to many-septate or muriform ascospores (Senwanna et al. 2024). Morphologically, *Dothiora* exhibits a dothichiza-like asexual form and a hormonema-like synasexual morph in culture (Crous & Groenewald 2017). The majority of *Dothiora* species are identified on dead parts of various host plants in tropical and temperate zones (Hongsanan et al. 2020a, Pem et al. 2024). The asexual morph of *D. pyrenophora* has been reported as *Dothichiza sorbi* by Sivanesan (1984) based on the formation of pycnidia in cultures (Thambugala et al. 2014). Crous & Groenewald (2016) suggested that members of *Dothiora* could be saprobes or potentially mild pathogens under conditions of plant tissue stress.

Out of the 60 species presently recorded in Index Fungorum (2025), Prof. Kevin D. Hyde and his team have described five species of *Dothiora*. In recognition of his remarkable contributions to mycology, we hereby present *Dothiora sorbi* as a new host record. This gesture honors his enduring influence on the research of *Dothiora* and mycology in general. We also provide the updated phylogenetic tree for *Dothiora* (Fig. 1).

Dothiora sorbi (Wahlenb.) Fuckel, Jb. nassau. Ver. Naturk. 23–24: 275 (1870) Fig. 2

Index Fungorum number: IF233104; Facesoffungi number: FoF17369

Saprobic on dead branches. Sexual morph: Undetermined. Asexual morph: hormonema-like. *Conidiomata* 50–200 × 75–150 µm ($\overline{x}$ = 56 × 82 µm, n = 10), stromatic, solitary or aggregated in a stroma, numerous, dark brown to black, dry. *Conidiophores* 2.3–2.5 × 2.7–3.2 µm ($\overline{x}$ = 2.3 × 3.2 µm, n = 5), micronematous, reduced to conidiogenous cells. *Conidia* 13.2–24.5 × 14.1–30.3 µm ($\overline{x}$ = 20.2 × 20.5 µm, n = 10), holoblastic, solitary, or formed in chains, chlamydospore-like, smooth- and thin to thick-walled, dark brown, globose, ellipsoid or irregularly-shaped, with longitudinal or oblique secondary septa over time, giving rise to a 'muriform' appearance, prominently constricted at septa when mature.

Culture characteristics – Colonies on MEA ranging from 20–35 mm diam., after three weeks at 25 °C, with margin submerged, irregular or undulating, rough at surface, mucoid, gummy with masses of moist conidia from mycelial conidiogenesis gathering in damp droplets, breaking down agar and forming cracks, pale olive-brown to dark olive, reverse dark olive-grey to whitish-grey.

Material examined – Uzbekistan, Tashkent Province, Bustonliq District, Chatkal State Biosphere Reserve, Western Tien Shan Mountains, on dead branches of *Rosa webbiana* (*Rosaceae*), 20 May 2016, Y. Gafforov and M. Yarasheva (TASM 6177), living culture MFLUCC 25–0169.

GenBank numbers – LSU = PV158287, SSU = PV158289, ITS = PV163078.

Notes – Phylogenetic analysis of combined LSU, SSU, and ITS sequence data placed our isolate (TASM 6177) within the genus *Dothiora*, forming a well-supported clade with *Dothiora sorbi* (CBS 742.71 and CBS 742.72) (82% ML bootstrap, 0.99 PP, Fig. 1). The ITS divergence from *D. sorbi* is relatively low (0.7%, 4/501 bp). However, TASM 6177 differs morphologically by producing a hormonema-like synasexual morph, which has not been described for *D. sorbi*. Our

isolate develops stromatic, dark brown to black conidiomata directly on the host surface, along with large, muriform, thick-walled conidia that are globose to irregularly shaped–morphological features not previously documented in closely related species. Because the synasexual morph of *D. sorbi* remains unknown, direct morphological comparison was not possible. Therefore, we tentatively identified TASM 6177 as *D. sorbi*, denoting its close phylogenetic relationship while recognizing the need for additional data to confirm its identity. Although *Dothiora* species have previously been recorded in Uzbekistan, this is the first record of a *Dothiora* species on *Rosa webbiana*.

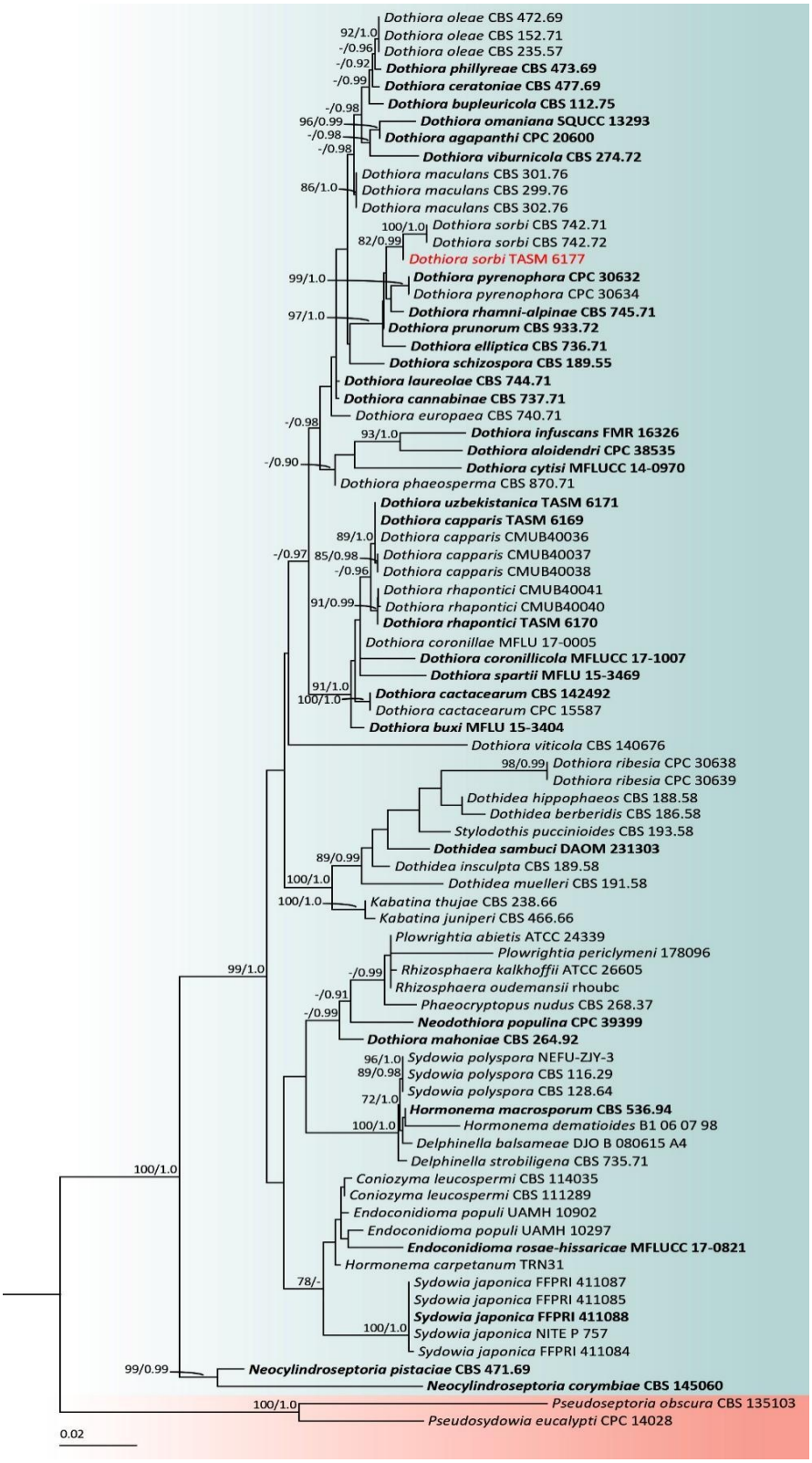


Figure 1 – Phylogram generated from maximum likelihood analysis based on combined LSU, SSU, and ITS sequence data from 82 taxa, comprising 2,270 characters (LSU = 898, SSU = 791, ITS = 581). The best-scoring RAxML tree with a final likelihood value of -8643.647 is presented. The matrix contained 505 distinct alignment patterns, with 38.88% of the characters being undetermined or gaps. Estimated base frequencies were as follows: A = 0.259, C = 0.220, G = 0.280, T = 0.241; substitution rates: AC = 1.553, AG = 2.735, AT = 1.613, CG = 0.917, CT = 7.508, GT = 1.0; gamma distribution shape parameter α = 0.553. Bootstrap support values for maximum likelihood (ML) equal to or greater than 70% and clade credibility values greater than 0.90 (rounded to two decimal places) from Bayesian inference analysis are labeled at each node. Ex-type strains are in bold, while the new isolate is indicated in red. The tree is rooted to *Pseudosydowia eucalypti* (CPC 14028) and *Pseudoseptoria obscura* (CBS 135103).

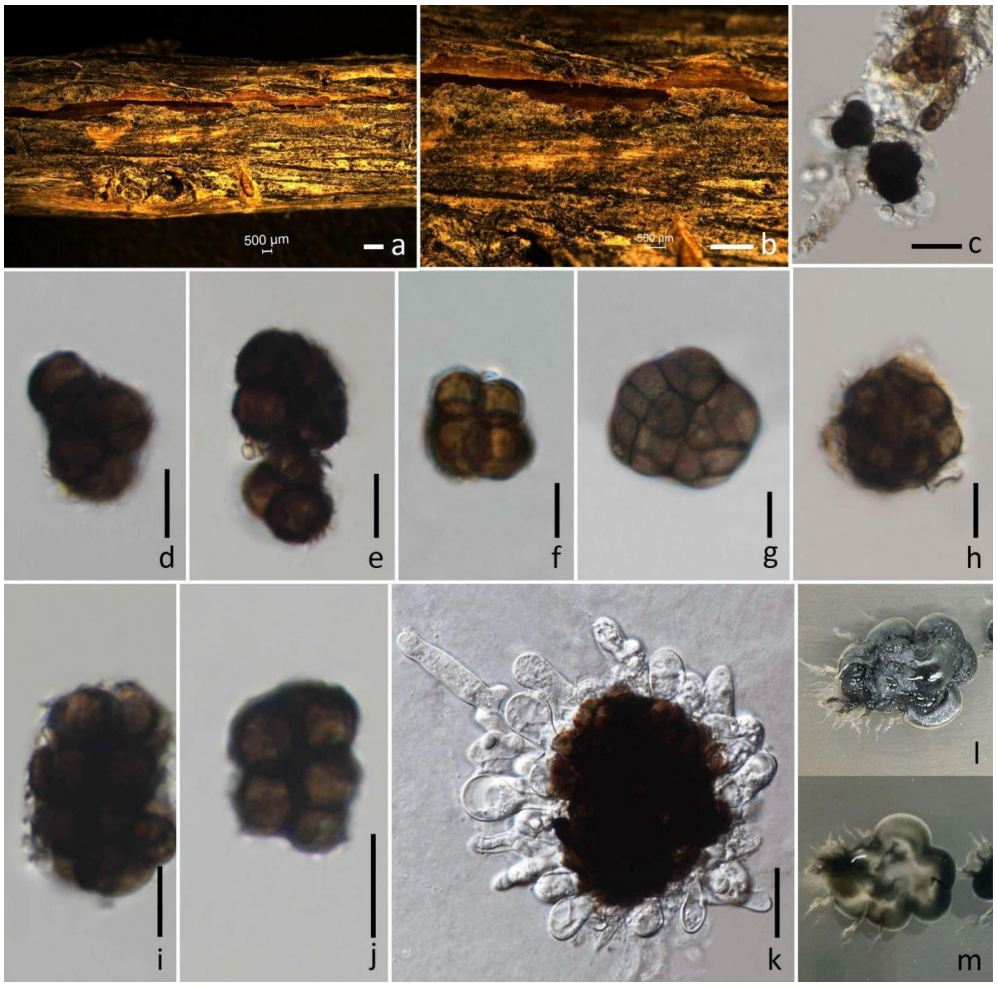


Figure 2 – *Dothiora sorbi* (TASM 6177, new host record). a, b Conidiomata on the host surface. c Conidiophores, conidiogenous cells, and conidia on the host. d–j Conidia. k Germinated conidium. l, m Culture characteristics on MEA (l: above view, m: reverse view). Scale bars: a, b = 1 mm, c, k = 20 µm, d–j = 10 µm.

Mycosphaerellales (Nannf.) P.F. Cannon

Mycosphaerellaceae Lindau

Pseudocercospora Speg., Anales Mus. Nac. Hist. Nat. Buenos Aires ser. 3, 13: 438 (1911)

Index Fungorum number: IF9559; Facesoffungi number: FoF08551

Pseudocercospora is a diverse genus of cercosporoid fungi, comprising more than 100 species found worldwide. The genus was established by Spegazzini (1910), with *P. vitis* as the type species. A key distinguishing feature of this genus is its colored conidia and conidiophores, which

lack thickened or darkened conidiogenous loci and hila. In contrast, related genera such as *Cercospora*, *Mycovellosiella*, *Passalora*, *Pedrocrousiella*, and *Zasmidium* possess thickened or darkened conidiogenous loci, facilitating differentiation (Crous & Braun 2003, Braun et al. 2013, 2016, Videira et al. 2017). Molecular data reveal that most *Pseudocercospora* species are host-specific, reflecting their specialization to particular plant hosts (Crous et al. 2013). However, some species exhibit overlapping morphological traits that can be resolved through multi-gene phylogenetic analysis (Videira et al. 2017, Chen et al. 2022). *Pseudocercospora* species are of economic importance, as they can cause significant crop losses, underscoring their relevance in plant pathology (Crous et al. 2013, Bakhshi et al. 2014). This group encompasses more than 2,000 named species, as described by Crous & Braun (2003), Kamal (2010), Awasthi et al. (2016), Braun et al. (2013, 2016), Kumar & Singh (2015a, b, 2016), Singh et al. (2011, 2012, 2013, 2020, 2022), Yadav et al. (2021), Verma et al. (2021), Rajwar et al. (2025), suggesting that the diversity of such fungi is still insufficiently known.

Prof. Kevin D. Hyde has introduced several novel species in *Pseudocercospora*, including *P. chiangmaiensis* (Cheewangkoon et al. 2008), *P. christellae* (Phengsintham et al. 2010), *P. cratevae* (Phengsintham et al. 2013a), *P. dypsidis* (Chen et al. 2020), *P. getoniae* (Phengsintham et al. 2013b), *P. micromeli* (Phengsintham et al. 2013b), *P. radermachericola* (Phengsintham et al. 2010), *P. rosae* (Wanasinghe et al. 2018), *P. tamarindi* (Liu et al. 2015), *P. tectonae* (Phengsintham et al. 2013b), *P. vignae* (Bhunjun et al. 2022) and *P. wendlandiiphila* (Phengsintham et al. 2013b). In recognition of his exceptional contributions to mycology, we dedicate the new host record of *P. snelliana*, identified based on morphological characteristics and phylogenetic analyses.

Pseudocercospora snelliana (Reichert) U. Braun, H.D. Shin, C. Nakash. & Crous, Stud. Mycol. 75: 106 (2012) Figs 4, 5

Index Fungorum number: IF903720; Facesoffungi number: FoF17747; MycoBank: MB851116

Phytopathogenic, foliicolous. *Leaf spots* hypogenous, initially indistinct from the upper surface but distinct on the lower surface, initially light brown, latter becoming on became blackish brown, vein- limited, 2–3 mm in diam., eventually later on coalescing to cover entire lower leaf surface. *Colonies* hypogenous, brown, velvety. Sexual morph: Undetermined. Asexual morph: Hyphomycetous. *Mycelium* 1.5–2.0 µm, mostly superficial, branched, septate, smooth, light olivaceous brown. *Stromata* absent. *Conidiophores* 27−85 × 3.5−6 µm ($\overline{x}$ = 53.5 × 4.75 µm, n = 20), arises as a lateral branch of superficial hyphae, macronematous, solitary or rarely in fascicles of 2 develop on superficial hyphae, unbranched, rarely branched, cylindrical, erect to curved, geniculate at the tip, 1–5-septate, smooth, thin to thick-walled, pale olivaceous brown to dark brown. *Conidiogenous cells* integrated, terminal and intercalary, mono to polyblastic, unbranched, smooth, thin- to thick-walled, olivaceous to light brown, conidiogenous loci slightly protuberant, inconspicuous, unthickened to slightly thickened, 2−4 µm wide. *Conidia* 15−67 × 2−4 µm ($\overline{x}$ = 40.5 × 3 µm, n = 20), formed singly, pale olivaceous brown to dark brown, dry, obclavate to obclavate-cylindrical, straight to curved, smooth, thin-walled, base obconically truncated to rounded, tip obtuse, 1−6-septate, hila unthickened, sometimes slightly thickened and darkened, 1−2 µm wide.

Culture characteristics – Very slow growing, reached about 10 mm diam. on PDA after 1 week of inoculation at 25 ± 5 °C, top colour smoke grey to glaucous grey and reverse greenish black, subcircular, velvety, surface raised, folded, margin crenate.

Material examined – India, Uttar Pradesh, Gorakhpur, Kusumhi Forest, 26°45'N, 83°22'E, on leaves of *Morus alba* (L.) (*Moraceae*), 20 October 2020, S. Yadav (AMH 10332), living culture NFCCI 5004.

GenBank numbers – NFCCI 5004: ITS = MW805767, LSU = ON409474, *rpb2* = ON416878.

Notes – In the phylogenetic analysis of *Pseudocercospora* based on LSU, ITS, and *rpb2* sequence data, our collection (NFCCI 5004) formed a sister clade with *P. snelliana* (94% ML bootstrap, 1.00 BYPP values, Fig. 3), indicating a close genetic relationship. Morphologically, our

isolate (NFCCI 5004) resembles *P. snelliana*, but shows slight differences in having shorter conidiophores (27–85 × 3.5–6 µm vs. 15–100 × 3–6 µm), and occasionally fewer septa (1–5-septate vs. 0–12-septate). NFCCI 5004 has smaller conidia (15–67 × 2–4 µm vs. 30–70 × 4–6 µm) and fewer septate conidia (1–6-septate vs. 1–10-septate) compared to those of *P. snelliana*. However, these measurements still fall within the morphological range reported for *P. snelliana*. The nucleotide differences between our collection and *P. snelliana* (CPC 11654) are 1.39% (7/502 bp, including 1 gap) in the ITS region and 0.12% (1/833 bp, including 1 gap) in the LSU region. Based on phylogenetic analysis results and overlapping morphological features, our isolate is identified as *P. snelliana*. This represents a new host record of *P. snelliana* on *Morus alba*.

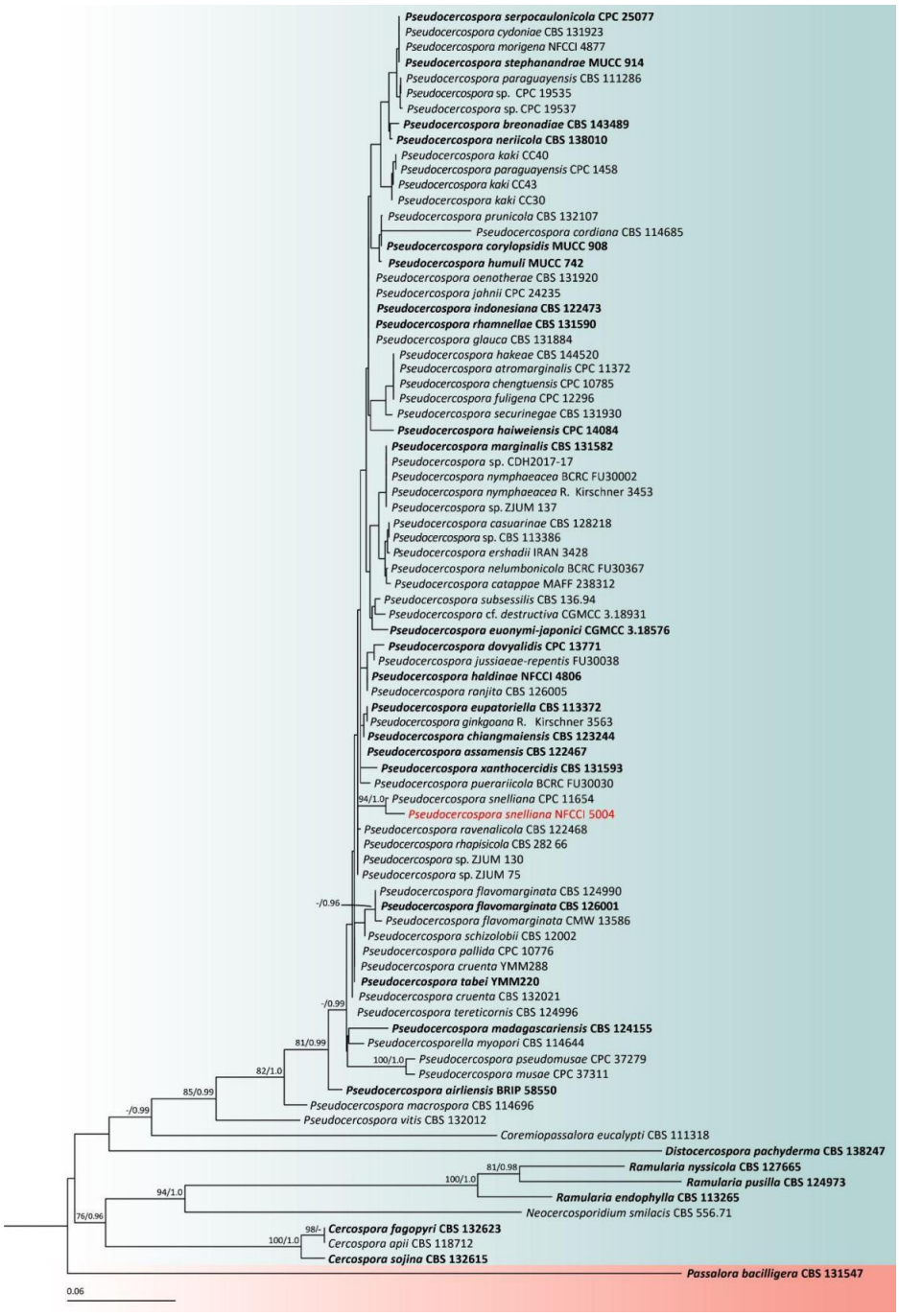


Figure 3 – Phylogram generated from maximum likelihood analysis based on combined LSU, ITS, and *rpb2* sequence data from 86 taxa, comprising 1,820 characters (LSU = 729, *rpb2* = 613, ITS = 478). The best-scoring RAxML tree with a final likelihood value of -10740.939 is presented. The matrix contained 582 distinct alignment patterns, with 29.06% of the characters being

undetermined or gaps. Estimated base frequencies were as follows: A = 0.294, C = 0.265, G = 0.266, T = 0.175; substitution rates: AC = 0.975, AG = 2.092, AT = 0.674, CG = 0.613, CT = 5.980, GT = 1.0; gamma distribution shape parameter α = 0.519. Bootstrap support values for maximum likelihood (ML) equal to or greater than 70% and clade credibility values greater than 0.90 (rounded to two decimal places) from Bayesian inference analysis are labeled at each node. Ex-type strains are in bold, while the new isolate is indicated in red. The tree is rooted to *Passalora bacilligera* (CBS 131547).

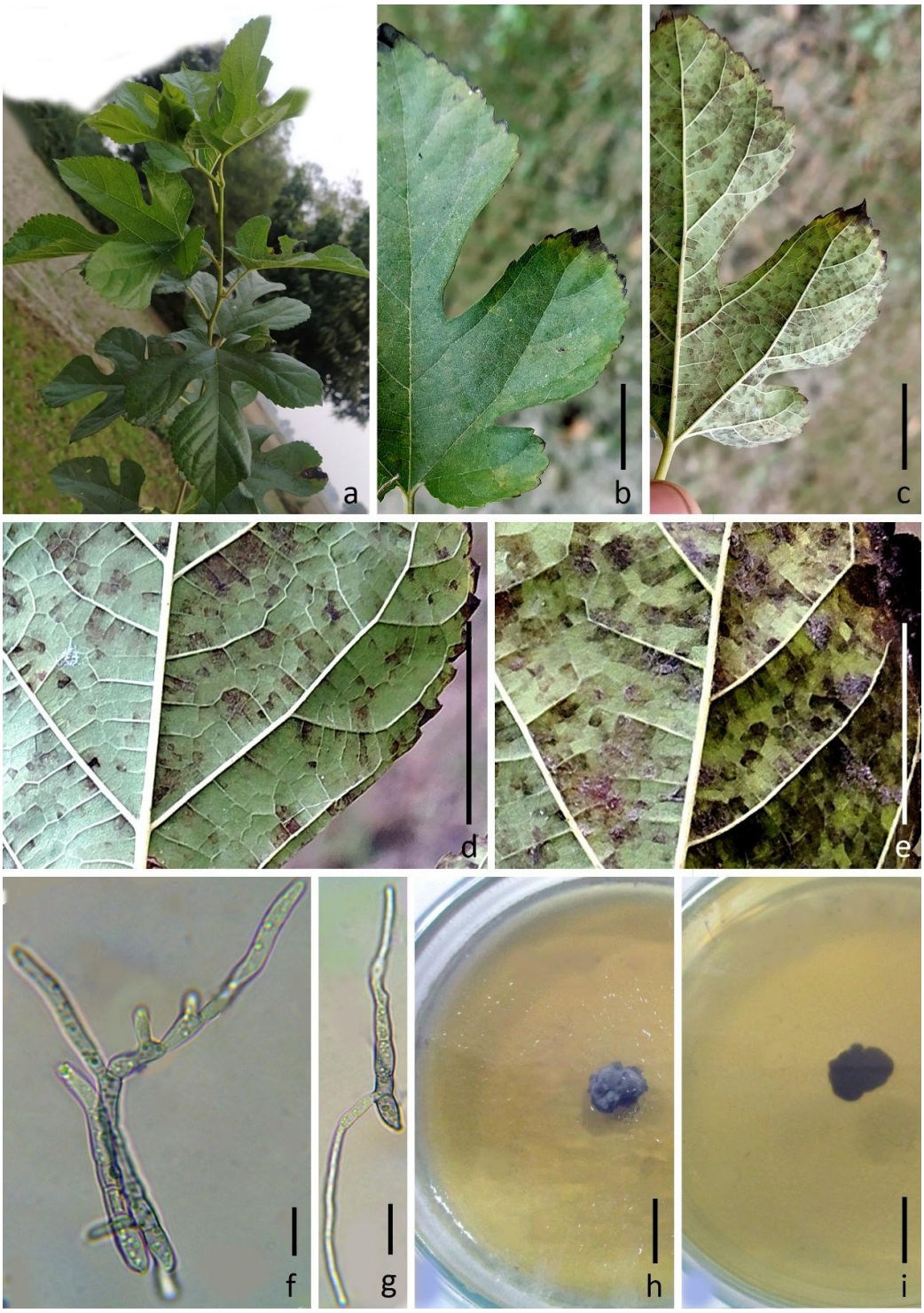


Figure 4 – *Pseudocercospora snelliana* (AMH 10332, new host record). a Host plant. b Initial stage of infection on the upper marginal surface of the leaf. c Initial stage of infection on the lower leaf surface. d, e Late stage of infection on the lower leaf surface. f, g Germinated conidia in

distilled water after 24 hours. h Top view of colony on PDA after 1 month. i Reverse view of the colony on PDA after 1 month. Scale bars: b–e = 20 mm, f, g = 10 µm, h, i = 10 mm.

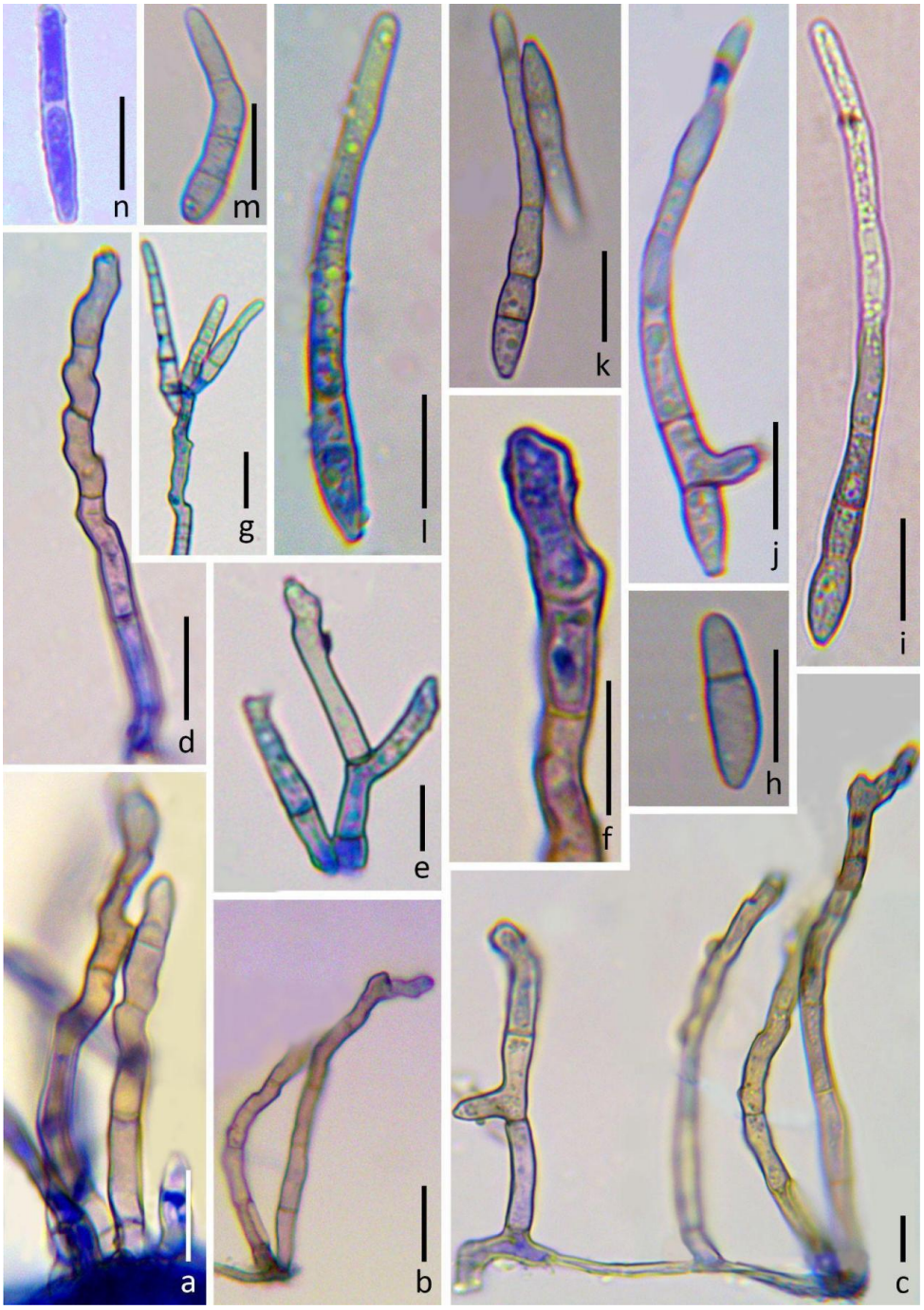


Figure 5 – Microphotographs of *Pseudocercospora snelliana* (AMH 10332, new host record). a–c Conidiophores arising from superficial hyphae. d Geniculate conidiogenous cells of conidiophores. e Branched conidiophores. f Polyblastic nature of conidiogenous cells. g Conidiophore with conidia. h–n Conidia. Scale bars: 10 µm.

Zasmidium Fr., Summa veg. Scand., Sectio Post. (Stockholm): 407 (1849)

Index Fungorum number: IF22396; Facesoffungi number: FoF08574

Zasmidium was introduced by Fries (1849), with *Z. cellare* designated as the type species and currently placed in the *Mycosphaerellaceae* within Dothideomycetes (Hyde et al. 2024c, Tan & Shivas 2024). *Zasmidium* is characterized by submerged, smooth, thin-walled, hyaline hyphae with thin septa, coarsely verrucose, olivaceous-green, thick-walled aerial hyphae with thin

septa, conidiophores not differentiated from vegetative hyphae, often reduced to conidiogenous cells, integrated, terminal, and lateral conidiogenous cells arising from aerial hyphae, cylindrical, and pale brown, cylindrical to fusiform, verrucose, obovate to obconical, pale brown conidia with a truncate base and a conspicuous, slightly pigmented, thickened, and refractive hilum, and subhyaline, verrucose or smooth-walled, 0–4-septate, fusiform to cylindrical primary conidia (Arzanlou et al. 2007). The molecular phylogenetic analysis of this genus is mainly based on sequences of ITS, LSU, *rpb2*, and *act* (Zhao et al. 2016, An et al. 2021, Osorio et al. 2021, Tan et al. 2022).

Out of the 254 species currently listed in Index Fungorum (2025), Prof. Kevin D. Hyde and his collaborators have described nine *Zasmidium* species. In recognition of his outstanding contributions to mycology, we introduce *Zasmidium hydei,* a pathogenic taxon named in honor of Prof. Kevin D. Hyde, with an updated phylogenetic tree for *Zasmidium* (Fig. 6).

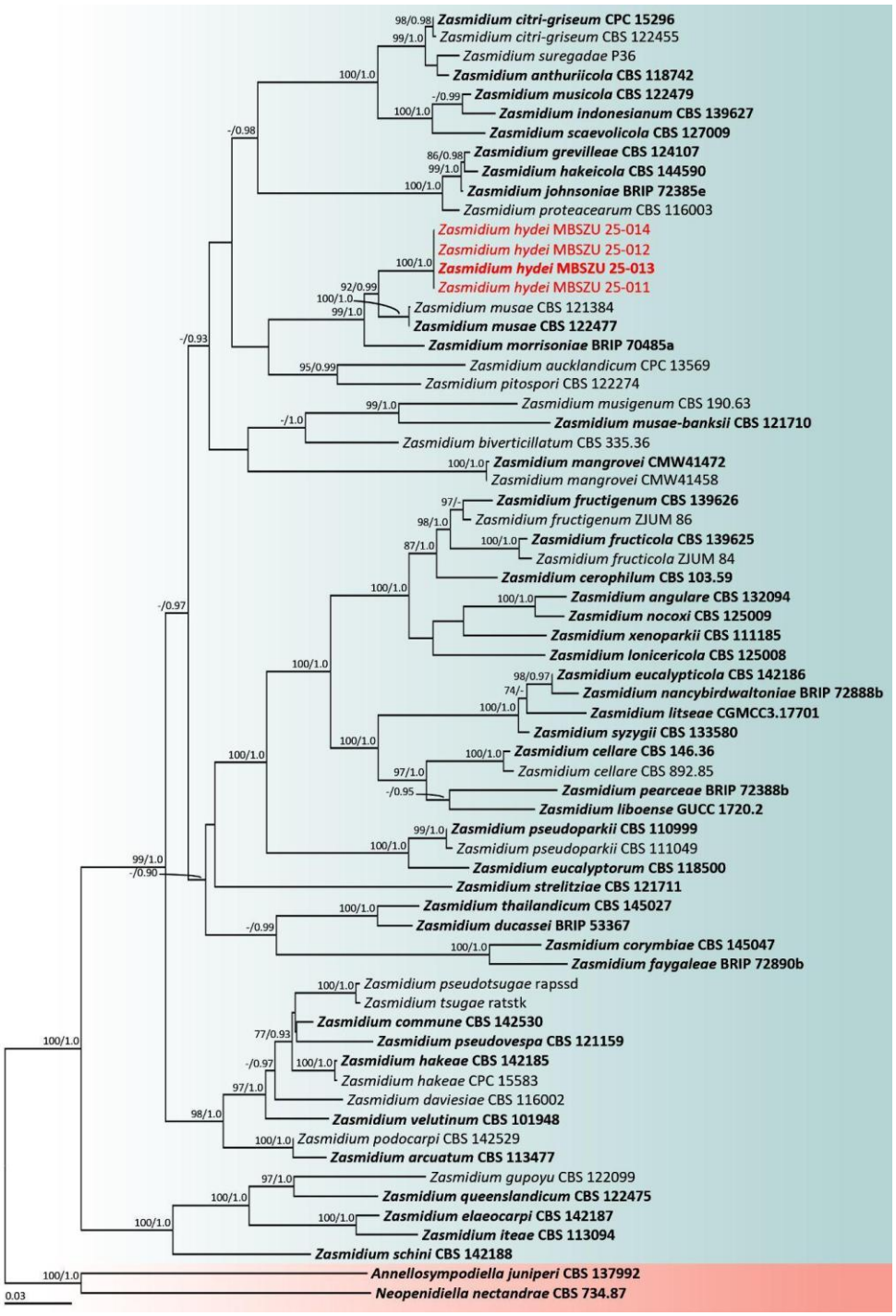


Figure 6 – Phylogram generated from maximum likelihood analysis based on combined LSU, ITS, *rpb2*, and *act* sequence data from 67 taxa, comprising 2,776 characters (LSU = 857, ITS = 620, *rpb2* = 1,063, *act* = 236). The best-scoring RAxML tree with a final likelihood value of -23015.118 is presented. The matrix contained 1,244 distinct alignment patterns, with 26.44% of the characters being undetermined or gaps. Estimated base frequencies were as follows: A = 0.243, C = 0.259, G = 0.286, T = 0.211; substitution rates: AC = 1.411, AG = 3.504, AT = 1.150, CG = 1.069, CT = 7.584, GT = 1.0; gamma distribution shape parameter α = 0.193. Bootstrap support values for maximum likelihood (ML) equal to or greater than 70% and clade credibility values greater than 0.90 (rounded to two decimal places) from Bayesian inference analysis are labeled at each node. Ex-type strains are in bold, while the new isolates are indicated in red. The tree is rooted to *Annellosympodiella juniperi* (CBS 137992) and *Neopenidiella nectandrae* (CBS 734.87).

Zasmidium hydei Khuna, Hongsanan & Xie N., sp. nov. Fig. 7

Index Fungorum number: IF903731; Facesoffungi number: FoF17748

Etymology – 'hydei' named in honor of the renowned mycologist Kevin D. Hyde, recognizing his significant contributions to mycology on the occasion of his 70th birthday.

Associated with leaf spot of *Cordyline fruticosa* (*Asparagaceae*). *Lesions on leaves* brown spots with a yellow halo surrounding each lesion, round to irregular, and measuring 1–31 × 1–13 mm. *Colonies* on PDA circular, flat, greyish-white; reverse dark brown. *Conidial mass* released from conidiomata formed on PDA after incubation for two months, globose or subglobose, yellow to yellow-brown. *Mycelium* 2.1–6.8 µm wide, composed of hyaline to pale brown, smooth, branched, uniform in width. Asexual morph: *Conidiophores* 56–140 × 1.4–5.0 µm ($\overline{x}$ = 89.3 × 3.4 µm, n = 20), arising from hyphae, hyaline, straight or slightly curved, unbranched, smooth and thick-walled. *Conidiogenous cells* 7–30 × 2.5–4.4 µm ($\overline{x}$ = 18.2 × 3.4 µm, n = 20), polyblastic, terminal, erect, unbranched, hyaline, smooth–walled. *Conidia* 4–10 × 2–5 µm ($\overline{x}$ = 6 × 3 µm, n = 100), solitary, hyaline, oval to ellipsoid, aseptate, smooth and thin-walled, granulate. Sexual morph: Undetermined.

Culture characteristics – Colonies on PDA and MEA were described at 25 °C after 14 days of incubation. Colonies on PDA were 21–25 mm diam., circular, flat, margin entirely to slightly undulate, greyish-white; reverse dark brown. Colonies on MEA grew to 27–31 mm diam., circular, flat, margin entire, white in the center, brown at the margin; reverse brown in the center, white at the margin.

Material examined – China, Guangdong Province, Zhuhai City, Xiangzhou District, 22°17'00.0" N, 113°35'20.0" E, leaf of Ti plant with leaf spot symptoms (*Cordyline fruticosa*, *Asparagaceae*), 23 November 2024, Khuna S., ex-type MBSZU 25–013; *ibid*., living cultures MBSZU 25–011, MBSZU 25–012, MBSZU 25–014.

GenBank numbers – MBSZU 25–011: LSU = PQ898037, ITS = PQ898041, *rpb2* = PV016589, *act* = PV016593; MBSZU 25–012: LSU = PQ898038, ITS = PQ898042, *rpb2* = PV016590, *act* = PV016594; MBSZU 25–013: LSU = PQ898039, ITS = PQ898043, *rpb2* = PV016591, *act* = PV016595; MBSZU 25–014: LSU = PQ898040, ITS = PQ898044, *rpb2* = PV016592, *act* = PV016596.

Notes – In the phylogenetic analysis based on combined LSU, ITS, *rpb2*, and *act* sequence data (Fig. 6), our new species (MBSZU 25–011, MBSZU 25–012, MBSZU 25–013, and MBSZU 25–014) formed a distinct clade among *Zasmidium* species and are closely related to *Z. musae* (CBS 121384 and CBS 122477) and *Z. morrisoniae* (BRIP 70485a). The base-pair differences in ITS and *act* between the type strain of *Z. musae* (CBS 122477) and our new species are 1.94% and 4.69% (10/514 and 10/213 bp, including gaps), while the differences in ITS, LSU, *rpb2*, and *act* between *Z. musae* (CBS 121384) and our new species are 2.01, 0.55, 5.10, and 5.14% (10/497, 4/732, 45/883, and 11/214 bp, including gaps), respectively. In addition, the base-pair differences in ITS, LSU, *rpb2*, *act*, and *tef1-α* between the type strain of *Z. morrisoniae* (BRIP 70485a) and our new species are 2.36%, 0.12%, 7.81%, 6.15%, and 16.42% (15/635, 1/814, 69/884, 12/195, and 78/475 bp, including gaps), respectively. The growth of *Z. hydei* on PDA was displayed faster than

that of *Z. musae* (CBS 122477) (27–31 mm diam. after 14 days vs. 30 mm diam. after 30 days). Based on micromorphological characteristics, *Z. hydei* has larger mycelia (2.1–6.8 µm vs. 2–3 µm wide), longer conidiophores (56–140 × 1.4–5 µm vs. up to 30 × 2–2.5 µm), wider conidiogenous cells (2.5–4.4 µm diam. vs. 1–1.5 µm diam.), and shorter conidia (4–10 × 2–5 µm vs. 7–70 × 1.5–3 µm) than *Z. musae* (CBS 122477) (Arzanlou et al. 2008). When compared to *Z. morrisoniae*, *Z. hydei* has longer conidiophores (56–140 × 1.4–5.0 µm vs. 15–40 × 3–4 µm) and shorter conidia (4–10 × 2–5 µm vs. 12–90 × 2–3 µm) (Tan & Shivas 2024). In addition, the conidia of *Z. hydei* are hyaline, oval to ellipsoid, smooth-walled, aseptate, and granulate, while those of *Z. musae* (CBS 122477) are pale brown, subcylindrical to obclavate, finely verrucose, and 0–7-septate (Arzanlou et al. 2008), and those of *Z. morrisoniae* are pale brown, cylindrical, finely verruculose, and 0–4-septate (Tan & Shivas 2024). Therefore, based on morphology and phylogeny, we introduce our collection as a new species, *Zasmidium hydei*.

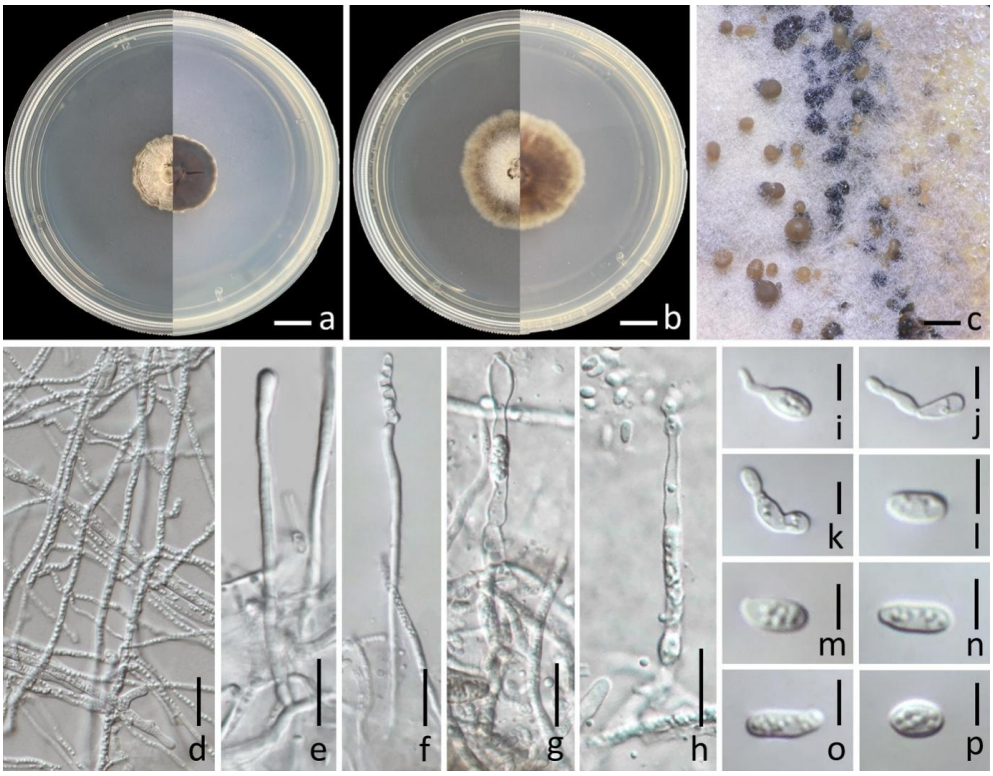


Figure 7 – *Zasmidium hydei* (MBSZU 25–013, ex-type). Colonies incubated at 25 °C for two weeks. a PDA. b MEA (left, surface view and right, reverse). c Conidial mass released from conidiomata. d Mycelium masses. e–h Conidiophores and conidiogenous cells. i–k Conidia germination. l–p Conidia. Scale bars: a, b = 10 mm, c = 1 mm, d–h = 20 µm, i–p = 5 µm.

Subclass Pleosporomycetidae C.L. Schoch, Spatafora, Crous & Shoemaker
Hysteriales Lindau
Hysteriaceae Chevall.
Hysterobrevium E. Boehm & C.L. Schoch, in Boehm, Mugambi, Miller, Huhndorf, Marincowitz, Spatafora & Schoch, Stud. Mycol. 64: 62 (2009)

Index Fungorum number: IF515329; Facesoffungi number: FoF08056

Hysterobrevium was introduced by Boehm et al. (2009) to accommodate three species, *H. mori*, *H. constrictum*, and *H. smilacis*, which were previously classified as *Hysterographium mori*, *Gloniopsis constricta*, and *G. smilacis*, respectively. This genus was proposed due to the phylogenetic distinctiveness of these species from their respective genera. *Hysterobrevium* is characterized by navicular hysterothecia with a prominent longitudinal slit, bitunicate and cylindrical to clavate asci, ovoid to obovoid, pigmented or hyaline dictyospores, with either obtuse

or acuminate ends, constricted at the median septum, highly variable, with a gelatinous sheath when young, and dissipating with age (Boehm et al. 2009, Jayasiri et al. 2018, Hongsanan et al. 2020a, Senanayake et al. 2023).

Prof. Kevin D. Hyde's contributions to the fungal taxonomy of hysteriform Dothideomycetes include the discovery of two new *Hysterobrevium* species (Jayasiri et al. 2018), which are among the nine species currently listed in Index Fungorum (2025). His work on *Hysterobrevium* has significantly expanded our understanding of this genus. In recognition of his outstanding contributions to mycology, herein we introduce *Hysterobrevium hydei*, which has been named in honor of Prof. Kevin D. Hyde. We also provide the updated phylogenetic tree for *Hysterobrevium* (Fig. 8).

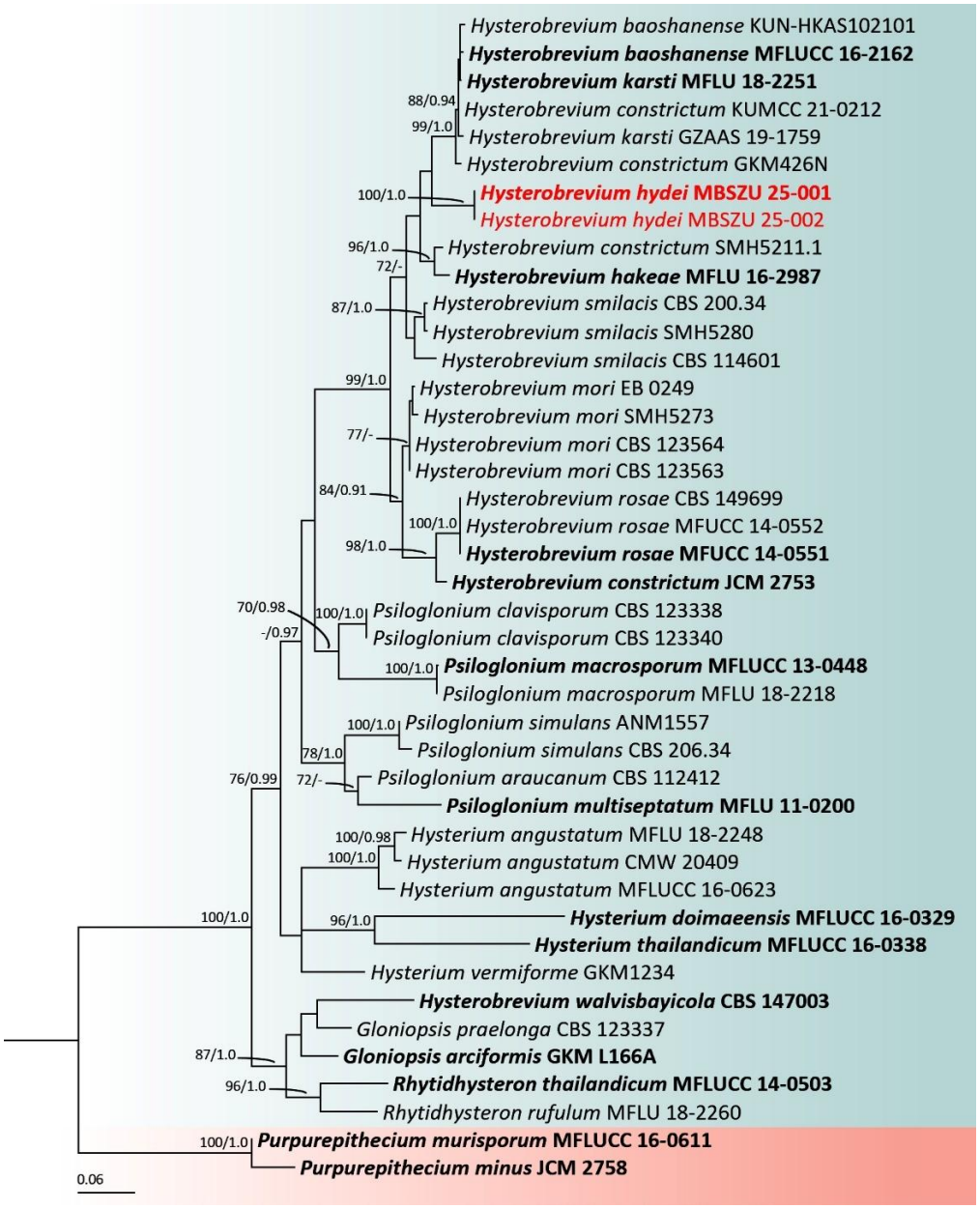


Figure 8 – Phylogram generated from maximum likelihood analysis based on combined ITS, LSU, SSU, and *tef1-α* sequence data from 42 taxa, comprising 3,935 characters (ITS = 868, LSU = 1,046, SSU = 1,038, *tef1-α* = 983). The best-scoring RAxML tree with a final likelihood value of -15742.495 is presented. The matrix contained 1,243 distinct alignment patterns, with 44.52% of the characters being undetermined or gaps. Estimated base frequencies were as follows: A = 0.247, C = 0.243, G = 0.275, T = 0.235; substitution rates: AC = 1.330, AG = 2.378, AT = 1.440, CG = 0.809,

CT = 7.750, GT = 1.0; gamma distribution shape parameter α = 0.432. Bootstrap support values for maximum likelihood (ML) equal to or greater than 70% and clade credibility values greater than 0.90 (rounded to two decimal places) from Bayesian inference analysis are labeled at each node. Ex-type strains are in bold, while the new isolates are indicated in red. The tree is rooted to *Purpurepithecium minus* (JCM 2758) and *P. murisporum* (MFLUCC 16–0611).

Hysterobrevium hydei Hongsanan, Khuna & Xie N., sp. nov. Fig. 9

Index Fungorum number: IF903732; Facesoffungi number: FoF17749

Etymology – 'hydei' named in honor of the renowned mycologist Kevin D. Hyde, recognizing his significant contributions to mycology on the occasion of his 70th birthday.

Holotype – SZU25–001

Saprobic on dead twigs of unidentified host. Sexual morph: *Ascomata* 250–322 diam. × 240–345 high μm ($\overline{x}$ = 285 × 290 μm, n = 10), hysterothecial, superficial, semi-immersed at the basal, scattered, solitary or clustered, usually surrounded at the base by ruptured epidermis or periderm cells, longitudinally striated, navicular with tapering ends, uni-loculate, black, flexuous, glabrous, with a thick slit-like opening. *Peridium* 45–80 μm wide, thick-walled, thinner at the base, thicker at the sides towards its apex, widest at mid-point, carbonaceous and brittle when dry, with several layers of dark brown to black, *textura angularis* cells. *Hamathecium* composed of 1–2 μm wide, dense, filamentous, septate, unbranched, cellular pseudoparaphyses, hyaline, not constricted at the septa, anastomosing at the apex, embedded in a gelatinous matrix. *Asci* 85–120 × 18–25 μm, ($\overline{x}$ = 95 × 19, n = 10), 8-spored, bitunicate, fissitunicate, cylindric-clavate, short pedicellate, apically rounded. *Ascospores* 20–34 × 8–12 ($\overline{x}$ = 24 × 9.5 μm, n = 20), overlapping uniseriate, to biseriate, hyaline, becoming pale brown at maturity, fusiform to ellipsoidal, or obvoid, tapering at both ends, dictyospores, 1–7 transverse septa, 1–3 longitudinal septa, with several segments, constricted at the transverse septa, especially at the median cells, smooth-walled, with guttules, surrounded by a mucilagenous sheath that usually dissipates upon maturation. Asexual morph: Undetermined.

Culture characteristics – Colonies on PDA reaching 1.3 cm diam., after 14 days at 25 °C, circular, irregular, with dense aerial mycelium on the surface, flattened to slightly raised, with initially white, turn in to greenish to grey or dark grey when old, paler greenish or pale grey hair-like at the center, Reverse dark greenish to black, dense, with pale to dark brown edge, surface smooth, velvety to cottony, producing brown pigment on PDA.

Material examined – China, Guangdong Province, Huizhou City, Xunliao Residential District, 22°35'23.5" N, 114°45'02.3" E, on decaying twigs of unidentified host, Hongsanan S., 22 September 2024, WY02.1 (SZU25–001, holotype), ex-type MBSZU 25–001; *ibid*., on decaying twigs of unidentified host, Khuna S., 22 September 2024, WY02.2 (SZU25–002), living culture MBSZU 25–002.

GenBank numbers – MBSZU 25–001: ITS = PQ849538, LSU = PQ849540, *rpb2* = PQ868898, SSU = PQ849542, *tef1-α* = PQ868902; MBSZU 25–002: ITS = PQ849539, LSU = PQ849541, *rpb2* = PQ868899, SSU = PQ849543, *tef1-α* = PQ868903.

Notes – In the phylogenetic analysis based on combined ITS, LSU, SSU, and *tef1-α* sequence data (Fig. 8), our new species (MBSZU 25–001 and MBSZU 25–002) formed a distinct clade within *Hysterobrevium*. This clade is closely related to the clade containing *H. baoshanense* (MFLUCC 16–2162, type; KUN-HKAS102101), *H. karsti* (MFLU 18–2251, type; GZAAS 19–1759), and *H. constrictum* (GKM426N, KUMCC 21–0212). The species within the sister clade are not well-resolved based on the current phylogenetic analyses and may represent a single species. However, further studies, including additional molecular data and morphological comparisons, are required to clarify their taxonomic status. The base-pair difference between the new species and *H. baoshanense* (MFLUCC 16–2162, type) was 9.69% (56/578 bp, including 4 gaps) in the ITS region, while the differences in LSU, SSU and *tef1-α* were 1.02% (8/787 bp, without gaps), 1.30% (13/1001 bp, including 8 gaps), and 5.99% (58/969 bp, including 2 gaps), respectively. The base-pair difference of the new species and *H. karsti* (MFLU 18-2251, type) was

9.55% (58/607 bp, including 5 gaps) in the ITS region, while the differences in LSU, SSU and *tef1-α* were 0.95% (8/838 bp, without gaps), 0.1% (1/1021 bp, without gaps), and 4.54% (43/947 bp, without gaps), respectively. Morphologically, *H. hydei* fits well with the generic concept of *Hysterobrevium* in having navicular hysterothecia with a prominent longitudinal slit, bitunicate and cylindrical to clavate asci, fusiform to ellipsoidal, or obvoid, pigmented or hyaline dictyospores, constricted at least at the median septum (Boehm et al. 2009, Jayasiri et al. 2018). Based on morphology and phylogeny, we introduce our collection as a new species, *Hysterobrevium hydei*.

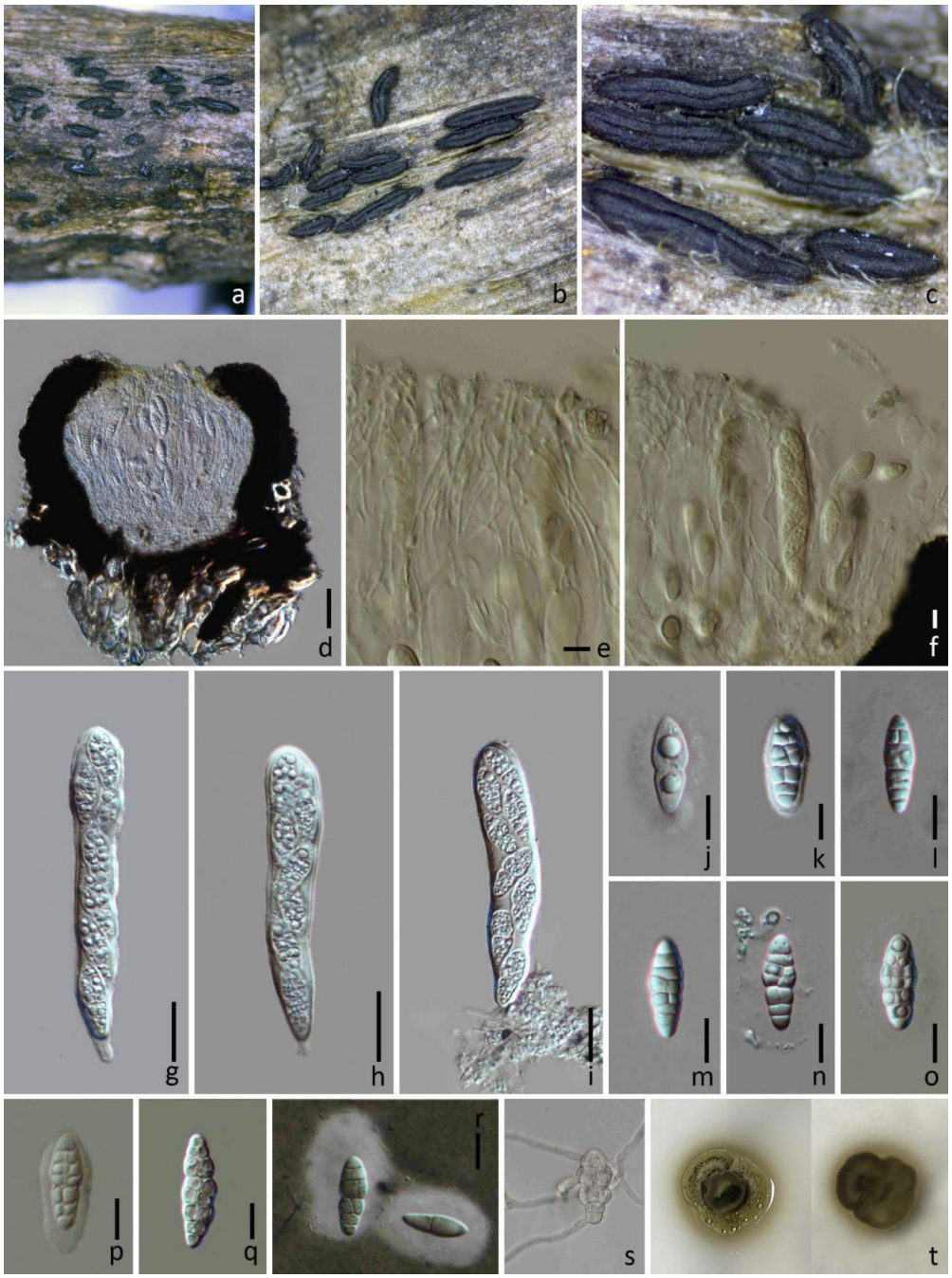


Figure 9 – *Hysterobrevium hydei* (SZU25-001, holotype). a–c Appearance of ascomata on woody substrate. d Vertical cross-section of an ascoma. e Hamathecium. f Asci embedded in a gelatinous matrix (stained in Melzer's reagent). g–i Asci. j–r Ascospores (o–q stained in Melzer's reagent; r stained in Indian ink's reagent). s Germinated ascospore. t Upper and reverse views of the colony on PDA. Scale bars: d = 50 µm, g–i = 20 µm, e, f, j–r = 10 µm.

Pleosporales Luttr. ex M.E. Barr

Amorosiaceae Thambug. & K.D. Hyde

Amorocoelophoma Jayasiri, E.B.G. Jones & K.D. Hyde

Index Fungorum number: IF555529; Facesoffungi number: FoF05230

The coelomycetous genus *Amorocoelophoma* was introduced by Jayasiri et al. (2019) to accommodate the type species *A. cassia*. Based on the phylogenetic analysis of combined ITS, LSU, SSU, *rpb2*, and *tef1-α*, *Amorocoelophoma* was considered to be polyphyletic, as *A. camelliae* forms a distinct clade and is well-separated from other *Amorocoelophoma* species (viz. *A. cassiae*, *A. neoregeliae*, and *A. sinensis*) (Yu et al. 2022, Zhang et al. 2024a). Our phylogenetic analysis also confirmed that *Amorocoelophoma* is polyphyletic (Fig. 10). Currently, this genus comprises four species with distinct ecological roles and geographic distributions. *Amorocoelophoma cassiae* and *A. sinensis* have been identified as saprobes from Thailand and China, respectively (Jayasiri et al. 2019, Zhang et al. 2024a). In contrast, *A. camelliae* and *A. neoregeliae* were isolated from leaf spots in China and New Zealand, respectively; however, pathogenicity has not been confirmed for these species (Ariyawansa et al. 2020, Crous et al. 2021a). Members of *Amorocoelophoma* are reported only as asexual morphs, and it is characterized by pycnidial conidiomata, solitary to gregarious, ovoid to globose, brown, phialidic conidiogenous cells, hyaline with cylindrical and aseptate conidia, smooth- and thin-walled, and guttulate concentrated at ends (Jayasiri et al. 2019).

Four species are currently listed in Index Fungorum (2025), and Prof. Kevin D. Hyde and his collaborators have introduced one species in this genus. In recognition of his outstanding contributions to mycology, we introduce *Amorocoelophoma hydei*, which has been named in honor of Prof. Kevin D. Hyde. We also provide the updated phylogenetic tree for *Amorocoelophoma* (Fig. 10), which suggests that *Amorocoelophoma* remains polyphyletic. Therefore, further collections are required to address these discrepancies.

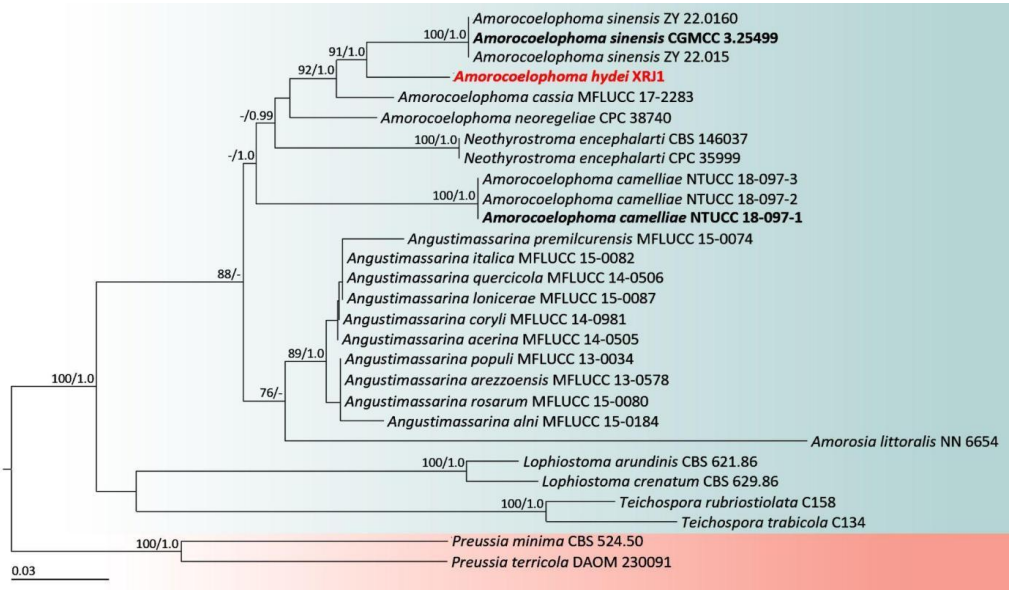


Figure 10 – Phylogram generated from maximum likelihood analysis based on combined ITS, LSU, SSU, *rpb2*, and *tef1-α* sequence data from 28 taxa, comprising 3,967 characters (ITS = 537, LSU = 889, SSU = 919, *rpb2* = 1,446, *tef1-α* = 711). The best-scoring RAxML tree with a final likelihood value of -15955.585 is presented. The matrix contained 1,092 distinct alignment patterns, with 27.06% of the characters being undetermined or gaps. Estimated base frequencies were as follows: A = 0.248, C = 0.248, G = 0.271, T = 0.233; substitution rates: AC = 1.406, AG = 4.034, AT = 2.112, CG = 1.247, CT = 9.330, GT = 1.0; gamma distribution shape parameter α = 0.159. Bootstrap support values for maximum likelihood (ML) equal to or greater than 70% and clade credibility values greater than 0.90 (rounded to two decimal places) from Bayesian inference analysis are labeled at each node. Ex-type strains are in bold, while the new isolate is indicated in red bold. The tree is rooted to *Preussia minima* (CBS 524.50) and *P. terricola* (DAOM 230091).

Amorocoelophoma hydei L. Lu & Tibpromma, sp. nov. Fig. 11

Index Fungorum number: IF903707; Facesoffungi number: FoF05231

Etymology – 'hydei' named in honor of the renowned mycologist Kevin D. Hyde, recognizing his significant contributions to mycology on the occasion of his 70th birthday.

Holotype – MFLU 25–0105

Saprobic on decaying branches of an unknown host in freshwater habitats. Sexual morph: Undetermined. Asexual morph: Coelomycetous. *Conidiomata* 100–150 × 12–180 μm ($\overline{x}$ = 121 × 148 μm, n = 15), pycnidial, immersed, solitary to gregarious, ovoid to subglobose, brown to black, uni-loculate, without ostiolate. *Conidiomata wall* 10–15 μm wide ($\overline{x}$ = 12 μm, n = 20), comprising two-layered, inner layer hyaline *textura angularis* cells, outer layer *textura angularis* cells, brown, dense, fusion with host tissue. *Conidiophores* reduced to conidiogenous cells. *Conidiogenous cells* 6–9 × 2.5–5 μm ($\overline{x}$ = 8 × 3.5 μm, n = 30), phialidic, solitary, ampulliform or subcylindrical, straight, hyaline, smooth-walled. *Conidia* 6.5–9 × 4–5.5 μm ($\overline{x}$ =7.8 × 4.8 μm, n = 30), oval to ellipsoid, some ovoid, hyaline, aseptate, smooth and thin-walled, granulate.

Culture characteristics – Conidia germinating on PDA within 24 h. Colonies growing on PDA, reaching 15–20 mm in one month at 25 °C, surface flocculent, circular, entire margin, from above, brownish, darker in the center, from below, light brown.

Material examined – Thailand, Chiang Rai Province, on a decaying branch of unidentified host, 07 November 2023, Xiongju Xu, XRJ1 (MFLU 25–0105, holotype), ex-type MFLUCC 25–0191.

GenBank numbers – MFLUCC 25–0191: ITS = PV426446, LSU = PV426448, SSU = PV426452, *rpb2* = PV426709, *tef1-α* = PV426710.

Notes – Based on the phylogenetic analysis of combined ITS, LSU, SSU, *tef1-α*, and *rpb2* sequence data, the new strain *Amorocoelophoma hydei* (MFLUCC 25-0191) forms an independent branch within *Amorocoelophoma* (91% ML/1.00 BYPP) and sister to *A. sinensis* (ZY 22.015, ZY 22.016 and ZY 22.014, ex-type) (Fig. 10). Morphologically, our new isolate fits well in *Amorocoelophoma* while it could be distinguished from *A. sinensis* by oval to ellipsoid conidia that are different from the cylindrical conidia of *A. sinensis* (Zhang et al. 2024a). Base pair differences between *A. hydei* (MFLUCC 25–0191, ex-type) and *A. sinensis* (ZY 22.014, ex-type) are as follows: ITS exhibits 6.8% nucleotide differences (33/484 bp, without gaps), LSU 0.4% (4/813 bp, without gaps), SSU 0.2% (3/1039 bp, without gaps), *tef1-α* 4.6% (43/922 bp, without gaps), and *rpb2* 9% (97/1056 bp, without gaps). Based on both morphological characteristics and phylogenetic analysis, we introduce our collection as a new species, *A. hydei*.

Corynesporascaceae Sivan

Corynespora Güssow, J. Royal Agric. Soc. England 65: 272 (1905)

Index Fungorum number: IF7795; Facesoffungi number: FoF06663

Corynespora was introduced by Güssow (1905) and typified with *C. mazei*. The genus currently comprises 216 species (Index Fungorum 2025), of which 134 species are accepted, and sequence data are available for only 18 of these species. *Corynespora* species are commonly reported as saprobes and plant pathogens on both woody and herbaceous hosts (McKenzie 2010, Xu et al. 2020, Liu et al. 2023a, Manawasinghe et al. 2024). Some species are important plant pathogens, causing leaf spots on plants. For instance, *C. cassiicola* causes leaf spot diseases in many economically plants, including cucumber (*Cucumis sativus*), cotton (*Gossypium hirsutum*), rubber (*Hevea brasiliensis*), soybean (*Glycine max*), tomato (*Solanum lycopersicum*), and tobacco (*Nicotiana tabacum*) (Fajola & Alasoadura 1973, Koenning et al. 2006, Miyamoto et al. 2009, Déon et al. 2012, Conner et al. 2013, MacKenzie et al. 2018). *Corynespora* is characterized by distinct, determinate or percurrently extending conidiophores, monotretic, integrated, terminal conidiogenous cells, and solitary or sometimes catenate, distoseptate conidia (Ellis 1971, Liu et al. 2023a).

Prof. Kevin D. Hyde has introduced three novel species in this genus: *Corynespora lignicola*, *C. submersa* (Hyde et al. 2020b), and *C. septata* (Zhang et al. 2025). In this paper, in honor of Prof. Kevin D. Hyde, we introduce a new species, *C. hydei*, and report a new host record of *C. cassicola*. An updated phylogenetic tree of the genus *Corynespora* is also provided (Fig. 12).

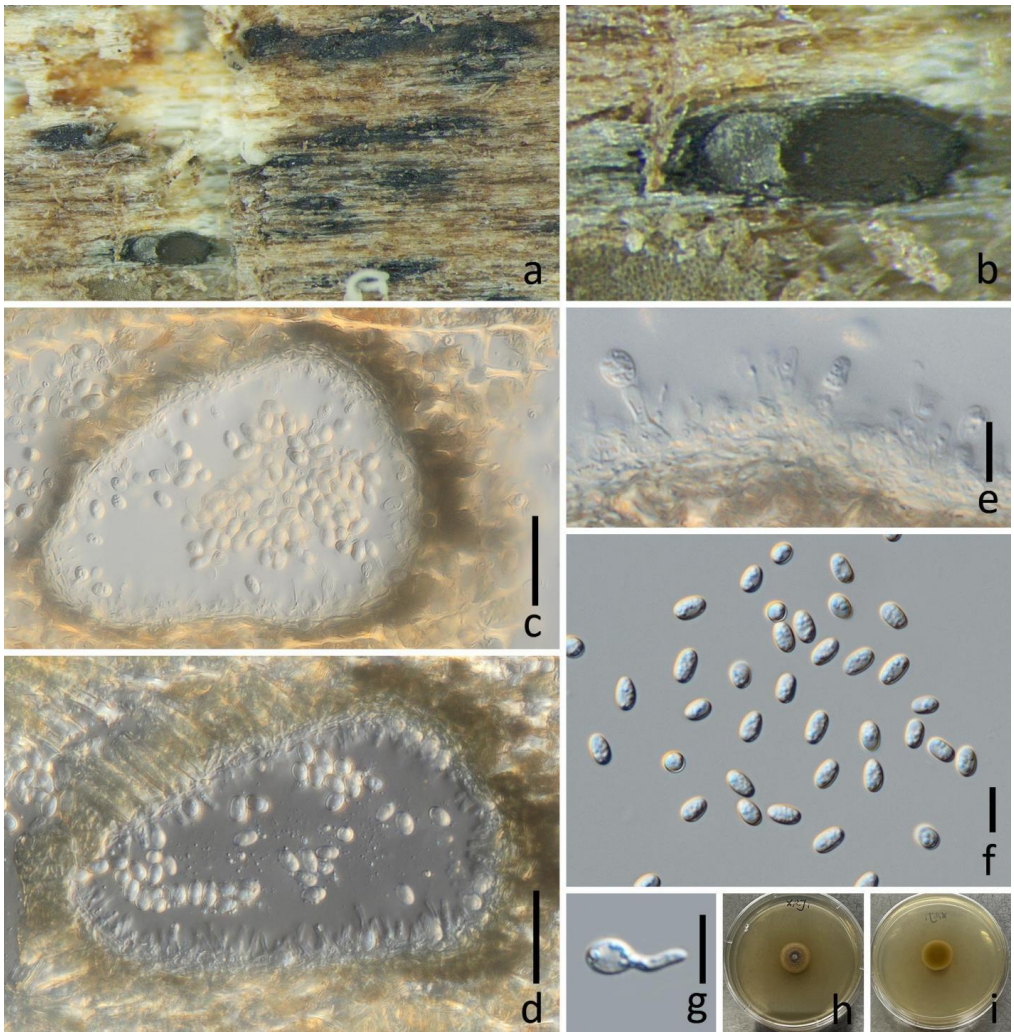


Figure 11 – *Amorocoelophoma hydei* (MFLU 25–0105, holotype). a, b Conidiomata on the host surface. c, d Longitudinal section through conidiomata. e Conidiomata wall and conidiogenous cells with conidia. f Conidia. g Germinated conidium. h, i Culture on PDA from surface and reverse. Scale bars: c, d = 30 µm, e–g = 10 µm.

Corynespora cassiicola (Berk. & M.A. Curtis) C.T. Wei, Mycol. Pap. 34: 5 (1950) Fig. 13

Index Fungorum number: IF296024; Facesoffungi number: FoF06664

Phytopathogenic, *foliicolous*. *Infection spots* amphigenous, circular, subcircular to irregular, concentric, necrotic, 5–40 mm in diam., whitish-red to brownish. *Colonies* on host, epiphyllous, effuse, brownish. *Mycelium* internal on natural host; branched, septate, hyaline, smooth-walled on culture. Sexual morph: Undetermined. Asexual morph: Hyphomycetous. *Stromata* absent. *Conidiophores* solitary, macronematous, mononematous, cylindrical, erect to procumbent, straight to flexuous, slightly curved, unbranched, thick-walled, smooth, 3–13-septate, brown, 55–115 × 2.5–3.5 µm ($\overline{x}$ = 85 × 3 µm, n = 10). *Conidiogenous cells* integrated, terminal, brown, smooth, monotretic, scars unthickened. *Conidia* acrogenous, dry, solitary, unbranched, thin-walled, smooth, straight to slightly curved, usually obclavate to obclavate-cylindrical, 3–17-distoseptate, 35–75 × 3.5–5.5 µm ($\overline{x}$ = 55 × 4.5 µm, n = 10), apex obtuse to rounded, olivaceous to light brown, hilum unthickened, 1.5–2.5 µm wide, germinating conidia present.

Culture characteristics – Colonies on PDA attain a diameter of 45 mm in 7 days at 25 °C, exhibiting a circular, flat morphology with an entire margin. The texture is velvety to fluffy, appearing white from above, while the reverse is dark brown at the center, gradually transitioning to light creamish to yellowish towards the margin.

Material examined – India, Kerala, Kannur, Aralam Wildlife Sanctuary, on living leaves of *Dipterocarpus bourdillonii* (*Dipterocarpaceae*), 29 July 2019, Shambhu Kumar (KFRIMH 102), living culture KFRIMCC 102.

GenBank numbers – ITS = MZ413592, LSU = MZ413594.

Notes – In this study, KFRIMCC 102 was isolated from symptomatic spots on *Dipterocarpus bourdillonii*. Phylogenetic analysis placed the isolate within *Corynespora*, forming a lineage closely related to *C. cassicola* (CBS 100822). The base-pair differences between our new isolate (KFRIMCC 102) and *C. cassiicola* (CBS 100822) showed 0.86% difference (4/466 bp, including 2 gaps) in the ITS locus, and 0.73% difference (6/820 bp, including 3 gaps) in the LSU locus. Morphologically, our collection resembles *C. cassiicola* but differs slightly by having smaller conidiophores and conidia, as well as fewer septa (conidiophores 55–115 × 2.5–3.5 µm vs. 110–850 × 4–11 µm; conidia 35–75 × 3.5–5.5 µm vs. 40–220 × 9–22 µm, 3–17-distoseptate vs. 4–20-distoseptate). However, *C. cassiicola* is known to be highly variable in conidial size and septation depending on host and environment (Nghia et al. 2008, Kurre et al. 2019). Thus, KFRIMCC 102 is identified as *C. cassiicola* based on both morphology and phylogenetic analysis. This is the new host record of *C. cassiicola* on *Dipterocarpus bourdillonii* or its family *Dipterocarpaceae* (Farr & Rossman 2024).

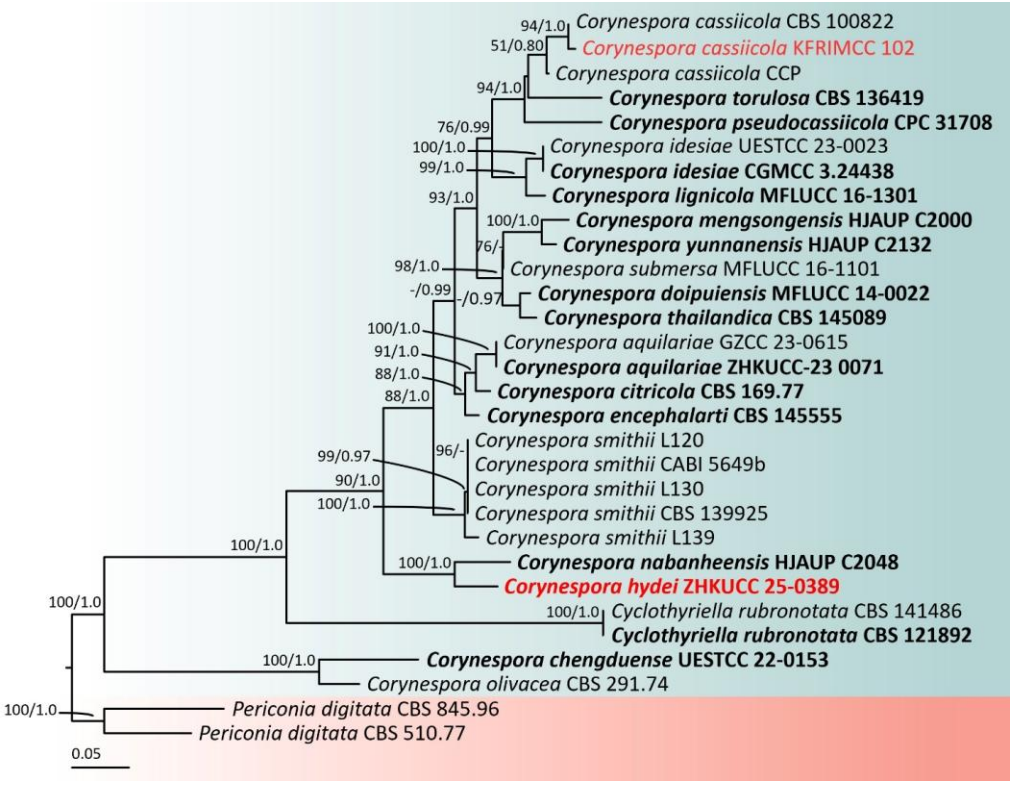


Figure 12 – Phylogram generated from maximum likelihood analysis based on combined LSU, ITS, SSU, *rpb2*, and *tef1-α* sequence data from 30 taxa, comprising 4,031 characters (LSU = 832, ITS = 522, SSU = 1,012, *rpb2* = 926, *tef1-α* = 735). The best-scoring RAxML tree with a final likelihood value of -14273.616 is presented. The matrix contained 897 distinct alignment patterns, with 36.98% of the characters being undetermined or gaps. Estimated base frequencies were as follows: A = 0.244, C = 0.254, G = 0.275, T = 0.226; substitution rates: AC = 2.393, AG = 3.199, AT = 1.680, CG = 1.453, CT = 9.353, GT = 1.0; gamma distribution shape parameter α = 0.147. Bootstrap support values for maximum likelihood (ML) equal to or greater than 70% and clade

credibility values greater than 0.90 (rounded to two decimal places) from Bayesian inference analysis are labeled at each node. Ex-type strains are in bold, while new isolates are indicated in red. The tree is rooted to *Periconia digitata* (CBS 510.77 and CBS 845.96).

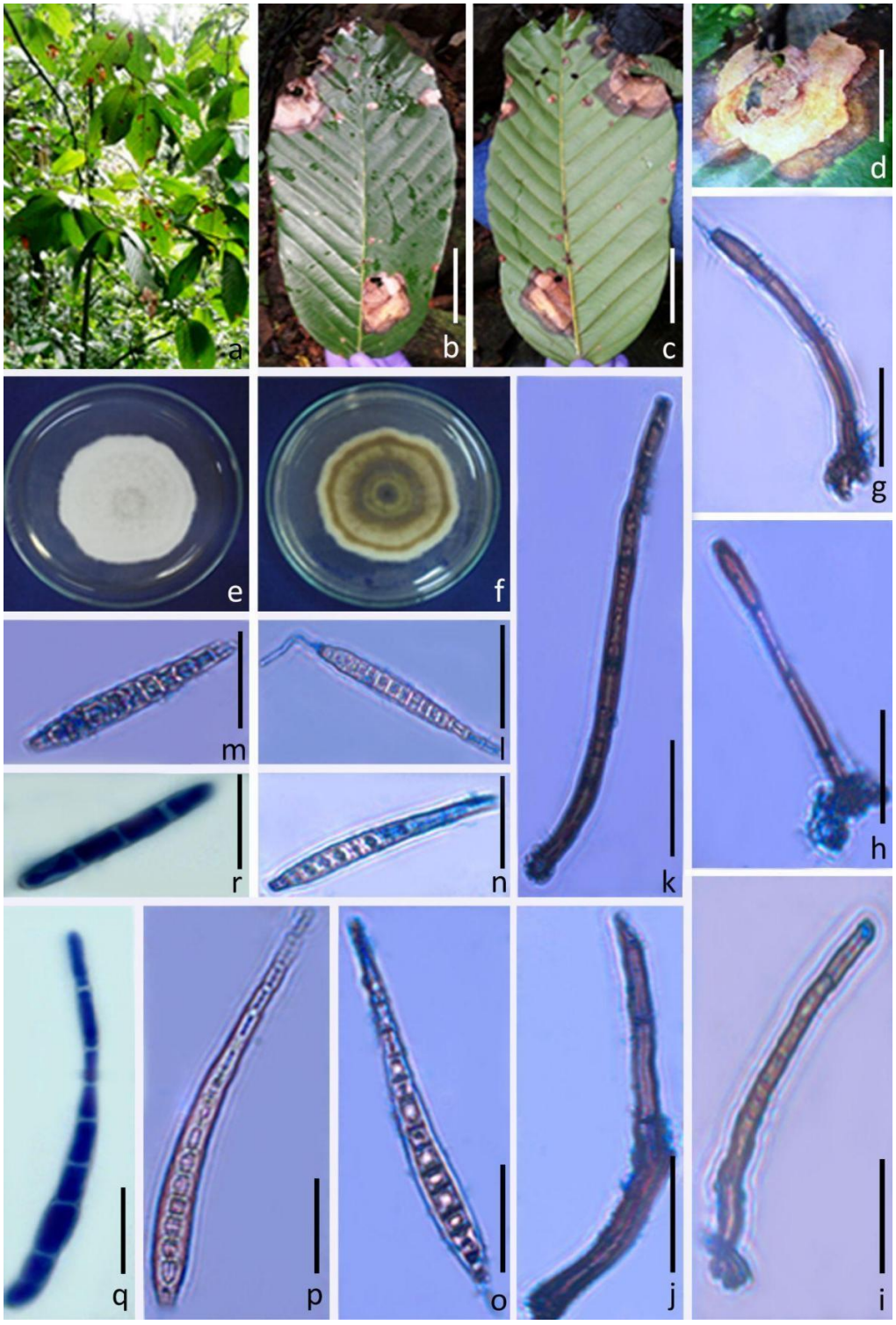


Figure 13 – *Corynespora cassiicola* (KFRIMH 102, new host record). a Host plant habitat b Upper surface of infected leaf. c Lower surface of infected leaf. d Enlarged view of symptom. e, f Front and reverse view of fungus colony on PDA. g–i Conidiophores on host. k, l Conidiophores on culture. l–p Conidia on host. q–r Conidia on culture. Scale bars: c = 20 mm, f–g = 20 µm.

Corynespora hydei C.F. Liao & Doilom, sp. nov. Fig. 14

Index Fungorum number: IF903705; Facesoffungi number: FoF17750

Etymology – 'hydei' named in honor of the renowned mycologist Kevin D. Hyde, recognizing his significant contributions to mycology on the occasion of his 70th birthday.

Holotype – MHZU 25–1051

Saprobic on decaying wood of unidentified host. Sexual morph: Undetermined. Asexual morph: *Conidiophores* 410–775 × 15–23 μm ($\overline{x}$ = 605 × 18 μm, n = 20), macronematous, mononematous, solitary or gregarious, cylindrical, straight to flexuous, unbranched, brown to black, 6–13-septate, smooth-walled. *Conidiogenous cells* monotretic, integrated, terminal, cylindrical, pale brown, smooth-walled, inconspicuous. *Conidia* 125–243 × 19–35 μm ($\overline{x}$ = 185 × 27 μm, n = 30), acrogenous, straight or slightly flexuous, obclavate to rostrate, pale brown to blackish brown, tapering towards the apex, sometimes swollen in lower portion, 12–22-distoseptate, rounded at tip, truncate at the base, with 2–4 protuberant dark brown hilum, thick-walled, verruculose.

Culture characteristics – Colonies on PDA reaching 2.6–3 cm diam., after 1 month at 25 °C, circular, flat, filiform, black-brown from above and reverse, no pigmentation.

Material examined – China, Yunnan Province, Baoshan City, Shidian County, on decaying wood, 29 July 2022, CF Liao, YN04 (MHZU 25–1051, holotype), ex-type ZHKUCC 25–0389.

GenBank numbers – ITS = PV446209, LSU = PV446210, SSU = PV573999.

Notes – In the phylogenetic analysis, our strain formed a distinct branch with the type strain of *Corynespora nabanheensis* (HJAUP C2048), supported by 100% ML and 1.00 BYPP bootstrap values (Fig. 12). Morphologically, our collection differs from *C. nabanheensis* in having 6–13-septate and simple conidiophores with inconspicuous conidiogenous cells, and 12–22-distoseptate conidia that are rounded at the tip, truncate at the base, with 2–4 protuberant dark brown hila. In contrast, *C. nabanheensis* has 10–17-septate conidiophores bearing 3–4 successive cylindrical extensions, conspicuous cylindrical conidiogenous cells, and 9–13-distoseptate conidia that are typically expanded into a rounded apex, 4–6 μm near the apex and truncated at the base, with a single protuberant dark brown hilum. Conidia of *C. hydei* are pale brown to blackish brown and verruculose, whereas those of *C. nabanheensis* are brown to golden brown and smooth-walled (Liu et al. 2023a). In addition, our collection can be distinguished from *C. nabanheensis* by its longer conidiophores (410–775 × 15–23 μm vs. 282–528 × 6–8 μm) and larger conidia (125–243 × 19–35 μm vs. 56–84 × 12–14 μm). A comparison of the ITS, LSU, and SSU sequences between our strain (ZHKUCC 25–0389) and the ex-type strain of *C. nabanheensis* (HJAUP C2048) revealed nucleotide differences of 2.36% (13/552 bp), 2.00% (11/549 bp), and 1.48% (15/1008 bp), respectively. Based on these morphological and phylogenetic differences, we identify *C. hydei* as a novel species.

Hermatomycetaceae Locq. ex A. Hashim. & Kaz. Tanaka, Persoonia 39: 56 (2017).

Hermatomyces Speg., Anal. Mus. nac. B. Aires, Ser. 3 13: 445 (1910).

Index Fungorum number: IF8517; Facesoffungi number: FoF08252

Hermatomyces was introduced in 1910, with *H. tucumanensis* as the type species (Spegazzini 1910). The prominent characteristics of *Hermatomyces* are lenticular to cylindrical, muriform conidia, often with subhyaline to pale brown peripheral cells, and dark brown central cells. Conidia are cylindrical and comprise 1–4 columns with 2–11 cells and are irregularly pigmented (Tibpromma et al. 2016, Doilom et al. 2017, Hashimoto et al. 2017, Koukol et al. 2018, Ren et al. 2021). *Hermatomyces* are widely distributed and have been reported from both temperate and tropical regions, mainly from Thailand (Doilom et al. 2017, Tibpromma et al. 2016, Hashimoto et al. 2017, Koukol et al. 2018, Boonmee et al. 2021, Ren et al. 2021, de Silva et al. 2022, Shen et al. 2023).

Prof. Kevin D. Hyde's contributions to the study of *Hermatomyces* have been pivotal by discovering numerous new species within this genus. Currently, Index Fungorum (2025) and MycoBank (2025) list 37 taxa under *Hermatomyces*. Prof. Kevin D. Hyde and his collaborators have introduced 19 species. In recognition of Prof. Kevin D. Hyde's outstanding contributions to

mycology, we herein present a new host record of *Hermatomyces indicus*. We also provide an updated phylogenetic tree for *Hermatomyces* (Fig. 15).



Figure 14 – *Corynespora hydei* (MHZU 25–1051, holotype). a–c Appearance of conidiophores and conidia on woody substrate. d–f Conidiophores. g–k Conidia. l Germinated conidium. m Colony on PDA (front and below). Scale bars: d–f = 100 µm, g–i = 20 µm, j–l = 50 µm.

Hermatomyces indicus Prasher & Sushma, Nova Hedwigia 94(3–4): 552 (2014) Fig. 16

Index Fungorum number: IF805645; Facesoffungi number: FoF01851

Synonym – *Hermatomyces thailandicus* Doilom et al. (2017).

Saprobic on dead wood. Sexual morph: Undetermined. Asexual morph: Colonies on natural substrate formed a dull zone, superficial, scattered to gregarious, conspicuous, glistening, brown to black. *Conidiophores* 2.0–4.0 µm in width, mononematous, cylindrical, erect, short, subhyaline or pale brown, unbranched, smooth, closely packed together, sometimes reduced to conidiogenous cells, thick-walled. *Conidiogenous cells* 4–6 × 3–5 µm monoblastic, terminal, integrated, short, determinate, often arising directly on the superficial mycelium. *Conidia* dimorphic: turbinate and lenticular. *Turbinate conidia* 22.5–38 × 11–23 µm ($\overline{x}$ = 32.9 × 18.0 µm, n = 20) composed of 3–6 cells arranged in 1 or 2 rows, grey-brown on the upper side, becoming hyaline towards the lower side. *Lenticular conidia* 28.5–37×18–26 µm ($\overline{x}$ = 33 × 21.9 µm, n = 30), solitary, elliptical to almost round in one plane, comprising dark-brown cells in the center, subhyaline to pale brown in peripheral cells.

Culture characteristics – Conidia germinated within 8 hours in PDA; colonies grew rapidly reaching around 20–30 mm within 30 days at 25 °C in the dark. Obverse: colonies circular, centrally raised, floccose, coloration from hyaline turn to grey with maturity, smoke grey at the center, light-grey at the margin, clearly visible sparse mycelium extended. Reverse: black-brown in

the middle area, brown to grey olivaceous near the margin, visible extended mycelium, without pigments produced in PDA.

Material examined – China, Guangdong Province, Guangzhou City, 23°5'44" N 113°16'39" E, on dead wood, October 2022, H. Li (MHZU 24–1191), living culture ZHKUCC 24–1820 and ZHKUCC 24–1821.

GenBank numbers – ZHKUCC 24–1820: ITS = PV446095, LSU = PV446097, SSU = PV446093, *tef1-α* = PV492568, *rpb2* = PV492566; ZHKUCC 24–1821: ITS = PV446096, LSU = PV446098, SSU = PV446094, *tef1-α* = PV492569, *rpb2* = PV492567.

Notes – In the phylogenetic analysis of *Hermatomyces* (Fig. 15), the new collections (ZHKUCC 24–1820 and 24–1821) clustered with *Hermatomyces indicus*. Morphologically, our collection is similar to *H. indicus* by turbinate conidia (22.4–35.4 × 11.4–21.6 µm vs. 22.5–38 × 11–23 µm), and lenticular conidia, which are solitary, elliptical to almost round in one plane, smooth, muriform, and with pale peripheral cells surrounding central dark brown to black cells (Prasher et al. 2014). In addition, base pair differences in ITS, SSU, *tef1-α,* and *rpb2* of our new isolates and *H. indicus* (MFLUCC 14–1143) were compared without gaps. They were 0.4% (2/484 bp) in the ITS locus, 0.3% (3/1001 bp) in the SSU locus, 0.4% (4/918 bp) in the *tef1-α* locus, and 0.1% (1/878 bp) in the *rpb2* locus. *Hermatomyces indicus* has been previously reported from *Phoenix rupicola* from India (Tibpromma et al. 2016) and *Tectona grandis* from Thailand (Hyde et al. 2018). In the study, we were unable to identify the host species. Based on phylogenetic analysis and available data, we introduce our new collection as *H. indicus*, which is reported for the first time in China.

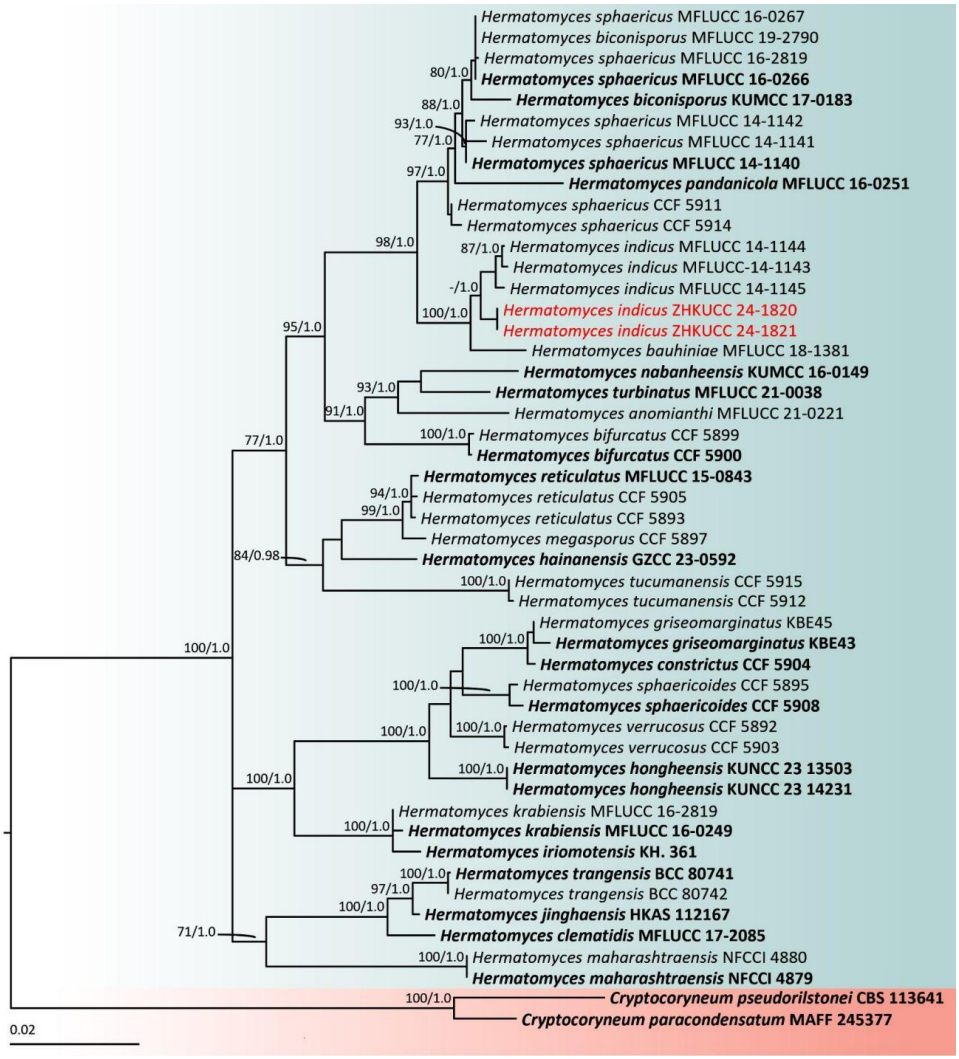


Figure 15 – Phylogram generated from maximum likelihood analysis based on the combined LSU, ITS, SSU, *tef1-α*, and *rpb2* sequence dataset representing *Hermatomyces*. Fifty strains are included in the combined analyses, comprising 4,341 characters including gaps (LSU = 824, ITS = 546, SSU = 1,049, *tef1-α* = 1,003, *rpb2* = 919). The best-scoring RAxML tree with a final likelihood value of -15234.798 is presented. The matrix had 1,053 distinct alignment patterns, with 30.32% of the characters being undetermined or gaps. Estimated base frequencies were as follows: A = 0.248, C = 0.256, G = 0.262, T = 0.234; substitution rates AC = 1.311, AG = 4.919, AT = 1.412, CG = 1.008, CT = 12.283, GT = 1.0; gamma distribution shape parameter α = 0.721. Bayesian posterior probabilities (BYPP) from MCMC were evaluated, yielding a final average standard deviation of split frequencies of less than 0.01. Bootstrap support values for maximum likelihood (ML) greater than 70% and Bayesian posterior probabilities (BYPP) greater than 0.95 are defined above the nodes as ML/BYPP. Ex-type strains are in bold, while new isolates are indicated in red. The tree is rooted to *Cryptocoryneum paracondensatum* (MAFF 245377) and *C. pseudorilstonei* (CBS 113641).

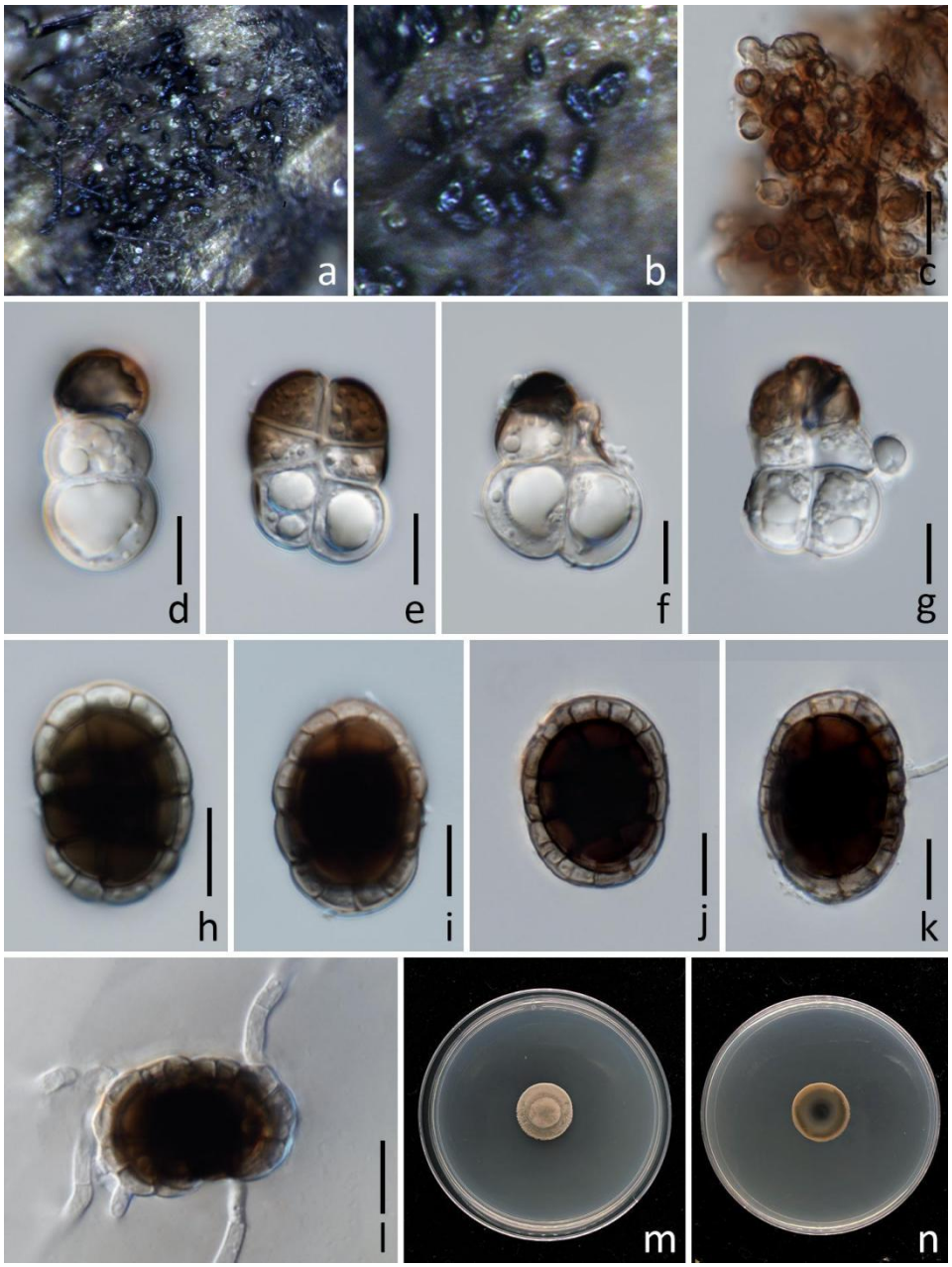


Figure 16 – *Hermatomyces indicus* (MHZU 24–1191, new geographical record). a, b Colonies on the natural substrate. c Conidiogenous cell. d–j Conidiophores, conidiogenous cells and conidia.

h–k Conidia. l Germinated conidium. m, n Colony on PDA (front and below). Scale bars: c–l = 10 μm.

Massarinaceae **Munk**

Heterohelminthosporium Khuna, Hongsanan & Xie N., gen. nov.

Index Fungorum number: IF903729; Facesoffungi number: FoF17751

Etymology – Refers to the new genus's similarity to *Helminthosporium*.

Type species – *Heterohelminthosporium hydei* Khuna, Hongsanan & Xie N

Endophytic in leaves of *Pandanus tectorius* (*Pandanaceae*). *Mycelia* superficial and immersed, composed of septate, branched, hyaline, with smooth and thick-walled hyphae. Sexual morph: *Ascomata* brown to black, semi-immersed to superficial, covered with mycelia, globose to subglobose, irregular, solitary or aggregated. *Peridium* thin-walled, 6–7-layered, composed of light brown compressed cells of *textura angularis*, cells towards inside lighter and somewhat flattened, at the outside, darker, fusing and indistinguishable from the host tissues. *Asci* 8-spored bitunicate, fissitunicate, cylindrical-clavate, apically rounded, slightly curved, sessile. *Ascospores* uniseriate or biseriate, hyaline when immature, pale brown to brown when mature, fusoid with rounded ends, tapering towards both ends, asymmetrical, straight or slightly curved, with 1 eccentric primary septum and often with 2-eusepta, constricted at the primary septum, slightly constricted at eusepta, smooth-walled with guttules, without mucilaginous sheath or appendages. Asexual morph: Undetermined.

Notes – The phylogenetic analysis based on a multi-locus dataset (SSU, LSU, ITS, *tef1-α*, and *rpb2*, Fig. 17) indicated that our collections (MBSZU 25–015 and MBSZU 25–016) formed an independent lineage within *Massarinaceae* sister to the genus *Massarina* (*M. tangneyae* and *M. pandanicola*) with high statistical support (Fig. 17). Morphologically, our collection can be distinguished from *Massarina* species in having pale brown to brown, fusoid, 1-sepate ascospores without mucilaginous sheath whereas *Massarina* has hyaline, broadly fusiform, multi-septate ascospores with mucilaginous sheath or appendages (Aptroot 1998, Hyde & Aptroot 1998, Tanaka & Harada 2003, Zhang et al. 2009, Hongsanan et al. 2020a). In addition, our collection shares similarities with *Helminthosporium* by pale brown, asymmetrical ascospores (Voglmayr & Jaklitsch 2017). However, *Helminthosporium* differs from our collection in having few to numerous ring-like thickenings of the inner wall, which gives the inner wall an irregularly wavy outline (Voglmayr & Jaklitsch 2017). Therefore, we identify our collection as a novel genus within *Massarinaceae*, based on both morphological and phylogenetic evidence. However, additional taxon sampling is essentially required to resolve the phylogenetic affinities of *Massarina*, *Helminthosporium*, and *Heterohelminthosporium*.

Heterohelminthosporium hydei Khuna, Hongsanan & Xie N., sp. nov. Fig. 18

Index Fungorum number: IF903730; Facesoffungi number: FoF17752

Etymology – 'hydei' named in honor of the renowned mycologist Kevin D. Hyde, recognizing his significant contributions to mycology on the occasion of his 70th birthday.

Ex-type – MBSZU 25–015

Endophytic in leaves of *Pandanus tectorius* (*Pandanaceae*). Sexual morph: *Ascomata* 125–1455 × 105–1112 μm ($\overline{x}$ = 508 × 382 μm, n = 50), brown to black, semi-immersed to superficial, covered with mycelia, globose to subglobose, irregular, solitary or aggregated. *Peridium* 17–31 μm wide, thin-walled, 6–7-layered, composed of light brown compressed cells of *textura angularis*, cells towards the inside lighter and somewhat flattened, at the outside, darker, fusing and indistinguishable from the host tissues. *Asci* 74–170 × 9–26 μm ($\overline{x}$ = 105 × 19 μm, n = 15), 8-spored, bitunicate, fissitunicate, cylindrical-clavate, apically rounded, slightly curved, sessile. *Ascospores* 21–35 × 7–11 μm ($\overline{x}$ = 25 × 8 μm, n = 50), uniseriate or biseriate, hyaline when immature, pale brown to brown when mature, fusoid with rounded ends, tapering towards both ends, asymmetrical, straight or slightly curved, with 1 eccentric primary septum and often with

2-eusepta, constricted at the primary septum, slightly constricted at eusepta, smooth-walled with guttules, without mucilaginous sheath or appendages. Asexual morph: Undetermined.

Culture characteristics – Colonies on PDA and MEA were described at 25 °C after 14 days of incubation. Colonies on PDA were 60–65 mm diam., circular, flat, margin entire to slightly undulate, white to yellow-white; reverse yellow in the center, yellow-white at the margin. Colonies on MEA grew to 46–50 mm diam., thin, flat, margin entire, brownish-white; reverse brown in the center, brownish-white at the margin. *Mycelia* superficial and immersed, composed of septate, branched, 1.5–5.4 µm wide, hyaline, with smooth and thick-walled hyphae.

Material examined – China, Guangdong Province, Huizhou City, Huidong County, Pinghaizhen, 22°37'31.4" N, 114°55'01.4" E, endophytes live within plant tissues of screw pine (*Pandanus tectorius*, *Pandanaceae*), Khuna S., 22 September 2024, ex-type MBSZU 25–015; *ibid*., living culture MBSZU 25–016.

GenBank numbers – MBSZU 25–015: SSU = PV017681, ITS = PV017664, LSU = PV017679, *tef1-α* = PV029251, *rpb2* = PV029252; MBSZU 25–016: SSU = PV017682, ITS = PV017665, LSU = PV017680, *tef1-α* = PV029253, *rpb2* = PV029254.

Notes – According to the multi-gene phylogeny, *Heterohelminthosporium hydei* (MBSZU 25–015 and MBSZU 25–016) clusters with *Massarina tangneyae* (BRlP 72527f) and *M. pandanicola* (MFLUCC 17–0596). The base-pair differences in LSU and ITS between the type strain of *M. tangneyae* (BRlP 72527f) and *H. hydei* are 2.37 and 8.82 % (20/843 and 48/544 bp including gaps), respectively. In addition, the base-pair differences between SSU, LSU, ITS, and *tef1-α* of the type strain of *M. pandanicola* (MFLUCC 17–0596) and *H. hydei* are 1.05%, 3.57%, 13.68%, and 8.96% (10/950, 30/840, 52/380, and 75/837 bp including gaps), respectively. However, we were unable to compare the morphological characteristics with those of *M. tangneyae* and *M. pandanicola* due to a lack of detailed descriptions of sexual morphological characteristics (Tibpromma et al. 2018b, Tan & Shivas 2022a). The morphological similarities and differences between *Heterohelminthosporium*, *Massarina*, and *Helminthosporium* have been mentioned in the above generic description. Our collection is introduced as a novel species in the newly proposed genus, *Heterohelminthosporium*. However, future collections with asexual morphologies are essentially required to resolve the morphological and phylogenetic affinities between *Heterohelminthosporium* and *Massarina* species.

Periconiaceae Nann

Periconia Tode, Fung. mecklenb. sel. (Lüneburg) 2: 2 (1791)

Index Fungorum number: IF9263; Facesoffungi number: FoF06658

Periconia was introduced by Tode (1791) with *P. lichenoides* as the type species. Initially, *Periconia* was classified under *Massarinaceae* (Hyde et al. 2013). Later, based on phylogenetic analysis using SSU, LSU, and *tef1-α* sequence data, Tanaka et al. (2015) reclassified *Periconia* within *Periconiaceae*. This genus has 234 epithets listed in Index Fungorum (accessed February 19, 2025). However, most of these species lack morphological and sequence data (Tennakoon et al. 2021). Most *Periconia* species have been reported based solely on asexual morphs; however, six species have been reported based on their sexual morphs, namely *P. didymosporum*, *P. homothallica*, *P. igniaria*, *P. prolifica*, *P. pseudodigitata*, and *P. wurfbainiae* (Tanaka et al. 2015, Liao et al. 2024). The asexual morph is characterized by brown, branched, or unbranched conidiophores, conidial heads are brown, ovoid to clavate or spherical, conidiogenous cells are intercalary or terminal and catenate or solitary, golden brown to dark brown, globose to subglobose, smooth or verruculose conidia (Tanaka et al. 2015, Liu et al. 2017b, Markovskaja & Kačergius 2014, Calvillo-Medina et al. 2020, Hongsanan et al. 2020b). The sexual morph is characterized by immersed or erumpent, globose to subglobose, ostiolate ascomata, asci are 8-spored, bitunicate, cylindrical, and ascospores are guttulate, smooth-walled, and with an entire sheath (Yang et al. 2022, Su et al. 2023, Liao et al. 2024). *Periconia* species are typically reported as saprobes, endophytes, and pathogens in terrestrial habitats and are rarely found in aquatic and marine environments; some species can even infect humans (Goga 2000, Teles et al. 2006,

Phookamsak et al. 2019, Gunasekaran et al. 2021). For instance, *P. endophytica* was isolated from the healthy medicinal plant, *Wurfbainia villosa* (Liao et al. 2024); *P. circinate* and *P. igniaria* were reported to cause blackening, rotting of wheat roots, leaf spots, and leaf necrosis (Goga 2000, Kolomiets et al. 2008, Sarkar et al. 2019). Additionally, *Periconia* species play a significant role in producing economically important bioactive compounds. There are more than 100 compounds that have been isolated from *Periconia* species, including aromatic compounds, carbohydrate derivatives, cytochalasans, macrolides, macropshelides, meroterpenes, polyketides, and terpenoids (Teles et al. 2006, Azhari & Supratman 2021, Wu et al. 2015).

Of the 234 species currently listed in Index Fungorum, Prof. Kevin D. Hyde and his collaborators have introduced 18 species. In recognition of his outstanding contributions to mycology, herein we introduce *Periconia hydei*, which has been named in honor of Prof. Kevin D. Hyde. We also provide an updated phylogenetic tree for *Periconia* (Fig. 19). *Periconia hydei*, as a single species, receives strong support. In this genus, habitats (aquatic vs. terrestrial) and morphology exhibit considerable diversity. Therefore, further collections from various habitats are required to address these discrepancies.

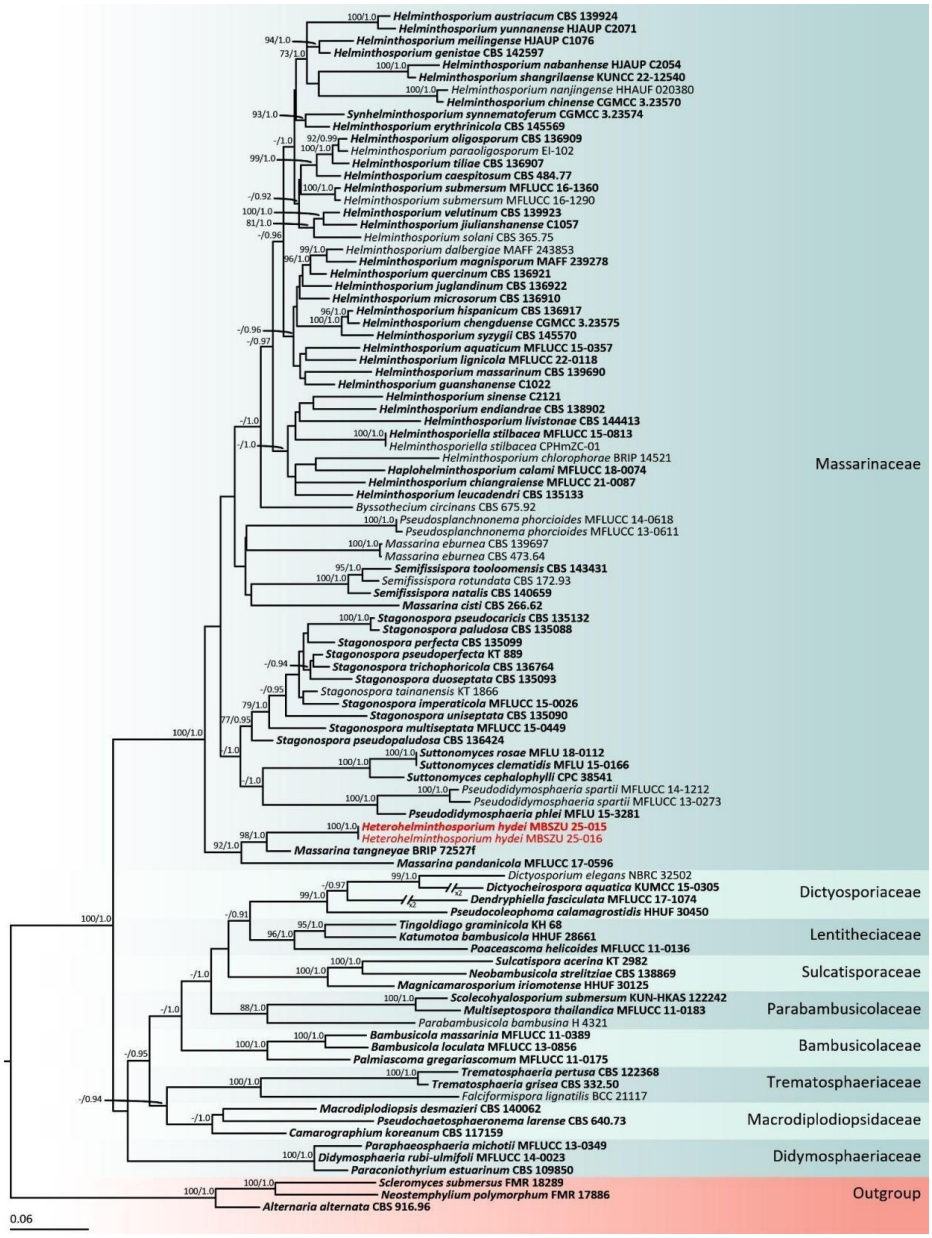


Figure 17 – Phylogram generated from maximum likelihood analysis based on combined SSU, LSU, ITS, *tef1-α*, and *rpb2* sequence data from 98 taxa, comprising 4,733 characters (SSU = 981,

LSU = 895, ITS = 799, *tef1-α* = 930, *rpb2* = 1,128). The best-scoring RAxML tree with a final likelihood value of -47552.061 is presented. The matrix contained 2,372 distinct alignment patterns, with 30.88% of the characters being undetermined or gaps. Estimated base frequencies were as follows: A = 0.241, C = 0.250, G = 0.271, T = 0.238; substitution rates: AC = 1.669, AG = 3.965, AT = 1.713, CG = 1.015, CT = 7.828, GT = 1.0; gamma distribution shape parameter α = 0.590. Bootstrap support values for maximum likelihood (ML) equal to or greater than 70% and clade credibility values greater than 0.90 (rounded to two decimal places) from Bayesian inference analysis are labeled at each node. Ex-type strains are in bold, while the new isolates are indicated in red. The tree is rooted to *Alternaria alternata* (CBS 916.96), *Neostemphylium polymorphum* (FMR 17886), and *Scleromyces submersus* (FMR 18289).

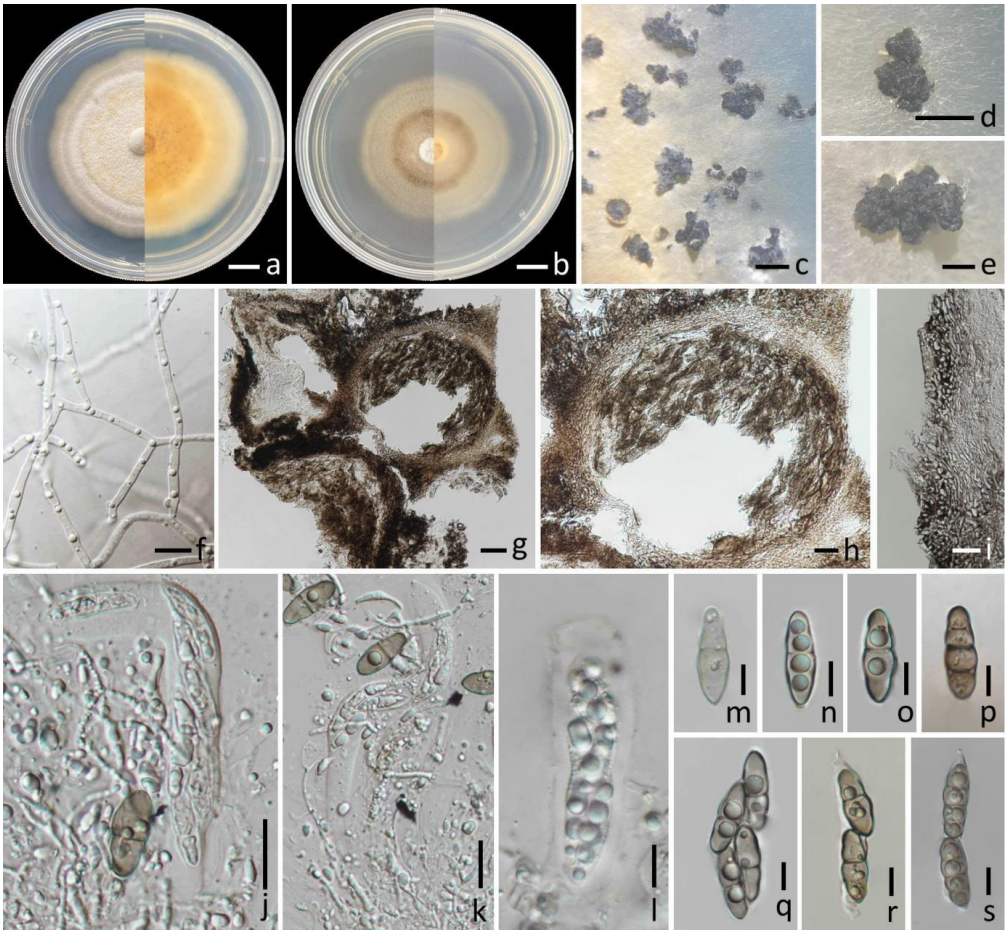


Figure 18 – *Heterohelminthosporium hydei* (MBSZU 25–015, ex-type). Colonies incubated at 25 °C for two weeks. a PDA. b MEA (left, surface view and right, reverse). c–e Ascomata forming on PDA after incubation at 25 °C for two months. f Mycelium masses. g, h Vertical cross-sections of ascomata. i Peridium. j–l Asci. m–s Ascospore. Scale bars: a, b = 10 mm, c = 2 mm, d, e = 1 mm, f, m–s = 10 µm, g–l = 20 µm.

Periconia hydei Y. H. Yang & Manawasinghe, sp. nov. Fig. 20

Index Fungorum number: IF903704; Facesoffungi number: FoF17753

Etymology – 'hydei' named in honor of the renowned mycologist Kevin D. Hyde, recognizing his significant contributions to mycology on the occasion of his 70th birthday.

Holotype – ZHKU 25–0442

Saprobic on dried twigs of *Stipa capillata*. Sexual morph: undetermined. Asexual morph: Colonies superficial on the host substrate, hairy, gregarious, brown to dark brown. *Setae* 1,260–1,580 µm wide ($\bar{x}$ = 1,420 µm, n = 10), erect, acicular, tapering towards the apex, slightly wider at the basal, unbranched, brown to dark brown, septate, smooth, straight or slightly flexuous.

Conidiophores 85–170 × 5–7 µm ($\bar{x}$ = 130 × 6 µm, n = 13), filiform, flexuous or straight, usually with one or a number of short branches at the apex, sparsely septate, shorter than setae, erect, slightly constricted at septa, rough-walled, verruculose, thin-walled, pale brown to brown. *Conidiogenous cells* 9–20 × 4–7 µm ($\bar{x}$ = 15 × 5 µm, n = 13), terminal, holoblastic, mono- and poly-blastic, integrated, long cylindrical or obovoid, obtuse or truncate at apical, pale brown to yellowish brown, verruculose. *Conidia* 6–9 × 5–8 µm ($\bar{x}$ = 8 × 7 µm, n = 28), globose to subglobose, solitary, aseptate, pale brown to dark brown, thin-walled, slightly verruculose.

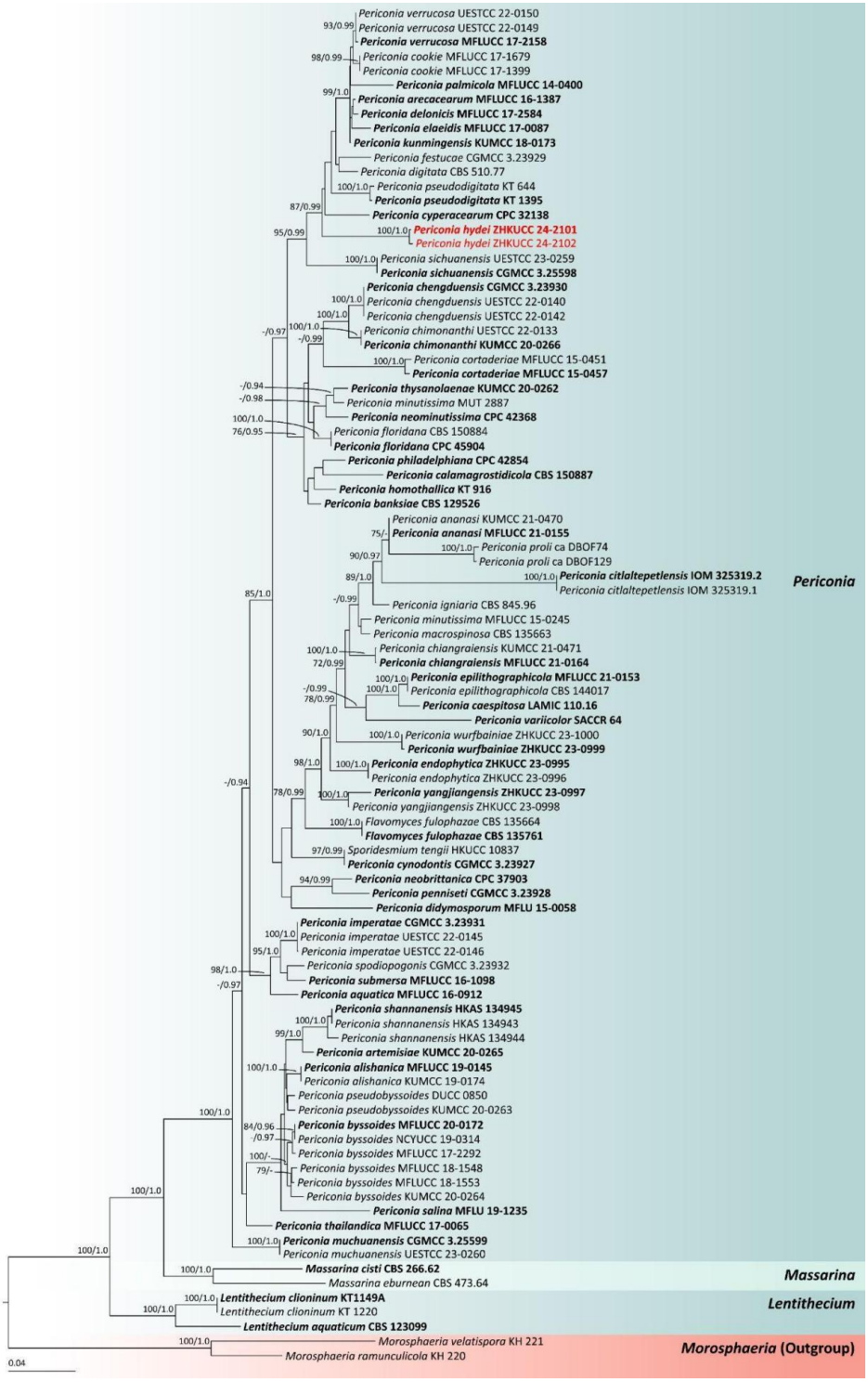


Figure 19 – Phylogram generated from maximum likelihood analysis based on combined ITS and LSU sequence data from 86 taxa, comprising 3,449 characters (ITS, LSU, SSU, and *tef1-α*). The best-scoring RAxML tree with a final likelihood value of -21023.370 is presented. The matrix

contained 330 distinct alignment patterns, with 16% of the characters being undetermined or gaps. Estimated base frequencies were as follows: A = 0.237, C = 0.256, G = 0.268, T = 0.238; substitution rates: AC = 1.692, AG = 2.677, AT = 1.777, CG = 1.199, CT = 10.523, GT = 1.0; gamma distribution shape parameter α = 0.208. Bootstrap support values for maximum likelihood (ML) equal to or greater than 70% and clade credibility values greater than 0.90 (rounded to two decimal places) from Bayesian inference analysis are labelled at each node. Ex-type strains are in bold, while the new isolates are indicated in red. The tree is rooted in *Morosphaeria velatispora* (KH 221) and *M. ramunculicola* (KH 220).

Material examined – China, Yunnan Province, Yuanmou City, Wumao Town, on submerged decaying twigs of *Stipa capillata*, 19 January 2023, YH Yang, MC03 (ZHKU 25–0442, holotype), ex-type ZHKUCC 24–2101; *ibid*., living culture ZHKUCC 24–2102.

GenBank numbers – ZHKUCC 24–2101: ITS = PV434171, LSU = PV436640, SSU = PV437586, *tef1-α* = PV588047; ZHKUCC 24–2102: ITS = PV434172, LSU = PV436641, SSU = PV437587, *tef1-α* = PV588048.

Notes – In phylogenetic analyses based on SSU, ITS, LSU and *tef1-α* sequence data, our collection formed a distinct lineage and clustered with other *Periconia* species with 87% ML and 0.99 BYPP (Fig. 19). Morphologically, our collection (ZHKUCC 24–210 and ZHKUCC 24–2102) resembles typical characteristics of *Periconia* species. Among them, some characteristics resemble those of *P. sichuanensis*, such as conidiogenous cells or several short branches at the apex (Yu et al. 2024). However, *P. hydei* has setae that are pale brown to brown, conidiogenous, and a wall with verrucula. Conidiogenous cells are long, cylindrical or obovoid, pale brown to yellowish brown, with verruculose walls, and solitary and larger conidia (4.5–5.5 µm vs. 8 × 7 µm) can be distinguished from *P. sichuanensis*. In comparison with the morphology of closely related species in our collection, we observe that *P. sichuanensis* has one or several short conidiogenous branches at the apex (Yu et al. 2024), unlike those found in our collection. In addition, *P. hydei* differs from *P. cyperacearum* and *P. pseudodigitata* by having acicular setae, conidiophores are shorter (130 vs. 150–350 µm vs. 250–450 µm), filiform, one or several short branches near the apex, conidiogenous cells are long, cylindrical, or obovoid, and conidia are solitary (Tanaka et al. 2015, Crous et al. 2018). Although the morphological characteristics of *P. hydei* differ from those of most saprobic *Periconia* species, it shares similarities with *P. endophytica* in terms of conidiogenous and conidiogenous cell morphology. *Periconia endophytica* was isolated from healthy plant tissue as an endophyte (Liao et al. 2024); however, these two species are placed in distinct clusters within the *Periconia* phylogenetic tree. In addition, we compared the base-pair differences between our new collection and the extype strains of *P. cyperacearum* (CPC 32138) and *P. pseudodigitata* (KT1395). The results showed that, in comparison with *P. cyperacearum* (CPC 32138), the ITS locus had 13% differences (71/545 bp, 19 gaps), LSU locus 5.7% (51/891 bp, 8 gaps), SSU locus 1% (11/1038 bp, 3 gaps), and *tef1-α* locus 3.3% (28/851 bp, no gaps). When compared with *P. pseudodigitata* (KT1395), the ITS locus showed 18.5% differences (109/588 bp, 38 gaps), LSU locus 4.6% (40/868 bp, 6 gaps), SSU locus 0.8% (8/1027 bp, 1 gaps), and *tef1-α* locus 3.79% (32/854 bp, no gaps). Based on morphological and phylogenetic evidence, we introduce *P. hydei* as a new species collected from Yunnan Province.

Phaeoseptaceae S. Boonmee, Thambugala & K.D. Hyde

Phaeoseptum Ying Zhang, J. Fourn. & K.D. Hyde, in Zhang, Fournier, Phookamsak, Bahkali & Hyde, Mycologia 105(3): 606 (2013)

Index Fungorum number: IF561890; Facesoffungi number: FoF08326

Phaeoseptum was introduced by Zhang et al. (2013) with *P. aquaticum* as the type species. The genus currently comprises eight species (Index Fungorum 2025). Species of this genus are generally found as saprobes in freshwater and terrestrial habitats, indicating a diverse range of environments (Phukhamsakda et al. 2019, Hongsanan et al. 2020b, Wanasinghe et al. 2020, Jayawardena et al. 2023, Zhang et al. 2024b). *Phaeoseptum* is characterized by immersed ascomata

with bitunicate, 8-spored asci and fusiform, slightly curved ascospores (Zhang et al. 2013). The asexual morph of *Phaeoseptum* has not been reported. To better understand the relationships between their asexual and sexual forms, as well as their host associations and habitats, further collections from various ecosystems are necessary.

Prof. Kevin D. Hyde has played a crucial role in advancing the knowledge of *Phaeoseptum*. His ongoing research has significantly enhanced our understanding of *Phaeoseptum* and has been instrumental in identifying new *Phaeoseptum* species. Prof. Kevin D. Hyde and collaborators have introduced four species from various substrates and habitats (Phukhamsakda et al. 2019, Hongsanan et al. 2020b, Wanasinghe et al. 2020, Jayawardena et al. 2023, Zhang et al. 2024b). Among these, *P. hydei* was introduced as a new terrestrial ascomycete by Wanasinghe et al. (2020). In recognition of his outstanding contributions to mycology, herein we introduce *Phaeoseptum kunmingensis* in honor of Prof. Kevin D. Hyde. We also provide an updated phylogenetic tree for *Phaeoseptum* (Fig. 21).

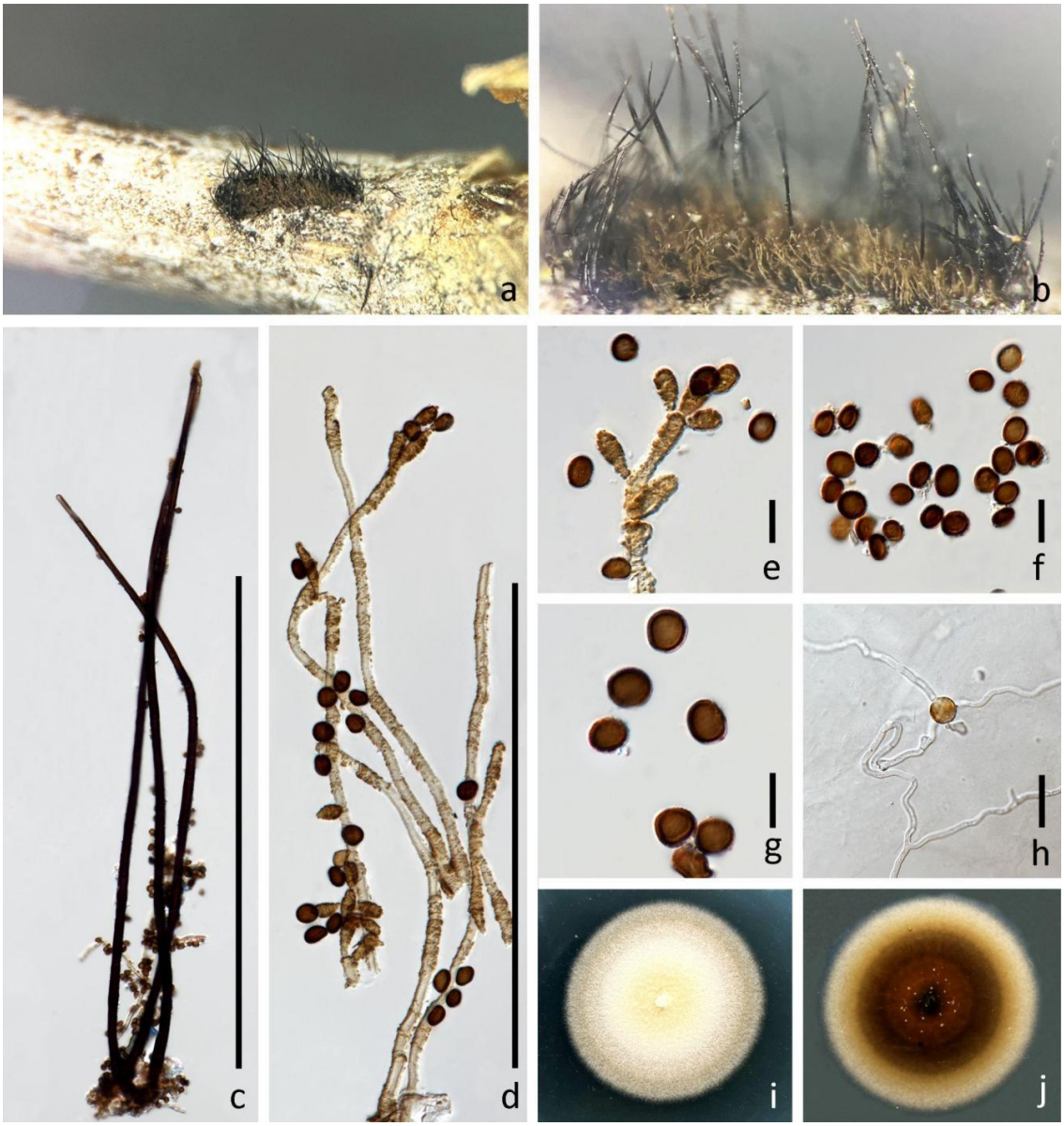


Figure 20 – *Periconia hydei* (ZHKU 25-0442, holotype). a, b Colonies on the host substrate. c Setae. d Conidiophores with conidia. e Conidiogenous cell with conidia. f, g Conidia. h Germinated conidium. i Surface view of colony on PDA. j Reverse view of colony on PDA. Scale bars: c = 1 mm, d = 100 µm, e–g = 10 µm, h = 20 µm.

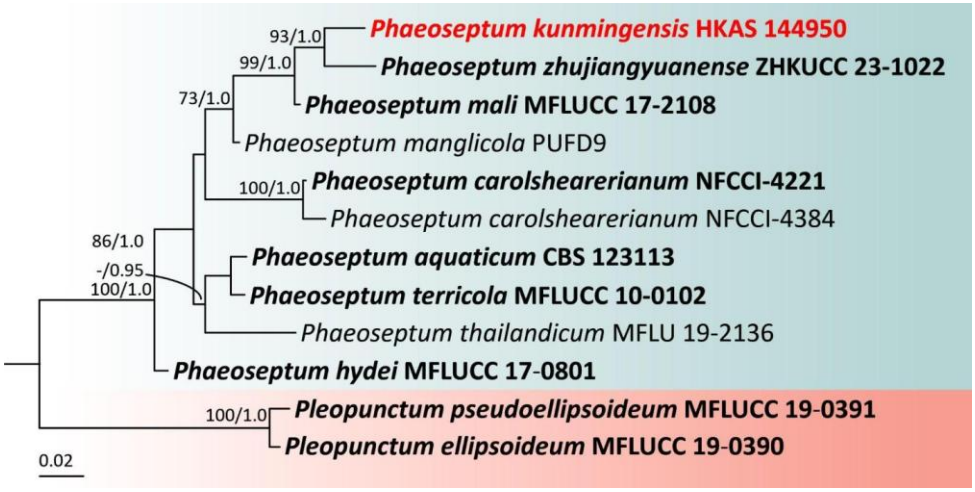


Figure 21 – Phylogram generated from maximum likelihood analysis based on combined ITS, LSU, SSU, and *tef1-α* sequence data from 12 taxa, comprising 3,805 characters after alignment (ITS = 885, LSU = 965, SSU = 1,013, *tef1-α* = 942). The best-scoring RAxML tree with a final likelihood value of -10389.513 is presented. The matrix contained 598 distinct alignment patterns, with 23.88% of the characters being undetermined or gaps. Estimated base frequencies were as follows: A = 0.232, C = 0.268, G = 0.280, T = 0.219; substitution rates: AC = 0.707, AG = 1.993, AT = 1.143, CG = 1.006, CT = 5.250, GT = 1.0; gamma distribution shape parameter α = 0.656. Bootstrap support values for maximum likelihood (ML) equal to or greater than 70% and clade credibility values greater than 0.90 (rounded to two decimal places) from Bayesian inference analysis are labeled at each node. Ex-type strains are in bold, while the new isolate is indicated in red bold. The tree is rooted to *Pleopunctum ellipsoideum* (MFLUCC 19–0390) and *P. pseudoellipsoideum* (MFLUCC 19–0391).

Phaeoseptum kunmingensis Z. L.T, sp. nov. Fig. 22

Index Fungorum number: IF901135; Facesoffungi number: FoF17656

Etymology – The epithet is derived from the type locality, Kunming, China.

Holotype – HKAS 144950

Saprobic on dead wood branches. Sexual morph: *Ascomata* 400–560 µm × 380–450 µm wide ($\bar{x}$ = 470 × 416 µm, n = 5), visible as black spots, semi-immersed, solitary, scattered or aggregated, globose to sub-globose, irregular, clypeate, dark brown, ostiolate. *Ostiole* 45–50 high × 21–26 µm diam. ($\bar{x}$ = 47 × 22 µm, n = 5), pale brown. *Peridium* 40–52 µm ($\bar{x}$ = 45 µm, n = 5) wide, comprising 4–5 layers of cells of *textura angularis*, thick-walled; cells fusing with host tissue with thick-walled and brown cells of outer layers, thin-walled and hyaline cells of inner layers. *Hamathecium* composed of 1.7–2 µm ($\bar{x}$ = 1.8 µm, n = 5) wide, numerous, branched, cellular, septate, pseudoparaphyses, longer than asci, and embedded in a gelatinous matrix. *Asci* 99–117 × 14–17 µm ($\bar{x}$ = 108 × 15 µm, n = 20), 8-spored, bitunicate, fissitunicate, cylindrical-clavate to elongate-clavate, apically rounded. *Ascospores* 28–36 × 8.7–11 µm ($\bar{x}$ = 31 × 9 µm, n = 20), uniseriate at base, 2–3-seriate above, hyaline when immature, turning pale to yellowish brown at maturity, oblong to broadly fusiform, 11–15 transverse septa and 1–2 longitudinal septa, broadly rounded ends, slightly curved, smooth-walled. Asexual morph: Undetermined.

Culture characters – Ascospores germinating on MEA within 24 hours, slow-growing, reaching 10 mm diam., after 15 days at 27 °C, flat or raised at the center, circular, irregular at the margin, grayish; reverse dark brown.

Material examined – China, Yunnan Province, Botanical Garden, Kunming Institute of Botany, 25.140833 N, 102.739444 E, 1892 m, on dead twigs of unidentified decaying branches, 10 October 2024, ZL Tun, 1C (HKAS 144950, holotype).

GenBank numbers – HKAS 144950: ITS = PV426819, LSU = PV426820, *tef1-α* = PV568315.

Notes – Based on the phylogenetic analyses of combined ITS, LSU, SSU, and *tef1-α* sequences (Fig. 21), our new species *Phaeoseptum kunmingensis* (HKAS 144950) clustered with *P. zhujiangyuanense* (ZHKUCC 23–1022) with 93% ML and 1.0 BYPP bootstrap support. *Phaeoseptum kunmingensis* can be distinguished from *P. zhujiangyuanense* by having larger ascomata (400–560 × 380–450 vs. 215–470 × 150–320 µm), smaller asci (99–117 × 14–17 vs. 105–165 × 22–35 µm), and smaller ascospores (28–36 × 8.7–11 vs. 35–42 × 9–15 µm) (Zhang et al. 2024b). *Phaeoseptum kunmingensis* is also closely related to *P. mali* (MFLUCC 17–2108) but can be distinguished by larger ascomata (400–560 × 380–450 vs. 320–375 × 320–360 µm), smaller asci (99–117 × 14–17 vs. 85–190 × 19–32µm), and smaller ascospores (28–36 × 8.7–11 vs. 27–38 × 8–13 µm) (Phukhamsakda et al. 2019). *Phaeoseptum mali* has eight to 11 layers of peridium wall, in contrast to *P. kunmingensis*, which has only four to five layers (Phukhamsakda et al. 2019).

When considering the base pair differences (excluding gaps) between *Phaeoseptum kunmingensis* and *P. zhujiangyuanense*, there were 2.2% differences (16/726 bp) in the ITS locus, 3.6% (40/1094 bp) in the LSU locus, and 0.9 % (9/963 bp) in the *tef1-α* locus. The base pair differences (without gaps) between *P. kunmingensis* and *P. mali* were 2.6% (22/840 bp) in the ITS locus, 3.2% (29/883 bp) in the LSU locus, and 0.8 % (9/963 bp) in the *tef1-α* locus. *Phaeoseptum kunmingensis* does not have SSU data available for comparison. Based on morphological characteristics, variations in genetic distance, and phylogenetic analysis, we propose that *P. kunmingensis* be recognized as a new species.



Figure 22 – *Phaeoseptum kunmingensis* (HKAS 144950, holotype). a Substrate. b Appearance of ascomata on host. c Vertical section of an ascoma. d Ostiole. e Peridium. f Pseudoparaphyses. g–i Asci. j–o Ascospores. Scale bars: b = 0.2 mm, c = 100 µm, d–o = 20 µm.

Pleosporaceae Nitschke

Comoclathris Clem., Gen. fung. (Minneapolis): 37 (1909).

Index Fungorum number: IF1198; Facesoffungi number: FoF00507

Comoclathris is characterised by semi-immersed to superficial, scattered ascomata, cylindrical to cylindro-clavate asci and fusiform, muriform, brown to reddish-brown ascospores, with or without a mucilaginous sheath (Hongsanan et al. 2020a). This genus has an alternaria-like asexual morph (Woudenberg et al. 2013). However, molecular data for the type species, *C. lanata*, remain unavailable. Shoemaker & Babcock (1992) provided a key to species of *Comoclathris*, including descriptions and illustrations. Zhang et al. (2011) transferred *Comoclathris* from *Diademaceae* to *Pleosporaceae* based on morphological features, specifically the prominent ostiolar opening in the ascomata, which results from the disintegration of the upper ascomatal wall, creating a large opening or circular lid as earlier noted by Shoemaker & Babcock (1992). Hongsanan et al. (2020a) and Pem et al. (2024) accepted *Comoclathris* in *Pleosporaceae* based on both morphological and phylogenetic evidence. Several researchers have introduced new species to *Comoclathris* (Brahmanage et al. 2020, Xu et al. 2024a).

Prof. Kevin D. Hyde's contributions to *Comoclathris* research have been crucial since the genus was initially introduced in 1909. Out of the 41 species presently listed in Index Fungorum (2025), Prof. Kevin D. Hyde and his team have described 15 species. In this study, we present *Comoclathris pimpinellae* as a new host record. We also provide the updated phylogenetic tree for *Comoclathris* (Fig. 23).

Comoclathris pimpinellae S. Konta, Bulgakov & K.D. Hyde, Fungal Diversity 78: 50 (2016)

Fig. 24

Index Fungorum number: IF551949; Facesoffungi number: FoF01769

Saprobic on dead branches of *Phlomis* sp. (*Lamiaceae*). Sexual morph: *Ascomata* 325–525 × 155–215 µm ($\overline{x}$ = 412 × 165.5 µm, n = 5), solitary, scattered or aggregated in small groups, semi-immersed to erumpent, subglobose, elongated, dark brown to black, shiny, presence of few dark brown setae without a distinct ostiole. *Peridium* 25–35 µm wide, consisting of an outer layer of dark brown cells of *textura angularis*, and inner layer of mostly hyaline flattened cells with *textura angularis*. *Hamathecium* 1.3–1.8 µm wide, numerous, septate, pseudoparaphyses, embedded in a gelatinous matrix. *Asci* 103–108 × 25–29 µm ($\overline{x}$ = 105.3 × 28.4 µm, n = 20), 8-spored, bitunicate, fissitunicate, cylindrical-clavate, short pedicellate, apically rounded, with an indistinct ocular chamber. *Ascospores* 25–32 × 10–13 µm ($\overline{x}$ = 29.8 × 11.6 µm, n = 40), 2–3-seriate, partially overlapping, broadly fusiform, 3-septate, brown to dark brown, muriform, broadly fusiform, with 3 transverse septa and a vertical septum in second and third cells, slightly constricted at the septa, with obtuse ends, smooth-walled, surrounded by a thick mucilaginous sheath. Asexual morph: Undetermined.

Culture characteristics – Colonies on PDA reaching 25 mm diam., after three weeks at 25 °C. Cultures from above, white to off-white, dense, ellipsoidal to irregular, umbonate, smooth, entire, thinly hairy, well-defined margin, white aerial mycelium, reverse brown in the middle, off-white to white at the edges.

Material examined – Uzbekistan, Tashkent Province, Bostanliq District, Beldorsoy, Katta Chimyon, Chatkal Range, Western Tien Shan Mountains, on dead branches of *Phlomis* sp. (*Lamiaceae*), 7 May 2016, Y. Gafforov (TASM 6178), living culture MFLUCC 25–0168.

GenBank numbers – LSU = PV158286, SSU = PV158288, ITS = PV163077.

Notes – Multi-locus phylogenetic analysis based on LSU, SSU, and ITS data places our isolate, within the *Comoclathris* clade, as a sister lineage to *Comoclathris pimpinellae* (MFLUCC 14–1159), with 95% ML support (Fig. 23). Although the ITS locus differs from *C. pimpinellae* by six bp (1.09%), it exhibits slight morphological differences, including larger ascomata, longer asci, and broader, muriform ascospores. *Comoclathris pimpinellae* was initially described from dead stems of *Pimpinella tragium* subsp. *titanophila* (*Apiaceae*) in Russia, while our isolate was found on *Phlomis* sp. in Uzbekistan. Based on both morphological characteristics and phylogenetic

analyses, we therefore identify this isolate as *C. pimpinellae.* This represents a new host record of the species on *Phlomis* sp.

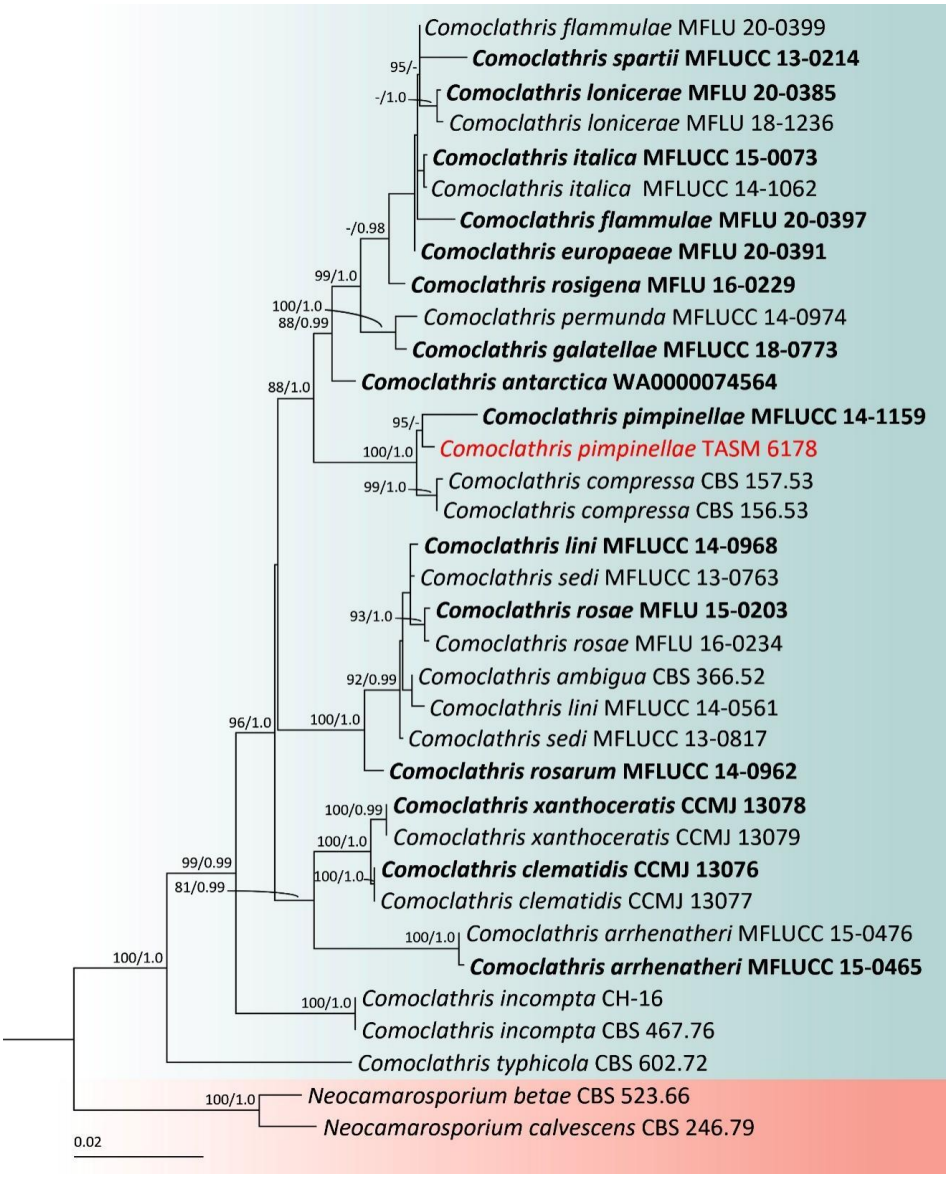


Figure 23 – Phylogram generated from maximum likelihood analysis based on combined LSU, SSU, and ITS sequence data from 35 taxa, comprising 2,470 characters (LSU = 862, SSU = 1,036, ITS = 572). The best-scoring RAxML tree with a final likelihood value of -7304.437 is presented. The matrix contained 497 distinct alignment patterns, with 14.26% of the characters being undetermined or gaps. Estimated base frequencies were as follows: A = 0.254, C = 0.213, G = 0.271, T = 0.262; substitution rates: AC = 2.057, AG = 3.401, AT = 1.523, CG = 0.653, CT = 6.159, GT = 1.0; gamma distribution shape parameter α = 0.841. Bootstrap support values for maximum likelihood (ML) equal to or greater than 70% and clade credibility values greater than 0.90 (rounded to two decimal places) from Bayesian inference analysis are labeled at each node. Ex-type strains are in bold, while the new isolate is indicated in red. The tree is rooted to *Neocamarosporium betae* (CBS 523.66) and *N. calvescens* (CBS 246.79).

Roussoellaceae Jian K. Liu, Phook., D.Q. Dai & K.D. Hyde

Roussoella Sacc., in Saccardo & Paoletti, Atti Inst. Veneto Sci. lett., ed Arti, Sér. 6 6: 410 (1888)

Index Fungorum number: IF4799; Facesoffungi number: FoF01689

Roussoella was introduced by Saccardo & Paoletti (1888), with *R. nitidula* as the type species, which was originally isolated from bamboo in Malaysia. *Roussoella* mostly occurs as a saprobe on monocotyledonous plants, such as bamboo and palms (Wu et al. 2023, Chen et al. 2024). Currently, approximately 56 species have been documented in this genus (Dai et al. 2022, Chen et al 2024, Manawasinghe et al. 2024, Shen et al. 2024a, Yu et al. 2024). *Roussoella* species are characterized by ascomata with darkened areas, cylindrical to clavate to clavate asci, ellipsoidal to fusiform, 1-septate, ornamented ascospores (Dai et al. 2022, Chen et al. 2024). The asexual morph of *Roussoella* is characterized by ampulliform, enteroblastic, conidiomata, oblong to ellipsoidal conidiogenous cells, hyaline to brown conidia (Dai et al. 2017, Wu et al. 2023).

Prof. Kevin D. Hyde has played a key role in advancing the study of *Roussoella* by discovering 22 species. These species, primarily found on bamboo, have also been observed on *Calamus* sp., palm, *Wisteria* sp., and wood. Additionally, they are distributed across Brunei, China, Ecuador, Japan, Queensland, Thailand, and the United States (Hyde et al. 1999, Zhou et al. 2003, Ariyawansa et al. 2015b, Dai et al. 2017, Jiang et al. 2019a, Dong et al. 2020, Hyde et al. 2023a). Prof. Hyde's work has not only enhanced our understanding of the diverse host plants of *Roussoella* species but also uncovered their broad geographical distribution across various countries and regions. In recognition of his outstanding contributions to the genus of *Roussoella*, herein we introduce a new species *Roussoella hydei*, which has been named in honor of Prof. Kevin D. Hyde.

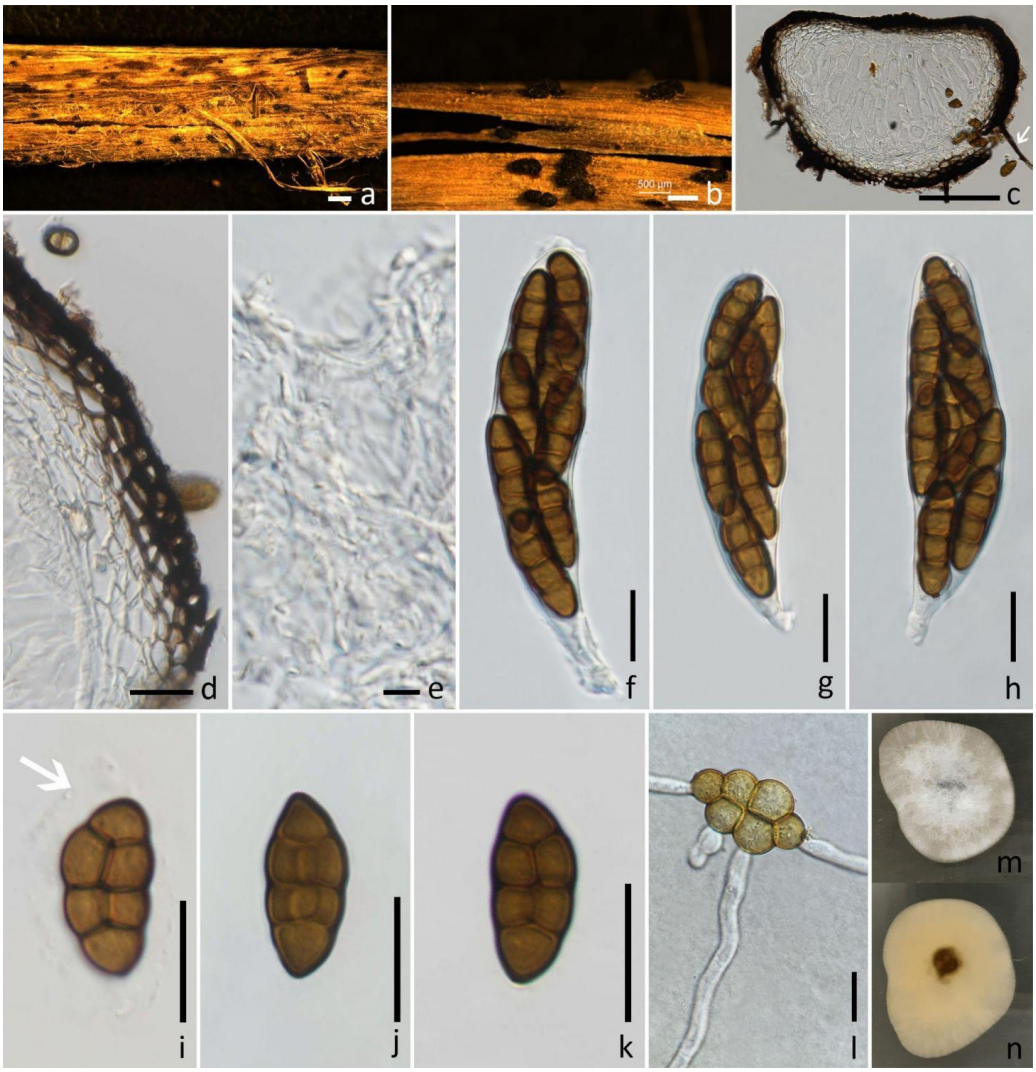


Figure 24 – *Comoclathris pimpinellae* (TASM 6178, new host record). a, b Appearance of ascomata on substrate. c Vertical cross-section of an ascoma (arrow indicates setae). d Peridium.

e Pseudoparaphyses. f–h Asci. i–k Ascospores (i: arrow indicates sheath). l Germinated ascospore. m, n Culture characteristics on MEA (m: above view, n: reverse view). Scale bars: a = 1 mm, b = 500 µm, c = 100 µm, d, f–l = 20 µm, e = 5 µm.

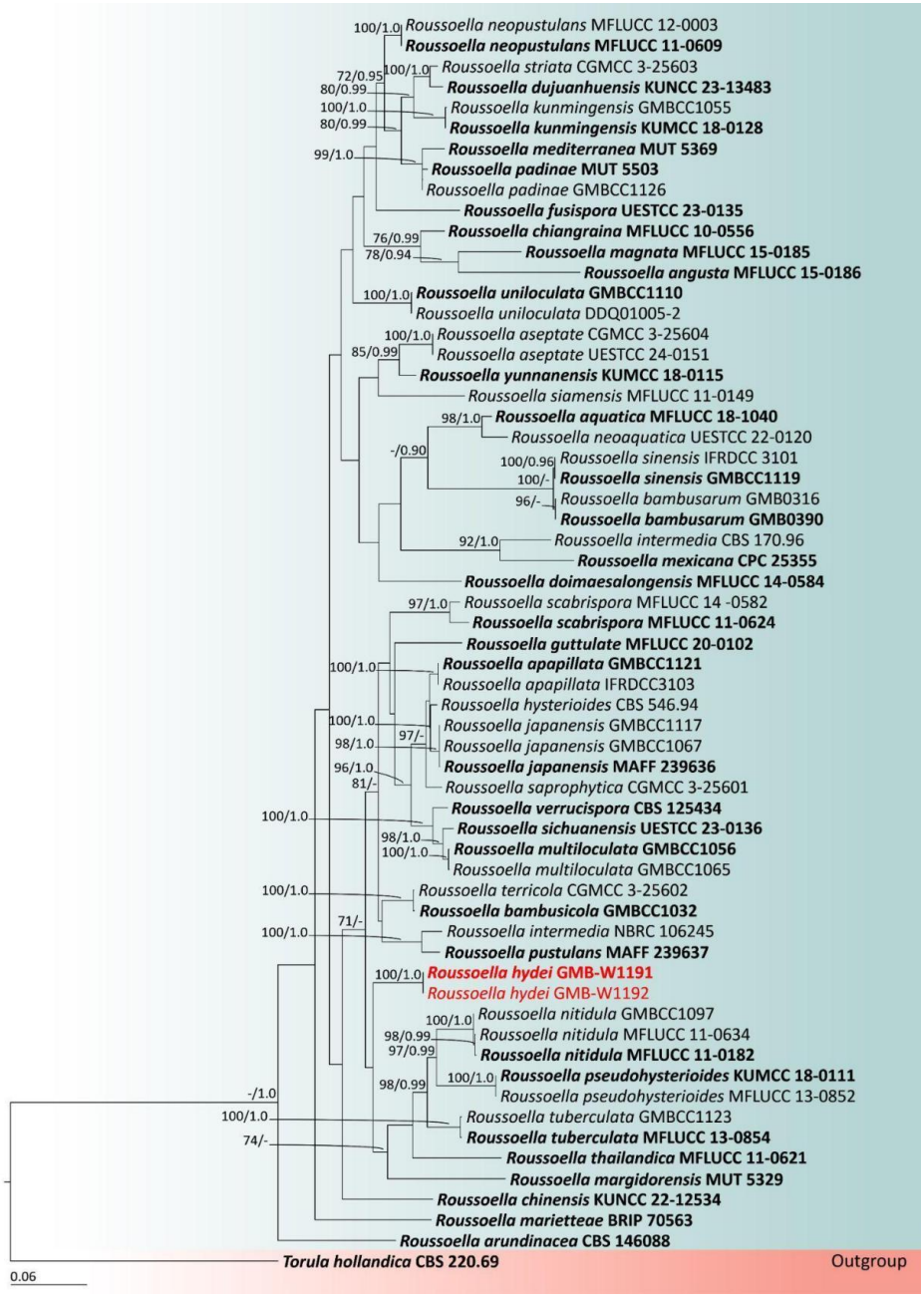


Figure 25 – Phylogram generated from maximum likelihood analysis based on combined ITS, LSU *rpb2*, and *tef1-α* sequence data from 59 taxa, comprising 3,278 characters (ITS = 492, LSU = 849, *rpb2* = 1,018, *tef1-α* = 919). The best-scoring RAxML tree with a final likelihood value of -20851.001 is presented. The matrix contained 1,227 distinct alignment patterns, with 22.56% of the characters being undetermined or gaps. Estimated base frequencies were as follows: A =0.242, C = 0.266, G = 0.268, T = 0.223; substitution rates: AC = 1.511, AG = 4.819, AT = 1.839, CG = 1.157, CT = 8.812, GT = 1.0; gamma distribution shape parameter α = 0.165. Bootstrap support values for maximum likelihood (ML) equal to or greater than 70% and clade credibility values greater than 0.90 (rounded to two decimal places) from Bayesian inference analysis are labeled at each node. Ex-type strains are in bold, while the new isolates are indicated in red. The tree is rooted to *Torula hollandica* (CBS 220.69).

Roussoella hydei L.S. Han & D.Q. Dai, sp. nov. Fig. 26

Index Fungorum number: IF903327; Facesoffungi number: FoF17304

Etymology – 'hydei' named in honor of the renowned mycologist Kevin D. Hyde, recognizing his significant contributions to mycology on the occasion of his 70th birthday.

Holotype – GMB-W1191

Saprobic on dead culms of bamboo. Sexual morph: Undetermined. Asexual morph: *Stromata* up to 700–1000 long × 150–230 μm high, forming under a blackened area, solitary to gregarious, ellipsoidal to irregular, raised at maturity, uniloculate to multi-loculate. *Conidiomata* loculate, immersed in the stromata, globose to subglobose, dark brown. *Conidiomatal wall* 20–35 μm wide, composed of several layers, with dark to brown cells of *textura angularis. Conidiophores* reduced to conidiogenous cells. *Conidiogenous cells* 10–20 × 2–4.5 μm ($\overline{x}$ = 13 × 3.5 μm, n = 20), obclavate, enteroblastic, phialidic, discrete, branched, cylindrical to ampulliform or irregular swollen cells, hyaline, smooth-walled. *Conidia* 4.5–5.2 × 3.5–4.7 μm ($\overline{x}$ = 4.8 × 4.2 μm, n = 20), oval to subglobose to globose, hyaline, with a guttule and smooth-walled when young, rounded at both ends, brown to dark brown, irregular edges, and verrucose, rough-walled when growing gradually, rounded at both ends, aseptate.

Material examined – China, Yunnan Province, Lijiang City, Liming Town, Laojun Mountain, on dead culms of bamboo, 21 July 2021, Dong-Qin Dai, DDQ2028 (GMB-W1191, holotype); *ibid*. DDQ2028-1 (GMB-W1192).

GenBank numbers – GMB-W1191: ITS = PV022386, LSU = PV022509, *tef1-α* = PV452824; GMB-W1192: ITS = PV022387, LSU = PV022510, *tef1-α* = PV452825.

Notes – In the phylogenetic tree (Fig. 25), our new isolates (GMB-W1191 and GMB-W1192) developed a distinct cluster with *Roussoella margidorensis* (MUT 5329), *R. nitidula* (GMBCC1097, MFLUCC 11–0634, MFLUCC 11–0812), *R. pseudohysterioides* (KUMCC 18–0111, MFLUCC 13–0852), *R. tuberculata* (GMBCC 1123, MFLUCC 13–0854), and *R. thailandica* (MFLUCC 11–0621). Morphologically, the new collections resemble *R. nitidula* and *R. tuberculata.* However, our new collections differ from *R. nitidula* and *R. tuberculata* by having oval to subglobose to globose conidia, whereas these two species have oblong to ellipsoidal conidia. Additionally, our new collections have smaller conidia compared to *R. nitidula* (4.5–5.2 ×3.5–4.7 vs. (6–)7–8 × 3–4), and *R. tuberculata* (4.5–5.2 ×3.5–4.7 vs. 8.5–10 × 4.5–5.5) (Liu et al. 2014, Dai et al. 2017). In addition, *R. pseudohysterioides* and *R. thailandica* have only been reported in their sexual morphs; however, they can be well distinguished by the molecular evidence (Liu et al. 2014, Dai et al. 2017). Furthermore, Poil et al. (2020) introduced *R. margidorensis*, while they did not provide a detailed description for this species, it can also be distinguished from our new collections through phylogenetic analysis (Fig. 25). Hence, we introduce *R. hydei* as a new species based on morphology and phylogeny.

Dothideomycetes orders *incertae sedis*

Dyfrolomycetales K.L. Pang, K.D. Hyde & E.B.G. Jones

Pleurotremataceae Walt. Watson

Melomastia Nitschke ex Fuckel, Jb. nassau. Ver. Naturk. 25–26: 306 (1871)

Index Fungorum number: IF92451; Facesoffungi number: FoF07673

Melomastia was established by Saccardo (1875), with *M. friesii* designated as the type species. Its taxonomic placement has been a subject of ongoing debate, with varying classifications proposed by different authors (Barr 1989, 1994, Hawksworth et al. 1995, Kirk et al. 2008, Lumbsch & Huhndorf 2010, Maharachchikumbura et al. 2015, 2016, Hyde et al. 2016, Wijayawardene et al. 2017, Norphanphoun et al. 2017, Pem et al. 2024). Based on phylogenetic analyses, Norphanphoun et al. (2017) provided a comprehensive understanding of *Melomastia*, revealing that it does not belong to Sordariomycetes but is a member of Dothideomycetes. In a more recent paper, Li et al. (2022) synonymized *Dyfrolomyces* under *Melomastia* based on both morphological characteristics and phylogenetic analyses, transferring 11 species to *Melomastia*. However, Kularathnage et al. (2023) resurrected *Dyfrolomyces* to accommodate *D. chromolaenae* and *D. tomanensis*, treating

these two as distinct genera. Molecular markers currently available for *Melomastia* include ITS, LSU, SSU, and *tef1-α* (Hyde et al. 2023a, Du et al. 2024, Pem et al. 2024). Species of *Melomastia* are characterized by immersed to semi-immersed, globose to subglobose, black, ostiolate ascomata, filamentous pseudoparaphyses, cylindrical and bitunicate asci, and ovoid or cylindrical, hyaline, 1–10-septate, with or without gelatinous sheath (Dayarathne et al. 2020, de Silva et al. 2022, Li et al. 2022, Kularathnage et al. 2023, Du et al. 2024, Xu et al. 2024b).

Prof. Kevin D. Hyde has made significant contributions to the taxonomy of *Melomastia*, particularly through the discovery and formal description of numerous taxonomic novelties. Among his notable achievements is the identification of 21 new species of *Melomastia*, contributing to the 70 species currently listed in Index Fungorum (2025). Of these, two species are retained under the genus *Dyfrolomyces*. His extensive work on *Melomastia* has greatly enhanced our understanding of this genus. In recognition of his exceptional contributions to mycology, we hereby introduce *Melomastia hydei*, named in honor of Prof. Kevin D. Hyde. Additionally, we present an updated phylogenetic tree for *Melomastia* (Fig. 27).

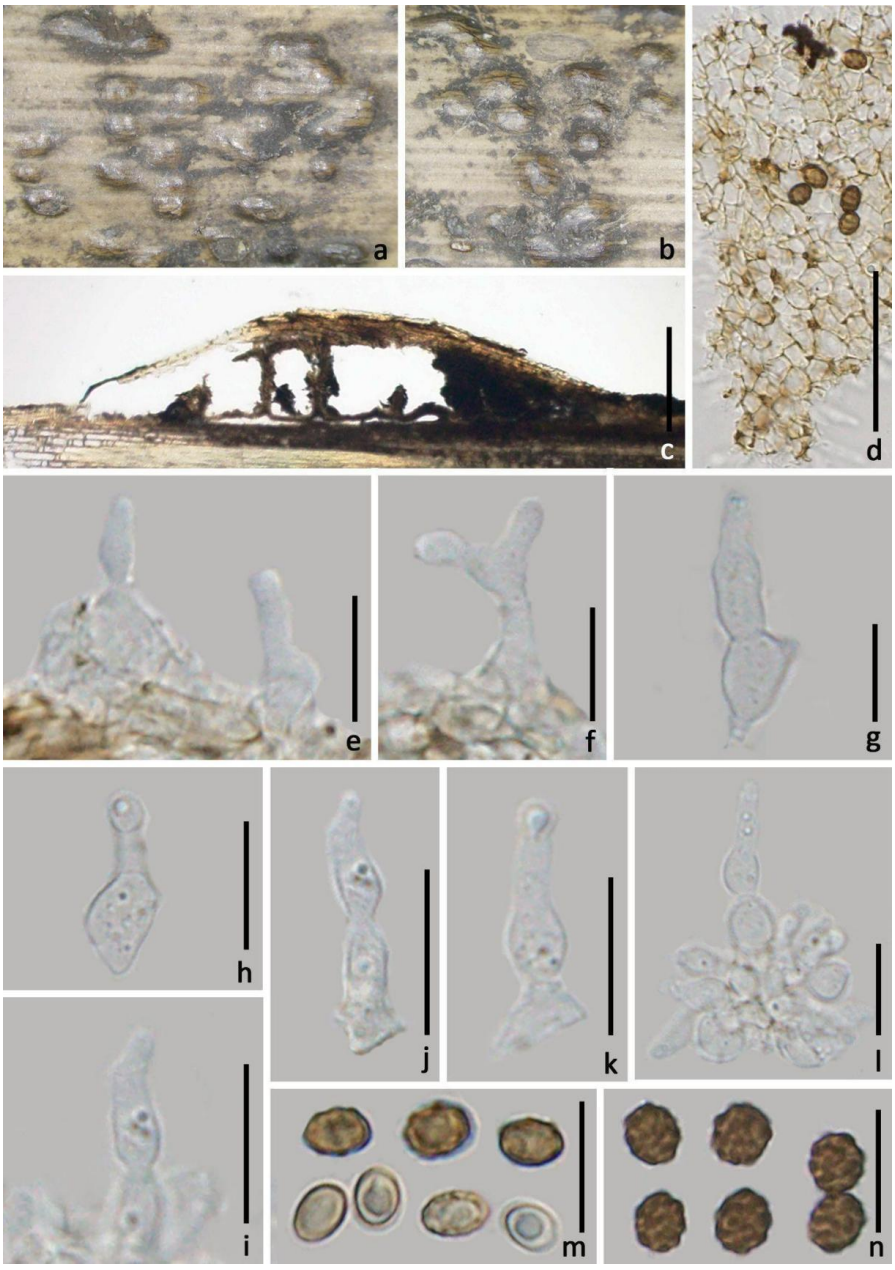


Figure 26 – *Roussoella hydei* (GMB-W1191, holotype). a, b Stromata on a bamboo culm. c Vertical sections of stromata showing loculate conidiomata. d Conidioma wall.

e–l Conidiogenous cells developing conidia. m, n Conidia. Scale bars: c = 300 µm, d = 30 µm, e–n = 10 µm.

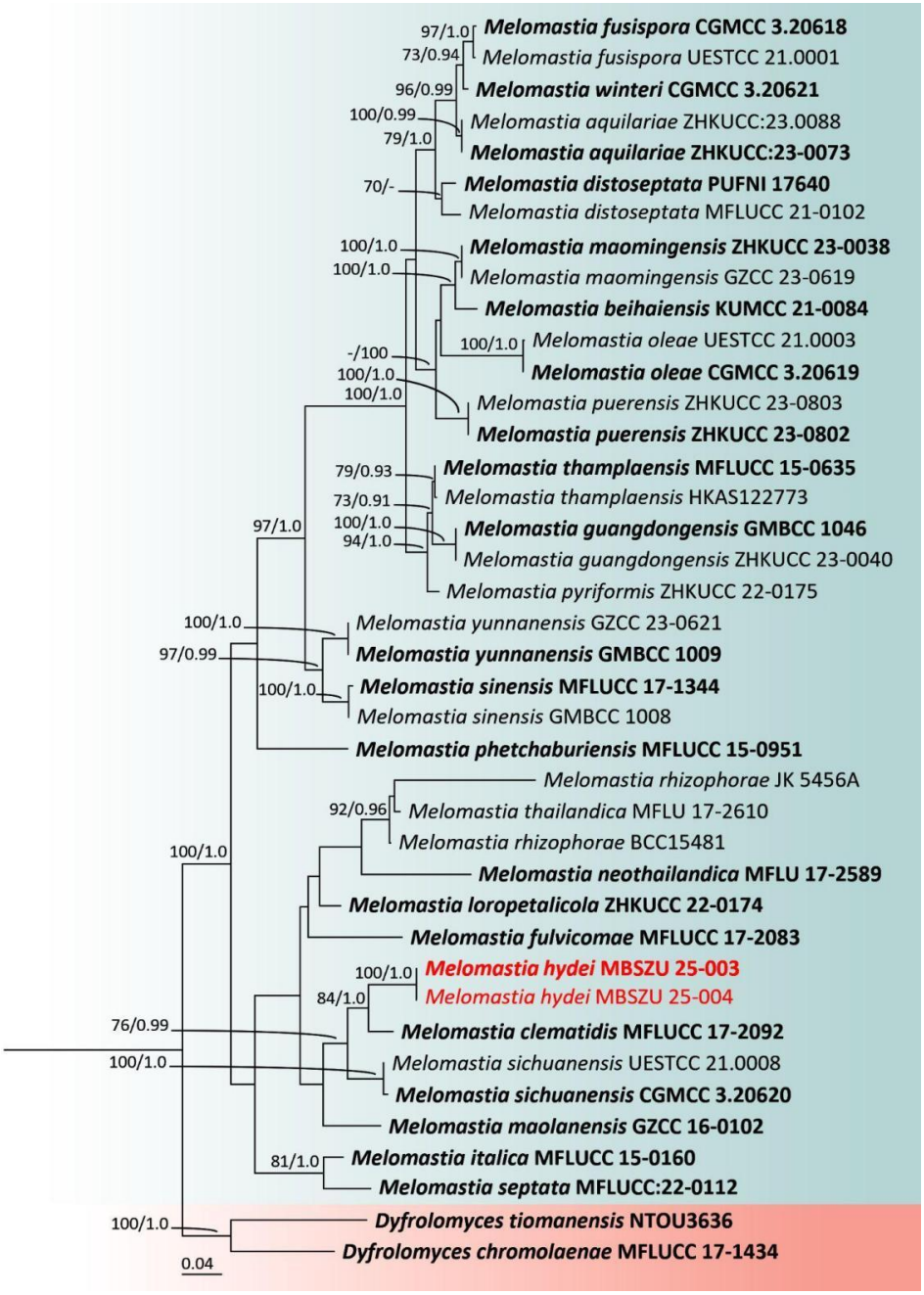


Figure 27 – Phylogram generated from maximum likelihood analysis based on combined ITS, LSU, SSU, and *tef1-α* sequence data from 42 taxa, comprising 3,749 characters (ITS = 831, LSU = 906, SSU = 1,020, *tef1-α* = 992). The best-scoring RAxML tree with a final likelihood value of -13889.121 is presented. The matrix contained 1,077 distinct alignment patterns, with 29.23% of the characters being undetermined or gaps. Estimated base frequencies were as follows: A = 0.231, C = 0.274, G = 0.291, T = 0.203; substitution rates: AC = 1.287, AG = 2.088, AT = 1.019, CG = 1.013, CT = 7.353, GT = 1.0; gamma distribution shape parameter α = 0.458. Bootstrap support values for maximum likelihood (ML) equal to or greater than 70% and clade credibility values greater than 0.90 (rounded to two decimal places) from Bayesian inference analysis are labeled at each node. Ex-type strains are in bold, while the new isolates are indicated in red bold. The tree is rooted to *Dyfrolomyces chromolaenae* (MFLUCC 17–1434) and *D. tiomanensis* (MFLUCC 13–0440).

Melomastia hydei Hongsanan, Khuna & Xie N., sp. nov. Fig. 28

Index Fungorum number: IF903733; Facesoffungi number: FoF17754

Etymology – 'hydei' named in honor of the renowned mycologist Kevin D. Hyde, recognizing his significant contributions to mycology on the occasion of his 70th birthday.

Holotype – SZU25–003

Saprobic on dead twigs of Beach Naupaka (*Scaevola taccada*). Sexual morph: *Ascomata* (excluding neck) 120–280 high × 180–325 diam. μm ($\overline{x}$ = 174 × 250 μm, n = 10), appear as numerous, black, cone-shaped structures on host surface, solitary, scattered to gregarious, immersed to erumpent through host tissue, globose to subglobose, black, coriaceous to carbonaceous, ostiolate. *Ostiolate* 135–170 high × 100–155 diam. μm ($\overline{x}$ = 150 × 130, n = 10), central, canal, dark brown to black, papillate, periphyses filling the ostiolar canal. *Peridium* 26–70 ($\overline{x}$ = 45, n = 10), thick-walled, brittle when dry, comprising several layers of dark brown to black cells of *textura angularis*, outer layers dark brown to black, becoming lighter inwardly. *Hamathecium* composed of 1–2 μm wide, numerous filamentous, cylindrical to broadly filiform, septate, not constricted at the septa, unbranched, hyaline pseudoparaphyses, embedded in a gelatinous matrix. *Asci* 70–110 × 5–7.5 μm ($\overline{x}$ = 87 × 6 μm, n = 15), 8-spored, bitunicate, cylindrical, short pedicel, straight or slightly curved, rounded apex, with an obvious ocular chamber. *Ascospores* 12.3–15 × 3.4–5 μm ($\overline{x}$ = 13.5 × 4.3 μm, n = 30), uniseriate, partial overlapping, broad fusiform, rounded ends, tapering towards both ends, straight or slightly curved, 3-septate, constricted at the septa, hyaline, with guttules in each cell, smooth-walled, with thin mucilaginous sheath. Asexual morph: Undetermined.

Culture characteristics – Colonies on PDA reaching 25 mm diam., after 14 days at 25 °C, circular, irregular, with dense aerial mycelium on the surface. The colony is flattened to slightly raised and umbonate, initially white, turns into cream, light yellow, or orange at the center, entire or slightly undulate edge, some areas later turn greenish-grey. Colonies reverse: yellowish to light cream at the margin, showing radial valleys that become dark greenish as the colony ages.

Material examined – China, Guangdong Province, Huizhou City, Xunliao Residential District, 22°35'23.5" N, 114°45'02.3" E, on decaying twigs of Beach Naupaka (*Scaevola taccada*, *Goodeniaceae*), Hongsanan S., 22 September 2024, WY01.1 (SZU25–003, holotype), ex-type MBSZU 25–003; *ibid*., WY01.2 (SZU25–004), living culture MBSZU 25–004.

GenBank numbers – MBSZU 25–003: ITS = PQ849544, LSU = PQ844642, SSU = PQ844644, *tef1-α* = PQ868900; MBSZU 25-004: ITS = PQ849545, LSU = PQ844643, SSU = PQ844645, *tef1-α* = PQ868901.

Notes – In the phylogenetic analysis based on combined ITS, LSU, SSU, and *tef1-α* sequence data (Fig. 27), our new species (MBSZU 25–003 and MBSZU 25–004), formed a distinct clade among *Melomastia* species and is closely related to *M. clematidis* (MFLUCC 17–2092). The base-pair difference between ITS locus of the type strain of *M. clematidis* (MFLUCC 17–2092) and our new species were 9.5% (59/621 bp, including 13 gaps), while these differences for LSU, SSU and *tef1-α* were 0.36% (3/825 bp, without gaps), 0.13% (1/764 bp, without gaps), and 4.33% (39/901 bp, without gaps), respectively. Morphologically, our new species *M. hydei* fits well with the generic concept of *Melomastia* in having immersed to semi-immersed, globose to subglobose, black, ostiolate ascomata, filamentous pseudoparaphyses, with cylindrical, bitunicate, pedicellate asci, and ovoid, or cylindrical, hyaline, septate ascospores, with gelatinous sheath (Dayarathne et al. 2020, de Silva et al. 2022, Li et al. 2022, Kularathnage et al. 2023, Du et al. 2024, Xu et al. 2024b). When compared to the closely related species, *M. clematidis* has larger ascomata (300–510 × 260–445 μm vs. 120–280 high × 180–325 diam. μm), longer asci (115–160 × 4–7 vs. 70–110× 5–7.5 μm), and longer ascospores (13–20 × 3.8–5 vs. 12.3–15× 3.4–5 μm) (Phukhamsakda et al. 2020, de Silva et al. 2022). Moreover, our new species exhibits distinct cultural characteristics, including differences in colony texture and coloration patterns. The colonies are initially white, then turn into cream, light yellow, or orange at the center, with greenish-grey areas developing over time. In contrast, *M. clematidis* has white colonies with a yellow ring and oil droplets. Therefore, based on morphology and phylogeny, we introduce our collection as a new species, *Melomastia hydei*.

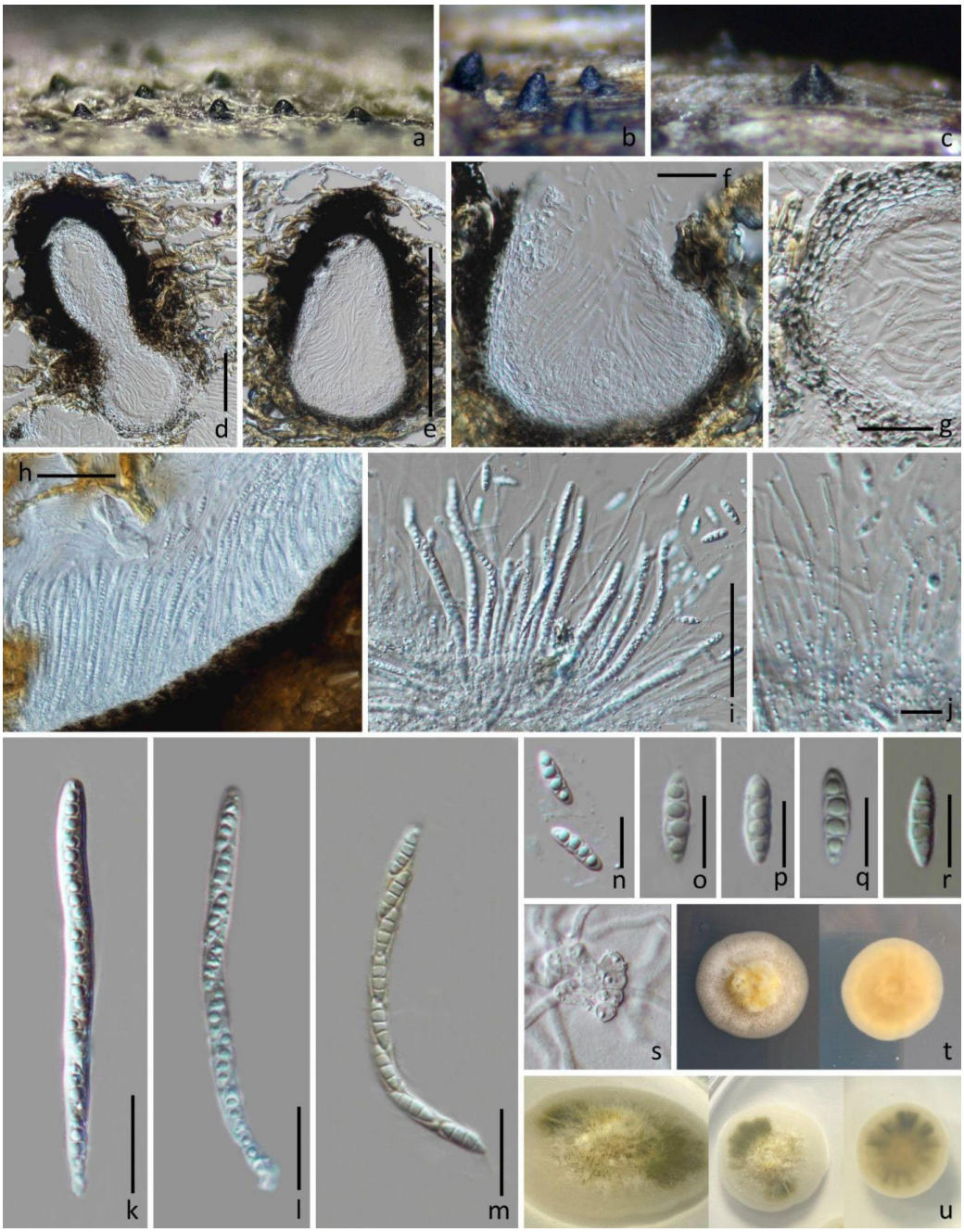


Figure 28 – *Melomastia hydei* (SZU25–003, holotype). a–c Appearance of ascomata on the substrate. d–f Vertical cross-section of ascomata. g Peridium. h, i Groups of asci. j Hamathecium. k–m Asci (m stained with Melzer's reagent). n–r Ascospores (r stained with Melzer's reagent). s Germinated ascospore. t Upper and reverse views of the colony on PDA when young. u Upper and reverse views of the colony on PDA when mature. Scale bars: d–f, h, i = 50 µm, g, k–m = 20 µm, j, n–r = 10 µm.

Monoblastiales Lücking, M.P. Nelsen & K.D. Hyde

Eriomycetaceae Huanraluek & K.D. Hyde

Neoheleiosa Mortimer, in Mortimer, Jeewon, Xu, Lumyong & Wanasinghe, Frontiers in Microbiology: 6 (2021)

Index Fungorum number: IF838517; Facesoffungi number: FoF11959

Neoheleiosa was recently established to accommodate its type species, *Neoheleiosa lincangensis*, which was found on dead twigs of *Pittosporum* sp. in Yunnan, China. Phylogenetic analysis based on SSU, LSU, ITS, *tef1-α*, and mtSSU sequence data placed *Neoheleiosa* in a well-

supported monophyletic clade, closely related to *Heleiosa barbatula* (Mortimer et al. 2021). Zhang et al. (2023a) added the second species, *N. guizhouensis*, based on morphological and molecular analyses of an herbaceous plant specimen from China. *Heleiosa* is a monotypic genus, previously reported from senescent leaves of *Juncus* in salt marshes on the Atlantic coast of the United States (Kohlmeyer et al. 1996). However, *Neoheleiosa* differs from *Heleiosa* primarily in ascospore morphology. The ascospores of *Heleiosa* possess ten or more short, curved, hair-like subapical appendages at each end and have smooth walls, whereas *Neoheleiosa* lacks appendages and exhibits longitudinally streaked ornamentation. Further, *Heleiosa* has a peridium composed of *textura angularis* cells, whereas *Neoheleiosa* has a peridium with *textura globulosa* cells (Mortimer et al. 2021).

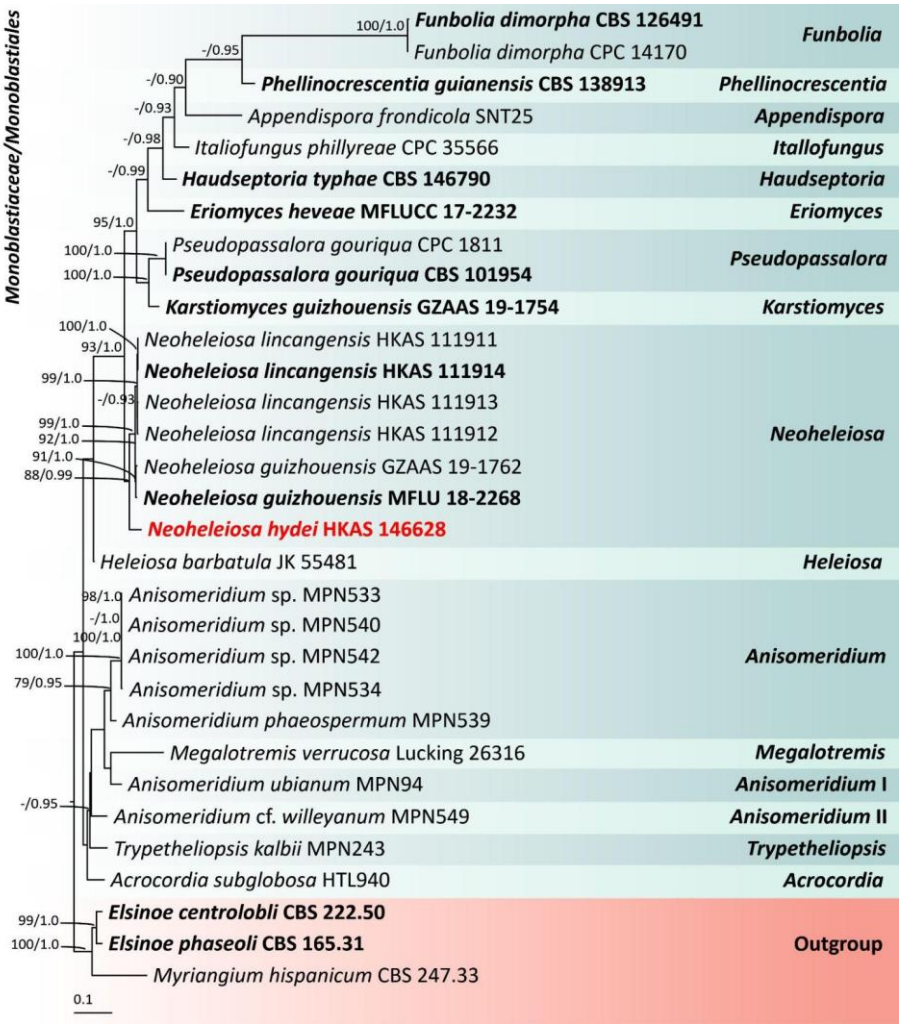


Figure 29 – Phylogram generated from maximum likelihood analysis based on combined SSU, LSU, ITS, and *tef1-α* sequence data from 31 taxa, comprising 3,912 characters (SSU = 1,225, LSU = 1,164, ITS = 604, *tef1-α* = 919). The best-scoring RAxML tree with a final likelihood value -17710.705 is presented. The matrix contained 1,356 distinct alignment patterns, with 47.67% of the characters being undetermined or gaps. Estimated base frequencies were as follows: A = 0.233, C = 0.259, G = 0.292, T = 0.216; substitution rates: AC = 1.109, AG = 1.939, AT = 1.006, CG = 1.421, CT = 5.918, GT = 1.0; gamma distribution shape parameter α = 0.140. Bootstrap support values for maximum likelihood (ML) equal to or greater than 70% and clade credibility values greater than 0.90 (rounded to two decimal places) from Bayesian inference analysis are labelled at each node. Ex-type strains are in bold, while the new isolate is indicated in red bold. The tree is rooted to *Myriangium hispanicum* (CBS 247.33), *Elsinoe phaseoli* (CBS 165.31) and *E. centrolobli* (CBS 222.50).

Neoheleiosa hydei Thiyagaraja, sp. nov. Fig. 30

Index Fungorum number: IF903738; Facesoffungi number: FoF11959

Etymology – 'hydei' named in honor of the renowned mycologist Kevin D. Hyde, recognizing his significant contributions to mycology on the occasion of his 70th birthday.

Holotype – HKAS 146628

Saprobic on dried twigs of an unidentified host. Sexual morph: *Perithecia* 210–240 × 130–190 µm ($\overline{x}$ = 220 × 160 µm, n = 10), solitary, scattered, immersed to erumpent, globose to subglobose or obpyriform, dark brown to black, coriaceous, ostiolate. *Peridium* 60–90 µm wide, composed of 5–7 layered, blackish dark brown cells of *textura angularis*. *Hamathecium* comprises 0.6–2 µm wide, comprising numerous, filamentous, branched, septate, pseudoparaphyses. *Asci* 60–105 × 8–10 µm ($\overline{x}$ = 80 × 9 µm, n = 20), 8-spored, bitunicate, fissitunicate, cylindrical, pedicel furcate, rounded and thick-walled at the apex, with an ocular chamber. *Ascospores* 12–20 × 6–10 µm ($\overline{x}$ = 15 × 8 µm, n = 20), overlapping uniseriate, hyaline at immature and becoming dark brown at maturity, with conically rounded ends, guttulate, thick-walled, smooth, and lacking a mucilaginous sheath or appendages. Asexual morph: Undetermined.

Material examined – China, Xishuangbanna, Mengla County, on decaying twigs of an unidentified host, 17 January 2024, Vinodhini Thiyagaraja, KIB55 (HKAS 146628, holotype).

GenBank numbers – HKAS 146628: SSU = PV469240, LSU = PV469239; ITS = PV469238, *tef1-α* = PV470946.

Notes – In the phylogenetic analysis (Fig. 29), our strain formed a sister clade to *Neoheleiosa lincangensis* and *N. guizhouensis* with 88% ML bootstrap and 0.99 BYPP values. Base pair comparisons between our strain and the type strain of *N. lincangensis* (HKAS 111914) revealed 0% difference in SSU (0/1245), 1.9% in LSU (23/1164), 4.6% in ITS (28/604), and 6.7% in *tef1-α* (59/870), including gaps. Similarly, the base pair differences between our strain and the type strain of *N. guizhouensis* (MFLU 18–2268) were 0% in SSU (0/1245), 2.6% in LSU (31/1164), 5.6% in ITS (34/604), and 6.7% in *tef1-α* (59/870), including gaps. However, the base pair differences between the type strains of *N. guizhouensis* (MFLU 18–2268) and *N. lincangensis* (HKAS 111914) revealed 0% in SSU (0/1245), 0.5% in LSU (6/1164), 1.4% in ITS (9/604), and 1.4% in *tef1-α* (13/870), including gaps. Zhang et al. (2023a) established *N. guizhouensis* as a new species based on differences in ascus and ascospore size from *N. lincangensis*, reporting smaller asci ((72–)79–85(–88) × 8–9.5 µm vs. 115–135 × 10–12 µm) and ascospores (12–15 × 5.5–7.5 µm vs. 16.5–17.5 × 7–9 µm) (Mortimer et al. 2021) along with phylogenetic analysis. However, these two species exhibit close morphological similarities and phylogenetic association, and could potentially be merged in the future following extensive sampling and detailed comparison with related species. Morphologically, our species aligns well with the *Neoheleiosa* species concept based on ascospore and peridium morphology. The ascospores of *N. lincangensis* possess longitudinal streaks, whereas our new species has smooth-surfaced ascospores. Further, *N. lincangensis* exhibits a *textura globulosa* peridium structure, while our species has a *textura angulari*s structure. Given the significant phylogenetic and morphological differences, we propose that our strain represents a new species. The continued discovery of *Neoheleiosa* species in China highlights the importance of extensive sampling in enhancing our understanding of species delineation within the genus.

Muyocopronales Mapook, Boonmee & K.D. Hyde

Muyocopronaceae K.D. Hyde

Muyocopron Speg., Anales Soc. Ci. Argent. 12(3): 113 (1881)

Index Fungorum number: IF3294; Facesoffungi number: FoF01887

Muyocopron was proposed by Spegazzini (1881), with *M. correntinum* as the type species. Currently, the genus comprises 79 species (Index Fungorum 2025) and is frequently reported as saprobic (Senwanna et al. 2019), pathogenic (Lye et al. 2022), or endophytic (Bill & Polishook 1992), with a broad global distribution. The sexual morph is characterized by ascomata that appear as small black spots on the surface of plant structures, and aseptate ascospores. The asexual morph exhibits conidiomata of the sporodochium type and lunate conidia with appendages at the

extremities and/or laterally (Hyde et al. 2013, Hernández-Restrepo et al. 2019). Prof. Kevin D. Hyde has made significant contributions to the study of *Muyocopron*, enhancing the knowledge of the genus and its diversity. Over the past decade, he has described 13 species, with the majority of these being described in the last decade.

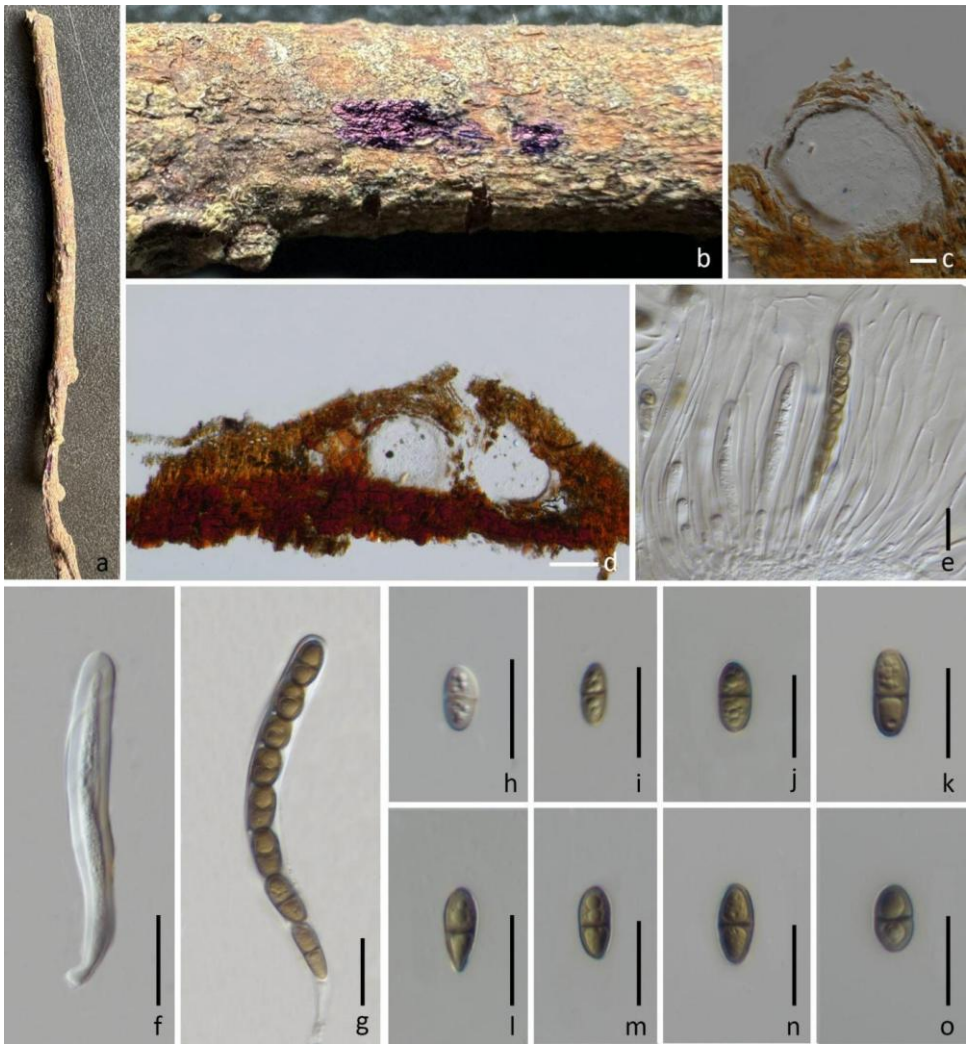


Figure 30 – *Neoheleiosa hydei* (HKAS 146628, holotype). a, b Appearance of ascomata on the woody substrate. c, d Vertical cross-section of ascomata. e Pseudoparaphyses. f, g Asci. h–o Ascospores. Scale bars: c = 20 µm, d = 100 µm, e–o = 20 µm.

Muyocopron cavernae A.S. Ferreira-Sá, L. Leonardo-Silva & S. Xavier-Santos, sp. nov. Fig. 32

Index Fungorum number: IF903290; Facesoffungi number: FoF172774

Etymology – Refers to the cave habitat where the species was isolated.

Holotype – HUEG-Fungi 18534

Isolated from the air in Sambaíba Cave. *Hyphae* septate, branched, 1.9–3.8 µm in width, hyaline, dark brown near the conidioma. *Conidioma* immersed in the medium, resembling a sporodochium, dark brown, with a circular appearance but without a defined outline, formed by aggregates of numerous conidiogenous cells, rounded to globose hyphae, brown (Korneup & Wanscher 1978). *Collarette* not observed. *Conidiogenous cells* of various shapes, due to the confluence of some spherical and arcuate cells, with thin, smooth walls, brown to dark brown, 13.5–24.4 × 14.5–25.6 µm diam., with pores of 1–2.8 µm. *Conidia* hyaline, smooth-walled, with granular contents, lunate, fusiform, 10.8–14.1 × 5.6–7.3 µm, with filiform, curved or straight appendages at both ends, 11.1–20.6 µm long apically and 12.6–21.8 µm basally, with 0–1(–1)

branches arising from ⅔ of the total length of the appendage. *Appressoria* lobed, irregular or clavate, smooth, 6.9 × 7.5 µm in diameter, light brown. Sexual morph: not observed.

Culture characteristics – After one week at 25 °C, the colonies exhibit distinct characteristics depending on the growth medium: on Oat Agar (OA): circular, cottony, reaching 29 mm in diameter, with greenish-grey mycelium, flat, greyish on the reverse; on Malt Extract Agar (MEA): 38 mm in diameter, olive-brown with whitish edges, sparse white aerial mycelium, the reverse gradually becoming blackened from the centre to the edges of the colony; on Potato Dextrose Agar (PDA): 43 mm in diam, exhibiting an olive-grey coloration with a grey reverse, sparse white aerial mycelium, and the production of brownish-yellow exudate after 20 days of incubation.

Material examined – Brazil, Goiás, São Domingos, Parque Estadual de Terra Ronca (PETER), 46°22'25.23"W 13°38'42.05"S, isolated from the air in Sambaíba Cave, 30 Nov. 2020 (HUEG-Fungi 18534, holotype), ex-type SXS 977.

GenBank numbers – HUEG 18534: ITS = OR944932, LSU = PQ643659, *rpb2* = PQ885599, *tef1-α* = PQ885598.

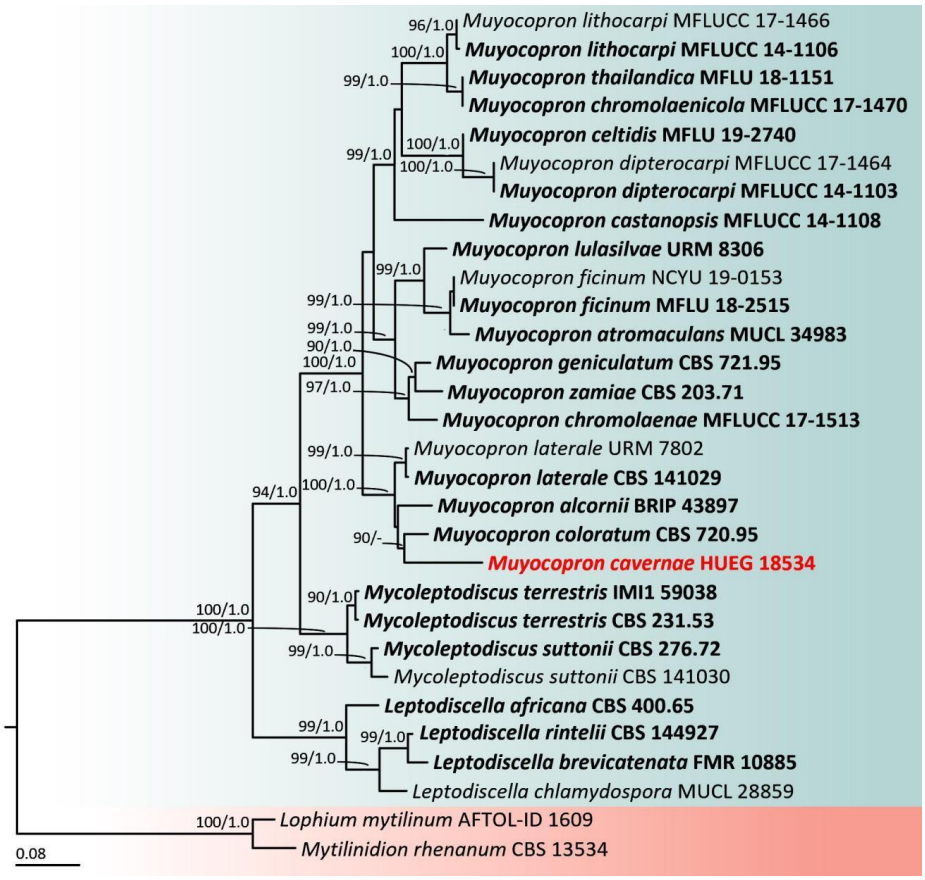


Figure 31 – Phylogram generated from maximum likelihood analysis based on combined ITS, LSU, *rpb2*, and *tef1-α* sequence data from 30 taxa, comprising 3,272 characters with gaps (ITS = 666, LSU = 876, *rpb2* = 847, *tef1-α* = 883). The best-scoring RAxML tree with a final likelihood value -18156.088 is presented. The matrix contained 1,278 distinct alignment patterns, with 28.73% of the characters being undetermined or gaps. Estimated base frequencies were as follows: A = 0.235, C = 0.273, G = 0.281, T = 0.110; substitution rates: AC = 1.326, AG = 3.429, AT = 1.326, CG = 1.000, CT = 8.253, GT = 1.0; gamma distribution shape parameter α = 0.439. Bootstrap support values for maximum likelihood (ML) equal to or greater than 70% and clade credibility values greater than 0.90 (rounded to two decimal places) from Bayesian inference analysis are labelled at each node. Ex-type strains are in bold, while the new isolate is indicated in red bold. The tree is rooted to *Lophium mytilinum* (AFTOL-ID 1609) and *Mytilinidin rhenanum* (CBS 13534).

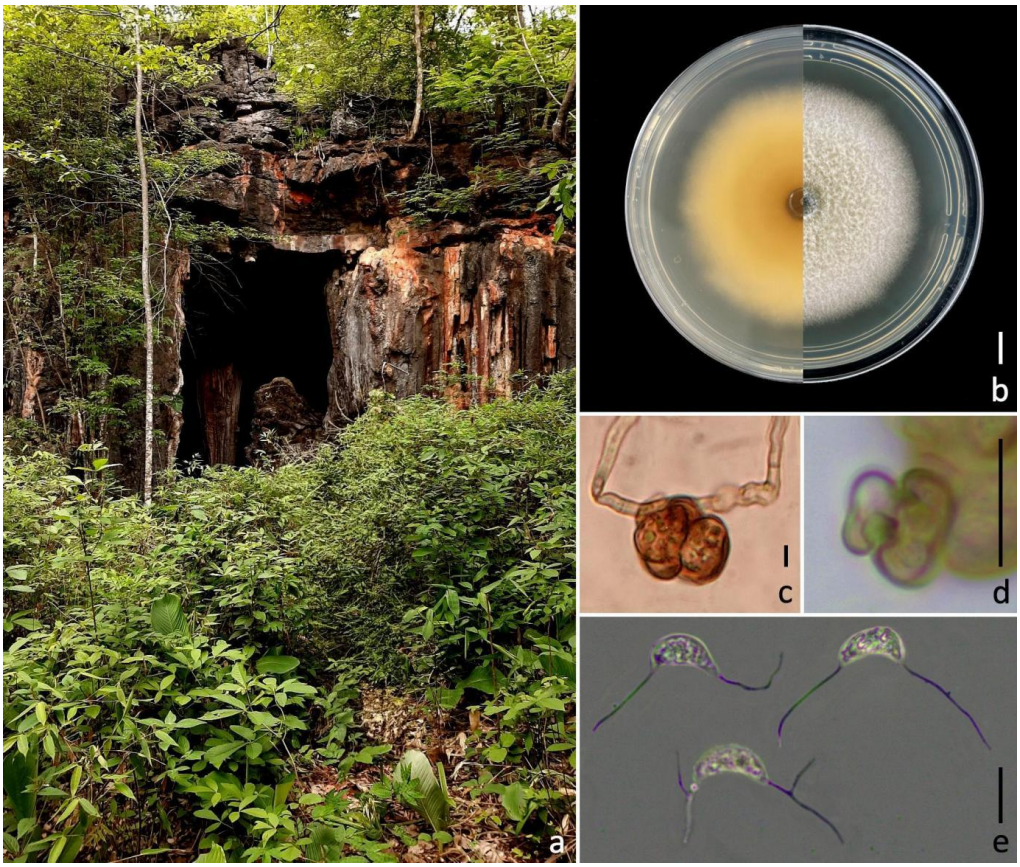


Figure 32 – *Muyocopron cavernae* (HUEG 18534). a Lapa de Sambaíba cave, where *Muyocopron cavernae* was isolated, in the Parque Estadual de Terra Ronca (PETER), Goiás, Brazil. b Colony producing conidia on nutrient-poor agar medium after two weeks. c Conidiogenous cells, d Appresoria. e Conidia. Scale bars: b = 1 cm, c–e = 10 µm.

Notes – *Muyocopron cavernae* was isolated from Lapa Sambaíba, a small cave approximately 600 metres in length, rarely visited by tourists and adventurers. The cave is characterized by a large opening and is situated within the semi-deciduous forest of the Cerrado biome. The phylogenetic analysis based on a combined dataset of ITS, LSU, *rpb2*, and *tef1-α* sequences reveals that the new collection is closely related to *M. coloratum* (Fig. 31). Base pair comparisons between the new species and the type strain of *M. coloratum* showed 19 % differences (95/503 bp, including 33 gaps) in the ITS locus, 0.9% (5/552 bp, without gaps) in the LSU locus, 36% (138/380 bp, without gaps) in the *rpb2* locus, and 4.7% (32/672 bp, without gaps) in the *tef1-α* locus. *Muyocopron cavernae* clustered phylogenetically closely with *M. coloratum* and *M. laterale*, based on ITS and *rpb2* phylogenetic analyses, and with *M. lithocarpi*, based on *tef1-α* phylogenetic analysis (data not shown). However, morphologically, our new species differs from the other members of the clade by exhibiting smaller conidia and longer appendages than those observed in *M. coloratum* and by lacking the lateral appendages present in *M. laterale.* Based on both morphological characteristics and phylogenetic analyses, we introduce our new collection as a new species, *Muyocopron cavernae*.

Dothideomycetes *genera incertae sedis*

Neottiosporina Subram., Proc. Natl. Inst. Sci. India, B 27: 238 (1961)

Index Fungorum number: IF9117

Neottiosporina was first established by Subramanian (1961) to accommodate *N. apoda* (basionym *Cryptostictis apoda*). It was later redescribed by Sutton & Alcorn (1974), and five species were added. The genus is characterized by separate, globose, black pycnidia, simple conidiophores, and septate, hyaline, fusiform conidia with gelatinous appendages of variable

shapes. Sutton (1980) accepted eight species in *Neottiosporina*, but none of them have molecular data available. Nag Raj (1993) discussed the differences between *Neottiosporina* and other morphologically similar genera, including *Allneottiosporina*, *Stagonospora*, *Tiarospora*, and *Tiarosporella*. *Paralloneottiosporina* is another newly introduced, morphologically similar genus that formed a sister group to *Alloneottiosporina* (Zeng et al. 2022). Phylogenetic results from the studies by Bhagya et al. (2024) and Tan & Shivas (2022b) suggested that *Neottiosporina* is closely related to the family *Massarinaceae*. According to Index Fungorum (2025), a total of 13 records are listed under *Neottiosporina.* Among them, *N. humerispora* and *N. infundibularis* were moved out. Wimalasena et al. (2025) introduced a new species of *Neottiosporina*, which was found as an endophytic fungus inhabiting aquatic plant species.

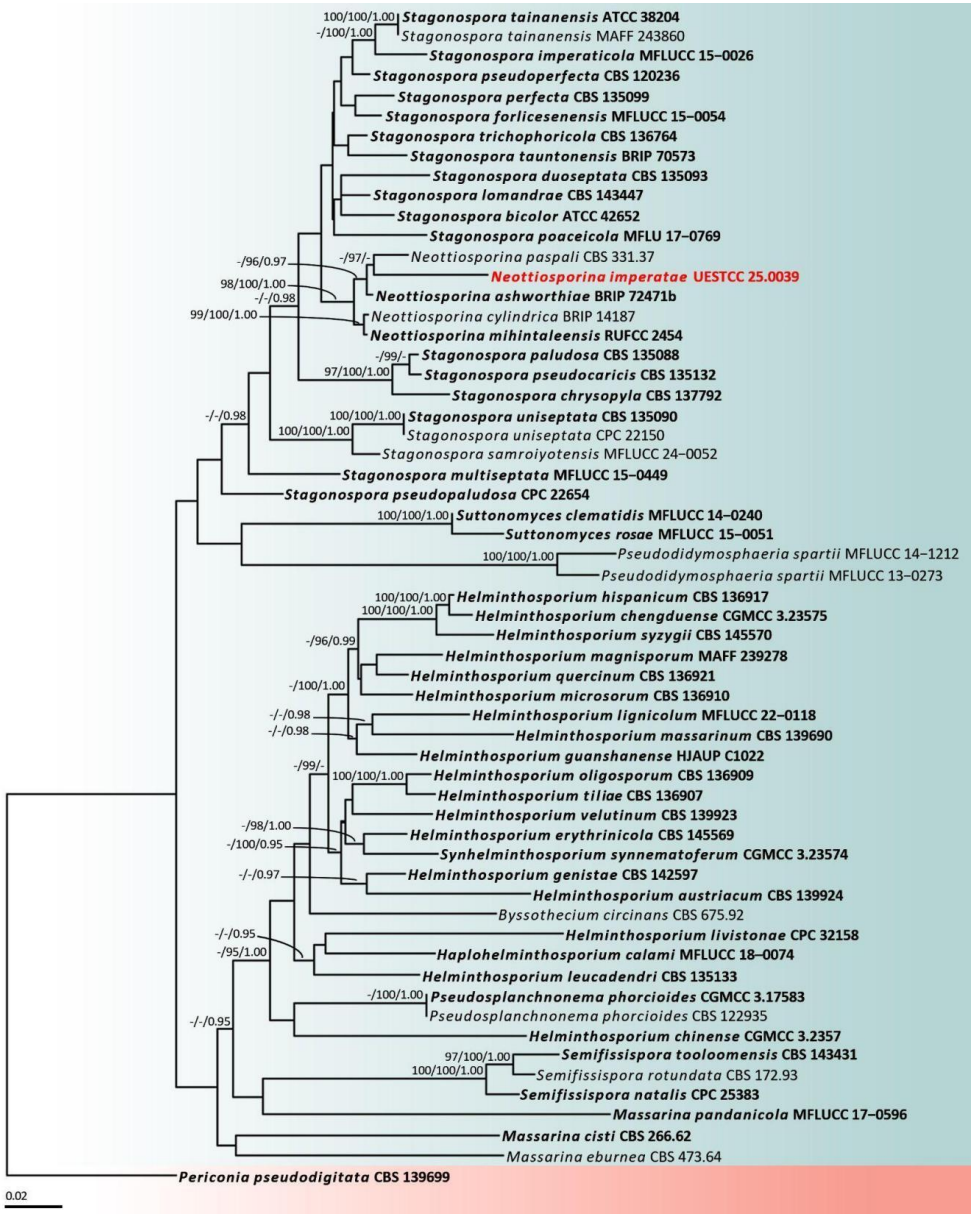


Figure 33 – Phylogram generated from maximum likelihood analysis based on combined SSU, ITS, LSU, *tef1-α*, and *rpb2* sequence data from 58 taxa, comprising 4,633 characters (SSU = 1,026, ITS = 546, LSU = 855, *tef1-α* = 1,116, *rpb2* = 1,090). The best-scoring ML tree with a final likelihood value of -26350.538 is presented. The matrix contained 1,593 distinct alignment patterns, with 40.76% of the characters being undetermined or gaps. Estimated base frequencies were as follows: A = 0.239, C = 0.248, G = 0.270, T = 0.244; substitution rates: AC = 1.617, AG = 4.390, AT = 1.636, CG = 0.976, CT = 8.207, GT = 1.0; gamma distribution shape parameter α = 0.178. Ultrafast bootstrap support values for maximum parsimony (MP) and maximum likelihood

(ML), and analyses equal to or greater than 95% and clade credibility values greater than 0.95 (rounded to two decimal places) from Bayesian inference analysis are labeled at each node. Ex-type strains are in bold, while the new isolate is indicated in red bold. The tree is rooted to *Pericnia pseudigitata* (CBS 139699).

Neottiosporina imperatae Y.P. Chen & Maharachch., sp. nov. Fig. 34

Index Fungorum number: IF555558; Facesoffungi number: FoF05264

Etymology – Refers to the host genus *Imperata* from which the species was isolated.

Holotype – HUEST 25.0034

Associated with disease symptoms on decaying stems of *Imperata cylindrica* (L.) P. Beauv. Sexual morph: Undetermined. Asexual morph: *Conidiamata* up 281 μm diam., pycnidial, immersed, solitary, black, conical. *Wall* composed of dark brown, pseudoparenchymatous cells, imperforate ostiole. *Conidiogenous cells* 5.8–18.0 × 1.9–5.7 μm ($\overline{x}$ = 13.3 × 3.5 μm, n = 30), produced from the inner cells lining the pycnidial wall, solitary, hyaline, holoblastic, determinate, short, cylindrical. *Conidia* 15.3–20.5 × 3.3–4.5 μm ($\overline{x}$ = 17.6 × 4.1 μm, n = 30), acrogenous, solitary, cylindrical, straight or slightly bent, hyaline, 1–2-septate, smooth-walled.

Culture characteristics – Conidia germinated on PDA within 12 hours at 25 °C in darkness. Colonies white to pale brown, circular, velvety, with distinct growing rings and slightly raised central area, reaching approximately 35 mm in diam., on PDA, after 17 days of incubation at 25 °C. On the reverse side, colonies were bright orange, dense, and exhibited a radiating, slightly wrinkled texture, with smooth and well-defined margins.

Material examined – China, Sichuan Province, Mianyang City, Zitong County, Shuangbanzheng, 31°49'40" N, 105°3'11" E, elevation 655 m, on decaying stems of *Imperata cylindrica* (L.) P. Beauv. (*Poaceae*) exhibiting distinct disease symptoms, 25 May 2022, P.W. Su, SBZ.S1 (HUEST 25.0034, holotype), ex-type UESTCC 25.0039.

GenBank numbers – UESTCC 25.0039: SSU = PQ891846, ITS = PQ891845, LSU = PQ891847, *tef1-α* = PQ999206, *rpb2* = PQ999207.

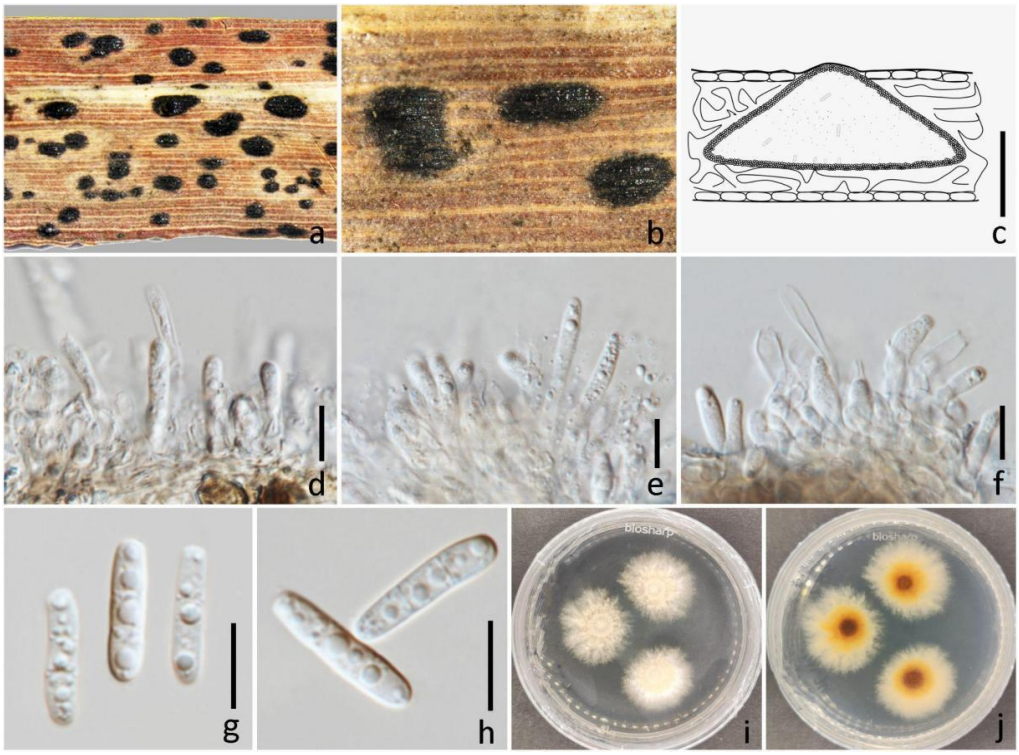


Figure 34 – *Neottiosporina imperatae* (HUEST 25.0034, holotype). a, b Conidiomata on host stems. c Drawing shows a vertical section of a pycnidial conidioma. d–f Conidiogenous cells and

developing conidia. g, h Conidia. i, j Cultures on PDA, front and back sides, after 17 days. Scale bars: f = 100 µm, d–h = 10 µm.

Notes – In combined SSU, ITS, LSU, *tef1-α*, and *rpb2* phylogenetic analysis (Fig. 33), our new collection developed a sister clade to *N. paspali.* Morphologically, our collection has the typical characteristics of *Neottiosporina*, including immersed pycnidial conidiomata, acrogenous, hyaline, and cylindrical conidia. In addition, our species develops distinct lesions, which are typical diseases caused by *Neottiosporina* species in *Poaceae* (Sutton & Alcorn 1974, Sutton & Marasas 1976, Sutton & Wu 1995). However, the conidia of *N. imperatae* are shorter than *N. paspali* (15.3–20.5 × 3.3–4.5 µm vs. 26–33 × 6.5–8 µm) (Sutton & Alcorn 1974). *Neottiosporina imperatae* also differs from other *Neottiosporina* species in the absence of appendages in conidia. The base pair difference between the ITS locus of the new species and *N. paspali* (CBS 331.37) was 7 % (35/494 bp, no gaps), while the differences in the SSU, LSU, *tef1-α* and *rpb2* regions were 0% (0/505 bp), 1.5% (13/851 bp, no gaps), 4.88% (42/860 bp, 2 gaps), and 6.80% (66/971 bp, no gaps), respectively. Based on these, we introduce our collection as a new species.

Class Eurotiomycetes O.E. Erikss. & Winka
Subclass Chaetothyriomycetidae Doweld
Chaetothyriales M.E. Barr
Chaetothyriaceae Hansf. ex M.E. Barr
Ceramothyrium Bat. & H. Maia, Publicações Inst. Micol. Recife 23(1–3): 5 (1956)

Index Fungorum number: IF880

Ceramothyrium was introduced by Batista & Maia (1956), and typified by *C. paivaeae*. Currently, there are 44 records in Index Fungorum (2025). Species in this genus are commonly found on leaves (Chomnunti et al. 2012, Zeng et al. 2016, Tennakoon et al. 2019). *Ceramothyrium* is characterized by a mycelial pellicle that covers the ascomata without setae, and hyaline, multi-septate to muriform ascospores (Chomnunti et al. 2012, Zeng et al. 2016, Tennakoon et al. 2019).). Prof. Kevin D. Hyde's contributions to the study of *Ceramothyrium* have been pivotal in the 21st century. Through his continued research, he has not only expanded our understanding of *Ceramothyrium* but has also played a key role in discovering new representative species within this genus. Of the 44 species currently listed in Index Fungorum, Prof. Kevin D. Hyde and his collaborators have introduced five species. His work, particularly in epifoliar fungi, has greatly advanced the field of fungal taxonomy. In recognition of his outstanding contributions to mycology, herein we introduce *Ceramothyrium hydei*, which has been named in honor of Prof. Kevin D. Hyde. We also provide the updated phylogenetic tree for *Ceramothyrium* (Fig. 35).

Ceramothyrium hydei T. Yang & X.Y. Zeng, sp. nov. Fig. 36

Index Fungorum number: IF903726; Facesoffungi number: FoF17755

Etymology – 'hydei' named in honor of the renowned mycologist Kevin D. Hyde, recognizing his significant contributions to mycology on the occasion of his 70th birthday.

Holotype – HGUP 23–0075

Epiphytic on leaves of *Cinnamomum* and *Eriobotrya*. Sexual morph: *Mycelial pellicle* subiculum-like, brown, reticulate, slightly constricted at septa, radiating outwards, anastomosing at central ostiole, with cells of the hyphal network. *Ascomata* 110–177 µm ($\overline{x}$ = 137 µm, n = 60) in diam., superficial, solitary, scattered, coriaceous, dark brown, flat spherical to subglobose. *Peridium* brown, with compressed hyaline inner cells of *textura prismatica*, and brown outer cells of *textura angularis*. *Asci* 31–53 × 15–23 µm ($\overline{x}$ = 42 × 19 µm, n = 10), 8-spored, bitunicate, obovoid to pyriform, with short pedicellate. *Ascospores* 13.2–15.7 × 6.5–7.6 µm ($\overline{x}$ = 14.5 × 7.0 µm, n = 20), 2-seriate, hyaline, oblong to ellipsoid, muriform, with 3 transversal septa and 2 longitudinal septa, slightly constricted at the septum, without a mucilaginous sheath. Asexual morph: Undetermined.

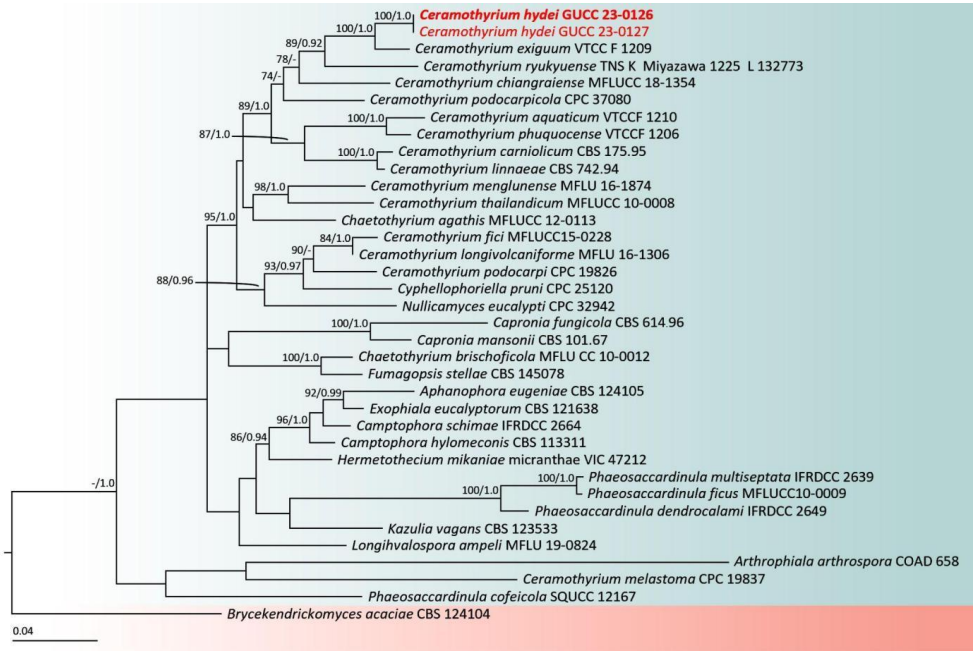


Figure 35 – Phylogram generated from maximum likelihood analysis based on combined ITS and LSU sequence data from 36 taxa, comprising 1,226 characters (ITS = 430, LSU = 836). The best-scoring ML tree with a final likelihood value of -8701.314 is presented. The matrix contained 422 distinct alignment patterns, comprising 840 invariant sites and 304 parsimony-informative sites. The best substitution model for ITS and LSU is TIM2e+I+G4 and TIM3e+I+G4, respectively. The estimated base frequencies for both ITS and LSU were equal. The rate parameters were as follow: ITS: AC = 3.492, AG = 3.943, AT = 3.493, CG = 1.000, CT = 9.777, GT = 1.0; LSU: AC = 0.549, AG = 2.465, AT = 1.000, CG = 0.549, CT = 4.471, GT = 1.0. Bootstrap support values for maximum likelihood (ML) equal to or greater than 70% and clade credibility values greater than 0.90 (rounded to two decimal places) from Bayesian inference analysis are labelled at each node. Ex-type strains are in bold, while the new isolates are indicated in red. The tree is rooted to *Brycekendrickomyces acaciae* (CBS 124104).

Material examined – China, Guizhou Province, Guiyang City, on leaves of *Cinnamomum* (*Lauraceae*), 23 April 2023, YW Liu, AH-4 (HGUP 23–0075, holotype), ex-type GUCC 23–0126; *ibid*., on leaves of *Eriobotrya japonica* (*Rosaceae*), 23 April 2023, YW Liu, QLS 3–2 (HGUP 23–0076), living culture GUCC 23–0127.

GenBank numbers – GUCC 23–0126: ITS = PQ877372, LSU = PQ877373; GUCC 23–0127: ITS = PQ871495, LSU = PQ871496.

Notes – Two strains (GUCC 23–0126 and GUCC 23–0127) from this study formed a distinct clade, sister to *Ceramothyrium exiguum* (VTCC F 1209), within the *Ceramothyrium* in ITS and LSU phylogenetic tree (Fig. 35). The type strain of our new species showed 9.3% differences (45/484 bp, 15 gaps) in the ITS locus and 1.85% differences (10/542 bp, 4 gaps), in the LSU locus compared to its sister species, *C. exiguum*. Morphologically, our collection is similar to four known *Ceramothyrium* species in terms of ascomata, ascus, and ascospore size. It has smaller ascomata and ascospores than *C. chiangraiense* (ascomata: 185–210 µm in diam., ascospores: 20–30 × 5–9 µm) (Wijesinghe et al. 2019), smaller ascomata, asci and ascospores than *C. menglunense* (ascomata: 245–255 µm in diam.; asci: 50–75 × 24–37 µm, ascospores: 25–35 × 10–12 µm) (Hyde et al. 2016), smaller asci and ascospores than *C. lycopodii* (asci: 50 × 30 µm, ascospores: 45 × 4 µm) (Constantinescu et al. 1989), and larger ascomata, asci and ascospores than *C. ryukyuense* (ascomata: 80–110 µm in diam., asci: 20–30 × 13–17 µm, ascospores: 8.7–13.8 × 3.4–4.9 µm) (Miyazawa et al. 2024). We hereby introduce our collections (GUCC 23–0126 and GUCC 23–0127) as *Ceramothyrium hydei* sp. nov., based on morphological comparisons and phylogenetic analysis results.

Class Lecanoromycetes O.E. Erikss. & Winka
Subclass Ostropomycetidae V. Reeb, Lutzoni & Cl. Roux
Graphidales Bessey
Graphidaceae Dumort.
Diorygma Eschw., Syst. Lich.: 25 (1824)

Index Fungorum number: IF1593; Facesoffungi number: FoF17756

Diorygma was described by Eschweiler (1824); however, no type species was designated at that time. Eschweiler merely mentioned *Opegrapha hieroglyphica* as a possible member of the genus and provided an illustration of another species, *D. tinctorium*. When Hawksworth & Sherwood (1981) suggested placing *Diorygma* under *Graphina*, they stated that the holotype of *Diorygma* was *D. tinctorium*. Later, Staiger (2002) synonymized *O. hieroglyphica* with *D. hieroglyphicum*, and formally designated *D. hieroglyphicum* as the lectotype. The genus is widely distributed, primarily found in tropical regions, and often thrives on the sheltered or overhanging sides of trees (Staiger 2002, Kalb et al. 2004). *Diorygma* is characterized by a crustose, white to pale olive green thallus and lirelliform to irregularly rounded ascomata with a pruinose disc; uncarbonized or slightly carbonized exciple; hyaline hymenium, not inspersed, branched or anastomosing paraphyses with a thick gelatinous wall; asci clavate, 1–8-spored; ascospores hyaline (rarely brownish), transversely septate to mostly muriform; produce substances such as norstictic or stictic acid or the protocetraric acid complex (Kalb et al. 2004, Li & Jia 2016, Aptroot et al. 2023).

In honor of Prof. Kevin D. Hyde's exceptional contributions to mycology, we introduce *Diorygma hydei* sp. nov. Additionally, we present a phylogenetic tree for *Graphidaceae* (Fig. 37), which supports the distinction of *D. hydei* as a single, unique species. This designation is based on its notably broad disc and distinctive chemical profile, confirming its status as a new species.

Diorygma hydei Meng & Wei Wu, sp. nov. Fig. 38

Index Fungorum number: IF903728; Facesoffungi number: FoF17757

Etymology – 'hydei' named in honor of the renowned mycologist Kevin D. Hyde, recognizing his significant contributions to mycology on the occasion of his 70th birthday.

Holotype – KUN-L0093722

Thallus corticolous, continuous, crustose, thin, and tightly attached to the substrate, with crystals present. Surface pale grey to greenish-grey, rough, dull, and lacking isidia or soredia; prothallus absent. *Ascomata* 1–4 × 0.5–2 mm, lirellate, oblong to elongated, ± flexuous, either simple or branched. *Discs* irregularly wide open, covered with a white pruina, and surrounded by entire, raised, swollen margins that are noticeably higher than the thallus surface. *Exciple* uncarbonized, not convergent, brownish both basally and laterally. *Epihymenium* 40–74 µm tall, brown, with crystals. *Hymenium* 250–310 µm tall, hyaline, non-inspersed, I+ violet. *Paraphyses* 1–2.5 µm wide, filiform, non-septate. *Hypothecium* 40–58 µm tall, brown. *Asci* 132–245 × 36–53 µm, fusiform to cylindrical, with an apically thickened wall when young, thinning as they mature, I–. *Ascospores* (86–)150–202(–238) × (32–)36–47(–50) µm ($\bar{x}$ = 176 × 42 µm, n = 20), 1–2 per ascus, hyaline, richly muriform, with peripheral and central locules approximately equal in size, 14–46/5–12 locular, I+ yellow. Pycnidia not seen.

Chemistry – Thallus K+ reddish brown, C–, KC+ yellow, P+ yellow, TLC: Constictic acid, salazinic acid, norstictic acid.

Material examined – China, Guizhou Province, Zunyi City, Zhengan County, Fuyan Nature Reserve, 28°46'4.82″N, 107°15'52.76″E, elev. 1373m, 10 May 2023, Shao-Bin Fu, ZA202 (KUN-L0093722, holotype).

GenBank numbers – KUN-L0093722: LSU = PQ810862, PQ810863; mtSSU = PQ810860, PQ810861.

Notes – The phylogenetic analysis of combined LSU and mtSSU sequences reveals that the new collection is closely related to *Diorygma tiantaiense* (Fig. 37). While the two species share similar ascospore size and characteristics, our collection can be distinguished by its 1–2-spored

asci, whereas *D. tiantaiense* consistently has 1-spored asci. Additionally, our collection exhibits a P+ yellow thallus reaction and a distinct chemical profile containing constictic acid, salazinic acid, and norstictic acid, whereas *D. tiantaiense* shows a P+ yellow to red reaction and contains only norstictic acid.

The members of *Diorygma* are divided into eight groups based on the number of ascospores per ascus: 1-spored, 4-spored, 8-spored, 1–2-spored, 1–4-spored, 2–4-spored, 4–6-spored, and 4–8-spored. Eleven species are included in the 1–2-spored group and are further divided into three subgroups based on ascospore size: those less than 100 µm long, those 100–150 µm, and those longer than 150 µm. The new species, with ascospores longer than 150 µm, closely resembles *D. excipuloconvergentum* in ascospore length, ascomatal size, and the presence of three chemical compounds (constictic, norstictic, and salazinic acids). However, it differs in having a wider disc (0.5–2 vs. 0.1–0.25 mm) and by lacking two additional chemical compounds: cryptostictic acid and methylstictic acid.

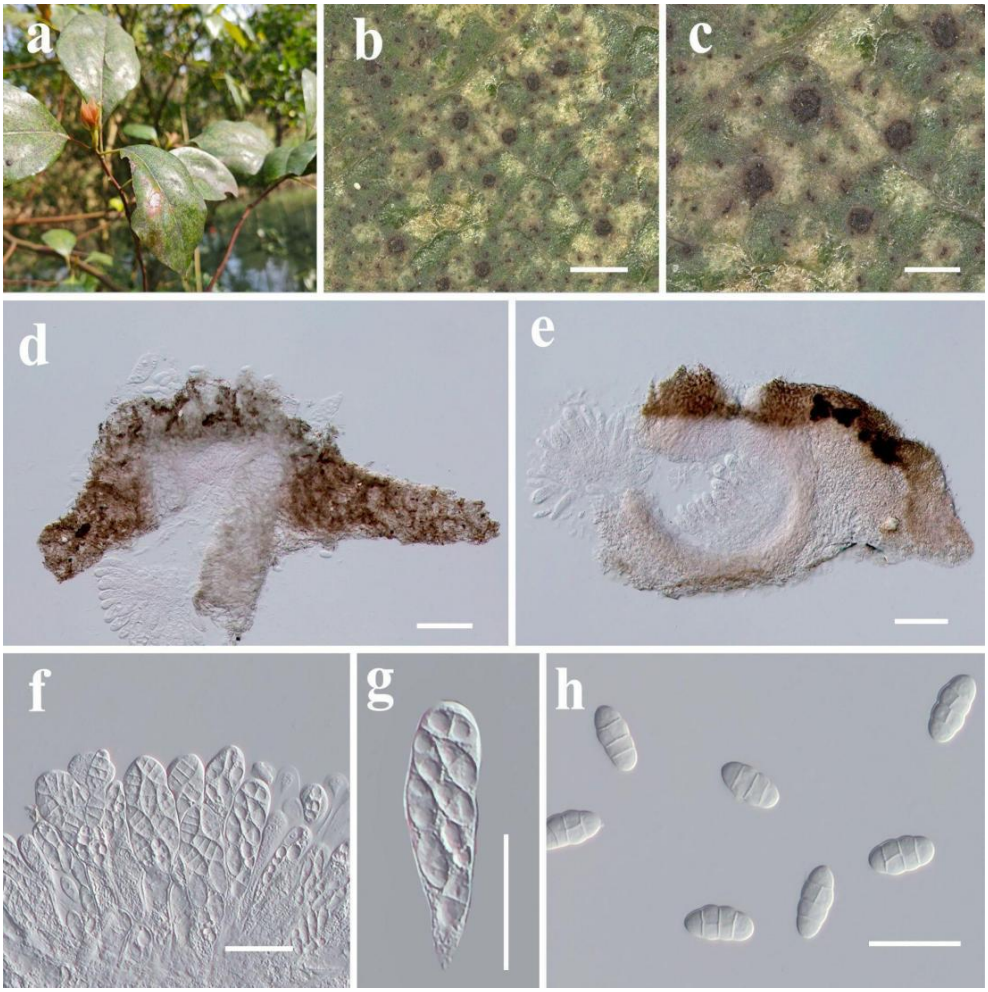


Figure 36 – *Ceramothyrium hydei* (HGUP 23–0075, holotype). a Host. b–c Ascostromata on the surface of the leaf. d–e Ascostroma. f–g Asci. h Ascospores. Scale bars: b = 500 µm, c = 250 µm, d–g = 50 µm, h = 20 µm.

Ostropales Nannf

Stictidaceae Fr.

Ostropomyces Thiyagaraja, Lücking, Ertz & K.D. Hyde, 2021

Index Fungorum number: IF556555; Faces of Fungi number: FoF 09511

The genus *Ostropomyces* was established by Thiyagaraja et al. (2021) to accommodate *O. pruinosellus* as the type species, along with *O. thailandicus.* This genus includes both the sexual

morph (*O. pruinosellus*) and the asexual morph (*O. thailandicus*), both of which were collected from unidentified stems in Thailand (Thiyagaraja et al. 2021). Later, another new species, *O. yunnanensis*, was introduced by Gao et al. (2024), bringing the total number of species in this genus to three (Index Fungorum 2025). Wei et al. (2021) expanded the knowledge of this genus through molecular analysis, utilizing ITS, LSU, and mtSSU sequence data to report new collections of *O. pruinosellus* and *O. thailandicus* from Thailand, as well as providing their cultural characteristics on PDA medium. Later, Lu et al. (2021) reported the asexual morph of *O. pruinosellus* on *Arabica coffee* in Yunnan Province, China, which expanded the geographical distribution of the genus. Most recently, Gao et al. (2024) enriched the genus by introducing a third species, *O. yunnanensis*, discovered on decaying stems of herbaceous plants in Yunnan Province, China. *Ostropomyces* is predominantly saprobic, inhabiting decaying wood and terrestrial environments (Lu et al. 2021, Thiyagaraja et al. 2021, Wei et al. 2021, Gao et al. 2024). The sexual morph of this genus is characterized by immersed ascomata with long-cylindrical, cylindrical, unitunicate, and thick-walled asci and filiform, multi-septate ascospores (Lu et al. 2021, Thiyagaraja et al. 2021, Wei et al. 2021). The asexual morph is characterized by erumpent pycnidia with ostioles, filiform, hyaline conidia, and guttulate at maturity (Lu et al. 2021, Thiyagaraja et al. 2021, Wei et al. 2021, Gao et al. 2024).

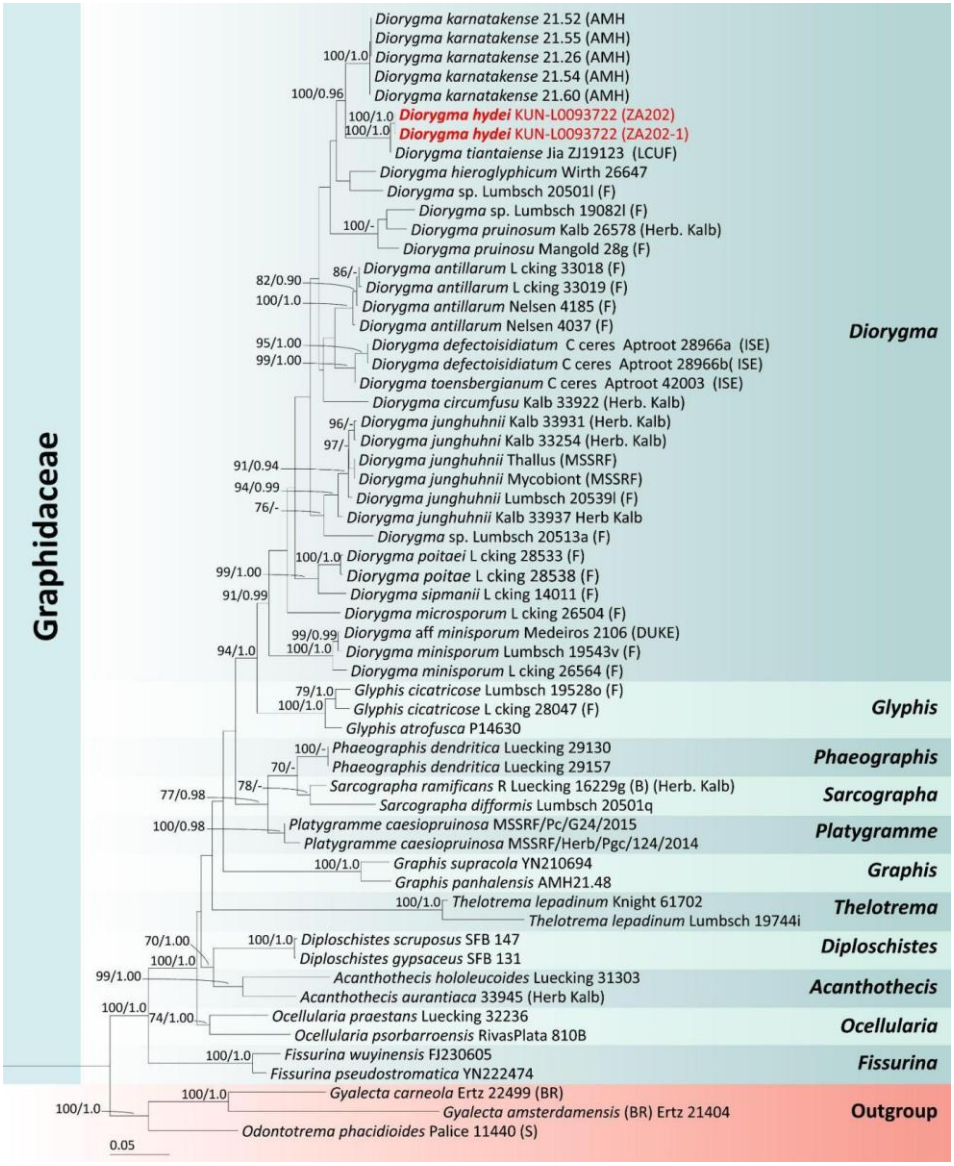


Figure 37 – Phylogram generated from maximum likelihood analysis based on combined LSU and mtSSU sequence data from 59 taxa, comprising 1,709 characters (LSU = 927, mtSSU = 782). The

best-scoring RAxML tree with a final likelihood value of -14131.033 is presented. The matrix contained 1,244 distinct alignment patterns, with 26.17% of the characters being undetermined or gaps. Estimated base frequencies were as follows: A = 0.292, C = 0.185, G = 0.265, T = 0.258; substitution rates: AC = 0.783, AG = 2.843, AT = 1.721, CG = 0.697, CT = 6.167, GT = 1.0; gamma distribution shape parameter α = 0.385. Bootstrap support values for maximum likelihood (ML) equal to or greater than 70% and clade credibility values greater than 0.90 (rounded to two decimal places) from Bayesian inference analysis are labeled at each node. New species are in red bold. The tree is rooted with *Gyalecta amsterdamensis* (BR Ertz 21404), *G. carneola* (BR Ertz 22499), and *Odontotrema phacidioides* (S Palice 11440).

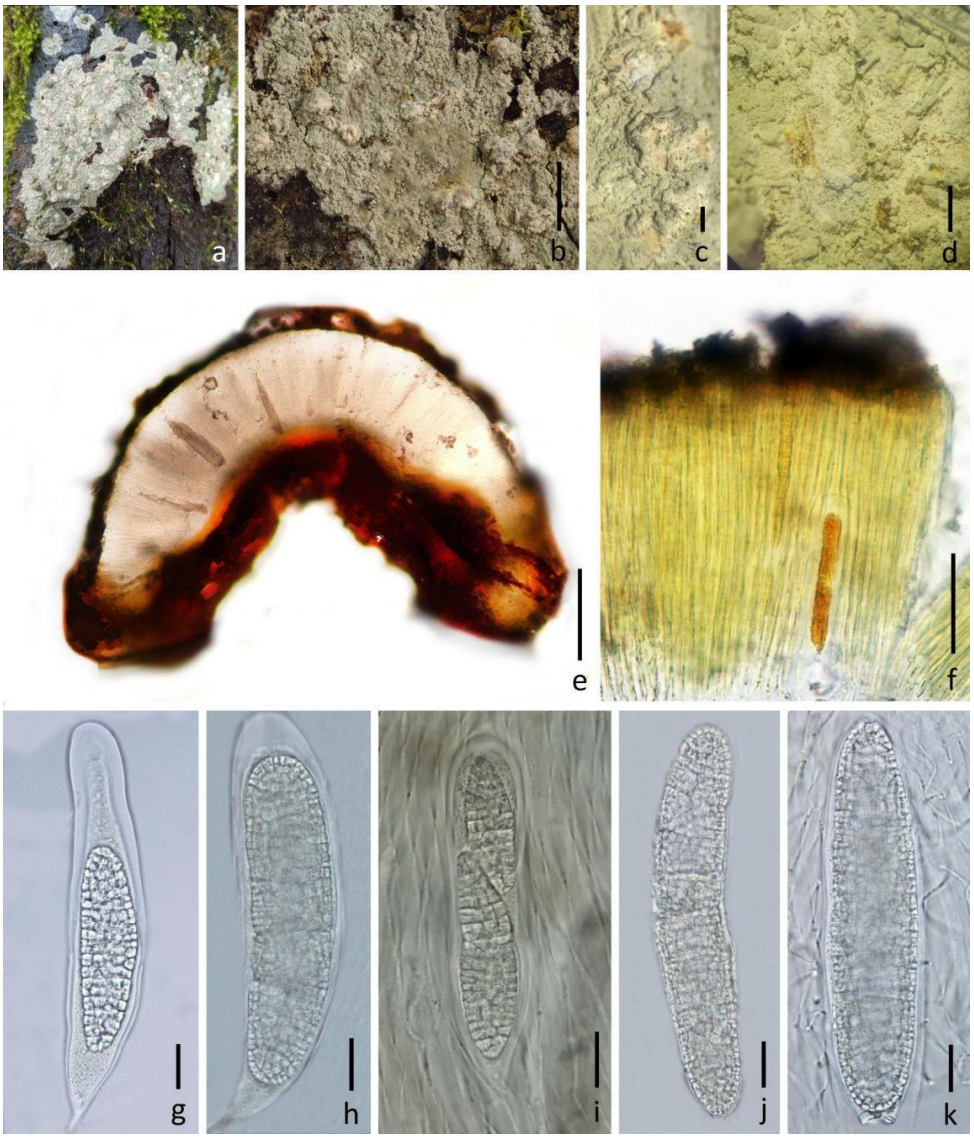


Figure 38 – *Diorygma hydei* (KUN-L0093722, holotype). a–d Thallus with ascomata. e Cross-section of apothecium. f Paraphyses. g–i Asci. j, k Ascospores (in water). Scale bars: b–d = 1 mm, e = 200 µm, f = 100 µm, g–k = 20 µm.

Out of the three species currently listed in Index Fungorum (2025), Prof. Kevin D. Hyde and his collaborators have described two new species. In recognition of his outstanding contributions to mycology, herein we introduce the fourth species, *Ostropomyces hydei*, which was named in honor of Prof. Kevin D. Hyde, commemorating his significant and enduring contributions to the study of *Ostropomyces* and mycology. We also provide the updated phylogenetic tree for *Ostropomyces* (Fig. 39).

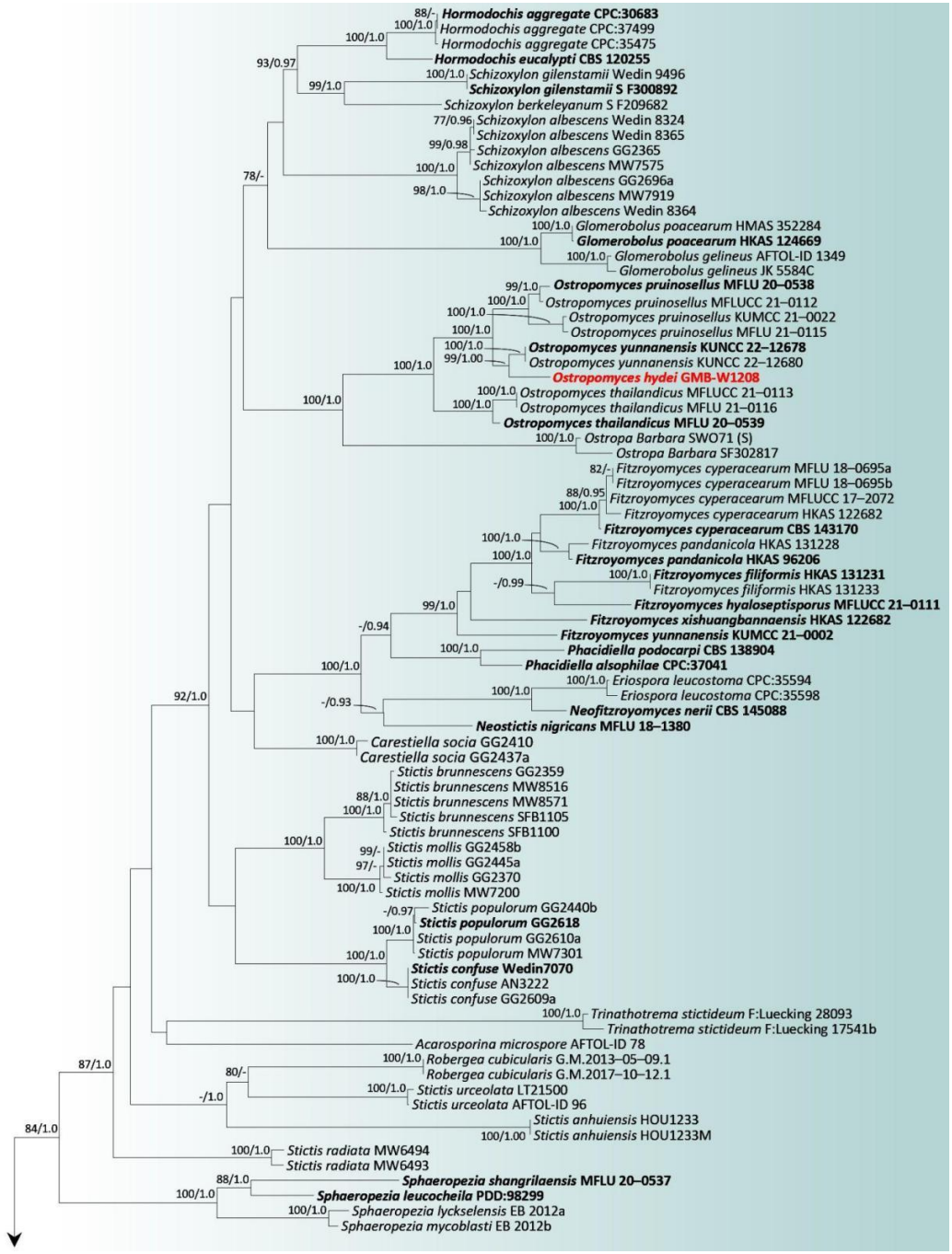


Figure 39 – Phylogram generated from maximum likelihood analysis based on combined ITS, LSU, and mtSSU sequence data from 110 taxa, comprising 2,257 characters (ITS = 597, LSU = 880, mtSSU = 780). The best-scoring RAxML tree with a final likelihood value of -30659.138 is presented. The matrix contained 1,515 distinct alignment patterns, with 29.34% of the characters being undetermined or gaps. Estimated base frequencies were as follows: A = 0.286, C = 0.208, G = 0.256, T = 0.250; substitution rates: AC = 1.084, AG = 2.420, AT = 2.028, CG = 0.776, CT = 5.343, GT = 1.0; gamma distribution shape parameter α = 0.384. Bootstrap support values for maximum likelihood (ML) equal to or greater than 70% and clade credibility values greater than 0.90 (rounded to two decimal places) from Bayesian inference analysis are labeled at each node. Ex-type strains are in bold, while the new isolate is indicated in red bold. The tree is rooted to *Orceolina kerguelensis* (Søchting 9398(C)), *Placopsis perrugosa* (KS137) and *Trapelia placodioides* (KS163).

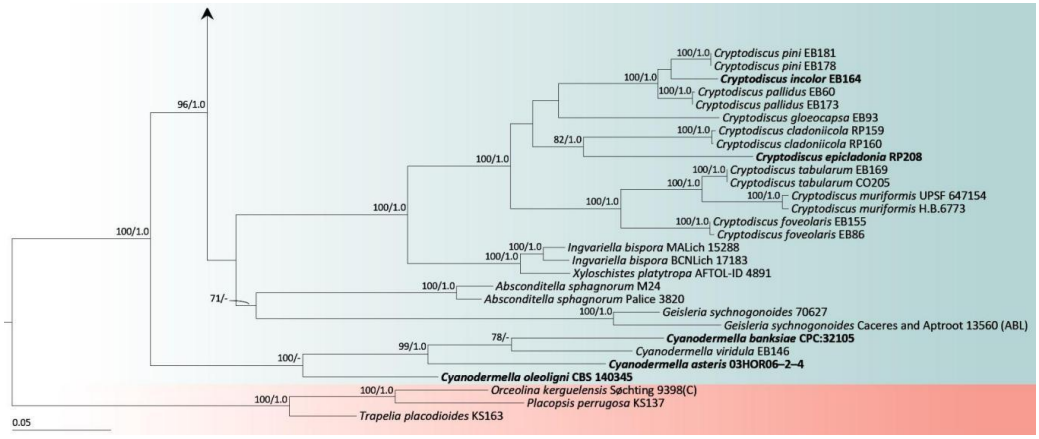


Figure 39 – Continued.

Ostropomyces hydei R.F. Xu, Tibpromma, sp. nov. Fig. 40

Index Fungorum number: IF903585; Facesoffungi number: FoF17618

Etymology – 'hydei' named in honor of the renowned mycologist Kevin D. Hyde, recognizing his significant contributions to mycology on the occasion of his 70th birthday.

Holotype – GMB-W1208

Saprobic on the decaying branch of *Hevea brasiliensis*. Sexual morph: *Ascomata* 435–655 (–705) × 710–975 µm ($\overline{x}$ = 543 × 810 µm, n = 5), perithecia, subglobose, orbicular in cross-section, unilocular, solitary, immersed to erumpent, immersed at first and raising the substrates into small pustules and later opening by entire pores, exposing the discs. *Discs* olivaceous, convex and covered by white pruinose substance. Inner mass creamy-yellow. *Exciple* 115–185 µm wide, composed of two layers, outer layer brown, inner layer hyaline with crystalline inclusions. *Hamathecium* consisted of paraphyses, lying parallel to the substrates. *Paraphyses* 2–3 µm wide ($\overline{x}$ = 2.5 µm, n = 15), hyaline, curve, anastomosing, aseptate, branched and longer than asci. *Asci* 245–455 × 10–19 µm ($\overline{x}$ = 375 × 15, n = 20), 4-spored, unitunicate, cylindrical, thick-walled, with short pedicle. *Ascospores* hyaline, filiform, multi-septate, long as asci and easily disarticulating into part-spores when mature. *Part-spores* 5–11 × 3–5 µm ($\overline{x}$ = 9 × 4, n = 20), oval or oblong, unicellular, with oil droplets. Asexual morph: Undetermined.

Material examined – China, Yunnan Province, Pu'er City, Puwen Town, on a dead branch of *Hevea brasiliensis*, 18 March 2023, Rui-Fang Xu, PWR-34 (GMB-W1208, holotype).

GenBank numbers – GMB-W1208: ITS = PV351455, LSU = PV351456, mtSSU = PV351457.

Notes – In phylogenetic analyses, our newly isolate, *O. hydei* (GMB-W1208) formed a sister branch to *O. yunnanensis* (KUNCC 22–12678 and KUNCC 22–12680) within *Ostropomyces*, with 99% ML bootstrap and 1.00 BYPP support (Fig. 39). Morphologically, *O. hydei* differs from *O. pruinosellus* in having larger ascomata (435–655 × 710–975 µm vs. 230–300 × 300–365 µm), convex discs covered by a white substance (vs. thick pruinose substance in *O. pruinosellus*), and longer asci (245–455 vs. 180–265 µm) (Thiyagaraja et al. 2021). While *O. thailandicus* and *O. yunnanensis* are only known from asexual morphs (Thiyagaraja et al. 2021, Wei et al. 2021, Gao et al. 2024), *O. hydei* was found in its sexual morph, precluding direct morphological comparison. Base pair differences in the ITS, LSU, and mtSSU sequences between *O. hydei* and other *Ostropomyces* species are detailed in Table 1. Based on morphological and phylogenetic evidence, we propose *O. hydei* as a new species.

Class Leotiomycetes O.E. Erikss. & Winka

Subclass Leotiomycetidae P.M. Kirk, P. Cannon, Minter & Stalpers

Helotiales Nannf. ex Korf & Lizoň

Lachnaceae Raitv.

Brunnipila Baral, in Baral & Krieglsteiner, Z. Mykol., Beil. Beih. 6: 49 (1985)

Index Fungorum number: IF25708; Facesoffungi number: FoF99595

Brunnipila was established by Baral & Krieglsteiner (1985), with *B. clandestina* designated as the type species. Currently, *Brunnipila* comprises eleven species (Index Fungorum 2025), that are primarily distributed in Europe, with hosts including *Caprifoliaceae*, *Cyperaceae*, *Fagaceae*, *Onagraceae*, *Poaceae*, *Rosaceae*, and *Solanaceae* (Bulliard 1789, Desmazières 1842, 1845, 1850, Rehm 1893, Baral & Krieglsteiner 1985, Nograsek & Matzer 1991, 1994, Raitviír & Järv 1997, Baral 2015, Læssøe & Petersen 2018, Tochihara et al. 2019, Acar & Karabıyık 2024). *Brunnipila* is characterized by brown, moderately thick-walled, densely granulated hairs with denser septation towards the slightly capitate apex and firmly attached, flat or octahedral crystals on top; the lanceolate, strongly protruding paraphyses consistently lack refractive vacuolar bodies (Acar & Karabıyık 2024). Additionally, we provide an updated phylogenetic tree for *Brunnipila* (Fig. 41).

Table 1 Nucleotide differences in the ITS, LSU, and mtSSU of *O. hydei* (GMB-W1208) compared with *O. pruinosellus*, *O. thailandicus*, and *O. yunnanensis*. "–" indicates no sequence data.

Strains	ITS	LSU	mtSSU
O. pruinosellus **(MFLU 20–0538, holotype)**	2.61% (37/498 bp, 13 gaps)	1.37% (12/875 bp, 3 gaps)	–
O. pruinosellus **(MFLU 21–0115)**	7.91% (39/493 bp, 19 gaps)	0.46% (4/876 bp, 1 gap)	5.94% (45/758 bp, 14 gaps)
O. thailandicus **(MFLU 20–0539, holotype)**	8.43% (42/498 bp, 17 gaps)	2.07% (18/868 bp, 1 gap)	–
O. thailandicus **(MFLU 21–0116)**	7.83% (38/498 bp, 13 gaps)	2.14% (18/840 bp, 1 gap)	11.58% (87/751 bp, 28 gaps)
O. yunnanensis **(KUNCC 22–12678, holotype)**	5.82% (29/498 bp, 12 gaps)	0.46% (4/867 bp, 1 gap)	2.53% (19/750 bp, 5 gaps)

Brunnipila hydei H.L. Su & Q. Zhao, sp. nov. Fig. 42

Index Fungorum number: IF903734; Facesoffungi number: FoF17666

Etymology – 'hydei' named in honor of the renowned mycologist Kevin D. Hyde, recognizing his significant contributions to mycology on the occasion of his 70th birthday.

Holotype – SZU25–009

Saprobic on decayed stems. Sexual morph: *Apothecia* scattered, gregarious, superficial, 1−2 mm in diameter, 0.5−1 mm high when dried, cupulate, stipitate, externally covered with abundant, long and brown hairs. *Disc* concave, surface slightly rough, white to brown. *Margin* involute, clothed with abundant, brown hairs. *Receptacle* cupulate to globose, brown, clothed with abundant, long, brown hairs entirely. *Hairs* 100−200 × 4.9−6.8 µm ($\overline{x}$ = 149 × 5.8 µm, n = 20), cylindric, straight to slightly curved, obtuse, multi-septate, thin-walled, rough, dark brown, some apex crowned by crystal. *Hymenium* 80–105 µm ($\overline{x}$ = 93 µm, n = 12), concave, surface slightly rough, white to light brown. *Medullary excipulum* 25–65 µm ($\overline{x}$ = 45 µm, n = 13) thick, hyaline to pale brown, thin-walled, smooth hyphae of *textura porrecta*, 1.7–4.0 µm ($\overline{x}$ = 2.5 µm, n = 56) in diameter. *Ectal excipulum* 20–35 µm ($\overline{x}$ = 31 µm, n = 10) thick, thick-walled, smooth, *textura angularis-globulosa*, with light brown to hyaline cell of 5.5–12.5 × 4.0–9.5 µm ($\overline{x}$ = 8.8 × 6.8 µm, n = 28). *Paraphyses* 75–105 × 3.1–5.9 µm, ($\overline{x}$ = 89 × 4.6 µm, n = 23), longer than asci, clavate, straight, multi-septate, hyaline, thin-walled, slightly rough-walled, with tapered, obtuse apex. *Asci* 50–58(–60) × (2.6–)2.8–4.0(–4.4) µm ($\overline{x}$ = 54 × 3.5 µm, n = 23), 8-spored, clavate, straight to slightly curved, inoperculate, hyaline, unitunicate, with an amyloid apex and slightly tapered base, croziers absent at the basal septa. *Ascospores* 6.5–9.2 × 1.6–2.5 µm, ($\overline{x}$ =7.7 × 1.9 µm, n = 59), mostly elliptic, few pyriform or bacilliform, aseptate, thin-walled, hyaline, rough, with obtuse ends, most bearing two guttules. Asexual morph: Unknown.

Material examined – China, Tibet Autonomous Region, Yadong County, on decayed stems on unidentified host, 1 July 2022, HL Su, SHL 1244 (SZU25–009, holotype); *ibid.*, SHL 1230 (SZU25–010, paratype).

GenBank numbers – SHL 1244: ITS = PV455902; SHL 1230: ITS = PV455903.

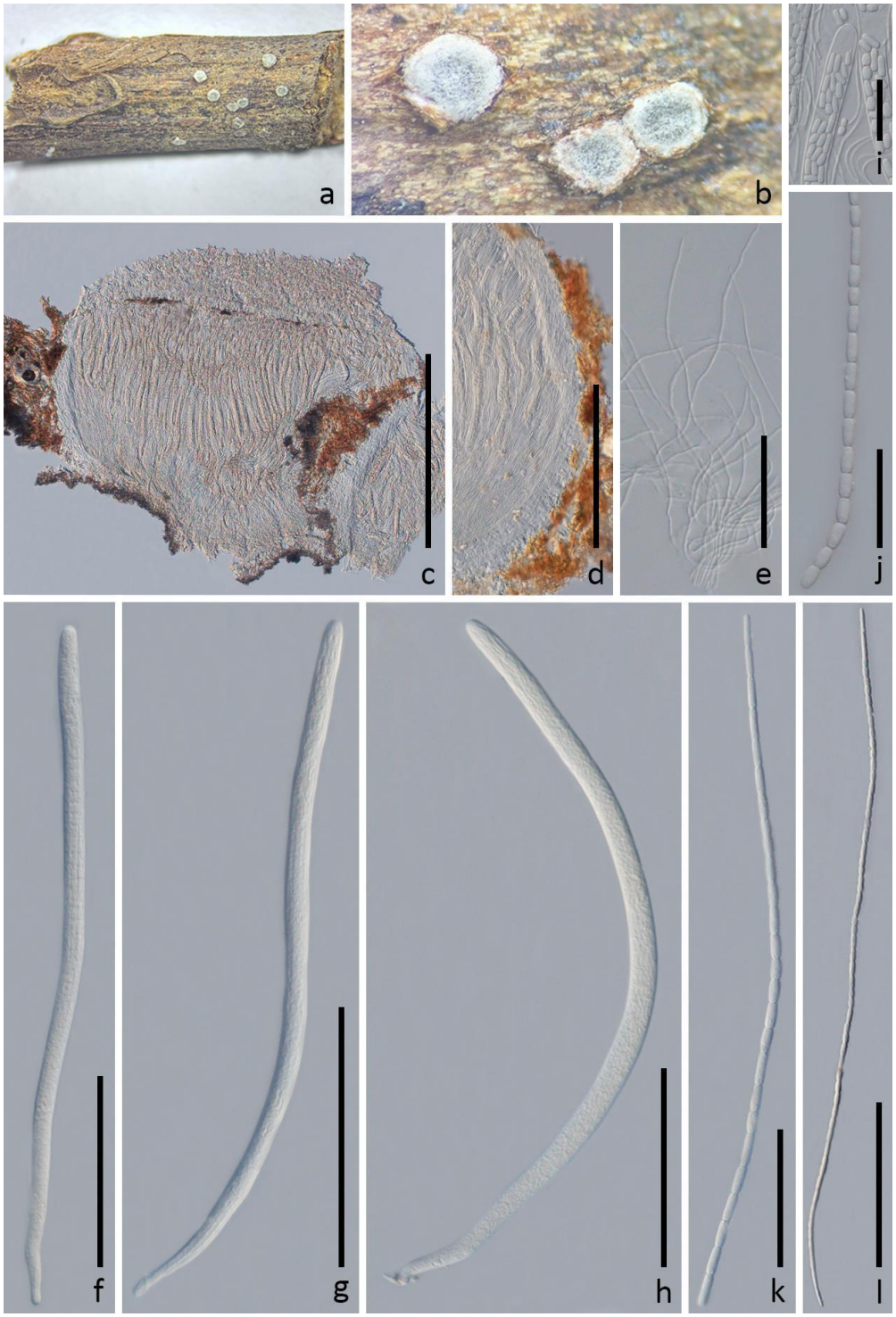


Figure 40 – *Ostropomyces hydei* (GMB-W1208, holotype). a, b ascomata on substrate. c Vertical section of an ascoma. d Exciple. e Paraphyses. f–h Asci. i Part-spores in the asci. j–l Ascospores. Scale bars: c = 200 µm, d, f–h, l = 100 µm, e, k = 50 µm, i, j = 30 µm.

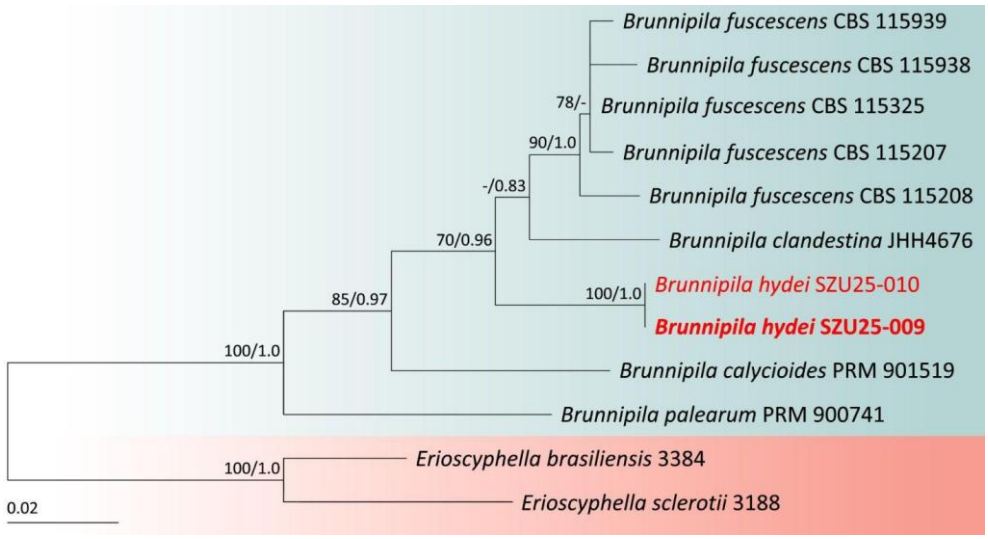


Figure 41 – Phylogram generated from maximum likelihood analysis based on combined ITS sequence data from 12 taxa, comprising 515 characters. The best-scoring RAxML tree with a final likelihood value of -1508.708 is presented. The matrix contained 121 distinct alignment patterns, with 7.46% of the characters being undetermined or gaps. Estimated base frequencies were as follows: A = 0.231, C = 0.242, G = 0.244, T = 0.283; substitution rates: AC = 0.676, AG = 1.665, AT = 0.954, CG = 0.524, CT = 3.308, GT = 1.0; gamma distribution shape parameter α = 0.704. Bootstrap support values for maximum likelihood (ML) equal to or greater than 70% and clade credibility values greater than 0.90 (rounded to two decimal places) from Bayesian inference analysis are labeled at each node. Ex-type strains are in bold, while the new isolates are indicated in red. The tree is rooted to *Erioscyphella brasiliensis* (3384) and *E. sclerotii* (3188).

Notes – In our phylogenetic analysis, the new collection *Brunnipila hydei* clustered with *B. fuscescens* (CBS 115938, CBS 115325, CBS 115939, CBS 115207, and CBS 115208) and *B. clandestina* (JHH4676) with 70% ML and 0.96 BYPP support (Fig. 41). We present the ITS base comparison in Table 2. Morphologically, *B. tibetensis* differs from *B. clandestina* and *B. fuscescens* by its larger asci without croziers (50–60 × 2.6–4.4 µm vs. 41–47 × 3.2–4.5 µm vs. 30–44 × 3–4.5 µm). Additionally, *B. tibetensis* differs from *B. clandestina* in its hair characteristics, as it has brown hairs, whereas *B. clandestina* has hairs with pale brown or hyaline apices (Suková 2005, Tochihara et al. 2019). Based on morphology and phylogenetic placement, we introduce our collection as a new species, *Brunnipila tibetensis*, from China.

Table 2 Nucleotide differences in the ITS region of *Brunnipila hydei* (SZU25–009) compared with strains of *B. clandestina* and *B. fuscescens*.

Compared strain	Comparison target	Nucleotide differences	Differences (%)
***B. fuscescens* (CBS 115939)**	*B. hydei* (SZU25-009)	30/458 bp (including 4 gaps)	6.55%
***B. fuscescens* (CBS 115938)**	*B. hydei* (SZU25-009)	29/449 bp (including 5 gaps)	6.46%
***B. fuscescens* (CBS 115325)**	*B. hydei* (SZU25-009)	26/457 bp (including 3 gaps)	5.69%
***B. fuscescens* (CBS 115207)**	*B. hydei* (SZU25-009)	27/457 bp (including 4 gaps)	5.91%
***B. fuscescens* (CBS 115208)**	*B. hydei* (SZU25-009)	28/456 bp (including 3 gaps)	6.14%
***B. clandestina* (JHH4676)**	*B. hydei* (SZU25-009)	28/489 bp (including 2 gaps)	5.73%

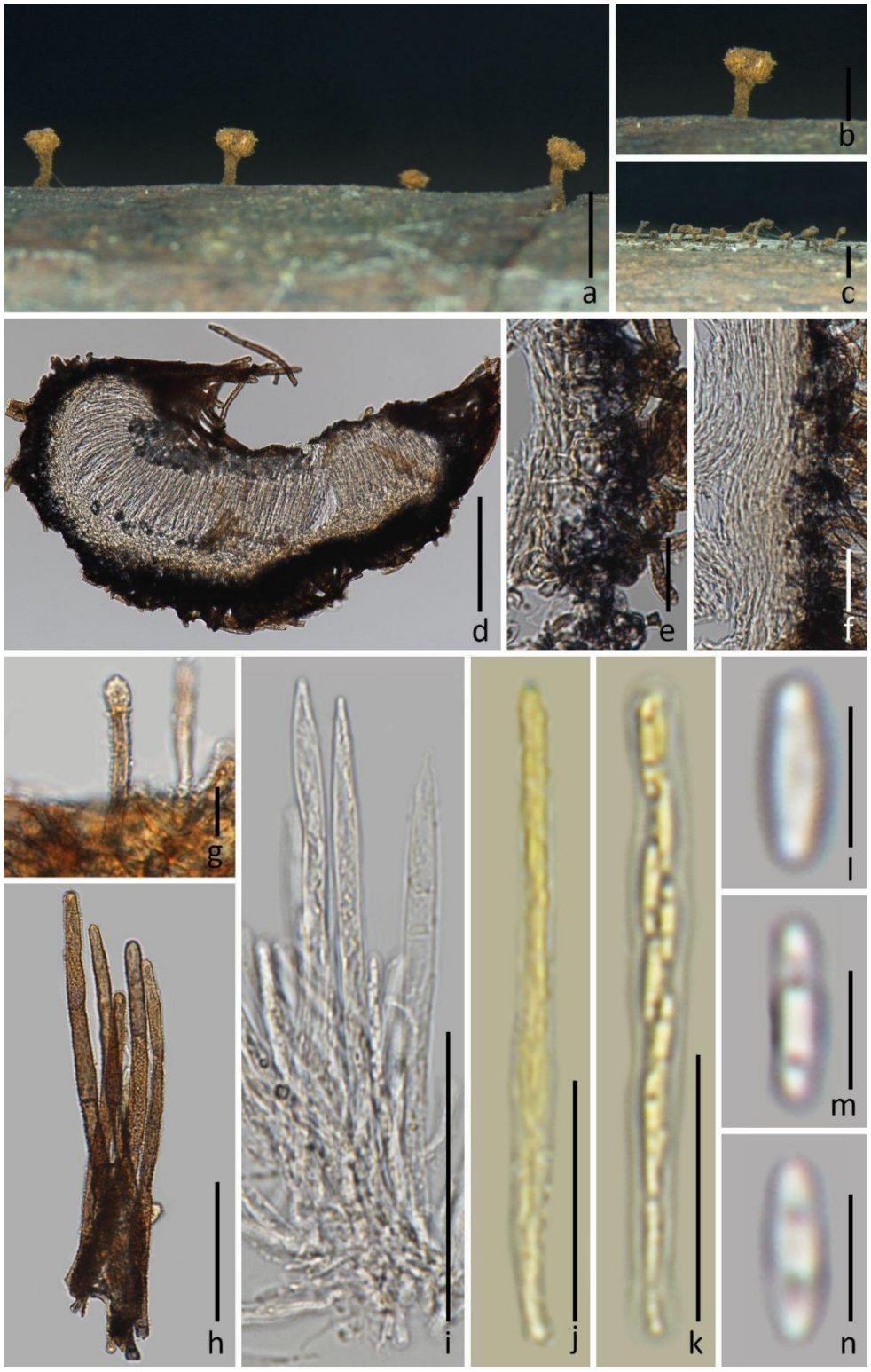


Figure 42 – *Brunnipila hydei* (SZU25–009, holotype). a–c Dried apothecia on woody host. d Vertical cross-section of an apothecium. e, f Excipulum. g Hair apex with crystals. h Hairs. i Paraphyses. j, k Asci in Melzer reagent. l–n Ascospores. Scale bars: a, c = 2 mm, b = 1 mm, d = 100 µm, e, f, j, k = 20 µm, g = 10 µm, h, i = 50 µm, l–n = 5 µm.

Class Orbiliomycetes O.E. Erikss. & Baral
Subclass Orbiliomycetidae P.M. Kirk, P.F. Cannon, Minter & Stalpers
Orbiliales Baral, O.E. Erikss., G. Marson & E. Weber

Orbiliaceae Nannf.

Orbilia ser. Drechslerella (Subram.) Baral & E. Weber, in Baral, Weber & Marson, Monogr. Orbiliomycetes: 1623 (2020)

Index Fungorum number: IF814996; Facesoffungi number: FoF17758

The genus *Orbilia* is a unique and significant group within the Orbiliomycetes, particularly among nematode-trapping fungi (NTF). The concept of sexual and asexual morphs in Orbiliomycetes was initially established by Brefeld (1891) and was further elucidated by Pfister (1997). The asexual morph states of *Orbiliaceae*, the sole family within Orbiliomycetes, encompass various genera: *Arthrobotrys*, *Dactylella*, *Dactylellina*, *Dicranidion*, *Drechslerella*, *Helicoon*, *Tridentaria*, and *Trinacrium*. Among these, *Arthrobotrys*, *Dactylellina*, and *Drechslerella* are notable for their nematode-trapping abilities. Baral et al. (2018) proposed that the generic concepts now used in Orbiliomycetes are incompatible regarding the two morphs: a broad concept depends on the sexual morphs, while a narrow concept is utilized for the asexual morphs. This has led to the creation of numerous additional generic names for the asexual morphs. Since many of the earlier generic conceptions were based on single characters without molecular backing, they are artificial. Baral et al. (2018) introduced three distinct general concepts within the Orbiliomycetes to address this mismatch: the large genus *Orbilia* was recognized by a broad concepts, and the majority of the listed names fall into synonyms, however they could still be considered infrageneric names, such as series *Drechslerella* under section *Arthrobotrys*; a moderate concept subdivided *Orbilia* into several genera, for example, all nematode-trapping fungi grouped under the genus and *Drechslerella* was regarded as subgenus under *Arthrobotrys*; a narrow generic concept accepts genera based on differences in trapping organs, which raised *Drechslerella* as a single genus. Baral et al. (2018) considered the broad idea to be the most practical due to insufficient evidence to support phylogenetic relationships. In their Monograph of Orbiliomycetes, *Orbilia ser. Drechslerella* was proposed (Baral et al. 2020).

Modern molecular biology techniques have significantly advanced the taxonomic understanding of *Orbiliaceae* nematode-trapping fungi in *Orbiliaceae*, revealing that species with adhesive networks often share similar molecular characteristics (Jiang et al. 2016, Zhang et al. 2022a). The genus *Drechslerella*, when applying a narrow generic concept, is typified by *D. acrochaeta* (Subramanian 1963). Historically, Scholler et al. (1999) synonymized *Dactylariopsis* with *Drechslerella* based on the presence of fusiform conidia with a long, filiform apical appendage and *Golovinia* with *Drechslerella* based on the presence of constricting rings. *Drechslerella* currently comprises 20 accepted species, as listed in the Index Fungorum (Accessed February 5, 2025). Despite earlier concerns raised by Liu & Zhang (1994) regarding the stability of the filamentous appendage as a defining feature, molecular phylogenetic analyses have since confirmed the monophyletic nature of *Drechslerell*a, characterized by three-celled constricting rings that capture nematodes through rapid mechanical expansion.

Drechslerella is distinguished from *Arthrobotrys* and *Dactylellina* by its adhesive networks to trap nematodes (Pfister 1997, Scholler et al. 1999, Baral et al. 2018). *Drechslerella* is considered a key group in the study of the origin and evolution of carnivorous fungi due to its unique method of nematode capture (Zhang et al. 2023b). The identification key for *Drechslerella* species, updated by Zhang et al. (2023b), prioritizes easily distinguishable features, such as conidial shape, the presence of supercells, and the branching of conidiophores, followed by more detailed characteristics, including macroconidial septation and size. Morphologically similar species are further distinguished by features such as microconidia, apical details of conidiophores, and characteristics of chlamydospores.

Orbilia longispora R. Yang & H. Zhang, sp. nov. Fig. 44

Index Fungorum number: IF903709; Facesoffungi number: FoF17657

Etymology – Referring to the long conidia.

Holotype – IFRD99020

Colonies on PDA yellowish, cottony, growing slowly, reaching 4.5 mm diam. after a month in the incubator at 28 °C. *Mycelium* partly superficial, partly immersed, composed of septate, branched, smooth, hyaline. *Conidiophores* 150–270 × 3.5–4.5 μm ($\overline{x}$ = 190.4 × 3.9 μm, n = 10), erect, septate, hyaline, unbranched, producing 3–12 short denticles near the apex, each denticle bearing a single conidium. *Conidia* 27–34 × 6–8 μm ($\overline{x}$ = 31.2 × 7.3 μm, n = 20), cylindrical, rounded above, slightly tapered-truncate below, 0–3-septate (mostly 3-septate), hyaline. *Chlamydospore* not observed. Capturing nematodes apparatus not seen.

Material examined – China, Yunnan Province, Ruili City, Moli Waterfall, on submerged decaying wood of unidentified plants, Rang Yang, 16 May 2024, YR127 (IFRD99020, holotype), ex-type IFRDCC25–0001.

GenBank numbers – ITS = PQ253052, LSU = PV469749.

Notes – The phylogenetic analysis based on combined ITS and LSU sequence data (Fig. 43) confirmed that the newly isolated strain belongs to *Orbilia ser. Drechslerella*. Notably, macroconidia and nematode-capturing apparatus were not observed in this isolate. *Orbilia longispora* is one of the few species within this genus that can be found in freshwater habitats. Previously, Zhang et al. (2023b) demonstrated that species within *Orbilia ser. Drechslerella* can be categorized into two groups based on the presence or absence of a supercell in their conidia. However, these groups are not phylogenetically distinct within the phylogenetic tree. In this context, *O. longispora* shares similarities with *O. brochapaga*, *Drechslerella dactyleoids*, *O. tonghaiensis* and *O. yunnanensis* in the absence of a super-cell (Zhang et al. 2023b). Nevertheless, differences in septation patterns are evident among these species: 0–1-septate in *D. dactyleoids* and *O. yunnanensis*, whereas 0–3-septate in *O. longispora* (Scholler et al. 1999). Furthermore, *O. longispora* is morphologically similar to *O. brochapaga* and *O. tonghaiensis* in that it has conidiophores that produce short denticles and cylindrical conidia (Scholler et al. 1999, Zhang et al. 2020). Despite these similarities, these species are phylogenetically distinguished from one another, highlighting the complexity of their evolutionary relationships within the *Orbilia ser. Drechslerella*.

Class Sordariomycetes O.E. Erikss. & Winka

Subclass Diaporthomycetidae Senan., Maharachch. & K.D. Hyde

Diaporthales Nannf.

Coryneaceae Corda

Coryneum Nees, Syst. Pilze (Würzburg): 34 (1816) [1816–17]

Index Fungorum number: IF7798; Facesoffungi number: FoF01464

Coryneum was first described by Nees von Esenbeck (1816) based on *C. umbonatum*, which is the asexual morph of *Pseudovalsa longipes* (Jiang et al. 2018). However, in single-name nomenclature, these two genera become synonyms. Rossman et al. (2015) considered the genus name *Coryneum* to have priority over *Pseudovalsa* and recommended it for future use. *Coryneum* is the only genus in the family *Coryneaceae* (*Diaporthales*). There are 236 records for *Coryneum* in the Index Fungorum (2025). *Coryneum* species are generally considered highly host-specific, especially when occurring on hardwood trees such as those in the *Betulaceae* and *Fagaceae* (Sutton 1975, Jiang et al. 2018). The majority of *Coryneum* species are phytopathogens that cause cankers and dieback of shoots and twigs, particularly on hosts belonging to the *Betulaceae* and *Fagaceae* families (Sutton 1975, Jiang et al. 2018, Wijesinghe et al. 2022). The sexual morph is characterized by having solitary, scattered pseudostromata, globose to subglobose, uniloculate perithecia, long ostiolar necks, 8-spored, unitunicate, cylindrical asci, fusiform to ellipsoidal, 1-septate, hyaline, guttulate ascospores (Jiang et al. 2018, Wijesinghe et al. 2022). The asexual morph is coelomycetous, characterized by acervuli conidiomata, cylindrical, straight, septate conidiophores, holoblastic, cylindrical, annellidic conidiogenous cells, and clavate to subcylindrical, club-shaped, hyaline to brown, 3–6-euseptate, guttulate conidia (Jiang et al. 2018, Wijesinghe et al. 2022). Phylogenetic analyses based on combined ITS, LSU, *tef1-α*, and *rpb2* sequence data have been used to distinguish *Coryneum* species (Jiang et al. 2018, 2019b, Wijesinghe et al. 2022).

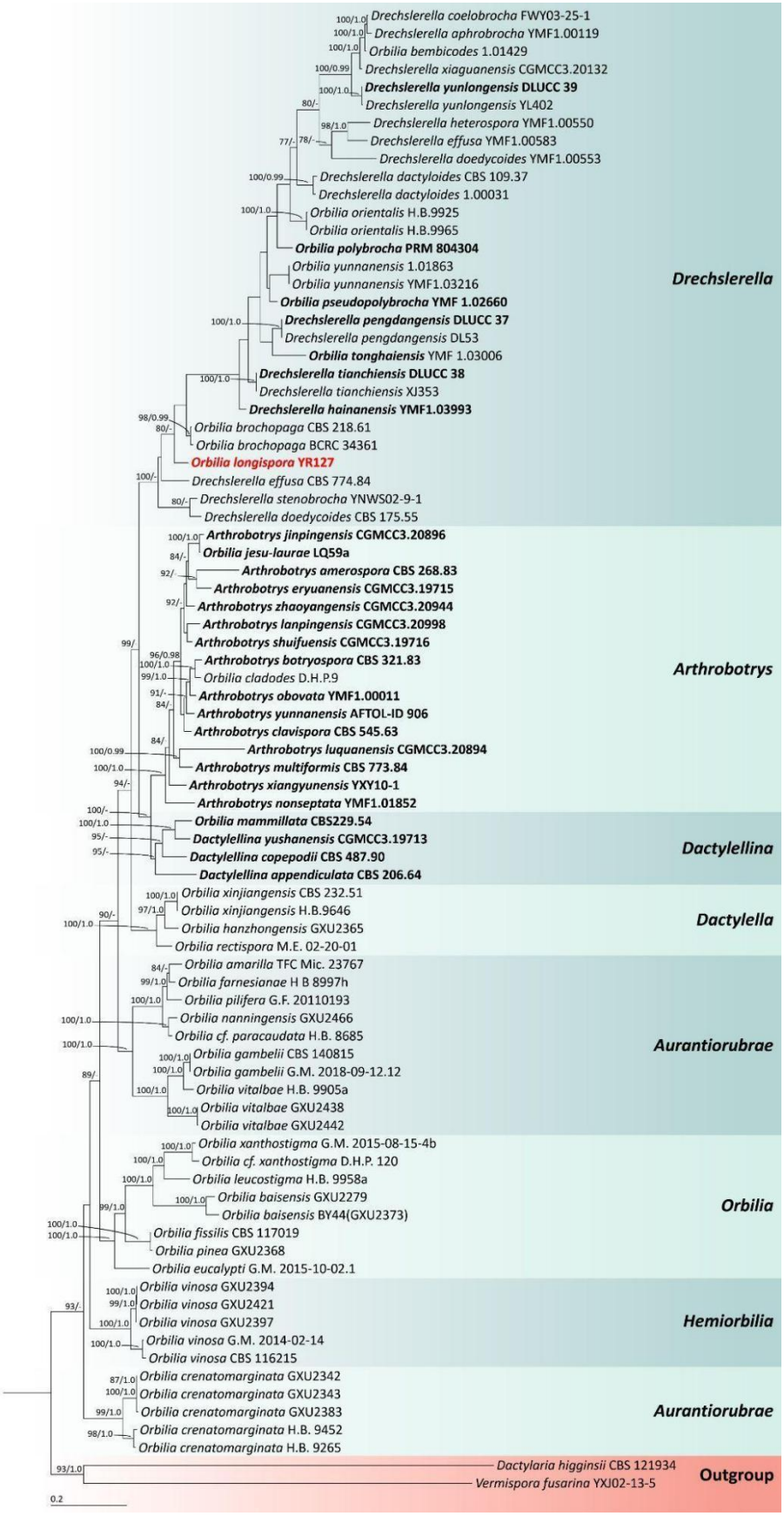


Figure 43 – Phylogram generated from maximum likelihood analysis based on combined LSU and ITS sequence data from 83 taxa, comprising 2,909 characters (LSU = 928, ITS = 1,981). The best-scoring RAxML tree with a final likelihood value of -29630.181 is presented. The matrix contained 1,511 distinct alignment patterns, with 56.47% of the characters being undetermined or gaps.

Estimated base frequencies were as follows: A = 0.264, C = 0.227, G = 0.262, T = 0.247; substitution rates: AC = 1.204, AG = 2.269, AT = 1.449, CG = 0.780, CT = 4.537, GT = 1.0; gamma distribution shape parameter α = 0.282. Bootstrap support values for maximum likelihood (ML, first value) equal to or greater than 70% and clade credibility values greater than 0.90 (rounded to two decimal places) from Bayesian inference analysis are labeled at each node. Ex-type strains are in bold, while the new isolate is indicated in red bold. The tree is rooted in *Dactylaria higginsii* (CBS 121934) and *Vermispora fusarina* (YXJ02–13–5).

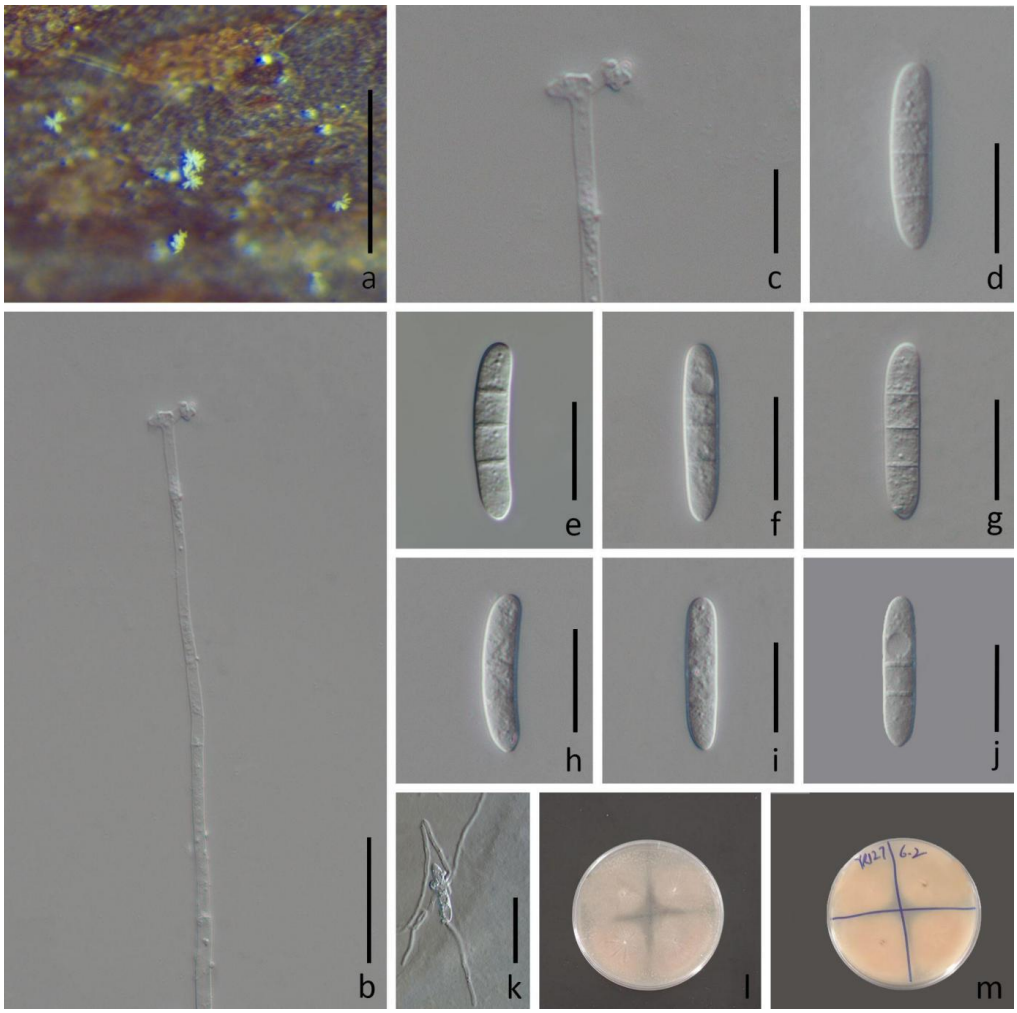


Figure 44 – *Orbilia longispora* (YR127, holotype). a Colonies on the natural substratum. b Conidiophore. c Conidiogenous cell. d–j Conidia. k Germinated conidium. l Colonies on PDA (from front). m Colonies on PDA (from reverse). Scale bars: a = 200 μm, b = 25 μm, c = 10 μm, d–j = 15 μm, k = 30 μm.

In recognition of Prof. Hyde's outstanding contributions to mycology, herein we introduce *Coryneum hydei*, which has been named in honor of Prof. Kevin D. Hyde. We also provide an updated phylogenetic tree for *Coryneum* (Fig. 45).

Coryneum hydei H.Y. Du & S.K. Huang, sp. nov. Fig. 46

Index Fungorum number: lF903736; Facesoffungi number: FoF17759

Etymology – 'hydei' named in honor of the renowned mycologist Kevin D. Hyde, recognizing his significant contributions to mycology on the occasion of his 70th birthday.

Holotype – HKAS 146642

Saprobic on decayed branches. Sexual morph: Undetermined. Asexual morph: *Conidiomata* 0.1–0.7 mm wide, 0.05–0.26 mm high, acervular, solitary, semi-immersed to erupting through the

host surface, scattered, with slightly convex surface tissues composed of thick-walled, brown *textura angularis*. *Conidiophores* 51.5–72.9 long × 6.9–11.1 µm wide, cylindrical, pale brown at the apex, gradually lighter towards the base, smooth, septate, unbranched, emerging from the basal stroma. *Conidiogenous cells* annellidic, integrated, terminal, cylindrical, widening towards the apex, pale brown, smooth, exhibiting 1–3 slightly percurrent proliferations. *Conidia* 46.6–73.9 × 8.7–12.5 µm ($\bar{x}$ = 61.2×10.5 µm, n = 20), variable in shape, curved, broadly fusiform to fusiform, dark brown, smooth-walled, with 4–9 distosepta; the apical cell bears a hyaline tip, while the base is black and truncate.

Culture characteristics – Colonies on PDA reaching 40 mm diam., within 14 days at 25 °C, circular, slightly raised, irregular margin, grey to dark brown with plenty of whitish aerial mycelium covering the surface; Reverse dark brown center with white outer zone.

Material examined – China, Guizhou Province, Zunyi City, Yunmentun Mountain, on dead branches of unidentified plant, 10 July 2024, H.Y. Du, YMT1–1 (HKAS 146642, holotype), ex-type ZNUZCC013030.

GenBank numbers – YMT1–1: ITS = PQ816944, *tef1-α* = PQ899252.

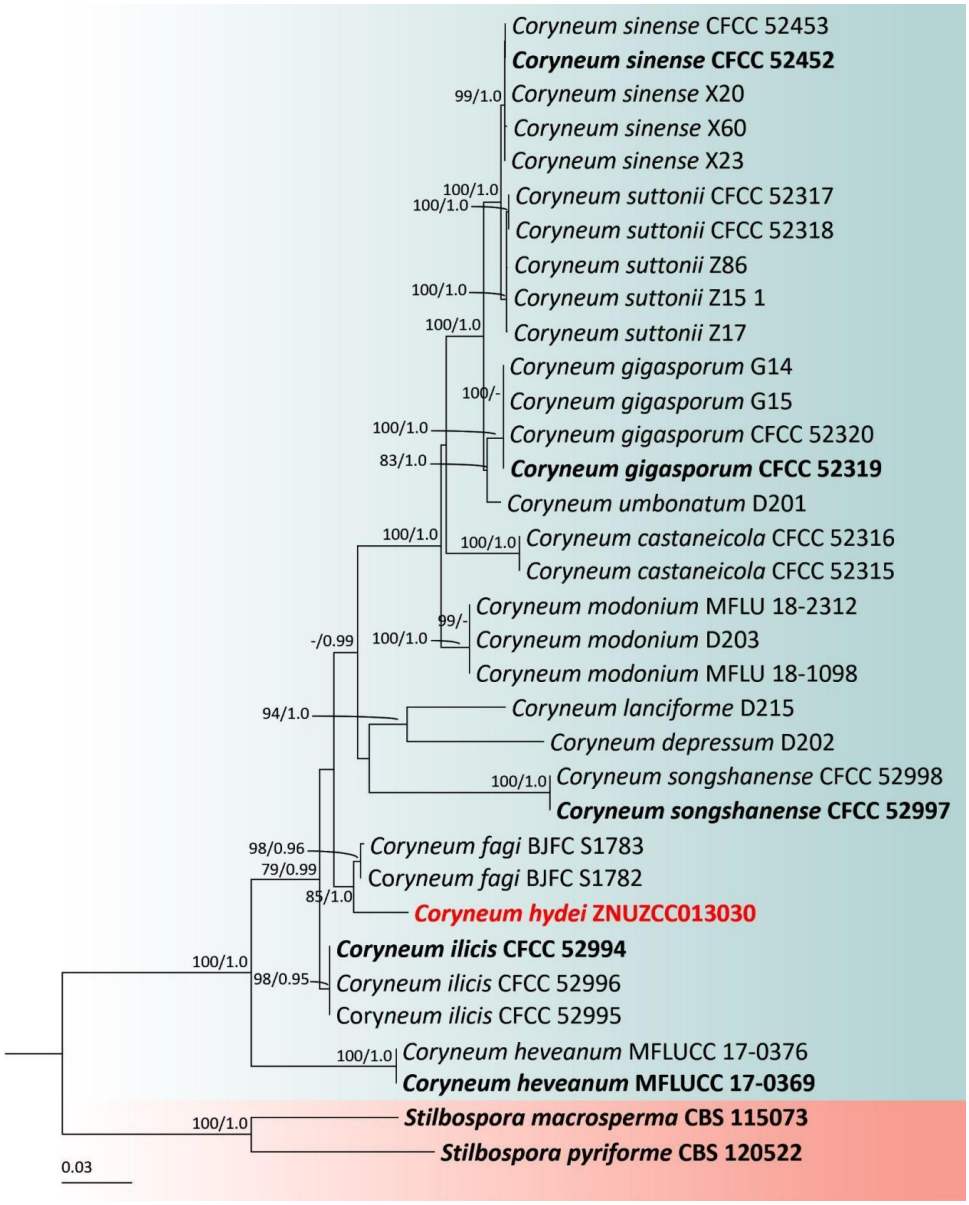


Figure 45 – Phylogram generated from maximum likelihood analysis based on combined ITS, LSU, *rpb2*, and *tef1-α* sequence data from 34 taxa, comprising 3,608 characters (ITS = 639, LSU = 841, *rpb2* = 1,110, *tef1-α* = 1,018). The best-scoring RAxML tree with a final likelihood value of -

12817.279 is presented. The matrix contained 933 distinct alignment patterns, with 29.47% of the characters being undetermined or gaps. Estimated base frequencies were as follows: A = 0.240, C = 0.273, G = 0.275, T = 0.211; substitution rates: AC = 1.445, AG = 2.128, AT = 1.242, CG = 1.055, CT = 6.021, GT = 1.0; gamma distribution shape parameter α = 0.252. Bootstrap support values for maximum likelihood (ML, first value) equal to or greater than 70% and clade credibility values greater than 0.90 (rounded to two decimal places) from Bayesian inference analysis are labeled at each node. Ex-type strains are in bold, while the new isolate is indicated in red bold. The tree is rooted to *Stilbospora macrosperma* (CBS 115073) and *S. pyriforme* (CBS 120522).



Figure 46 – *Coryneum hydei* (YMT1–1, holotype). a Habitat of the sampling site. b–c Conidiomata on the dead branch. d Vertical cross-section of a conidioma. e Developing conidia from conidiogenous cells. f–g Conidia. h–i Germinated conidia. j–k Colony on PDA (j obverse, k reverse). Scale bars: c = 1000 μm, d–i = 50 μm.

Notes – The phylogenetic analysis based on a combined ITS, LSU, *rpb2*, and *tef1-α* sequence dataset (Fig. 45) confirmed that the newly isolated strain belongs to *Coryneum* and is sister to *C. fagi* (BJFC S1782 and BJFC S1783) with 85% bootstrap (ML) and 1.0 BYPP support. However, sequence data for the type strain of *C. fagi* is not available. A base pair comparison between the new species and two strains of *C. fagi* reveals a 1.97% difference (11/557 bp) in the ITS region. LSU data is not available for our new species, and *tef1-α* data is not available for *C. fagi*, so we were unable to compare base pair differences in these gene regions. *Coryneum hydei* is

morphologically similar to *C. fagi*, but the conidia of the latter are slightly thicker (46.6–73.9 × 8.7–12.5 µm in *C. hydei* vs. 45–75 × 10–15.5 µm in *C. fagi*) (Boonmee et al. 2021). *Coryneum fagi* was found as a saprobe or weak pathogen on branches of *Fagus* sp. (Boonmee et al. 2021), whereas *C. hydei* was found as a saprobe on decayed branches. Based on morphology and phylogenetic analyses, we herein introduce our collection as a new species, *C. hydei*, from China.

Diaporthaceae Höhn. ex Wehm.

Diaporthe Nitschke, Pyrenomycetes Germanici 2: 240 (1870)

Index Fungorum number: IF92244; Facesoffungi number: FoF00146

Diaporthe was introduced by Nitschke (1870) and typified with *D. eres*. The genus encompasses important plant pathogenic, endophytic, and saprobic species with a diverse host range and a global distribution (Gomes et al. 2013, Hyde et al. 2014, Dissanayake et al. 2017, Abeywickrama et al. 2022, Hilário & Gonçalves 2023). Currently, Index Fungorum (2025) and MycoBank (2025) list more than 1,300 taxa under *Diaporthe* and almost 1,000 species in *Phomopsis* (accessed January 2025). Considering all available type isolates of *Diaporthe*, the genus is divided into seven sections by Dissanayake et al. (2024a). Prof. Kevin D. Hyde and his collaborators have introduced more than 90 species. His work, particularly in the context of his students' research on resolving the complexity of *Diaporthe*, as presented Norphanphoun et al. (2022), Hongsanan et al. (2023), and Dissanayake et al. (2024a), has significantly advanced the *Diaporthe* taxonomy.

In recognition of his outstanding contributions to mycology, herein we introduce *Diaporthe hydei*, which has been named in honor of Prof. Kevin D. Hyde. We also provide an updated phylogenetic tree for *Diaporthe* (Fig. 47).

Diaporthe hydei Y.R. Xiong & Manawas., sp. nov. Fig. 48

Index Fungorum number: IF903748; Facesoffungi number: FoF17760

Etymology – 'hydei' named in honor of the renowned mycologist Kevin D. Hyde, recognizing his significant contributions to mycology on the occasion of his 70th birthday.

Holotype – MFLU25–0147

Saprobic on a decaying petiole of *Calamus* sp. Sexual morph: *Ascomata* 450–600 × 300–400 µm ($\overline{x}$ = 517 × 350 µm, n = 10), perithecial, immersed, erumpent through the epidermis or clypeus, scattered to aggregate, solitary, globose, black, coriaceous, ostiolate. *Ostiole* central, black, elongate, mostly immersed in the epidermis, with a papillate apex protruding on the substrate surface. *Peridium* 20–50 µm wide, composed of 3–5 layered, brown to dark brown cells of *textura angularis*. *Asci* 25–30 × 5–8 µm ($\overline{x}$ = 27.5 × 6.2 µm, n = 20), 8-spored, unitunicate, clavate, sessile, widest at centre and truncate towards the apices, distinct ocular chamber. *Ascospores* 7–9 × 2.5–3.5 µm ($\overline{x}$ = 7.9 × 3.1 µm, n = 25), overlapping, bi-seriate, fusoid to ellipsoid, hyaline, 1-septate, with 4–6 guttules, one at each end and 1–2 near the septum, slightly constricted at the septum. Asexual morph: Undetermined.

Culture characteristics – Colonies on PDA reaching 5 cm diam. after 2 weeks at 25 °C, circular, slightly raised, initially white, turn into light green on surface when old, plenty of whitish aerial mycelia around center, Reverse olive-green center.

Material examined – Thailand, Narathiwat Province, on an unidentified branch, on a decaying petiole of *Calamus* sp., 6 August 2023, Y.R. Xiong, XG330 (MFLU25–0147, holotype), ex-type MFLUCC 25–0204, living culture MFLUCC 25–0205.

GenBank numbers – MFLUCC 25–0204: ITS = PV469907, *tef1-α* = PV483807, *tub*2 = PV483809; MFLUCC 25–0205: ITS = PV469908, *tef1-α* = PV483808, *tub*2 = PV483810.

Notes – Together with our strain, *Diaporthe acutispora* and *D. hsinchuensis* formed a distinct clade within *Diaporthe* (Section *Foeniculina*, Dissanayake et al. 2024a). The base pair differences of the ITS, *tub*2, and *tef1-α* loci between our isolate (MFLUCC 25-0204, type), and related species are as follows: compared to *Diaporthe acutispora* (CGMCC3 18285), the differences were 4.05% (22/543) in the ITS locus, 5.08% (25/492 bp) in *tub*2, and 13.35% (45/337 bp) in *tef1-α*. In comparison with *D. hsinchuensis* (NTUPPMCC 18-153), the differences were 5.26% (30/570) in

ITS, 6.35% (31/488 bp) in *tub*2, and 12.03% (38/316 bp) in *tef1-α*. However, we only obtained the sexual morph of our collection, whereas *D. acutispora* and *D. hsinchuensis* were described based on their asexual morph (Gao et al. 2017, Ariyawansa et al. 2021). Therefore, it was not possible to compare the morphology of our collection with *D. acutispora* and *D. hsinchuensis*. Thus, we introduce our collection as a new species *Diaporthe hydei*.

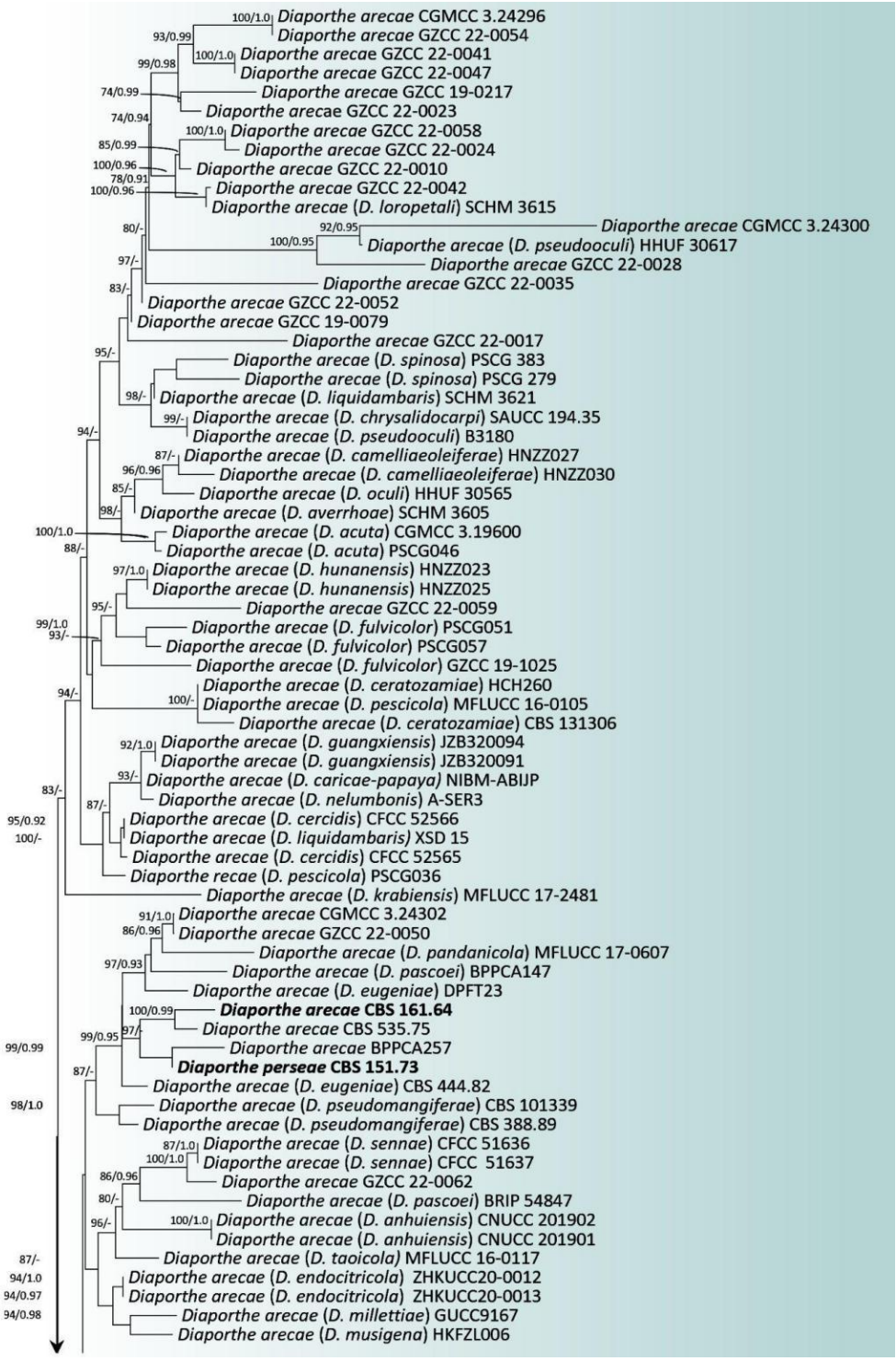


Figure 47 – Phylogram generated from maximum likelihood analysis based on combined ITS, *tef1-α*, *tub2*, *cal*, and *his* sequence data from 228 taxa, comprising 2,586 characters (ITS = 397, *tef1-α* = 610, *tub2* = 401, *cal* = 691, *his* = 487). The best-scoring RAxML tree with a final likelihood value of -38511.169 is presented. The matrix contained 336 distinct alignment patterns, with 13.4% of the characters being undetermined or gaps. Estimated base frequencies were as follows: A = 0.213, C =

0.321, G = 0.240, T = 0.227; substitution rates: AC = 1.279, AG = 3.264, AT = 1.279, CG = 1.000, CT = 4.483, GT = 1.0; gamma distribution shape parameter α = 0.646. Bootstrap support values for maximum likelihood (ML) equal to or greater than 50% and clade credibility values greater than 0.90 (rounded to two decimal places) from Bayesian inference analysis are labeled at each node. Ex-type strains are in bold, while the new isolates are indicated in red. The tree is rooted to *Diaporthe eres* (AR5193).

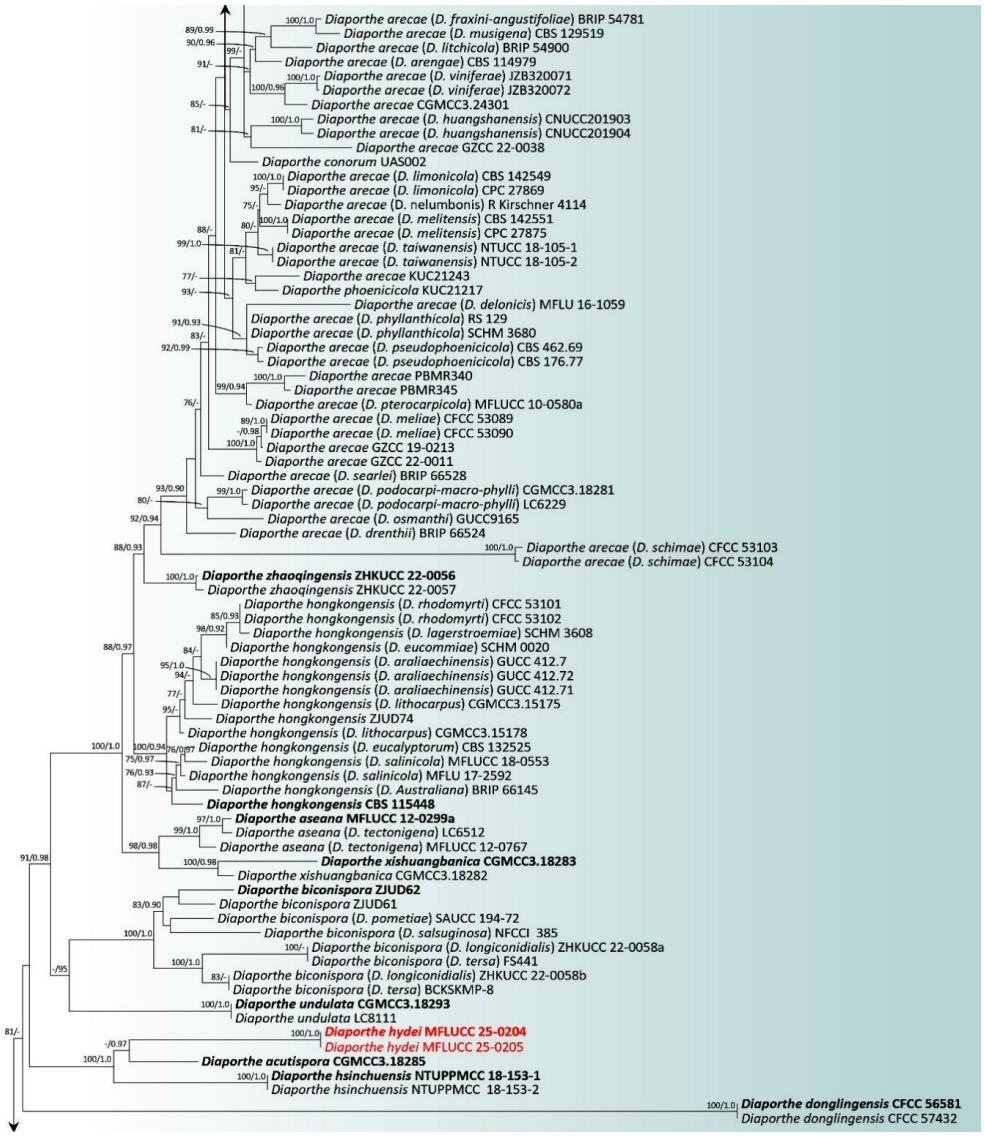


Figure 47 – Continued.

Distoseptisporales Z.L. Luo, H.Y. Su & K.D. Hyde

Distoseptisporaceae K.D. Hyde & McKenzie

Distoseptispora K.D. Hyde, McKenzie & Maharachch.

Index Fungorum number: IF551833; Facesoffungi number: FoF01755

Distoseptispora was introduced by Su et al. (2016) and typified by *D. fluminicola*. In less than a decade, more than 90 species have been introduced to *Distoseptispora* (Index Fungorum 2025), with most of these species being found on dead wood in terrestrial and freshwater habitats (Sun et al. 2020, Zhang et al. 2022b, Dissanayake et al. 2024b, Shen et al. 2024b). *Distoseptispora* is characterized by erect, unbranched, cylindrical, septate conidiophores, terminal, monoblastic or polyblastic conidiogenous cells, and acrogenous, obclavate, rostrate, distoseptate or euseptate conidia in asexual morph (Luo et al. 2018, 2019, Karimi et al. 2024), cylindrical, pedicellate asci

with an apical ring, and fusiform, septate or aseptate ascospores with a mucilaginous sheath in sexual morph (Yang et al. 2021, Konta et al. 2023, Yu et al. 2024).

In the realm of the ever-growing inventory of introduced *Distoseptispora* species, Prof. Kevin D. Hyde and his collaborators are the main contributors. Their research has been both extensive and impactful. These efforts have significantly enhanced our understanding of the genus, from its morphological intricacies to its genetic makeup, thus laying a solid foundation for further research in the field of *Distoseptispora* fungi. In recognition of Prof. Kevin D. Hyde's outstanding contributions to this genus, we introduce the new species, *Distoseptispora kevinia*, herein.

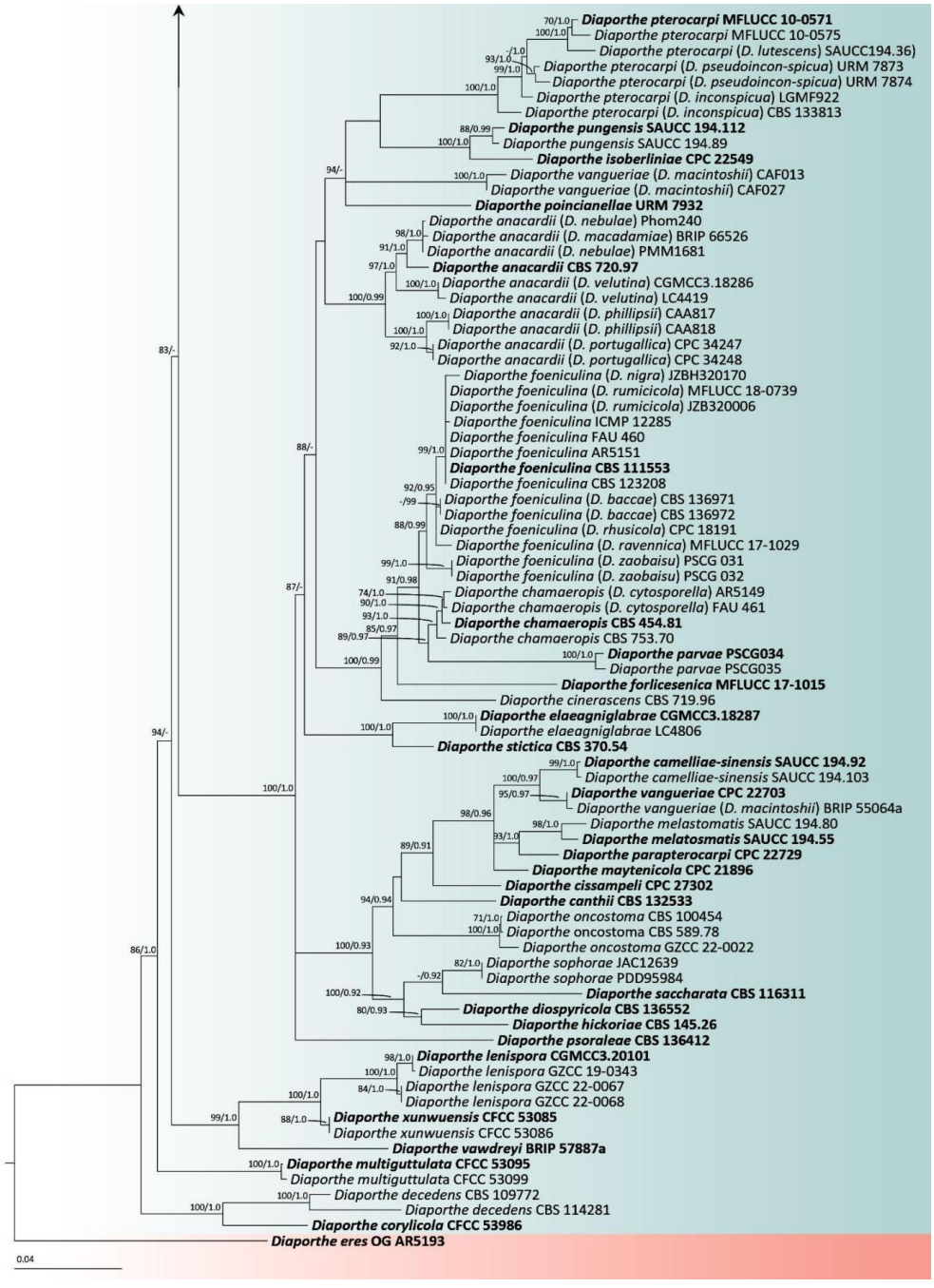


Figure 47 – Continued.

Distoseptispora monospora W.P. Wang & Z.L. Luo, sp. nov. Fig. 50

Index Fungorum number: IF903346; Facesoffungi number: FoF17297

Etymology – Refers to the conidiophores that produce only one conidia.

Holotype – HKAS 145690

Saprobic on submerged decaying wood. Asexual morph: *Colonies* superficial, hair, effuse, brown, glistening. *Mycelium* immersed, composed of unbranched, septate, smooth, hyaline to pale brown hyphae. *Conidiophores* 62–117 × 3–5.1 µm ($\overline{x}$ = 85 × 4 µm, n = 20), macronematous, mononematous, erect, solitary, unbranched, cylindrical, 3–7-septate, straight or slightly flexuous, brown, smooth, thick-walled, rounded at the apex. *Conidiogenous cells* 12–20 × 3–4.3 µm ($\overline{x}$ = 16 × 3.8 µm, n = 20), monoblastic, integrated, terminal, determinate, cylindrical, brown. *Conidia* 27–126 × 6.2–8.9 µm ($\overline{x}$ = 75 × 7.6 µm, n = 20), acrogenous, solitary, narrowly obclavate, rostrate, tapering towards the apex, straight or slightly curved at the base, 2–13-euseptate, smooth to slightly verrucose walled, brown, paler at the apex, truncate and darkened scar at the base, guttulate. Sexual morph: Undetermined.

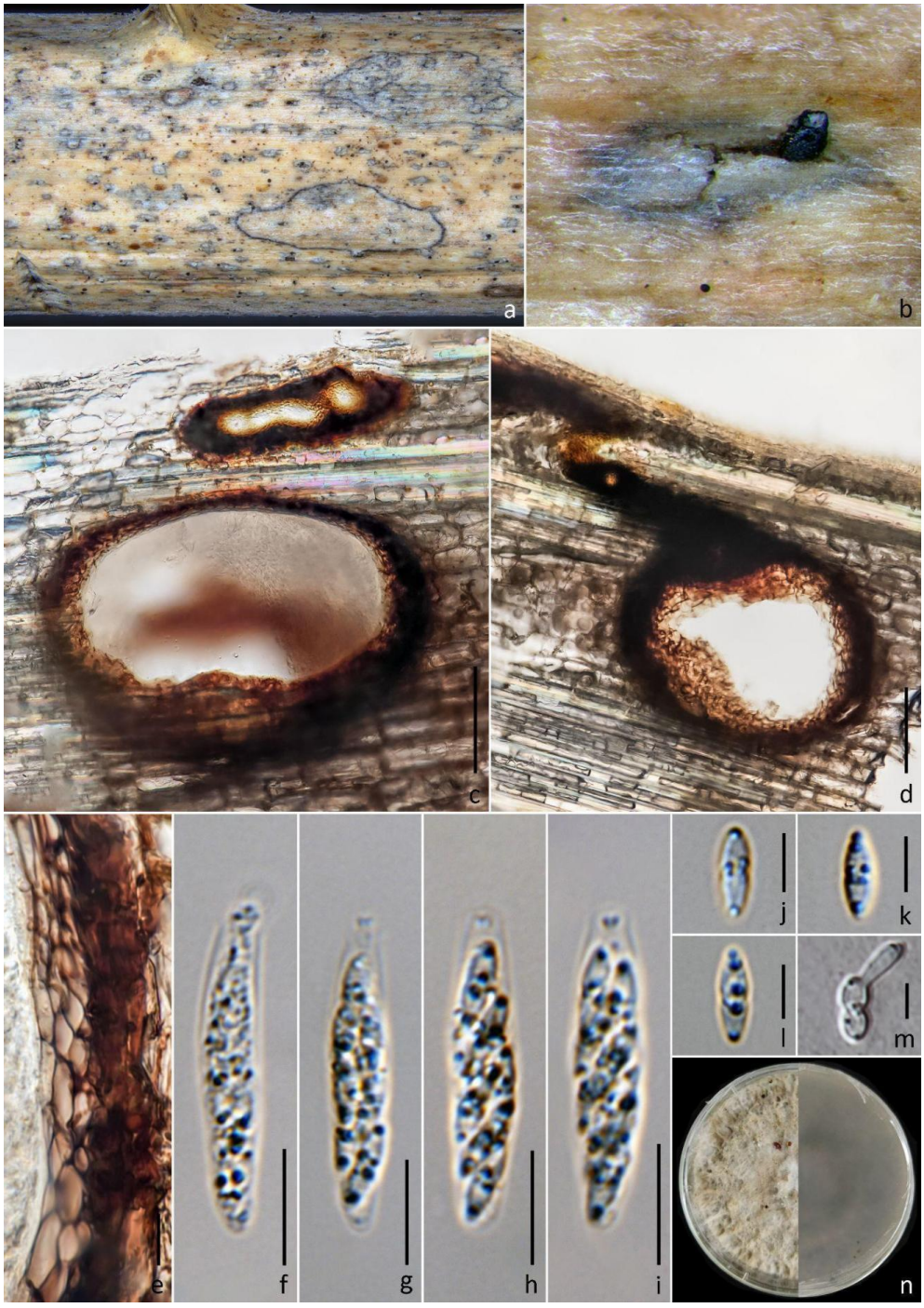


Figure 48 – *Diaporthe hydei* (MFLU25–0147, holotype). a, b Appearance of ascomata on woody substrate. c, d Vertical cross-section of an ascoma. e Peridium. f–i Asci. j–l Ascospores.

m Germinating ascospores. n Surface view of colony on PDA and reverse view of colony on PDA. Scale bars: c, d = 100 µm, e–i = 10 µm, j–m = 5 µm.

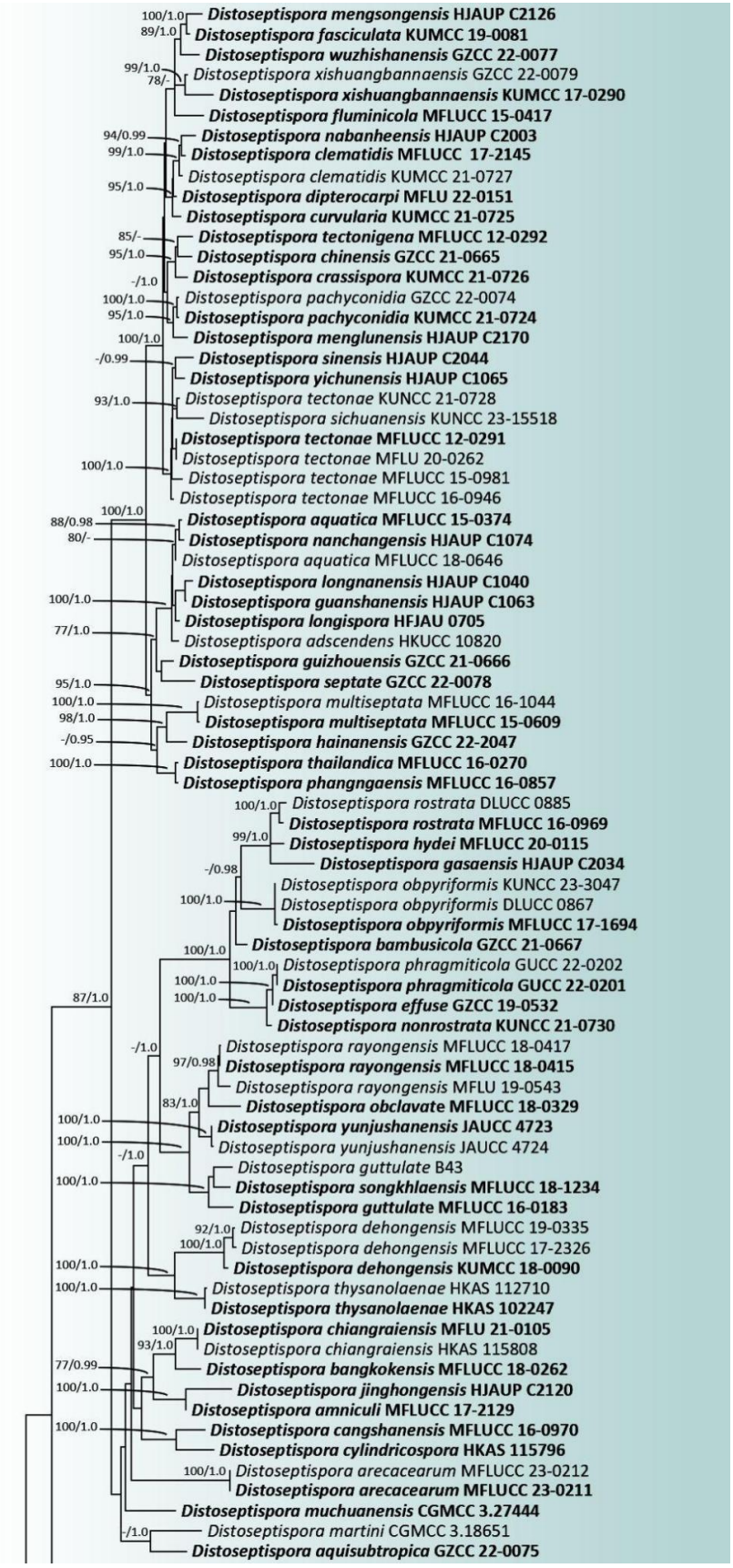


Figure 49 – Phylogram generated from maximum likelihood analysis based on combined LSU, ITS, *tef1-α*, and *rpb2* sequence data from 128 taxa, comprising 3,266 characters (LSU = 825, ITS =

528, *tef1-α* = 885, *rpb2* = 1,028). The best-scoring RAxML tree with a final likelihood value of -35469.751 is presented. The matrix contained 1,614 distinct alignment patterns, with 26.60% of the characters being undetermined or gaps. Estimated base frequencies were as follows: A = 0.239, C = 0.267, G = 0.282, T = 0.212; substitution rates: AC = 1.423, AG = 3.537, AT = 1.177, CG = 0.881, CT = 6.990, GT = 1.0; gamma distribution shape parameter α = 0.255. Bootstrap support values for maximum likelihood (ML) equal to or greater than 70% and clade credibility values greater than 0.90 (rounded to two decimal places) from Bayesian inference analysis are labeled at each node. Ex-type strains are in bold, while the new isolate is indicated in red. The tree is rooted to *Myrmecridium banksiae* (CBS 132536) and *M. schulzeri* (CBS 100.54).

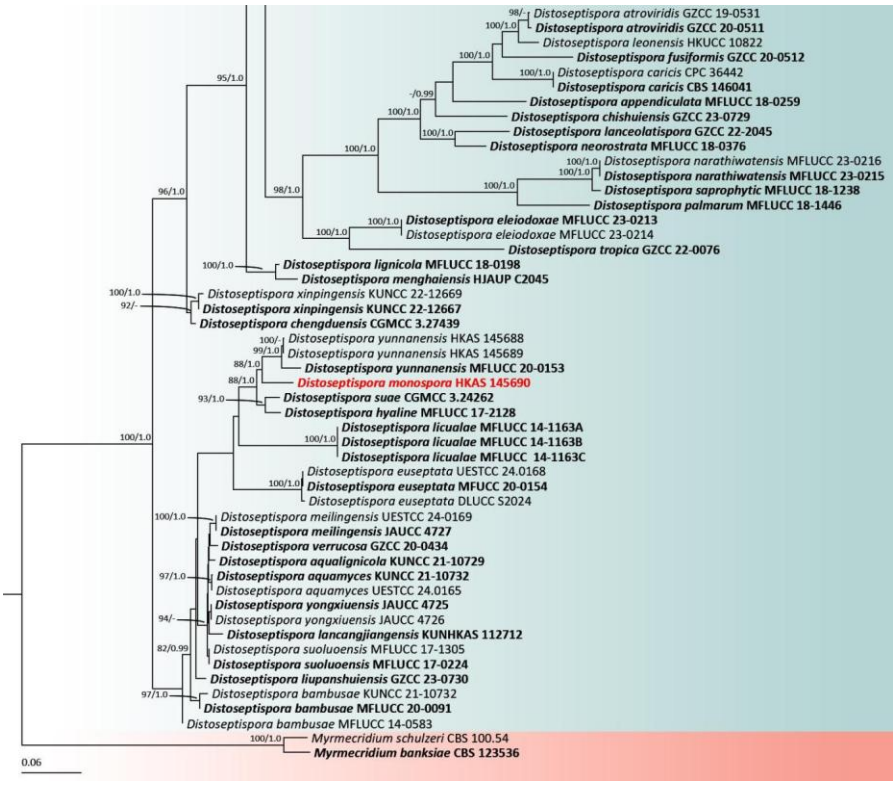


Figure 49 – Continued.

Culture characteristics – Conidia germinating on PDA within 12 h and germ tubes producing from the base. Colonies on PDA reaching 20 mm diameter after 4 weeks at room temperature. Colonies on the surface of PDA, circular, umbellate, velvety, regular edges, brown with pale brown edges. Reverse circular, smooth, split from the center, dark brown with brown edges.

Material examined – China, Yunnan Province, Xishuangbanna Dai Autonomous Prefecture, Xishuangbanna Tropical Botanical Garden, Chinese Academy of Sciences, 21°53′37.60″N; 101°16′30.98″E, 558 m, on submerged decaying wood in a freshwater stream, 12 July 2022, Long-Li Li, S-3972 (HKAS 145690, holotype).

GenBank numbers – HKAS 145690: ITS = PQ898696, LSU = PQ898699, *tef1-α* = PV001669, *rpb2* = PV001672.

Notes – In the phylogenetic tree, *Distoseptispora monospora* (HKAS 145690) and *D. hyalina* (MFLUCC 17–2128), *D. kevinia* (HKAS 145688 and HKAS 145689), *D. suae* (CGMCC 3.24262), and *D. yunnanensis* (MFLUCC 20–0153) clustered in a subclade with 88% and 1.00 BYPP support (Fig. 49). A comparison of the ITS sequences between *D. monospora* and the ex-type strains of *D. hyalina*, *D. kevinia*, *D. suae*, and *D. yunnanensis* showed differences of 3.52% (19/541, including 5 gaps), 4.53% (24/530, including 4 gaps), 3.52% (19/540, including 5 gaps), and 4.46% (24/538, including 5 gaps), respectively. Morphologically, *D. monospora*, *D. suae*, and *D. yunnanensis* have monoblastic conidiogenous cells, while the conidiogenous cells of *D. kevinia*

are polyblastic. *Distoseptispora monospora* has unbranched, cylindrical conidiophores (62–117 µm, with 3–7-septa) shorter than *D. yunnanensis* (131–175 µm, with 6–10-septa), but longer than *D. suae* ((21–) 25–41 (–53) µm, with 1–3-septa) (Li et al. 2021, Shen et al. 2024b). Based on morphological and molecular analyses, we therefore identify *D. monospora* as a new species within the genus *Distoseptispora*.

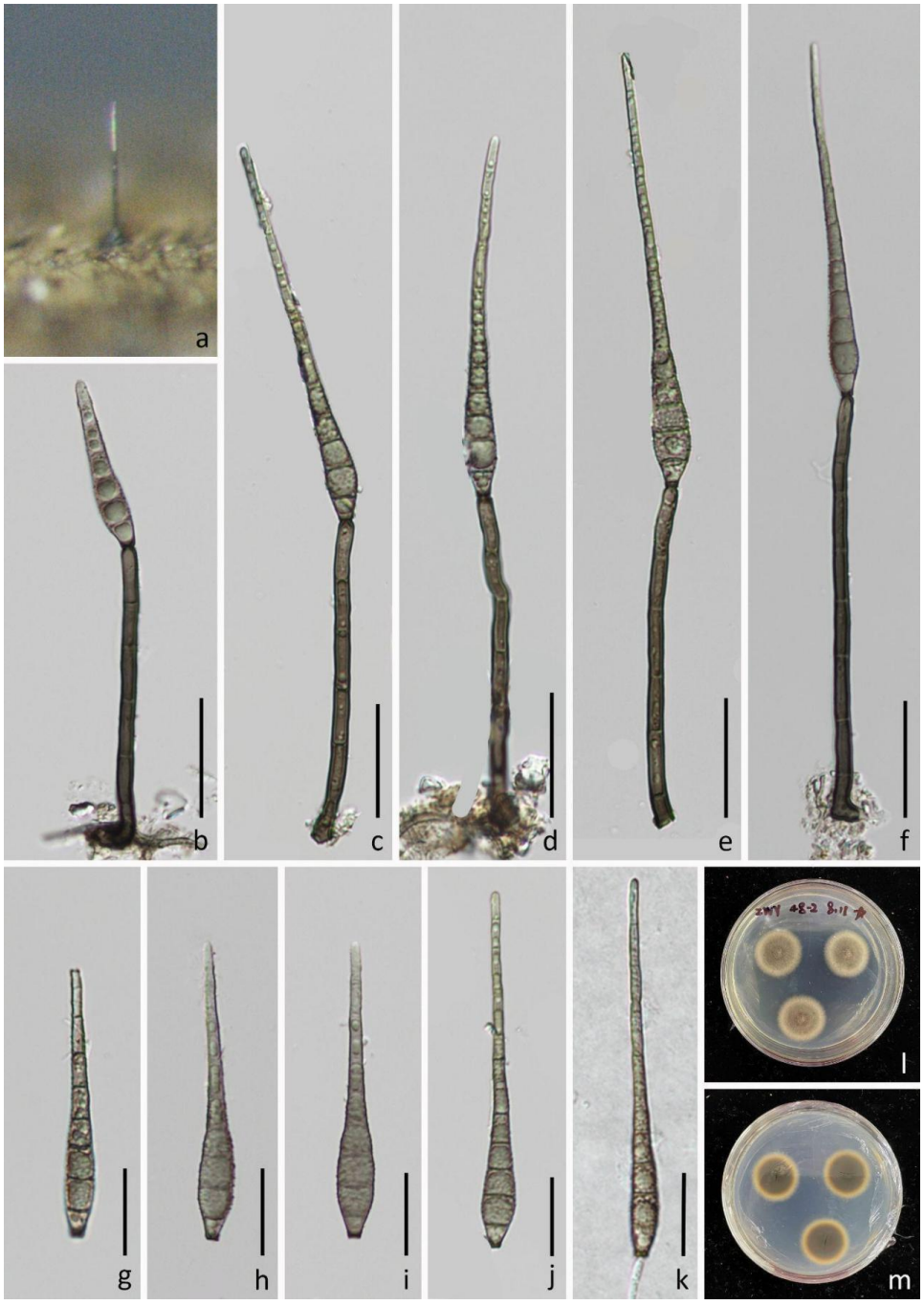


Figure 50 – *Distoseptispora monospora* (HKAS 145690, holotype). a Colony on the substratum. b–f Conidiophores with conidia. g–j Conidia. k Germinating conidium. l, m Colonies on PDA from surface and reverse. Scale bars: b–f =30 µm, g–k =20 µm.

Diaporthomycetidae families *incertae sedis*

Woswasiaceae H. Zhang, K.D. Hyde & Maharachch.

Xylochrysis Réblová, Mycologia 106(3): 567 (2014)

Index Fungorum number: IF805253; Facesoffungi number: FoF10306

The genus *Xylochrysis* was introduced by Réblová et al. (2014), with *X. lucida* designated as the type species, collected from the decaying wood and bark of a twig of *Rhododendron* species in Germany. The type species was reported to have a hyphomycetous asexual morph in culture (Réblová et al. 2014). The second species, *Xylochrysis aquatica*, was reported from submerged decaying wood in Sichuan Province, China (Song et al. 2023). Currently, the genus comprises two species, and the ITS, LSU, SSU, *tef1-α*, and *rpb2* gene regions were used to determine the species (Song et al. 2023). This paper introduces the third species of *Xylochrysis* from Qujing, Yunnan Province, China.

Xylochrysis hydei G.Q. Zhang & Wijayaw., sp. nov. Fig. 52

Index Fungorum number: IF903437; Facesoffungi number: FoF17342

Etymology – 'hydei' named in honor of the renowned mycologist Kevin D. Hyde, recognizing his significant contributions to mycology on the occasion of his 70th birthday.

Holotype – GMB-W 1199

Saprobic on dead wood branches in terrestrial habitats. Sexual morph: *Ascomata* 185–420 µm long, 130–300 µm diam. ($\overline{x}$ = 290 × 200 µm, n = 10), semi-immersed to superficial on decorticated wood under the peeled off periderm or erumpent through the periderm, seven or more aggregated or confluent into groups commonly, rarely solitary, scattered, globose to subglobose, nonstromatic, uniloculate, ostiolate. *Ostiole* 80–200 µm long, 40–80 µm diam. ($\overline{x}$ = 115 × 55 µm, n = 10), black, papillate. *Ascomatal wall* multi-layered, outer layers 20–35 µm thick, composed of brown to dark brown cells of *textura angularis*, form a thicker layer in the lower part of the ostiole; inner layers 15–35 µm, thin, composed of flattened, hyaline cells of *textura prismatica*. *Hamathecium* 2.5–6 µm, may be lacking at maturity but usually present, narrowly cylindrical to filiform, septate paraphyses, not embedded in a gelatinous matrix. *Asci* 70–115 × 3.5–5 µm ($\overline{x}$ = 90 ×4 µm, n = 25), 8-spored, unitunicate, cylindrical, long pedicellate, tapering to the bulbose base, apically rounded with an apical ring. *Ascospores* 5.0–7.0 ×2.5–3.5 µm ($\overline{x}$ = 6 × 3 µm, n = 30), L/W 1.5–2.5 µm ($\overline{x}$ = 2.0 µm, n = 30), uniseriate, ellipsoidal, hyaline, aseptate, straight, 2-guttulate, thin-walled, smooth-walled, without mucilaginous sheath or appendages. Asexual morph: Undetermined.

Culture characteristics – Culture is unavailable

Material examined – China. Yunnan Province, Qujing City, Qujing Normal University premises, 01 September 2023, Gui-Qing Zhang & Nalin N. Wijayawardene, QJNU07 (GMB-W 1199, holotype); *ibid.* (GMB-W 1120, isotype).

GenBank numbers – GMB-W 1199: ITS = PV113466, LSU = PV113468, *tef1-α* = PV134364, *rpb2* = PV134362; GMB-W 1120: ITS = PV113467, LSU = PV113469, *tef1-α* = PV134365, *rpb2* = PV134363.

Notes – The phylogenetic analyses based on a combined dataset of ITS, LSU, *tef1-α*, and *rpb*2 gene regions (Fig. 51) showed that our collections (GMB-W1119 holotype, and GMB-W11200) are placed in the genus *Xylochrysis*, and formed a distinct branch with *X. lucida* (CBS 135996) and *X. aquatica* (GMBCC 3.23639) with 100% ML and 1.00 PP support. Based on nucleotide comparisons, our species *Xylochrysis hydei* (GMB-W 1119, holotype) differs from *X. lucida* (CBS 135996) by 1.5% (8/519 bp) in the ITS locus, 0.2% (2/847 bp) in the LSU locus, and 0% (0/1071) in the *rpb*2 locus, while it differs from *X. aquatica* (GMBCC 3.23639) by 2.3% (12/511 bp) in the ITS locus, 0% (1/814 bp) in the LSU locus, and 1.3% (13/935) in the *tef1-α* locus. Morphologically, our species *X. hydei* matches the morphology of *Xylochrysis* well in having papillate ostiolate ascomata with a multi-layered ascomatal wall, hamathecium septate, unitunicate hamathecium, cylindrical asci with an apical ring, and ascospores hyaline, aseptate ascospores (Réblová et al. 2014, Song et al. 2023). However, our species *X. hydei* can be distinguished from the type species *X. lucida* by smaller ascomata (185–420 µm × 130–300 µm vs. 350–500 µm × 350–500 µm), rare hamathecium, narrow ostiolar neck (40–80 µm in base vs. 100–120 µm in base), and its longer asci (70–115 µm long vs. 59–73 µm long) (Réblová et al. 2014). While our species shows similarity to the ascomata of *X. lucida*, aggregated or confluent in groups, but can be separated by *X. lucida* ascomata surrounded by a golden yellow layer of cells (Réblová et al. 2014).

Furthermore, *Xylochrysis hydei* is easily distinguished from *X. aquatica* by its rarely solitary, scattered, seven or more aggregated or confluent into groups, broader ascomata (185–420 µm in diam. vs. 160–265 µm in diam.), rare hamathecium, longer and narrower ostiolar neck (80–200 × 40–80 µm vs. 65–135 µm × 65–130 µm) (Song et al. 2023). Therefore, based on morphology and phylogeny, we introduce our collection as a new species, *Xylochrysis hydei.*

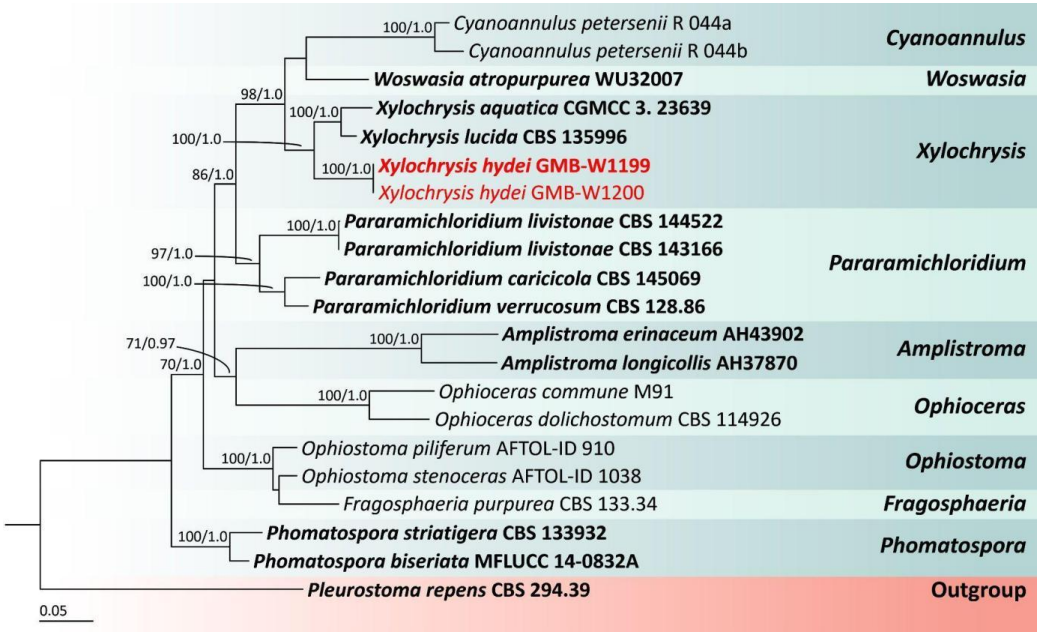


Figure 51 – Phylogram generated from maximum likelihood analysis based on combined ITS, LSU, *tef1-α*, and *rpb2* sequence data from 21 taxa, comprising 3,202 characters (ITS = 511, LSU = 813, *tef1-α* = 876, *rpb2* = 1,002). The best-scoring RAxML tree with a final likelihood value of -16551.679. The matrix contained 1,155 distinct alignment patterns, with 41.97% of the characters being undetermined or gaps. Estimated base frequencies were as follows: A = 0.234, C = 0.270, G = 0.289, T = 0.206; substitution rates: AC = 1.101, AG = 1.854, AT = 1.083, CG = 1.209, CT = 5.335, GT = 1.0; gamma distribution shape parameter α = 0.429. Bootstrap support values for maximum likelihood (ML) equal to or greater than 70% and clade credibility values greater than 0.90 (rounded to two decimal places) from Bayesian inference analysis are labeled at each node. Ex-type strains are in bold, while the new isolates are indicated in red bold. The tree is rooted to *Pleurostoma repens* (CBS 294.39).

Subclass Hypocreomycetidae O.E. Erikss. & Winka

Hypocreales Lindau

Bionectriaceae Samuels & Rossman

Stilbocrea Pat., Bull. Soc. mycol. Fr. 16(4): 186 (1900)

Index Fungorum number: IF5263; Facesoffungi number: FoF10908

Stilbocrea is a genus in the family *Bionectriaceae* of the order *Hypocreales*, established by Patouillard (1900a) based on the type species *S. dussii* found on dead stems of *Daphnopsis caribaea* in Guadeloupe, France. Eleven epithets are listed under *Stilbocrea*, and of which two have been transferred to other genera (Index Fungorum 2025). Species in this genus can be found on dead plant material globally. Some species of *Stilbocrea* are known to cause wood discoloration and trunk diseases (Bolboli et al. 2022). For instance, *S. colubrensis* has been reported on *Bambusa vulgaris* (Lechat & Fournier 2019) and *S. walteri* on *Quercus ilex* (Voglmayr & Jaklitsch 2019) and diverse Citrus species, including *Citrus aurantifolia*, *C. aurantium*, and *C. limon* (Esparham et al. 2020). *Stilbocrea macrostoma* has been implicated in wood necrosis and decline symptoms on oak (*Quercus brantii*) trees in Iran (Di Lecce et al. 2021). The genus is known by its sexual morph and asexual morphs. The sexual morph is characterized by fleshy, spreading, superficial, non-black

stroma, immersed perithecia, thecae octospores, without paraphyses, colorless, uniseptate spores, conidiophores with stipitate head, born on the aseophoric stroma (Patouillard 1900a). The asexual morph in culture is characterized by dark colonies, globose or allantoid conidia, phialides that are terminally and laterally formed, cylindrical to lageniform, and branched or verticillioid (Voglmayr & Jaklitsch 2019, Bolboli et al. 2022).

In recognition of Prof. Kevin D. Hyde's outstanding contributions to mycology, we herein introduce two new species, *Stilbocrea hydei* and *S. yunnanensis*. We also provide an updated phylogenetic tree for *Stilbocrea* (Fig. 53).

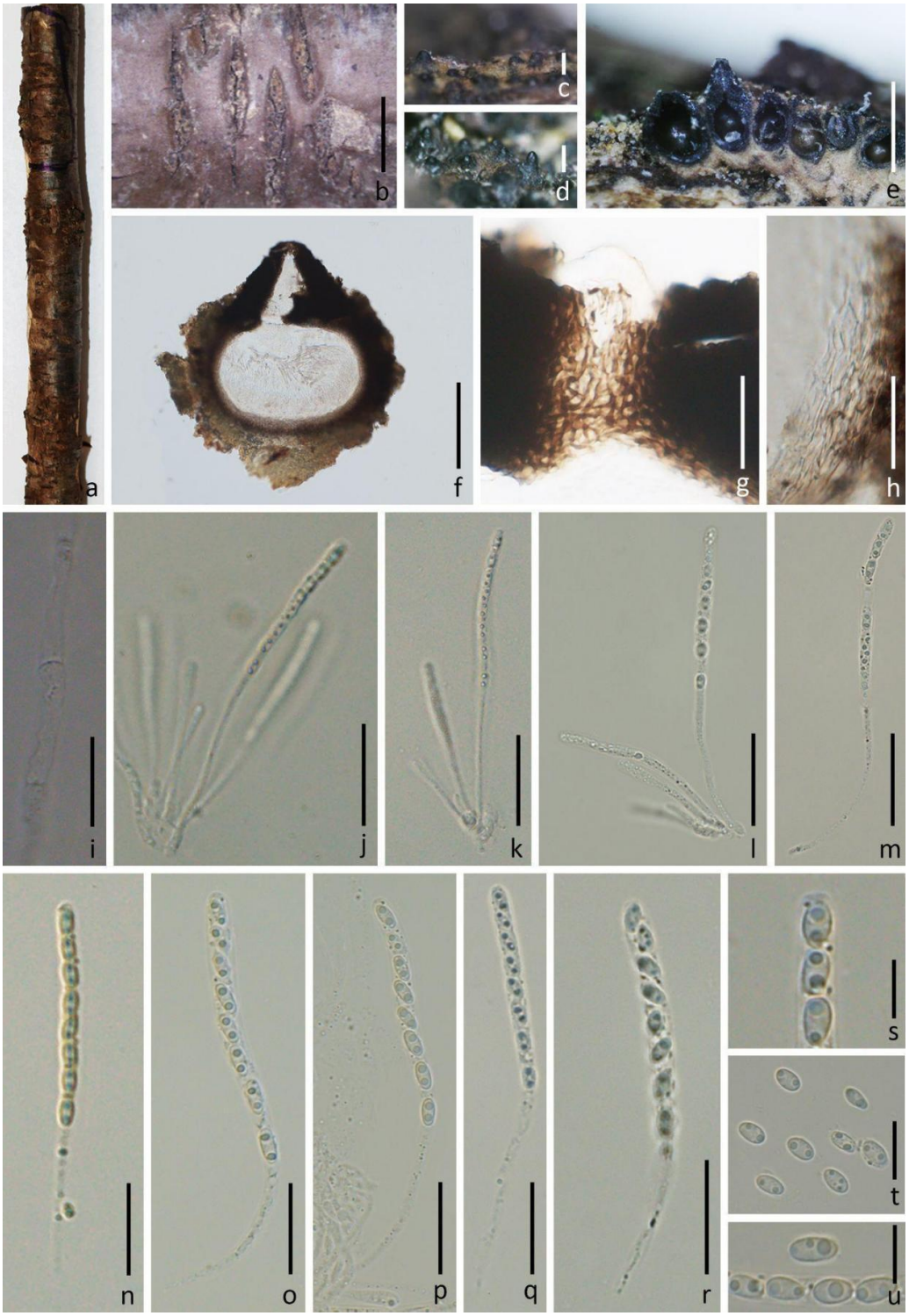


Figure 52 – *Xylochrysis hydei* (GMB-W1199, holotype). a Habit of ascomata on a branch. b–d Appearance of ascomata on host substrate. e, f Vertical section of ascomata. g Ostiole.

h Vertical section through ascomatal wall. I Hamathecium. j–r Asci (q, r stained with Lugol's iodine reagent). s Apical ring stained with Lugol's iodine reagent. t, u Ascospores. Scale bars: b = 550 μm, c, g–l = 30 μm, d = 40 μm; e = 400 μm, f = 150 μm, i, r–t = 10 μm, m–q = 20 μm.

Stilbocrea hydei X.C. Peng, & T.C. Wen, sp. nov. Fig. 54

Index Fungorum number: IF903300; Facesoffungi number: FoF17281

Etymology – 'hydei' named in honor of the renowned mycologist Kevin D. Hyde, recognizing his significant contributions to mycology on the occasion of his 70th birthday.

Holotype – HKAS 145716

Sexual morph: *Stroma* ca. 1 high × 3–4 mm diam., solitary, orange, pulvinate, orange in section. *Perithecia* 220–350 × 155–265 μm ($\overline{x}$ = 286 × 219 μm, n = 10), immersed, elliptical, with ostiolate. *Peridium* 14–43 μm thick ($\overline{x}$ = 26 μm, n = 20). *Asci* 74–111 × 5–10 μm ($\overline{x}$ = 90 × 7.1 μm, n = 15), oblong, narrowly clavate, upper part with eight uniseriate ascospores, lower part stipe-like, 35–60 μm long. *Ascospores* 10–15 × 4–6 μm ($\overline{x}$ = 12.3 × 5 μm, n = 60), ellipsoid, oblong or fusoid, hyaline, with a median or slightly eccentric septum, straight, symmetric or slightly curved, slightly constricted at the septum, with blunt or rounded ends. Asexual morph: Undetermined.

Material examined – China, Yunnan Province, Kunming City, Yeya Lake, on an unidentified stick, 22 July 2024, Xing-Can Peng, YYH240722105 (HKAS 145716, holotype).

GenBank numbers – HKAS 145716: ITS = PQ849524, LSU = PQ849525, SSU = PQ849526, *rpb1* = PQ848109.

Notes – In phylogenetic analysis based on the combined LSU, ITS, *rpb2*, and *tef1-α* sequence dataset (Fig. 53), *Stilbocrea macrostoma* strains 1.11 and CBS 141849 were grouped within *S. gracilipes* (CLLM16015) with 76% ML bootstrap support and 0.98 BYPP values. Cruz et al. (2021) and Hou et al. (2023) provided molecular data for *S. macrostoma* strains 1.11 and CBS 141849, respectively; however, neither study reported morphological analyses. The molecular data and morphological examination of *S. gracilipes* (CLLM16015) were provided by Lechat & Fournier (2019). A pairwise nucleotide comparison revealed that the isolate *S. macrostoma* (CBS 141849) differs from *S. gracilipes* (CLLM16015) in 2/513 bp of ITS (0.39%, excluding gaps), while the LSU sequences of *S. macrostoma* (1.11) and *S. gracilipes* (MFLU 19–0966) are 100% identical. Therefore, *S. macrostoma* strains 1.11 and CBS 141849 should be renamed to *S. gracilipes* (Fig. 54). The new species, *S. hydei* is sister to *S. macrostoma* (CLLG18056, CLLG18033, and SM) and regarded as a different species, supported by 100% bootstrap (ML) and 1.00 BYPP values. The phylogenetic analysis reveals that *S. macrostoma* is not monophyletic, suggesting that it may be split into multiple species in the future (Fig. 54, Voglmayr & Jaklitsch 2019). *Stilbocrea macrostoma* isolates G.J.S. 02–125, CBS 114375, and GJS 73-26 are characterized solely by molecular data. *Stilbocrea macrostoma* isolates CLLG18056, CLLG18033, and SM have both molecular data and illustrations but lack a description of their sexual morph. Guu et al. (2010) described the sexual morph of *S. macrostoma* in Taiwan, China, without providing molecular data. The difference between *S. hydei* and *S. macrostoma* (Guu et al. 2010) is that the peridium of the former is thicker (14–43 μm vs. 12–26 μm), and the asci and ascospores are longer (asci: 74–111 × 5–10 μm vs. 68–100 × 5–9 μm; ascospores: 10–15 × 4–6 μm vs. 9–14 × 4–6 μm). Our base pair comparisons have unveiled significant genetic differences between *S. hydei* (HKAS 145716) and *S. macrostoma* (SM). These differences amount to 1.56% (9/577 bp, no gaps) in the ITS region, 0.62% (5/810 bp, no gaps) in the LSU region, 2.56% (18/703 bp, no gaps) in the *rpb1* region, and 0.62% (5/810 bp, no gaps) in the SSU region. Further comparisons between *S. hydei* (HKAS 145716) and *S. macrostoma* (CLLG18033) revealed 1.81% differences (10/553 bp, no gaps) in the ITS region, and 0.62% (5/810 bp, no gaps) in the LSU region. When compared with *S. macrostoma* (CLLG18056), the differences were 1.63% (9/551 bp, including 1 gap) in the ITS region, and 0.62% (5/810 bp, no gaps) in the LSU region. These findings lead us to introduce our new collection as a novel and distinct species, *S. hydei*.

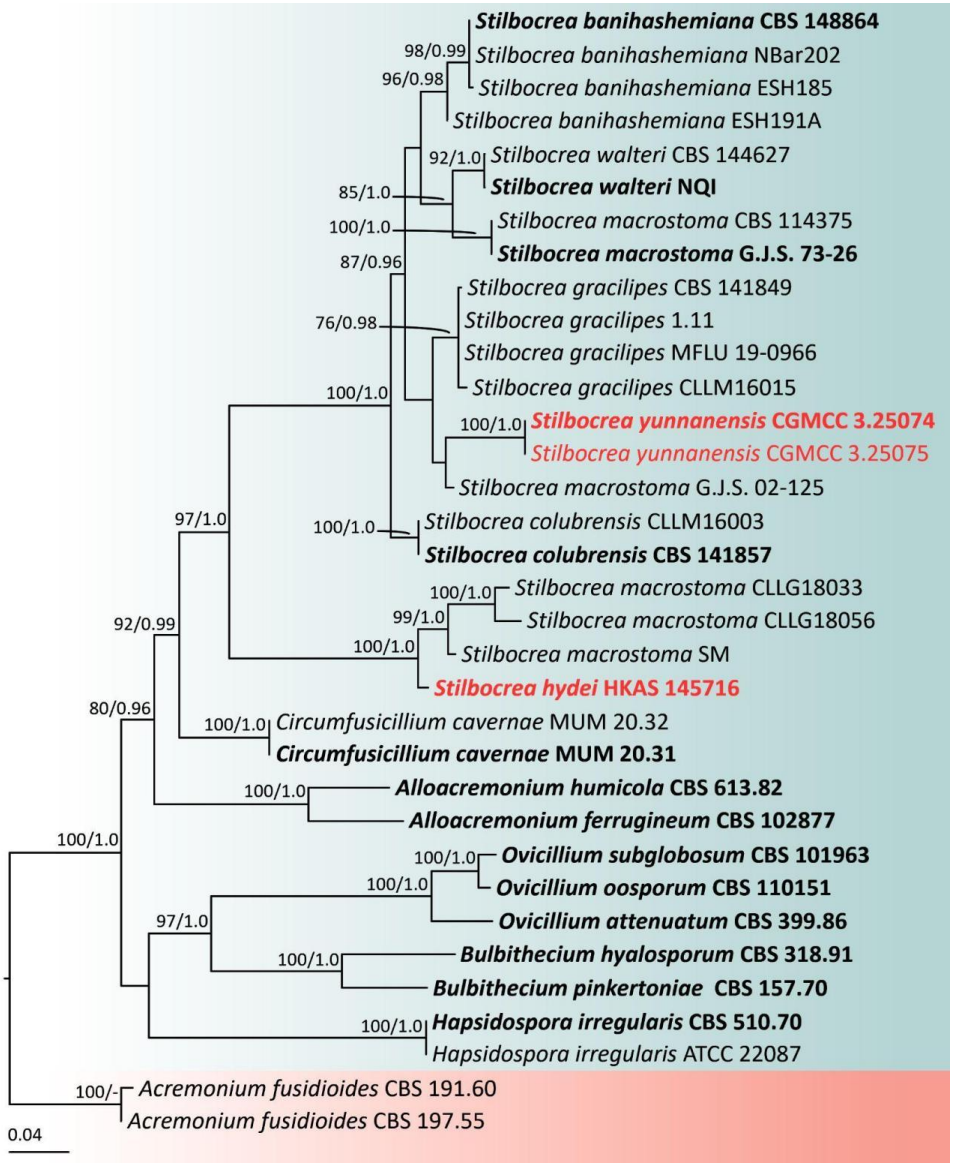


Figure 53 – Phylogram generated from maximum likelihood analysis based on combined LSU, ITS, *rpb2*, and *tef1-α* sequence data from 34 taxa, comprising 5,977 characters (LSU = 2,016, ITS = 1,623, *rpb2* = 1,004, *tef1-α* = 1,334). The best-scoring RAxML tree with a final likelihood value of -18754.906 is presented. The matrix contained 1,114 distinct alignment patterns, with 63.87% of the characters being undetermined or gaps. Estimated base frequencies were as follows: A = 0.240, C = 0.263, G = 0.275, T = 0.222; substitution rates: AC = 1.295, AG = 2.237, AT = 1.260, CG = 0.730, CT = 6.047, GT = 1.0; gamma distribution shape parameter α = 0.491. Bootstrap support values for maximum likelihood (ML) equal to or greater than 70% and clade credibility values greater than 0.90 (rounded to two decimal places) from Bayesian inference analysis are labeled at each node. Ex-type strains are in bold, while the new isolates are indicated in red. The tree is rooted to *Acremonium fusidioides* (CBS 191.60) and *A. fusidioides* (CBS 191.60 and CBS 197.55).

Stilbocrea yunnanensis Y. Gao & H. Gui, sp. nov. Fig. 55

Index Fungorum number: IF901620; Facesoffungi number: FoF17761

Etymology – The epithet refers to the type locality, Yunnan Province, China.

Holotype – HKAS 145986

Saprobic on the dead wood of an unidentified plant. Sexual morph: Undetermined. Asexual morph: *Synnemata* up to 1500 µm high, 140–220 µm wide in the middle, erumpent through host epidermis, scattered, gregarious, cylindrical-capitate, subulate-capitate to spatulate, nodding or sinuous, straight, slender, unbranched, smooth to hirsute, stipe red-brown with pink white.

Conidiophore branching once or twice. *Phialides* 3–6 × 2–3 µm ($\bar{x}$ = 4.7 × 2.6 µm, n = 20), subulate or cylindrical, straight or curved, proliferating percurrently, collarettes sometimes slightly flared, periclinal thickening present. *Conidial mass* 440–615 µm ($\bar{x}$ = 570 µm, n = 20), globose or subglobose, the shade of pink, opaque or translucent. *Conidia* 5.5–7 × 3–4 µm ($\bar{x}$ = 6.5 × 3.7 µm, n = 35), ellipsoidal, straight or slightly curved, hyaline, usually with two polar guttules, and with thickened walls.

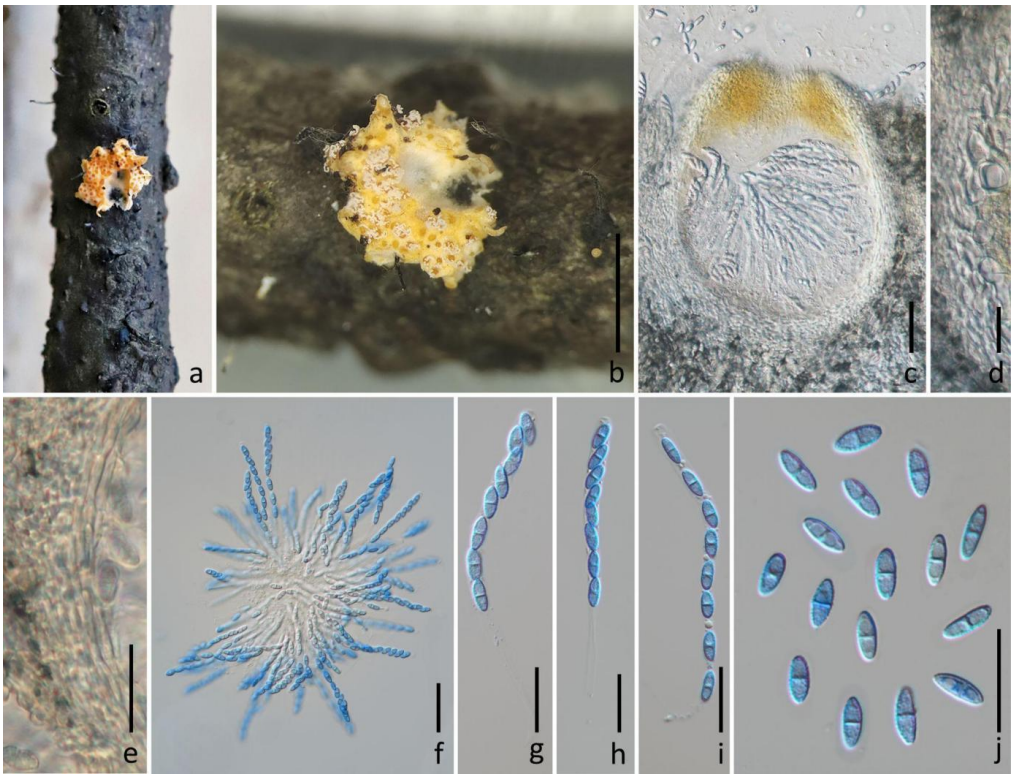


Figure 54 – *Stilbocrea hydei* (HKAS 145716, holotype). a, b Ascomata on a woody substrate. c Vertical cross-section of a perithecia. d, e Peridium in face view and vertical section. f–i Asci with ascospores in lactophenol cotton blue solution. j Ascospores in lactophenol cotton blue solution. scale bars: b = 2 mm, c, f = 50 µm, d–e, g–j = 25 µm.

Culture characteristics – Colonies on PDA reaching 4 cm diam., after 5 weeks at 27 °C, circular, slightly raised, wavy margin, initially white, turn into dark green inner zone and white outer zone when old, plenty of whitish aerial mycelia around the center, Reverse olive-green center with white outer zone. Cultures on PDA are dull-green, plane, aerial mycelium absent, and surface smooth with an entire margin. *Hyphae* 2–4 µm ($\bar{x}$ = 2.8 µm, n = 35), hyaline, branched, septate, guttulate. *Mononematous conidiophores* on PDA Acremonium-like, with phialides 5–15.5 × 2–3.5 µm ($\bar{x}$ = 10.5 × 2.8 µm, n = 35), arising from single hyphae or fascicles. *Conidia* 3.5–5.5 × 3–4 µm ($\bar{x}$ = 4.3 × 3.5 µm, n = 30), oblong-ellipsoidal, hyphae, guttulate.

Material examined – China, Yunnan Province, Kunming City, on dead wood of an unidentified plant, 13 May 2021, Y. Gao, GY164A (HKAS 145986, holotype), ex-type CGMCC 3.25074; *ibid.*, GY164B (HKAS 145995), living culture CGMCC 3.25075.

GenBank numbers – CGMCC 3.25074: ITS = PV154035, LSU = PV154037, *rpb1* = PV166241, *tef1-α* = PV166239; CGMCC 3.25075: ITS = PV154036, LSU = PV154037, *rpb1* = PV166242, *tef1-α* = PV166240.

Notes – In our phylogenetic analyses (Fig. 54), *Stilbocrea yunnanensis* formed a sister clade to *S. macrostoma* (G.J.S. 02-125); however, their relationship is not statistically supported by either ≥70% ML or 0.90 BYPP. Hirooka et al. (2010) provided molecular data of the isolate *S. macrostoma* (G.J.S. 02-125), but morphological characters were not reported. The LSU and *rpb1*

sequences of *S. yunnanensis* differ from those of *S. macrostoma* (G.J.S. 02-125) by 6/847 (0.71%) bp and 44/690 (6.38%) bp, respectively. Our species, *S. yunnanensis*, also clustered closer to *S. gracilipes* (CLLM16015) (Fig. 53). Sequence comparison for the ITS region between *S. yunnanensis* and *S. gracilipes* (CLLM16015) showed a 2.25% difference (13/578 bp, without gaps). Morphologically, *S. yunnanensis* is different from *S. gracilipes* (CLLM16015) in having synnemata that are red-brown with pink white, cylindrical-capitate vs. grey, grey brown to blackish, granulose in the upper part, 5.5–7 × 3–4 μm vs. 4–8(–9) × 2.5–3 μm conidia in nature, and 3.5–5.5 × 3–4 μm vs. 4.5–7 × 1.5–2 μm in culture) (Lechat & Fournier 2019). Therefore, we introduced our strains as a new species, namely *Stilbocrea yunnanensis* sp. nov., based on phylogenetic analyses and morphological characteristics

Cordycipitaceae Kreisel ex G.H. Sung, J.M. Sung, Hywel-Jones & Spatafora
Hevansia Luangsa-ard, Hywel-Jones & Spatafora

Index Fungorum number: IF820885; Facesoffungi number: FoF13127

Hevansia was introduced by Kepler et al. (2017) to accommodate *H. novoguineensis* as the type species, which was previously known as *Akanthomyces novoguineensis* (Samson & Brady 1982). *Hevansia* species are characterized by having immersed, ovoid, or sickle-shaped perithecia and hyaline, filiform ascospores. In addition, they have an akanthomyces-like asexual morph with white stroma, monophialidic conidiogenous cells, and hyaline, clavate conidia (Kepler et al. 2017, Mongkolsamrit et al. 2022). Currently, eight species are listed in Index Fungorum (2025), namely *H. arachnophila* (Sri Lanka, on *Araneida*), *H. longispora* (China, on *Araneae*), *H. mainiae* (Queensland, on *Araneae*), *H. minuta* (Thailand, on *Meotipa*), *H. nelumboides* (Japan, on *Araneae*), *H. novoguineensis* (Papua New Guinea, on *Araneae*), *H. ovalongata* (China, on *Araneae*), and *H. websteri* (Thailand, on *Araneae*). Most of the *Hevansia* species have been introduced based on asexual morphs that were reported from China, Papua New Guinea, Sri Lanka, and Thailand (Samson & Evans 1974, Samson & Brady 1982, Hywel-Jones 1996, Hsieh et al. 1997, Huang 2000, Kepler et al. 2017, Mongkolsamrit et al. 2022).

In recognition of Kevin D. Hyde's outstanding contributions to mycology, we hereby introduce *Hevansia hydei*. We provide an updated phylogenetic tree for *Hevansia* (Fig. 56).

Hevansia hydei J. X. Li & S. K. Huang, sp. nov. Fig. 57

Index Fungorum number: IF903737; Facesoffungi number: FoF17762

Etymology – 'hydei' named in honor of the renowned mycologist Kevin D. Hyde, recognizing his significant contributions to mycology on the occasion of his 70th birthday.

Holotype – HKAS 146639

On a dead spider on the underside of leaves. Sexual morph: Undetermined. Asexual morph: *Mycelium* completely covering the host, cream, comprised of hyaline, septate hyphae. *Synnemata* erect, simple, numerous, cylindrical, occasionally acuminate apex, white to cream, up to 1 mm long, 48–95 μm broad, composed of *textura porrecta*. *Conidiophores* covering the synnemata, reduced to conidiogenous cells, lateral on hyphae. *Conidogenous cells* 3.8–7.7 × 3–5.2 μm ($\overline{x}$ = 5.8 × 3.9 μm, n = 20), solitary, globose to subglobose, with a distinct cylindrical neck, 1.4–2.9 × 0.8–1.2 μm ($\overline{x}$ = 2.1 × 1.1 μm, n = 20). *Conidia* 5.8–8.9 × 1.1–1.9 μm ($\overline{x}$ = 7.6 × 1.4 μm, n = 20), in short chains, hyaline, cylindrical, aseptate.

Culture characteristics – Colonies on PDA attaining 15–17 mm diam., within 14 days at 25 °C, circular, slightly raised, red to reddish with plenty of whitish aerial mycelium covering the surface, reddish pigment diffusing in the medium; Reverse red center with white hyphal rim.

Material examined – China, Yunnan Province, Pu'er City, Sun River National Park, on spider attached to the underside of a dicot leaf of forest plants, 6 August 2024, S. K. Huang, TYH 9-3 (HKAS 146639, holotype); ex-type ZNUZCC010214.

GenBank numbers – ZNUZCC010214: ITS = PQ816943, *tef1-α* = PQ899251, *rpb2* = PQ899250.

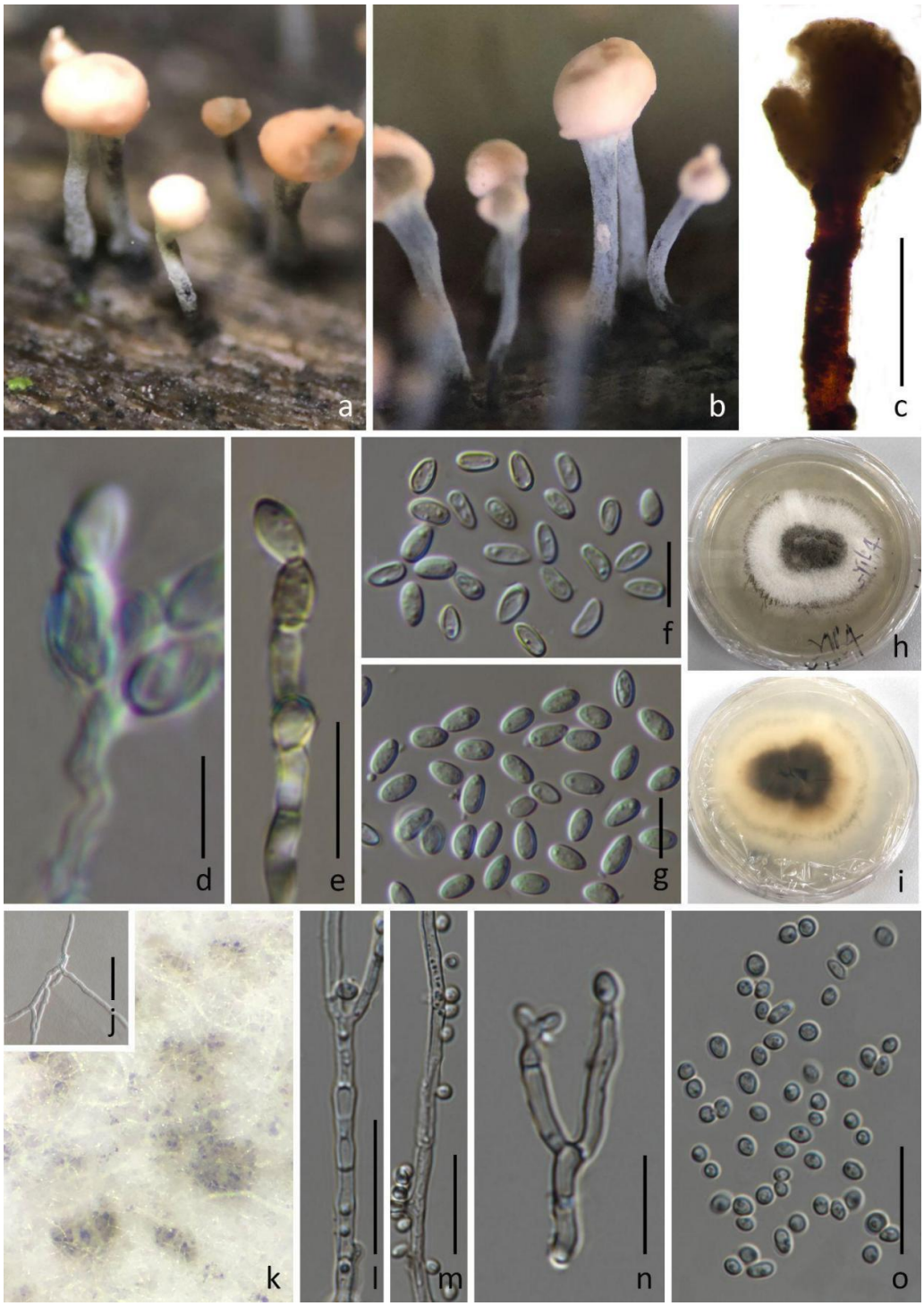


Figure 55 – *Stilbocrea yunnanensis* (CGMCC 3.25074, holotype). a–c Synnemata on substrate. d, e Conidiophores and phialides on natural substrate. f Conidia (when immature). g Conidia (when mature). h Surface view of the colony on PDA. i Reverse view of the colony on PDA. j Germinated conidium. k Hyphae with conidia masses forming on culture. l–n Conidiophores and phialides. o Conidia. Scale bars: c = 500 µm, j, l, m, o = 20 µm, e–g, n = 10 µm, d = 5 µm.

Notes – In the phylogenetic analysis based on combined ITS, LSU, *tef1-α*, *rpb1*, and *rpb2* sequence data (Fig. 56), our collection formed a sister clade with *Hevansia novoguineensis* (non-type strains, BCC 2190 and BCC 49323), with 94% ML and 0.94 PP support values. The type strain of *H. novoguineensis* (CBS 610.80) clusters separately with *H. mainiae* strains. Based on nucleotide comparison between our new species and the type strain of *H. novoguineensis* (CBS 610.80) showed 3.79% differences (21/554 bp, including 5 gaps) in the ITS region, 0.38% (3/794

bp, no gap) in the *tef1-α* region, and 1.45% (10/689 bp, no gap) in the *rpb2* region. We also compared our new species with three non-type strains of *H. novoguineensis*. Strain BCC 49323 showed 2.10% differences (11/224 bp, including 3 gaps), and strain BCC 42675 showed 2.69% differences (15/557 bp, including 3 gaps) in the ITS region, while BCC 2190 lacked ITS sequence data. For the *tef1-α* region, base pair differences between our species and BCC 49323, BCC 2190, and BCC 42675 were 0.25% (2/786 bp, no gaps), 1.15% (9/784 bp, including 1 gap), and 0.64% (5/786 bp, no gaps), respectively. In the *rpb2* region, the differences were 0.59% (4/679 bp, no gaps) and 0.92% (6/649 bp, no gaps) compared to BCC 49323 and BCC 42675, respectively, while *rpb2* sequence data were not available for BCC 2190. Morphologically, our new collection has significantly smaller conidia (*H. hydei*: 5.8–8.9 × 1.1–1.9 µm vs. *H. novoguineensis*: 10.5–17.5 × 1.5–3 µm) (Samson & Brady 1982). Most species of *Hevansia* grow on dead spiders and are often attached to the underside of living leaves (Petch 1923, Samson & Brady 1982, Mongkolsamrit et al. 2022). Previously, this genus has been reported in Anhui and Taiwan, China (Hsieh et al. 1997, Huang 2000). Therefore, we introduce our collection as a new species, *H. hydei*, and this is the first report of this genus in Yunnan, China.

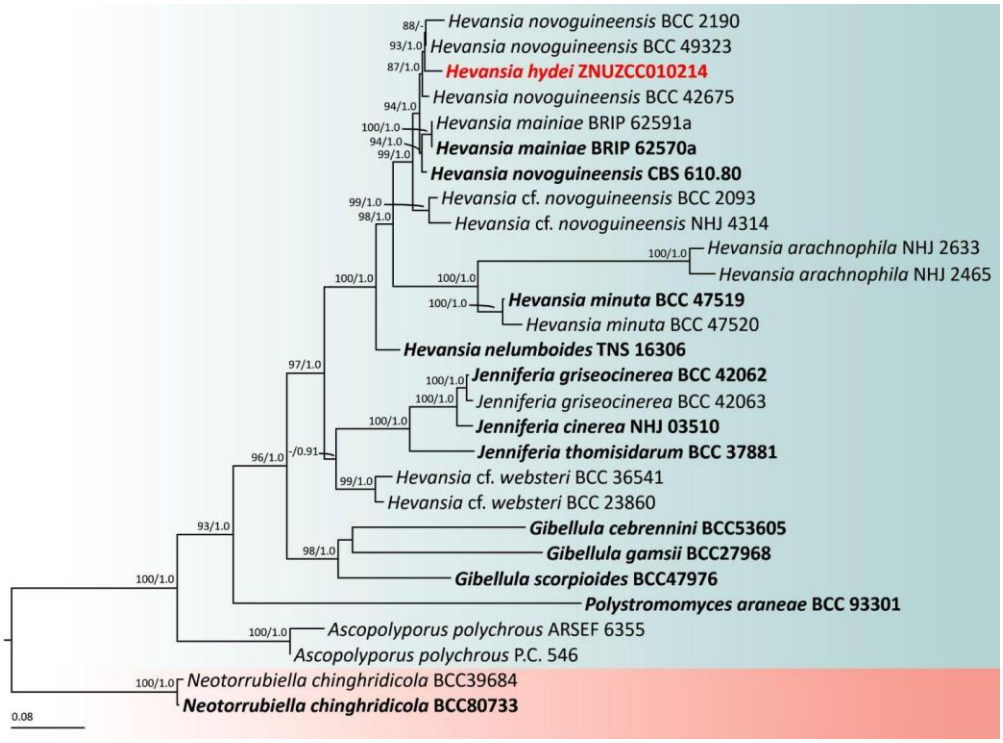


Figure 56 – Phylogram generated from maximum likelihood analysis based on combined ITS, LSU, *tef1-α*, *rpb1*, and *rpb2* sequence data from 28 taxa, comprising 4,123 characters (ITS = 681, LSU = 839, *tef1-α* = 900, *rpb1* = 760, *rpb2* = 943). The best-scoring RAxML tree with a final likelihood value of -19544.710 is presented. The matrix contained 1,418 distinct alignment patterns, with 27.94% of the characters being undetermined or gaps. Estimated base frequencies were as follows: A = 0.231, C = 0.292, G = 0.278, T = 0.198; substitution rates: AC = 1.252, AG = 3.735, AT = 0.788, CG = 1.104, CT = 9.579, GT = 1.0; gamma distribution shape parameter α = 0.901. Bootstrap support values for maximum likelihood (ML) equal to or greater than 70% and clade credibility values greater than 0.90 (rounded to two decimal places) from Bayesian inference analysis are labeled at each node. Ex-type strains are in bold, while the new isolate is indicated in red bold. The tree is rooted to *Neotorrubiella chinghridicola* (BCC39684 and BCC80733).

Leptobacillium Zare & W. Gams, Mycol. Progr. 15: 1001 (2016)

Index Fungorum number: IF815489; Facesoffungi number: FoF13129

Leptobacillium was established by Zare & Gams (2016) to accommodate the type species *L. leptobactrum* (≡ *Verticillium leptobactrum*), which was initially described with two varieties: *L. leptobactrum* var. *leptobactrum* and *L. leptobactrum* var. *calidius*. Morphologically, *Leptobacillium* resembles *Simplicillium*, but phylogenetic analysis based on combined LSU and SSU sequence data confirmed its distinction as a separate genus (Zare & Gams 2016). Subsequent studies transferred three species, *viz*., *L. chinense*, *L. coffeanum* (Okane et al. 2020), and *L. filiforme* (Chen et al. 2021) from *Simplicillium* to *Leptobacillium* based on combined ITS, LSU, and SSU phylogenetic analyses. Currently, *Leptobacillium* comprises ten verticillium-like species, characterized by whitish colonies and erect conidiophores (Index Fungorum 2025).

Species within *Leptobacillium* are primarily saprotrophic, with some exhibiting fungicolous lifestyles, colonizing various substrates (Zare & Gams 2016, Preedanon et al. 2023). When cultured on PDA, they form woolly colonies that range in color from white to greyish white, pinkish white, and cream. The reverse side of colonies varies from orange to orange-brown, pale luteous, or milky white to dark buff, sometimes diffusing yellow pigment into the agar (Zare & Gams 2016). The genus is characterized by a hyphomycetous asexual morph, with conidiophores bearing solitary phialides that are rarely irregularly branched, and rod-shaped to slightly fusiform conidia, forming very long, slender chains resembling simple hyphae.

Although Prof. Kevin D. Hyde has not directly contributed to research on *Leptobacillium*, his extensive work on *Simplicillium* and other genera within *Cordycipitaceae* (Wei et al. 2019) has significantly advanced the understanding of this fungal lineage. In this study, we report new geographical and habitat records of *Leptobacillium coffeanum*. An updated phylogenetic tree for *Leptobacillium* is provided (Fig. 58), along with illustrations depicting the morphological characteristics of *L. coffeanum* (Fig. 59).

Leptobacillium coffeanum (A.A.M. Gomes & O.L. Pereira) Okane, Nonaka, Kurihara, J.P. Abe & Yamaoka, Mycoscience 61(4): 169 (2020) Fig. 59

Index Fungorum number: IF834665; Facesoffungi number: FoF17777

Saprobic on decaying wood submerged in a freshwater environment. Sexual morph: Undetermined. Asexual morph: Hyphomycetous. *Hyphae* septate, branched, superficial or slightly immersed, hyaline. *Conidiophores* solitary, smooth-walled, cylindrical–subulate, hyaline-unbranched, and frequently reduced to conidiogenous cells. *Phialides* up to 25 µm long, 1.5–2.0 µm wide, slender, tapering toward the tip, hyaline. *Conidia* 2.0–3.5 × 1–1.5 µm ($\overline{x}$ = 3 × 1.3 µm, n = 10), mostly ovate, ellipsoidal, subcylindrical, aseptate, hyaline.

Culture characteristics – Colonies on PDA reaching 30–35 mm after 30 days at 25 °C, circular, slightly raised, entire margin, velvety and white from above, reverse radial crack and primrose-yellow on reverse. *Conidiophores* solitary or branched with two phialides, arising from procumbent hyphae, blastic, enteroblastic, phialidic, discrete, terminal, solitary. *Phialides* 3.1–35.1 × 0.6–2.0 µm ($\overline{x}$ = 16.4 × 1.1 µm) slender, tapering toward tip, hyaline. *Conidia* 3.37–6.54 × 0.85–1.75 µm ($\overline{x}$ = 5.04 × 1.14 µm), slightly fusiform to narrowly cylindrical, straight, aseptate, hyaline, forming long, slender, and inconspicuous chains. *Chlamydospores* absent.

Material examined – Philippines, Bohol, Loon, Danicop-Ticugan Spring, on a decaying wood submerged in a freshwater stream, 08 August 2023, T.A.R. Lopez, BHL–010–02–2 (UPVMI 23–094), living culture UPVMICC 23–094.

GenBank numbers – UPVMICC 23–094: ITS = PV468734, LSU = PV467067.

Notes – In the phylogenetic analysis based on a concatenated dataset of ITS and LSU sequences (Fig. 58), *Leptobacillum coffeanum* (UPVMICC 23–094) formed a well-supported sister clade with the holotype of *L. coffeanum* (COAD 2057) and other conspecific isolates, receiving maximum support values (100% ML and 1.00 BYPP). Pairwise comparison of the ITS region between UPVMICC 23–094 and COAD 2057 revealed a nucleotide divergence of 1.09% (6/548 bp), while no sequence differences were detected in the LSU region. Morphologically, UPVMICC 23–094 shows some variation compared to the holotype of *L. coffeanum* in phialide dimensions (3.1–35.1 × 0.6–2.0 µm vs. 11–44(–70) × 1.0–2.4 µm) and conidial characteristics. UPVMICC 23–

094 produces fusiform to narrowly cylindrical conidia (3.37–6.54 × 0.85–1.75 µm), whereas COAD 2057 forms slightly curved, spindle-shaped macroconidia (5.3–8.8 × 1.0–1.6 µm) and microconidia (2.2–3.8 × 0.8–1.5 µm) (Gomes et al. 2018). Despite these morphological differences, molecular evidence confirms the identification of UPVMICC 23–094 as *L. coffeanum*. This represents the first report of *Leptobacillum* from the Philippines and the first record of this genus in a freshwater ecosystem.

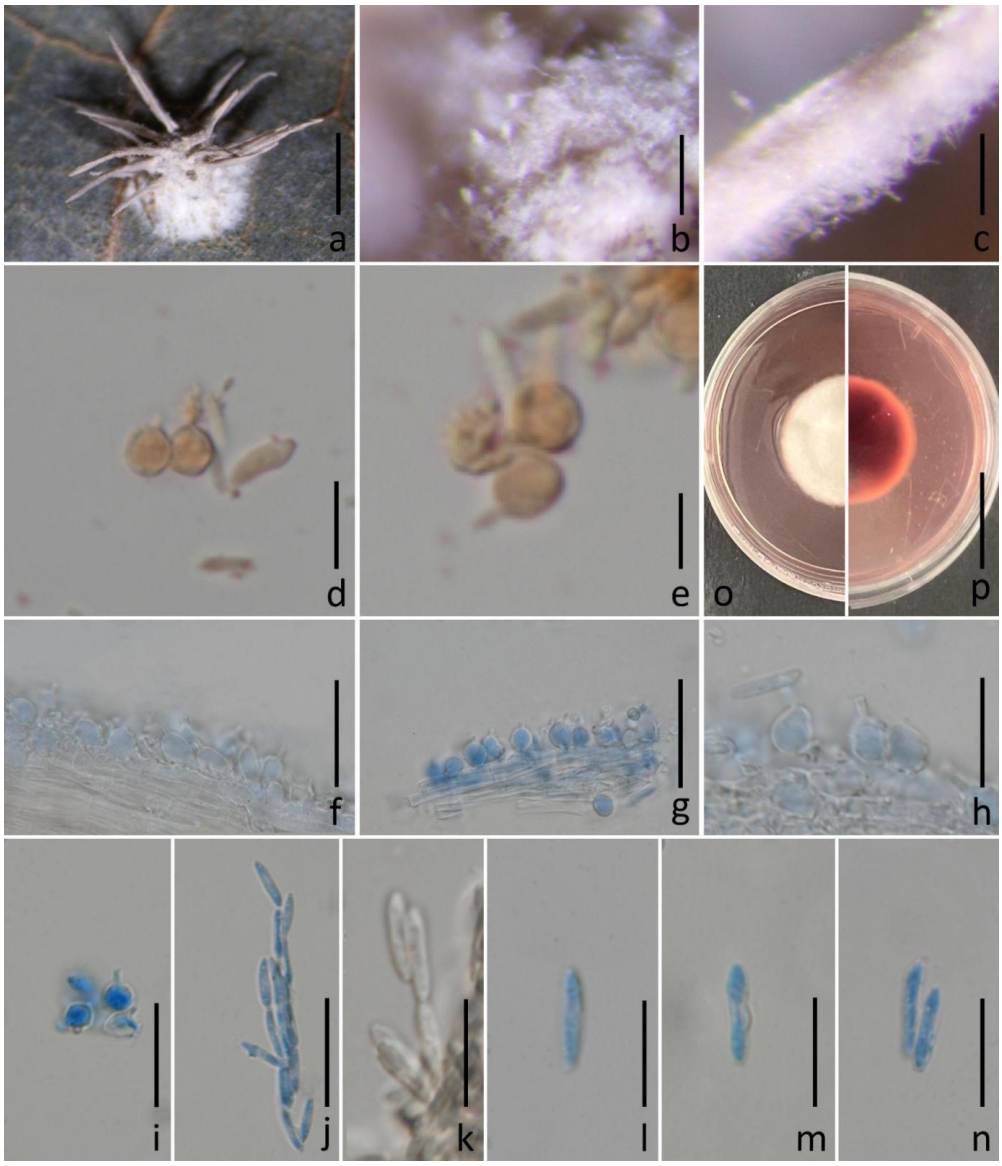


Figure 57 – *Hevansia hydei* (HKAS 146639, holotype). a Mycelium on an unidentified spider host. b White, densely arranged mycelium. c Conidiophores scattered along with the synnemata. d–i Conidiophores reduced conidiogenous cells. j–n Conidia. o–p Colonies on PDA (f obverse, g reverse). (d–e stained in Congo red, f–j, l–n mounted in cotton blue). Scale bars: a = 1000 µm, b–c = 100 µm, e = 5 µm, f, g, i–j = 20 µm, d, h, k–n = 10 µm, o–p = 10 mm.

Hypocreaceae De Not.

Trichoderma Pers., Neues Mag. Bot. 1: 92 (1794).

Index Fungorum number: IF10282; Facesoffungi number: FoF02075

Trichoderma was established by Persoon (1794) and typified by *T. viride*. *Trichoderma* is one of the largest genera in *Hypocreaceae*, with more than 500 accepted species (Cai & Druzhinina 2021, Cao et al. 2022, Yu et al. 2022, Zhang et al. 2022c, Sousa et al. 2023, Ye et al. 2023, Zhao et

al. 2023, 2024). They are frequently found in soil, decaying wood, plant leaves, bark, root systems, or other tissues, and even the human body (Vanderwolf et al. 2013, Jaklitsch & Voglmayr 2015, Zhu et al. 2017, Holz et al. 2018, Zhang & Li 2019, Karunarathna et al. 2020, Bustamante et al. 2021, Liu et al. 2023b). The species of *Trichoderma* are one of the most useful groups of microbes, which can serve as effective biocontrol agents and producers of enzymes, antibiotics, and heterologous proteins for food, feed, textile, and biofuel industries (Mukherjee et al. 2013, Zhu et al. 2017, Bustamante et al. 2021, Cai & Druzhinina 2021, Liu et al. 2023, Zhao et al. 2023, 2024). They play a pivotal role in agriculture and ecology as biocontrol agents of plant pathogens and promoters of plant growth (Samuels 1996, Harman et al. 2004, Anand et al. 2006, Lorito et al. 2010, Mazyar 2010, Tripathi et al. 2013, Zhang et al. 2023c, Zhao et al. 2024). However, *Trichoderma* species have also been reported as pathogens of mushrooms and animals, and can even cause nosocomial mycoses in immunocompromised humans (Chouaki et al. 2002, Myoken et al. 2002, Kredics et al. 2003, 2010, Komoń-Zelazowska et al. 2007, Liu et al. 2023, Zeng et al. 2024). Morphology, combined with the phylogenetic analysis of the ITS, *rpb2*, and *tef1-α* loci, is commonly used in species identification of *Trichoderma* (Zhao et al. 2023, 2024, Zeng et al. 2024). Prof. Kevin D. Hyde and his team introduced more than 10 *Trichoderma* species, out of the 522 known species in Index Fungorum. In recognition of his outstanding contributions to mycology, we introduce *Trichoderma hydei* as a new species. We also provide an updated phylogenetic tree for the *Trichoderma* Harzianum clade (Fig. 60).

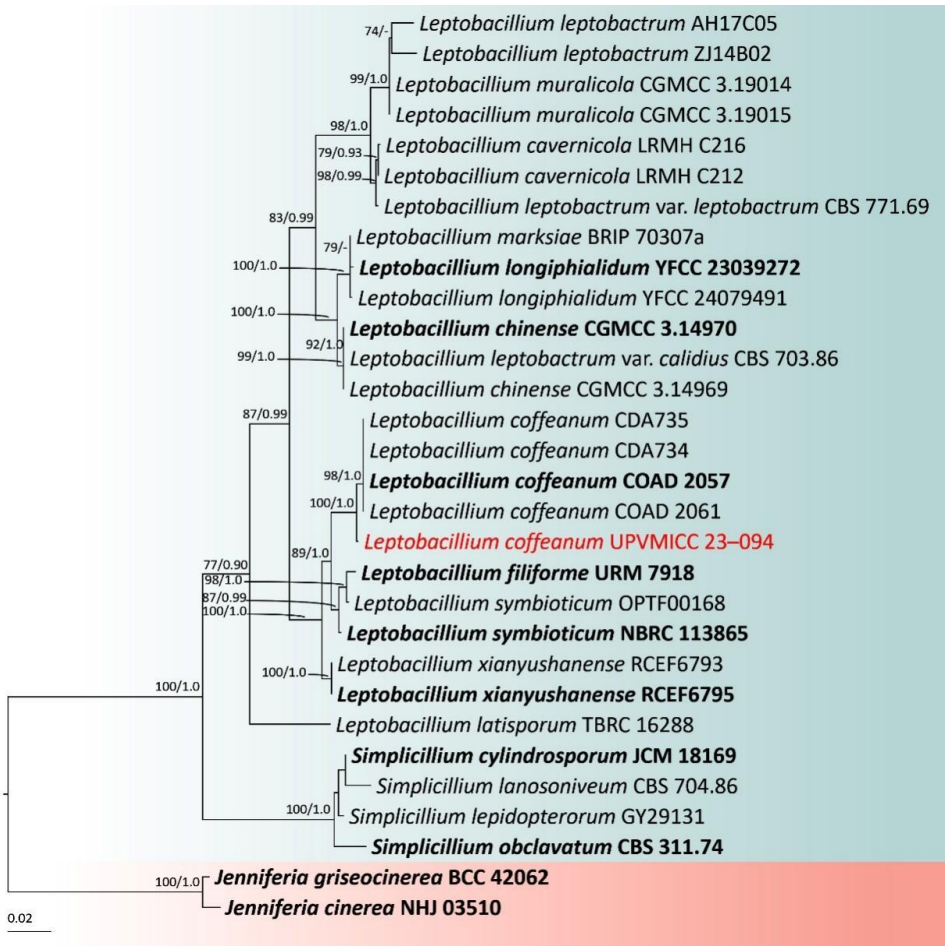


Figure 58 – Phylogram generated from maximum likelihood analysis based on combined ITS and LSU sequence data from 30 taxa, comprising 1,520 characters (ITS = 657, LSU = 863). The best-scoring RAxML tree with a final likelihood value of -4833.601 is presented. The matrix contained 424 distinct alignment patterns, with 20.79% of the characters being undetermined or gaps. Estimated base frequencies were as follows: A = 0.245, C = 0.251, G = 0.285, T = 0.219; substitution rates: AC = 1.659, AG = 2.475, AT = 1.495, CG = 1.078, CT = 6.331, GT = 1.0;

gamma distribution shape parameter α = 0.181. Bootstrap support values for maximum likelihood (ML) equal to or greater than 70% and clade credibility values greater than 0.90 (rounded to two decimal places) from Bayesian inference analysis are labeled at each node. Ex-type strains are in bold, while the new isolate is indicated in red bold. The tree is rooted to *Jenniferia cinerea* (NHJ 03510) and *J. griseocinerea* (BCC 42062).

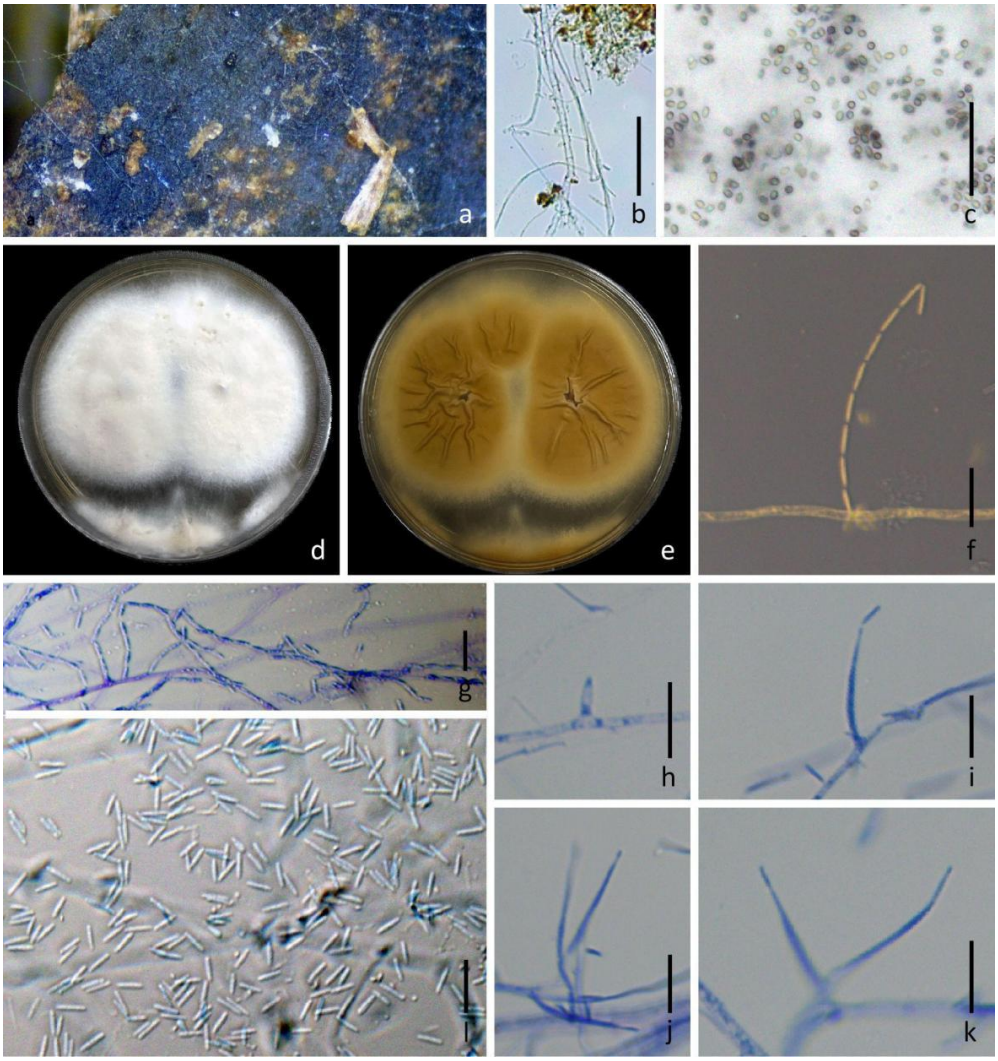


Figure 59 – *Leptobacillium coffeanum* (UPVMI 23–094, new geographical and habitat records). a Appearance of colonies on woody substrate. b Septate hyphae and phialides. c Conidia. d, e Colonies on PDF after 25 days. g Catenulate conidia and phialides. h–k Phialides and conidia. l Conidia. Scale bars: b = 25 µm, c = 5 µm, f–l = 10 µm.

Trichoderma hydei X.F. Liu, Karun. & Tibpromma, sp. nov. Fig. 61

Index Fungorum number: IF903282; Facesoffungi Number: FoF17763

Etymology – 'hydei' named in honor of the renowned mycologist Kevin D. Hyde, recognizing his significant contributions to mycology on the occasion of his 70th birthday.

Holotype – GMB-W1190

Asexual morph on PDA: *Vegetative hyphae* 2–6 µm wide, septate, branched, hyaline, smooth-walled. *Conidiophores* pyramidal with verticillate, comprising a recognizable main axis, branches pairs or solitary, paired lateral branches, longer branches near the base, and short branches or solitary phialides arising near the tip. *Phialides* 6–17 × 2–4 µm ($\overline{x}$ = 9.7 × 2.7 µm, n = 100), ampulliform to lageniform, generally formed on terminal branches in divergent whorls of 2–3. *Supporting cells* 6–15 × 2–4 µm ($\overline{x}$ = 10.7 × 2.6 µm, n = 50). *Conidia* 2–4 × 2–3 µm ($\overline{x}$ = 2.9 × 2.6 µm, n = 100), ellipsoidal to ovoid, straight to slightly curved, light grey to green, smooth-walled.

Chlamydospores 3–8 × 2–7 µm ($\bar{x}$ = 5.3 × 4.0 µm, n = 60), single or in clusters, terminal and intercalary, variable in shape, mostly subglobose to globous, thick-walled, hyaline, granulate. Sexual morph: Undetermined.

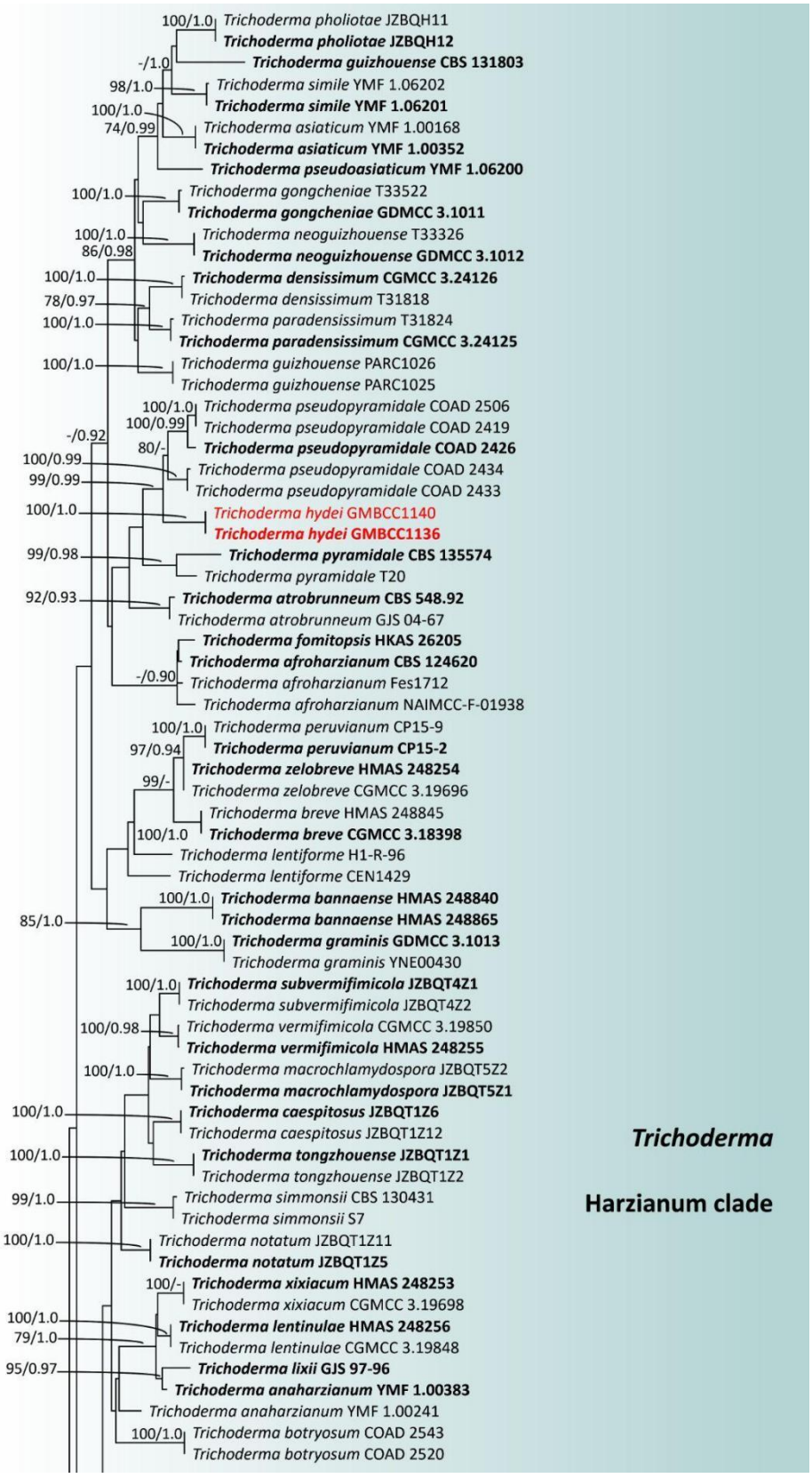


Figure 60 – Phylogram generated from maximum likelihood analysis based on combined ITS, *rpb2*, and *tef1-α* sequence data from 66 taxa, comprising 2,857 characters (ITS = 526, *rpb2* =

1,072, *tef1-α* = 1,259). The best-scoring RAxML tree with a final likelihood value of -16310.515 is presented. The matrix contained 986 distinct alignment patterns, with 33.31% of the characters being undetermined or gaps. Estimated base frequencies were as follows: A = 0.236, C = 0.275, G = 0.244, T = 0.244; substitution rates: AC = 0.975, AG = 3.790, AT = 1.272, CG = 0.857, CT = 5.572, GT = 1.0; gamma distribution shape parameter α = 0.661. Bootstrap support values for maximum likelihood (ML) equal to or greater than 70% and clade credibility values greater than 0.90 (rounded to two decimal places) from Bayesian inference analysis are labeled at each node. Ex-type strains are in bold, while the new isolates are indicated in red. The tree is rooted to *Trichoderma rossicum* (DAOM 230010) and *T. stromaticum* (DAOM 231100).

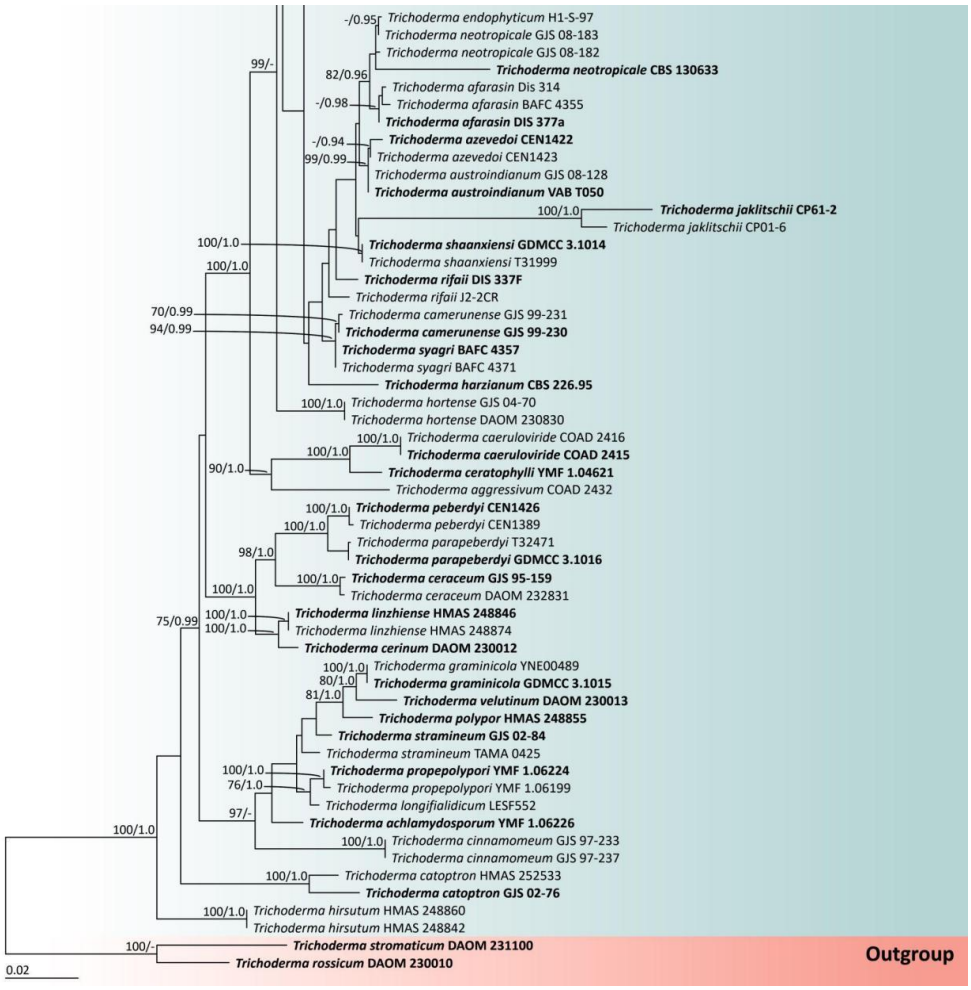


Figure 60 – Continued.

Culture characteristics – Colonies on PDA attaining 60 mm after 7 days at room temperature (20–25 °C), white, grey to green, sparse aerial mycelium on the surface; reverse white to reddish brown. The white reproductive mycelium covers the stromatic colonies after 30 days. Odor absent.

Material examined – China, Yunnan Province, Dehong Dai and Jingpo Autonomous Prefecture, Mang City, Mengga Town, Sanxian Cave, on rock surface, N 98.426103, E 24.232220, elev. 1528.89 m, 23 April 2024, Xiangfu Liu and Xuemei Chen, MS34C (GMB-W1190, holotype), ex-type GMBCC1136; *ibid*., MS34C2, ex-isotype GMBCC1140.

GenBank numbers – GMBCC1136: ITS = PV061860, *rpb2*= PV448526, *tef1-α* = PV448528; GMBCC1140: ITS = PV061861, *rpb2* = PV448527, *tef1-α* = PV448529.

Notes – In our phylogenetic analyses of ITS, *rpb2*, and *tef1-α* (Fig. 60), *Trichoderma hydei* forms a distinct lineage, sister to *T. pseudopyramidale* strains with 99% ML and 0.99 BYPP support. It is also related to *T. pyramidale* strains within the Harzianum clade. However, nucleotide comparisons between *T. hydei* (GMBCC1136, type) and *T. pseudopyramidale* (COAD 2426, type)

revealed 1.88% differences (17/905 bp, without gaps) in the *rpb2* region and 1.85% (9/486 bp, with 3 gaps) in the *tef1-α* region. *Trichoderma hydei* (GMBCC1136, type) and *T. pyramidale* (CBS 135574, type) revealed 3.51% differences (38/1084 bp, without gaps) in the *rpb2* region and 1.32% (6/454 bp, with 2 gaps) in the *tef1-α* region. Cai & Druzhinina (2021) established a standard for the molecular identification of *Trichoderma* species, which can be considered a new species if the unique sequence similarity meets the criteria of *rpb2* < 99% or *tef1-α* < 97%. Our species has met this standard. Morphologically, *T. hydei* differs from *T. pseudopyramidale* by the latter produces a yellow pigmentation reverse on PDA, smaller phialides (6–17 × 2–4 µm vs. 5.3–8.6 × 2.2–2.9 µm), smaller supporting cells (6–15 × 2–4 µm vs. 3.3–7.1 × 1.9–2.8 µm), slightly smaller conidia (2–4 × 2–3 µm vs. 2.1–2.9 × 2.3–2.9 µm) (Rodríguez et al. 2021). *Trichoderma hydei* differs from *T. pyramidale* by the latter having more (2–3 whorls vs. 2–4(–5) whorls) and lageniform, smaller phialides (6–17 × 2–4 µm vs. 5.5–11.5 × 2.8–3.7 µm), and absent chlamydospores (Chaverri et al. 2015). Based on the phylogenetic analyses, morphological characteristics, and the guidelines of Cai & Druzhinina (2021), *T. hydei* is introduced as a new species.

Nectriaceae Tul. & C. Tul.

Fusarium Link, Mag. Gesell. naturf. Freunde, Berlin 3(1–2): 10 (1809)

Index Fungorum number: IF8284; Facesoffungi number: FoF00149

Fusarium was introduced by Link (1809) and typified with *F. sambucinum*. The genus currently comprises 20 species complexes or lineages (Crous et al. 2021b), and the number of species is still increasing, with 1,850 *Fusarium* epithets listed in Index Fungorum (2025). This genus is characterized by dark blue to black perithecia that produce clavate asci, which bear ellipsoidal to cylindrical, 1- to multiseptate ascospores. The asexual morph consists of conidiophores arising from aerial hyphae with mono- and/or polyphialides. Conidiogenous cells produce both micro- and macroconidia, and sometimes mesoconidia, or only macroconidia are produced in sporodochia. Chlamydospores form within the hyphae (Crous et al. 2021b).

In the current list of Index Fungorum, Prof. Kevin D. Hyde and his collaborators have introduced ten species. In recognition of Prof. Kevin D. Hyde's outstanding contributions to mycology, we herein report both a new host record and a new geographical record of *F. guangdongense*. Additionally, we provide an updated phylogenetic tree of the *Fusarium fujikuroi* species complex (Fig. 62).

Fusarium guangdongense Y.X. Zhang, K.D. Hyde, L.T. Nie & Manawas., Mycosphere 15(1): 6674 (2024) Fig. 63

Index Fungorum number: IF902567; Facesoffungi Number: FoF15239

Endophytic in a healthy peel of *Citrus grandis* cv. "Tomentosa". Sexual morph: Undetermined. Asexual morph: *Sporodochia* peach, formed on twigs of *C. grandis* cv. "Tomentosa". *Conidiophores* in sporodochia densely aggregated, irregularly branched and densely packed. *Sporodochia conidiogenous cells* subulate to subcylindrical, 21–37 × 2–3 µm, smooth. *Sporodochial conidia* falcate, slightly curved with almost parallel sides tapering slightly towards both ends, with papillate to hooked curved apical cell, basal cell blunt flat, hyaline, smooth and thin-walled with 1–3-septate: 1-septate conidia: 11–21 × 2–3 µm ($\overline{x}$ = 15.4 ± 2.4 × 2.6 ± 0.2 µm, n = 50); 2-septate conidia: 17–25 × 2–4 µm ($\overline{x}$ = 19.6 ± 1.5 × 2.8 ± 0.2 µm, n = 50); 3-septate conidia: 21–32 × 2–4 µm ($\overline{x}$ = 24.6 ± 2.5 × 2.9 ± 0.2 µm, n = 50). *Conidiophores* on CLA and SNA are densely distributed, dense on the apex of aerial mycelium, solitary, commonly unbranched, straight or flexuous, smooth- and thin-walled. *Microconidia* formed densely, hyaline and aseptate 6–13 × 2–4 µm ($\overline{x}$ = 7.9 ± 1.9× 3.1 ± 0.3, n = 50 µm). *Chlamydospores* not observed.

Culture characteristics – Colonies on PDA grown in the dark reaching 6–7 cm diam., after 7 days at 25 ℃, raised, aerial mycelia dense, colony margin rhizoid, surface rosy buff; reverse ochreous in the center, pale ochreous at the margin. Colonies on SNA under a 12/12 h near-ultraviolet light/dark cycle at 25 ℃, raised, aerial mycelia dense, colony margin entire, surface and reverse smoke grey.



Figure 61 – *Trichoderma hydei* (GMB-W1190, holotype). a, b Colony on PDA (above and below). c Sporulation on PDA (35 days old culture). d–g Conidiophores, phialides and conidia. h Chlamydospores. i Conidia. Scale bars: d–g = 20 µm, h, i = 10 µm.

Material examined – CHINA, Guangdong Province, Maoming, isolated from healthy fruits of *C. grandis* cv. "Tomentosa", May 2021, B.Y. Cen, dried culture (MHKU 22-0167), living culture ZHKUCC 22–0317, ZHKUCC 22–0318 and ZHKUCC 22–0319.

GenBank numbers – ZHKUCC 22–0317: *tef1-α* = OP981760, *rpb1* = OP981760, *rpb2* = OP946547, *tub2* = PP551537; ZHKUCC 22–0318: *tef1-α* = OP981761, *rpb1* = OP981761, *rpb2* = OP946548, *tub2* = PP551538; ZHKUCC 22–0319: *tef1-α* = OP981762, *rpb1* = OP981762, *rpb2* = OP946549, *tub2* = PP551539.

Notes – In the phylogenetic analysis of the *Fusarium fujikuroi* species complex, three newly isolated isolates clustered with *F. guangdongense* (Fig. 62). Our isolates differ from its closely

related species by producing macroconidia with fewer septa (1–3-septate vs. 1–10-septate) and smaller macroconidia (11–32 × 2–4 µm vs. 34–120 × 4–6 µm) (Zhang et al. 2024c). The base-pair difference between the type strain of *F. guangdongense* (ZHKUCC 23–0920) and ZHKUCC 22–0317 is 1.32% (23/1744 bp, including 18 gaps) in the *rpb2* region. However, these strains have no nucleotide differences in the *rpb1*, *tef1-α*, and *tub2* regions. Although ZHKUCC 22–0317 shows some morphological differences from the type strain of *F. guangdongense* (ZHKUCC 23–0920), the absence of divergence in three gene regions and only limited variation in *rpb2* (1.32%) support its placement within *F. guangdongense*. Therefore, we identify these three isolates as *F. guangdongense*, while acknowledging the need for additional data to confirm intraspecific variation. The first report of *F. guangdongense* isolated from *C. grandis* cv. 'Tomentosa' is a significant addition to our understanding of fungal distribution and is a new geographical record of *F. guangdongense* in Maoming City, Guangdong province, China.

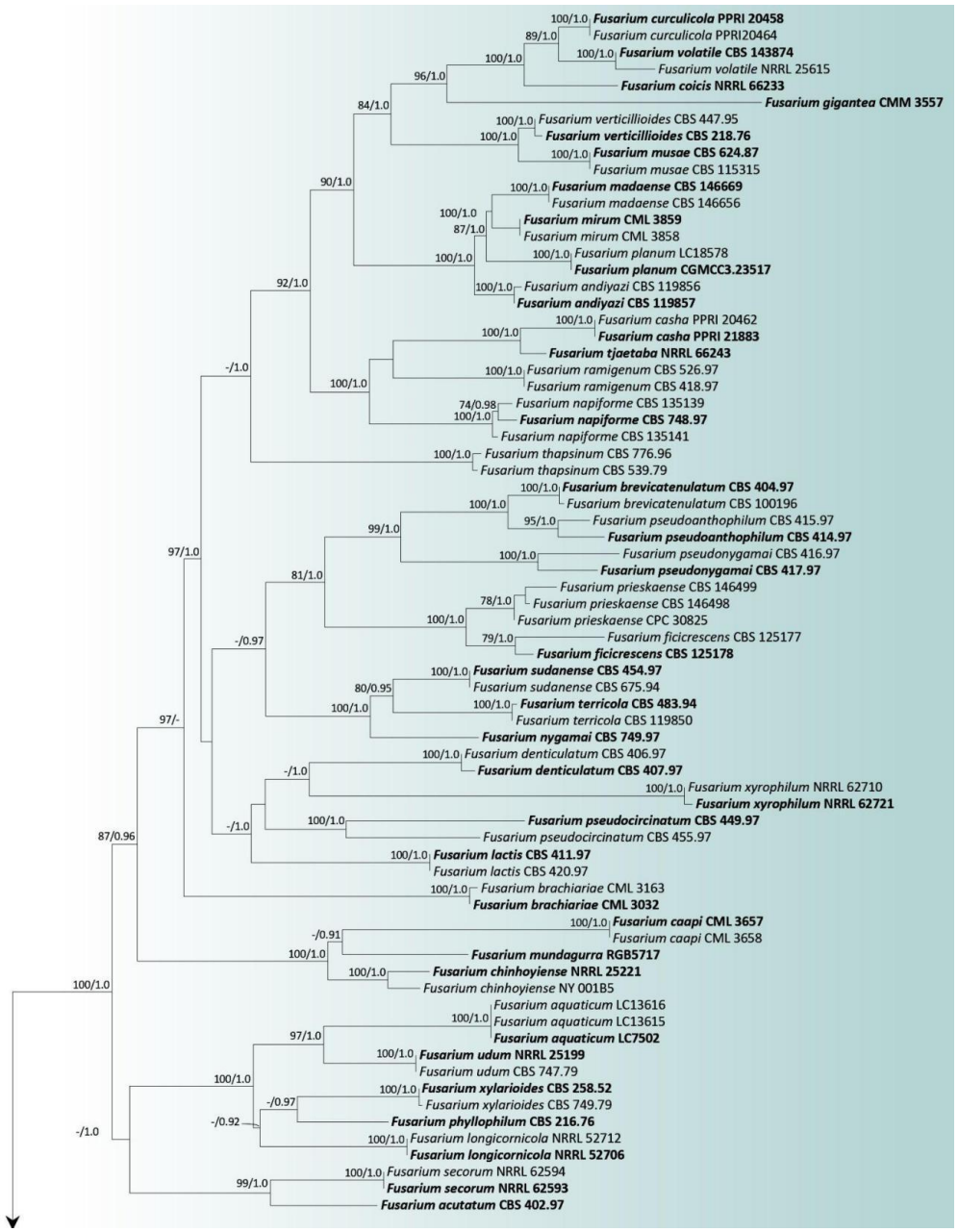


Figure 62 – Phylogram generated from maximum likelihood analysis based on combined *tef1-α*, *rpb2*, *rpb1*, and *tub2* sequence data from 171 strains, comprising 4,871 characters (*tef1-α* = 648, *rpb2* = 1,823, *rpb1* = 1,805, *tub2* = 595). The best-scoring RAxML tree with a final likelihood value of - 29030.137 is presented. The matrix contained 1,879 distinct alignment patterns, with

31.29% of the characters being undetermined or gaps. Estimated base frequencies were as follows: A = 0.251, C = 0.256, G = 0.244, T = 0.248; substitution rates: AC = 1.403, AG = 5.542, AT = 1.153, CG = 0.926, CT = 10.243, GT = 1.0; gamma distribution shape parameter α = 0.140. Bootstrap support values for maximum likelihood (ML) equal to or greater than 70% and clade credibility values greater than 0.90 (rounded to two decimal places) from Bayesian inference analysis are labeled at each node. Ex-type strains are in bold, while the new isolates are indicated in red. The tree is rooted to *Fusarium nirenbergiae* (CBS 744.97).



Figure 62 – Continued.

Ophiocordycipitaceae G.H. Sung, J.M. Sung, Hywel-Jones & Spatafora
Ophiocordyceps Petch, Trans. Br. mycol. Soc. 16(1): 73 (1931)

Index Fungorum number: IF3598; Facesoffungi number: FoF00828

Ophiocordyceps is a genus of entomopathogenic fungi in the family *Ophiocordycipitaceae* (*Hypocreales*), with more than 300 epithets recorded in Index Fungorum (2025). First described by Petch (1931), *Ophiocordyceps* was initially classified under *Cordyceps*, but was later elevated to

genus rank by Sung et al. (2007) based on phylogenetic analyses. *Ophiocordyceps* is characterized by dark, tough, and flexible stromata with varied morphologies, including filiform, wiry, clavate, or fibrous structures, and perithecia that are either superficial or immersed (Sung et al. 2007, Ban et al. 2015). The genus has a broad host range, parasitizing insects such as larval lepidopterans, coleopterans, adult hymenopterans (ants), hemipterans, dipterans, and rarely spiders (Kobayasi 1941, Mains 1958, Sung et al. 2007, Ban et al. 2015). Quandt et al. (2014) revised this genus through morphological observations and phylogenetic analyses.

Prof. Kevin D. Hyde and his collaborators have made pivotal contributions to the study of *Ophiocordyceps*, including the discovery of 13 species. In recognition of Prof. Kevin D. Hyde's outstanding contributions to mycology, we herein introduce the new species, *O. bannaensis*, in his honor, commemorating his significant and enduring impact on the field. We also provide an updated phylogenetic tree for *Ophiocordyceps* (Fig. 64).

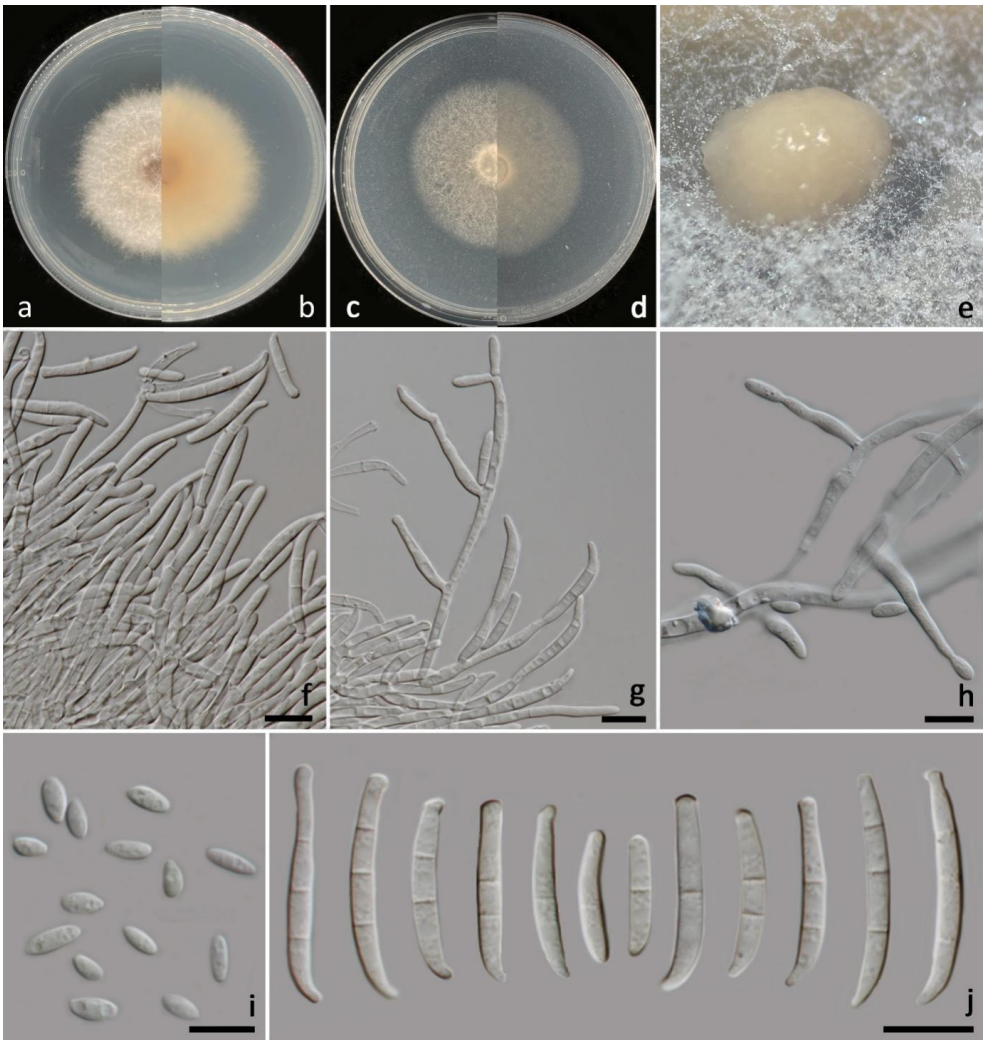


Figure 63 – *Fusarium guangdongense* (ZHKUCC 22–0317, new host and geographical record). a, b Upper and reverse sides of cultures on PDA 7 days at 25 °C in the dark. c, d Upper and reverse sides of cultures on SNA 7 days under a 12/12 h near-ultraviolet light/dark cycle at 25 °C. e Sporodochia on twig of *Citrus grandis* cv. "Tomentosa". f, g Conidiophores in sporodochia. h Conidiophores. i Aerial conidia (microconidia). j Sporodochial conidia. Scale bars: f–j = 10 μm.

Ophiocordyceps bannaensis X. Zhang & T. C. Wen, sp. nov. Fig. 65

Index Fungorum number: IF903280; Facesoffungi number: FoF03919

Etymology – Refers to the type locality, Xishuangbanna City, China.

Holotype – GACP24–0801

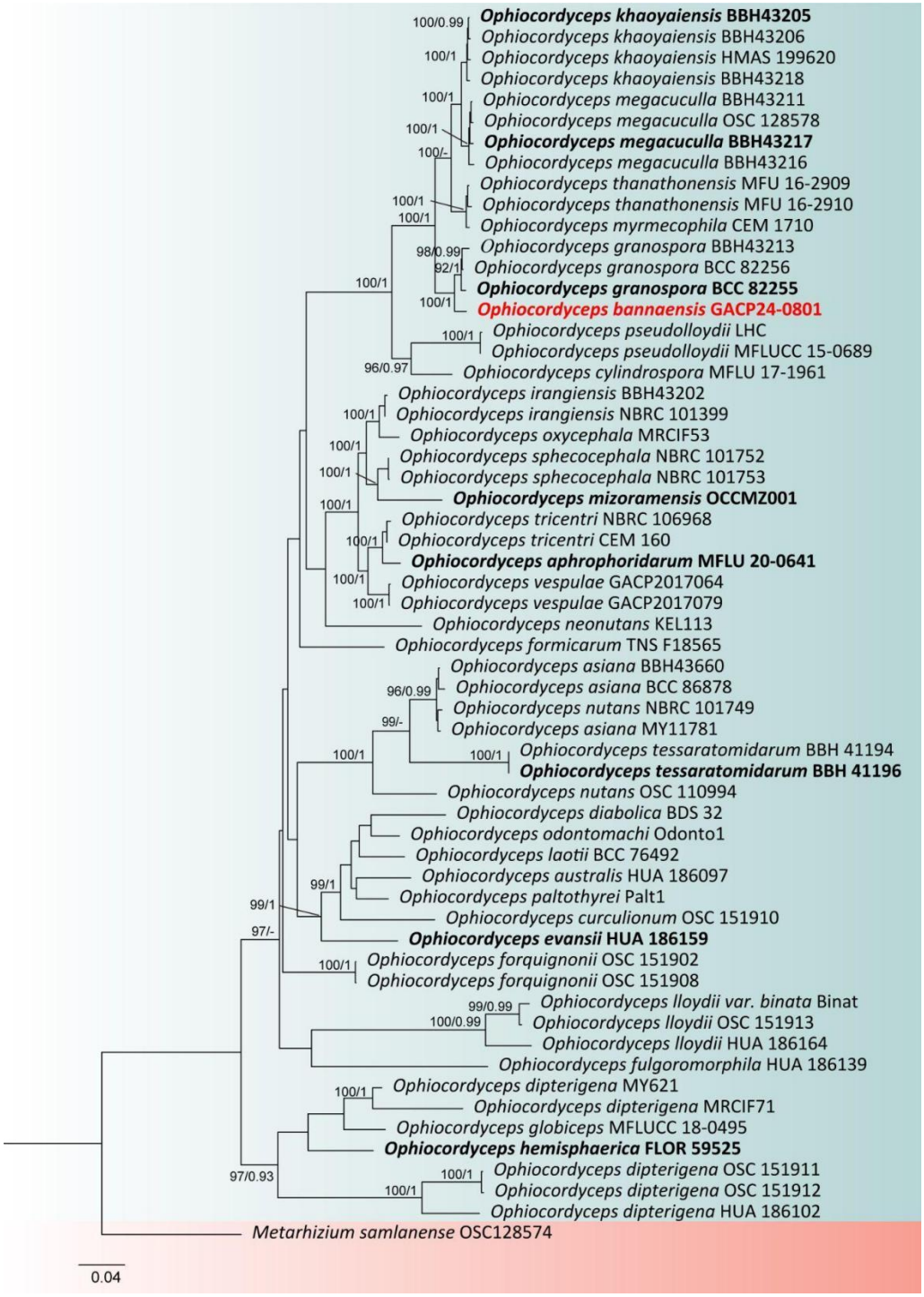


Figure 64 – Phylogram generated from maximum likelihood analysis based on combined ITS, LSU, SSU, *tef1-α*, *rpb1*, and *rpb2* sequence data from 59 taxa, comprising 6,165 characters (ITS = 608, LSU = 830, SSU = 1,751, *tef1-α* = 988, *rpb1* = 779, *rpb2* = 1,209). Maximum likelihood (ML) and Bayesian inference analyses were performed using OFPT (Zeng et al. 2023). The best-scoring RAxML tree with a final likelihood value of -36911.039 is presented. The matrix contained 2,487 distinct alignment patterns, with 50.59% of the characters being undetermined or gaps. Estimated base frequencies were as follows: A = 0.255, C = 0.245, G = 0.266, T = 0.234; substitution rates: AC = 1.119, AG = 3.705, AT = 1.497, CG = 0.831, CT = 7.156, GT = 1.0; gamma distribution shape parameter α = 0.676. Bootstrap support values for maximum likelihood (ML) equal to or greater than 70% and clade credibility values equal to or greater than 0.90 (rounded to two decimal places) from Bayesian inference analysis are labeled at each node. Ex-type strains are in bold, while the new isolate is indicated in red. The tree is rooted to *Metarhizium samlanense* (OSC128574).

Parasitic on *Camponotus* sp. (Formicidae, Hymenoptera), collected from the underside of leaf litter. Sexual morph: *Stroma* 3.6–4.0 cm long, arising from between the head and thorax of adult ants of *Camponotus* sp., simple, solitary, cream yellow to yellow orange. *Stipe* 33.4–38.5 long × 0.13–0.23 mm diam., with a fertile apex, becoming pale to yellow. *Fertile head* 1.5–1.7 × 0.4–0.8 mm diam., fusiform, yellow, surface roughened, ridged and furrowed. *Perithecia* 418–548 × 176–216 μm ($\overline{x}$ = 505 × 198 μm, n = 30), immersed, oblique, ovoid, obclavate. *Asci* 239–538 × 3.3–8.2 μm ($\overline{x}$ = 294 × 5.5 μm, n = 30), hyaline, cylindrical, with a thickened apex. *Apical cap* 4.6–6.7 × 6.5–8.1 μm ($\overline{x}$ = 5.5 × 7.1 μm, n = 30), rounded. *Ascospores* filiform, easily breaking into secondary ascospores. *Secondary ascospores* 6.5–8.6 × 1.8–2.3 μm ($\overline{x}$ = 7.4 × 2.0 μm, n = 40) fusiform to cylindrical, truncated at both ends, hyaline, smooth. Asexual morph: Undetermined

Material examined – China, Yunnan Province, Xishuangbanna City, Menghai County, Mengzhe Village, under leaf litter, 10 August 2024, BN-1 (GACP24–0801, holotype).

GenBank numbers – GACP24–0801: ITS = PQ826458, LSU: = PQ825960, SSU = PQ825959, *tef1-α* = PQ880174, *rpb1* = PQ880176, *rpb2* = PQ880175.

Notes – In the phylogenetic analysis of *Ophiocordyceps myrmecophila* complex based on combined ITS, LSU, SSU, *tef1-α*, *rpb1*, and *rpb2* sequence data (Fig. 64), our new collection develops a lineage closely related to *O. granospora.* The *Ophiocordyceps myrmecophila* complex comprises pathogens that are specifically adapted to infect ants. Species within this complex exhibit remarkable morphological similarities, making macroscopic differentiation a challenging task. To date, these fungi have been documented exclusively on formicine ants belonging to *Camponotus* and *Polyrhachis* (Khonsanit et al. 2019). The morphological characteristics of the newly described species closely resemble those of *O. granospora*, *O. khaoyaiensis*, and *O. megacuculla*, which are members of the same complex. However, the species had highest similarity to *O. granospora* BCC 82255 (type), with 3.45% differences in the ITS region (19/550 bp, including 1 gap), 2.43% in the LSU region (20/824 bp, including 3 gaps), 1.22% in the *tef1-α* region (9/740 bp), 4.07% in the *rpb1* region (29/713 bp), and 1.45% in the *rpb2* region (11/757 bp). Based on molecular phylogenetic relationships (supported by single-gene phylogenetic analyses) and sexual morphological characteristics, we introduce our collection as a new species.

Stachybotryaceae L. Lombard & Crous

Nigrosynnema C.F. Liao, K.D. Hyde & Doilom, in Liao, Doilom, Bhat, Chethana, Tangtrakulwanich, Yang, Al-Otibi, Hyde & Dong, MycoKeys 114: 310 (2025)

Index Fungorum number: IF902006; Facesoffungi Number: FoF15744

Nigrosynnema, introduced by Liao et al. (2025), is a genus that accommodates *N. guangdongense* (the type species) and *N. natarajanensis* (= *Virgatospora natarajanensis*), based on both morphological and molecular evidence. This genus is characterized by unusual olivaceous brown to black synnemata that are narrower towards the apex, black and glistening heads, enteroblastic, monophialidic, integrated, terminal, clavate to subcylindrical conidiogenous cells, and aseptate, fusiform to ellipsoidal conidia (Liao et al. 2025). *Nigrosynnema* has only been reported as asexual on *Calamus thwaitesii* and *Wurfbainia villosa* in China and India (D'Souza et al. 2002, Liao et al. 2025). Despite its morphological similarities to *Longitudinalis*, a species also found in China (on dead leaves of *Pandanus* spp.), *Nigrosynnema* shows significant differences in molecular data (ITS, LSU, and *tef1-α*) (Hyde et al. 2017b, Liao et al. 2025).

Herein, we introduce *Nigrosynnema hydei*, a species named in honor of Prof. Kevin D. Hyde for his outstanding career in mycology. This gesture is a celebration of his lasting impact on the study of mycology as a whole, a testament to his dedication and contribution. We also provide an updated phylogenetic tree for *Nigrosynnema* (Fig. 66).

Nigrosynnema hydei T.Y. Du, Tibpromma & Karun., sp. nov. Fig. 67

MycoBank number: MB858792; Facesoffungi number: FoF17764

Etymology – 'hydei' named in honor of the renowned mycologist Kevin D. Hyde, recognizing his significant contributions to mycology on the occasion of his 70th birthday.

Holotype – GMB-W1195

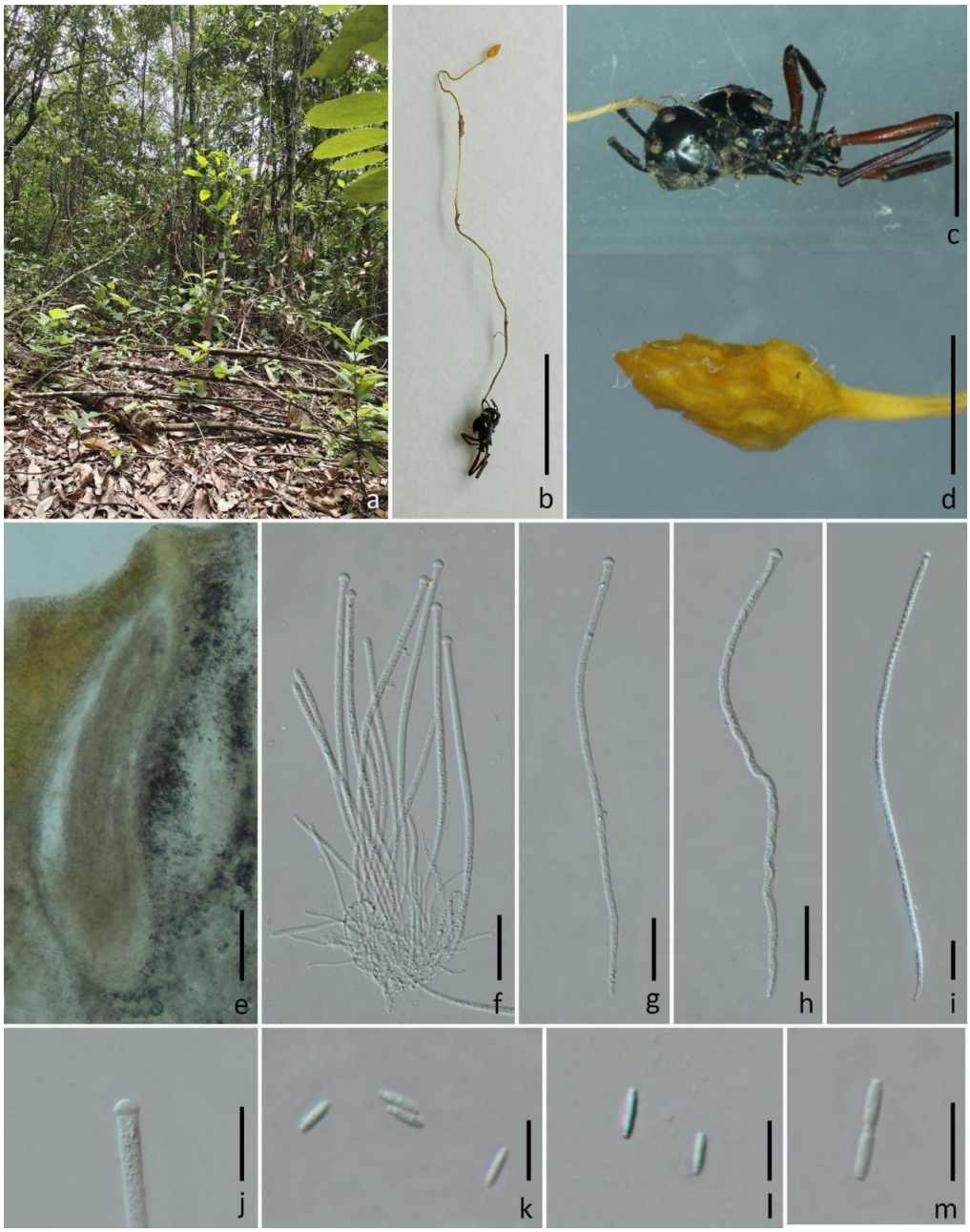


Figure 65 – *Ophiocordyceps bannaensis* (GACP24–0801, holotype). a Habitat of *Ophiocordyceps bannaensis*. b Stroma arising from the ant host. c Overview of host. d Fertile head. e Perithecia. f Immature asci of different lengths. g–i Immature to mature asci. j Apical cap of asci. k–l Secondary ascospores. m Part of ascospores. Scale bars: b = 1 cm, c = 2 mm, d = 1 mm, e = 100 µm, f–i = 40 µm, j = 20 µm, k–m = 10 µm.

Saprobic on leaf litter of *Poaceae.* Sexual morph: Undetermined. Asexual morph: *Conidiomata* synnemata, 300–700 × 20–40 um, in group, solitary, erect, unbranched, straight to somewhat flexuous, arising from a hyaline to yellow stroma, consisting of tightly aggregated bundles of conidiophores, narrowed towards fertile apex, subcylindrical, olivaceous green to dark brown, verruculose, multiseptate, giving rise to a globose head of conidia. *Terminal cells* giving rise subcylindrical conidiophores, 2–4 µm wide, olivaceous brown, branched, verrucose. *Conidiogenous cells* 8–16 × 2–4 µm ($\bar{x}$ = 12 × 3 µm, n = 20), enteroblastic, monophialidic, terminal, discrete, subcylindrical, phialidic, hyaline, verruculose. *Conidia* 15–22 × 4–5(–6) um ($\overline{x}$ =

18.5 × 4.8 µm, n = 30), fusoid, solitary, hyaline when immature and turn to green olivaceous to dark when mature, finely guttulate, apex subacute, with brown longitudinally striate, base truncate 1 um diam.

Material examined – China, Yunnan Province, Xishuangbanna, Jinghong City, Gasa Town, on leaf litter of *Poaceae*, 15 September 2021, TY Du, BND38 (GMB-W1195, holotype), ex-type GMBCC1141 = GMBCC1143.

GenBank numbers – GMBCC1141: *CaM* = PV471480, ITS = PV473917, LSU = PV469667, *rpb2* = PV483355, *tef1-α* = PV483353; GMBCC1143: *CaM* = PV471481, ITS = PV473918, LSU = PV469668, *rpb*2 = PV483356, *tef1-α* = PV483354.

Notes – In the phylogenetic analysis, our strains clustered with the recently introduced species, *Nigrosynnema guangdongense* (ZHKUCC 23–1014 and ZHKUCC 23–1015) with 66% ML and 0.95 BYPP bootstrap support (Fig. 66). Morphologically, our collection is also similar to *N. guangdongense* by the characteristics of synnemata conidiomata, tightly aggregated bundles of conidiophores, and aseptate, solitary, longitudinally striate conidia (Liao et al. 2025). However, our collection is different from *N. guangdongense* in having green olivaceous to dark conidia, and the conidia of our collection are narrower than those of *N. guangdongense* (18.5 × 4.8 µm vs. 11.5 × 4 µm) (Liao et al. 2025). In addition, the base pair differences in the *CaM*, ITS, LSU, *rpb2*, and *tef1-α* genes (without gaps) between our new strain (GMBCC1141, ex-type) and *N. guangdongense* (ZHKUCC 23–1014, ex-type) were also compared. The results show that they have nucleotide differences at different gene loci, *viz.*, 4.5% (23/511 bp) in the *CaM* region, 1.8% (9/498 bp) in the ITS region, 0.2% (2/826 bp) in the LSU region, 2.5% (28/1139 bp) in the *rpb2* region, and 0.9% (8/897 bp) in the *tef1-α* region. No sequence data are currently available for the *tub2* gene in our new strain. Therefore, based on morphology and phylogenetic evidence, we identify our collection as a new species, *Nigrosynnema hydei*, and this is the second report of this genus in China.

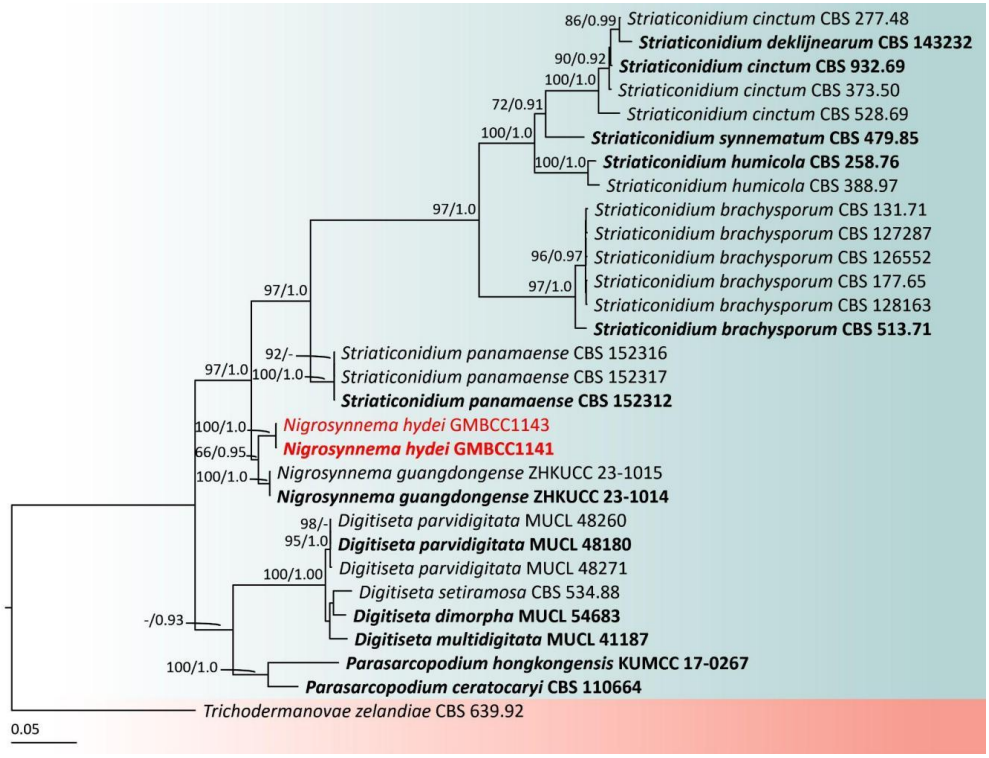


Figure 66 – Phylogram generated from maximum likelihood analysis based on combined *CaM*, ITS, LSU, *rpb*2, *tef1-α*, and *tub*2 sequence data from 30 taxa, comprising 4,654 characters (*CaM* = 613, ITS = 557, LSU = 1,043, *rpb2* = 1,138, *tef1-α* = 636, *tub2* = 667). The best-scoring RAxML tree with a final likelihood value of -16893.339 is presented. The matrix contained 1,164 distinct alignment patterns, with 33.62% of the characters being undetermined or gaps. Estimated base

frequencies were as follows: A = 0.236, C = 0.279, G = 0.269, T = 0.215; substitution rates: AC = 1.070, AG = 2.526, AT = 1.107, CG = 0.939, CT = 5.230, GT = 1.0; gamma distribution shape parameter α = 1.030.; gamma distribution shape parameter α = 0.667. Bootstrap support values for maximum likelihood (ML) equal to or greater than 70% and clade credibility values equal to or greater than 0.90 (rounded to two decimal places) from Bayesian inference analysis are labeled at each node. Ex-type strains are in bold, while the new isolates are indicated in red. The tree is rooted to *Trichodermanovae zelandiae* (CBS 639.92).



Figure 67 – *Nigrosynnema hydei* (GMB-W1195, holotype). a, b Appearance of conidiomata on leaf litter. c–f Microscopic morphology of bundles of conidiomata, conidiophores, conidiogenous cells, and conidia. g–i Conidia. j A germinated conidium. Scale bars: c = 100 µm, d–f = 50 µm, g–j = 10 µm.

Microascales Luttr. ex Benny & Kimbr.
Halosphaeriaceae E. Müll & Arx ex Kohlm
Keraliethelia P. Correia, E. Azevedo & M.F. Caeiro, J. Fungi 9(8, no. 841): 29 (2023)

Index Fungorum number: IF848496; Facesoffungi number: FoF17765

The genus *Keraliethelia* was introduced by Correia et al. (2023) to accommodate the type species *K. pulchella* (≡ *Corollospora pulchella*), which was previously classified in the genus *Corollospora*. *Keraliethelia* is characterized by its asexual and sexual morphs commonly found on wood or sand (Kohlmeyer & Kohlmeyer 1979, Corriea et al. 2023). The sexual morph of this genus is characterized by black, papillate ascomata, unitunicate asci, and fusiform, 7-septate ascospores (Kohlmeyer et al. 1967, Kohlmeyer & Kohlmeyer 1979). The asexual morph is characterized by tetraradiate conidia with bulbous cells at the base, and crowns radiating diverging arms, and catenulated chlamydospores (Shearer & Crane 1971, Kohlmeyer & Kohlmeyer 1979).

Prior to the establishment of this genus, Prof. Kevin D. Hyde's research primarily focused on the genus *Corollospora*, to which the type species previously belonged. His work on *K. pulchella* (≡ *Corollospora pulchella*) demonstrated how extended incubation periods increase the percentage occurrence of this species (Hyde 1992). This research significantly contributed to mycology by highlighting the role of incubation time in the occurrence of marine fungi, advancing our understanding of fungal ecology, and shaping modern mycological methodologies.

In recognition of Prof. Hyde's contributions to mycology, we introduce the new species, *Keraliethelia hydei*, named in his honor. This designation serves as a tribute to his pioneering work in the field. An updated phylogenetic tree for *Keraliethelia* is also provided (Fig. 68).

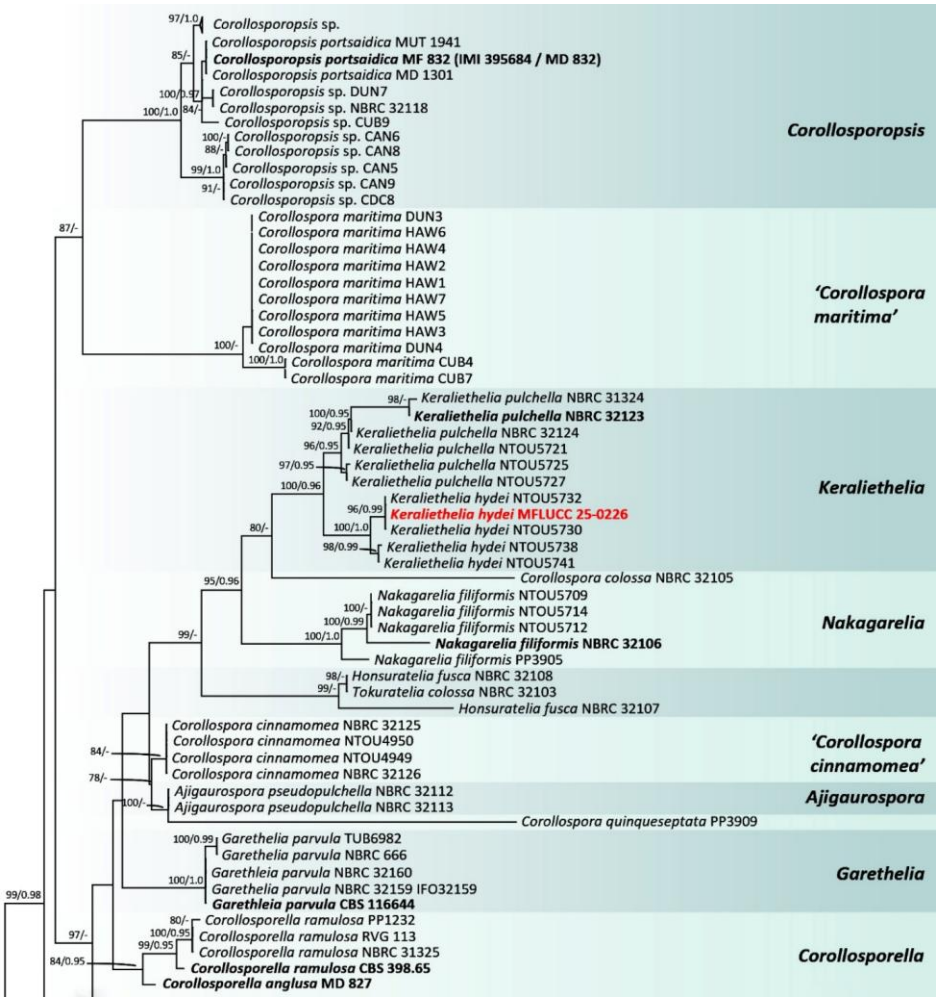


Figure 68 – Phylogram generated from maximum likelihood analysis based on combined SSU, ITS, and LSU sequence data from 258 taxa, comprising 3,772 characters (SSU = 2,186, ITS = 473,

LSU = 1,113). The best-scoring RAxML tree with a final likelihood value of -21075.573 is presented. The matrix contained 780 columns, 1,332 distinct patterns, 729 parsimony-informative characters, 477 singleton sites, and 2,574 constant sites. Estimated base frequencies were as follows: A = 0.239, C = 0.245, G = 0.287, T = 0.229; substitution rates: AC = 1.00, AG = 1.757, AT = 1.000, CG = 1.000, CT = 3.998, GT = 1.0; gamma distribution shape parameter α = 0.575. Bootstrap support values for maximum likelihood (ML) equal to or greater than 75% and clade credibility values greater than 0.95 (rounded to two decimal places) from Bayesian inference analysis are labeled at each node. Ex-type strains are in bold, while the new isolate is indicated in red bold. The tree is rooted to *Corollospora maritima* (3 P1815 and 20 D05), *Microascus cirrosus* (CBS 217.31), and *M. longirostris* (CBS 196.61 and CBS 415.64).

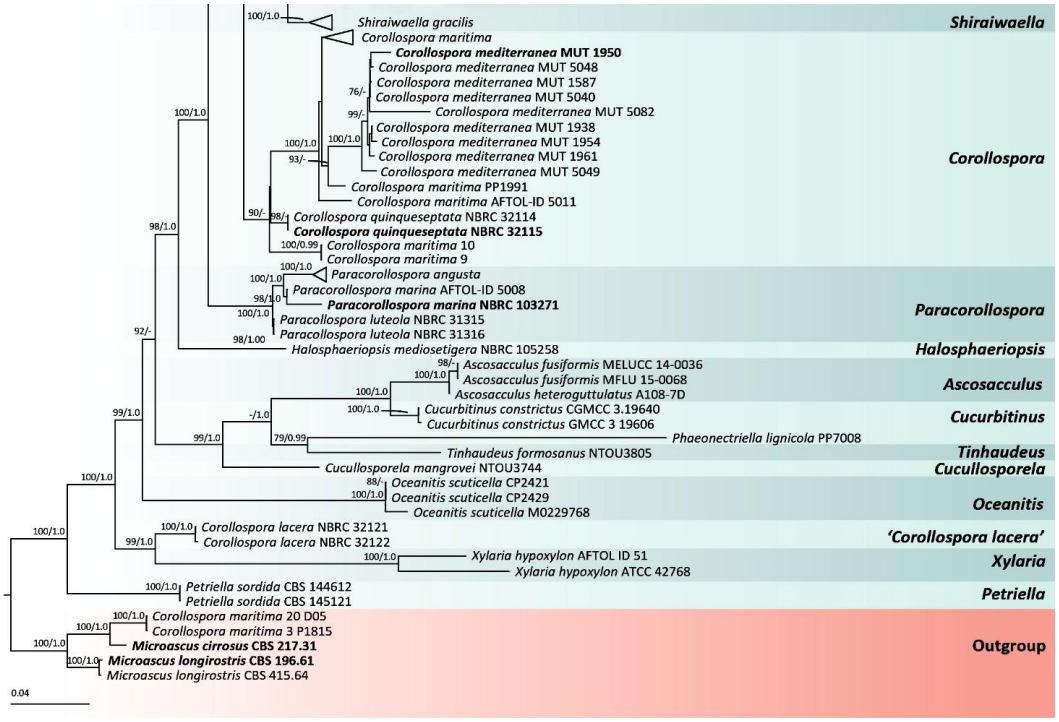


Figure 68 – Continued.

Keraliethelia hydei Bagacay, Opiña, & M.S. Calabon, sp. nov. Fig. 69

Index Fungorum number: IF903753; Facesoffungi number: FoF17766

Etymology – 'hydei' named in honor of the renowned mycologist Kevin D. Hyde, recognizing his significant contributions to mycology on the occasion of his 70th birthday.

Holotype – MFLU25–0158

Saprobic on dried twigs of an unidentified host. Sexual morph: Undetermined. Asexual morph: Hyphomycetous. *Hyphae* septate, branched, superficial or immersed, hyaline to pale brown. *Conidiophores* reduced to conidiogenous cells. *Conidiogenous cells* 16–28 × 8.2–12.4 µm (22.3 × 10.1 µm, *n* = 20), holoblastic, integrated, terminal, determinate. *Conidia* 79–140 × 13–46 µm ($\bar{x}$ = 122.9 × 23.1 µm, *n* =30), light to dark brown, solitary, scattered or gregarious, produced terminally or laterally on hyphae, curved, coiled, or irregularly coiled, initially hyaline then becoming brown, muriform, conidial groups form compactly intertwined and irregularly shaped masses of cells.

Culture characteristics – Colonies on MEA reaching 10–15 mm after 30 days at 25 °C, circular, slightly raised, undulate, light grayish brown inner zone, dark gray middle zone, then light brown outer zone, reverse brown with dark brown margin. *Conidia* 17.6–36.3 × 12.8–33.2 µm ($\bar{x}$ = 25.1 × 23.0 µm, n =30), initially hyaline then becoming dark brown, muriform, cell division in several planes, becoming a mass of irregularly-shaped cells. *Chlamydospores* 6.9–51.1 × 10.5–12.3 µm ($\bar{x}$ = 11.7 × 11.1 µm, n = 15), globose, olivaceous brown, catenulate, constricted at the septa, rarely branched, formed in acropetal succession.

Material examined – Thailand, Phuket Province, Thalang District, saprobic on a submerged decaying wood, 5 May 2018, M.S. Calabon, 27HY2 (MFLU25–0158, holotype), ex-type MFLUCC 25–0226.

GenBank numbers – MFLUCC 25–0226: ITS = PV468735, LSU = PV467068.

Notes – In the phylogenetic analysis of the combined ITS and LSU sequence data, *Keraliethelia hydei* MFLUCC 25–0226 clustered with the unidentified *Keraliethelia* strains (NTOU5730, NTOU5738, NTOU5741) with 100% ML and 1.00 BYPP support (Fig. 68). It also formed a clade basal to *K. pulchella*, including the holotype NBRC 32123. *Keraliethelia hydei* shares morphological similarities with *K. pulchella*, particularly in the presence of catenulated chlamydospores observed in culture (Shearer & Crane 1971, Kohlmeyer & Kohlmeyer 1979). However, our collection differs from the reported asexual morphology of *K. pulchella*, which produces tetraradiate conidia, whereas *K. hydei* exhibits curved and coiled conidia (Shearer & Crane 1971, Kohlmeyer & Kohlmeyer 1979). Base pair comparisons between the type strain of *K. hydei* (MFLUCC 25–0226) and the type strain of *K. pulchella* (NBRC 32123) revealed a 16.67% differences in the ITS region (68/408 bp, including 17 gaps), and a 3.06% differences in the LSU region (27/883 bp, including 5 gaps). Based on morphological characteristics and phylogenetic analyses, we introduce our collections as a new species, *K. hydei*.

Subclass Sordariomycetidae O.E. Erikss. & Winka (= Meliolomycetidae P.M. Kirk & K.D. Hyde)
Chaetosphaeriales Huhndorf, A.N. Mill. & F.A. Fernández
Chaetosphaeriaceae Réblová, M.E. Barr & Samuels
Lomaantha Subram., J. Indian bot. Soc. 33: 31 (1954)

Index Fungorum number: IF8788

Lomaantha was established by Subramanian (1954), with *L. pooga* as the type species. According to Index Fungorum (2025), ten species are currently recognized within this genus. Notably, in light of the recent classification of *Lomaantha* within the ellisembia-like chaetosphaeriaceous clade (Wu & Diao 2022), the genus has been reevaluated to more comprehensively encompass this taxonomic group. Six of these species were initially classified under the genus *Ellisembia* (*L. aquirostrata*, *L. aurantiaca*, *L. aurea*, *L. brachypus*, *L. folliculate*, and *L. reblovae*) (Delgado et al. 2024). *Lomaantha* has been expanded, which together constitute a distinct lineage within *Chaetosphaeriaceae* (Sordariomycetes) and are notably distant from *Sporidesmiaceae* (Delgado et al. 2024). Wu & Diao (2022) were the first to categorize *Lomaantha* (Subramanian 1954) within *Chaetosphaeriaceae*, based on specimens collected from China. They also proposed that *Lomaantha* could serve as a prospective generic designation for fungi resembling *Ellisembia* within *Chaetosphaeriaceae* (Wu & Diao 2022). *Lomaantha* is characterized by its conidiophores, conidiogenous cells, and conidial appendages (Ma et al. 2011). The morphology of conidia and the characteristic of percurrent proliferation of conidiogenous cells are the key features that differentiate species within this genus (Ma et al. 2011).

In recognition of Prof. Kevin D. Hyde's outstanding contributions to mycology, we herein introduce *Lomaantha guizhouensis* as a new species. We also provide an updated phylogenetic tree for *Lomaantha* (Fig. 70).

Lomaantha guizhouensis M.Y. Han. & Tibpromma, sp. nov. Fig. 71

Index Fungorum number: IF903329; Facesoffungi number: FoF17308

Etymology – The species name reflects the type location, "Guizhou Province", China.

Holotype – HKAS 136914

Saprobic on an unidentified decaying wood. Sexual morph: Undetermined. Asexual morph: *Colonies* on natural substrate effuse, pale brown to brown, hairy, often inconspicuous. *Mycelium* mostly superficial, partly immersed in the substratum, composed of pale brown, septate, unbranched hyphae. *Conidiophores* 31–110 × 7–13.5 µm ($\overline{x}$ = 73 × 11, n = 30), macronematous, mononematous, solitary or aggregated at the base, simple, cylindrical, straight or slightly fexuous, smooth, 2–8-septate, dark brown. *Conidiogenous cells* 11–23 × 5–10 µm ($\overline{x}$ = 17.5×7.5, n = 30),

integrated, terminal, lageniform, smooth, dark brown. *Conidia* 77–120 × 10–18 µm ($\overline{x}$ = 100 × 14, n = 30), acrogenous, solitary, dry, obclavate, rostrate, 9–15-distoseptate, not constricted at the septa, pale brown, becoming hyaline toward the apex, the 1 basal cell distinctly darker than the other cells, smooth-walled; *apical cell* extended into 1 filiform, hyaline, aseptate, branched appendage of 45–65 × 1–1.5 µm ($\overline{x}$ = 28.5 × 1.2, n = 30); basal cell conical-truncate, darker than other cells, 4–7.5 µm wide at the base.



Figure 69 – *Keraliethelia hydei* (MFLU25–0158, holotype). a–c Appearance of colonies on woody substrate. d–h Conidiophores and conidia in natural substrates. i–n Conidia found on hosts; o–p 25-day-old culture in MEA. q–t Conidiophores and conidia in culture. u–z Conidia in cultures. Scale bar: d = 200 µm, e–h, g–t, q–t = 50 µm, i–n, u–z = 20 µm.

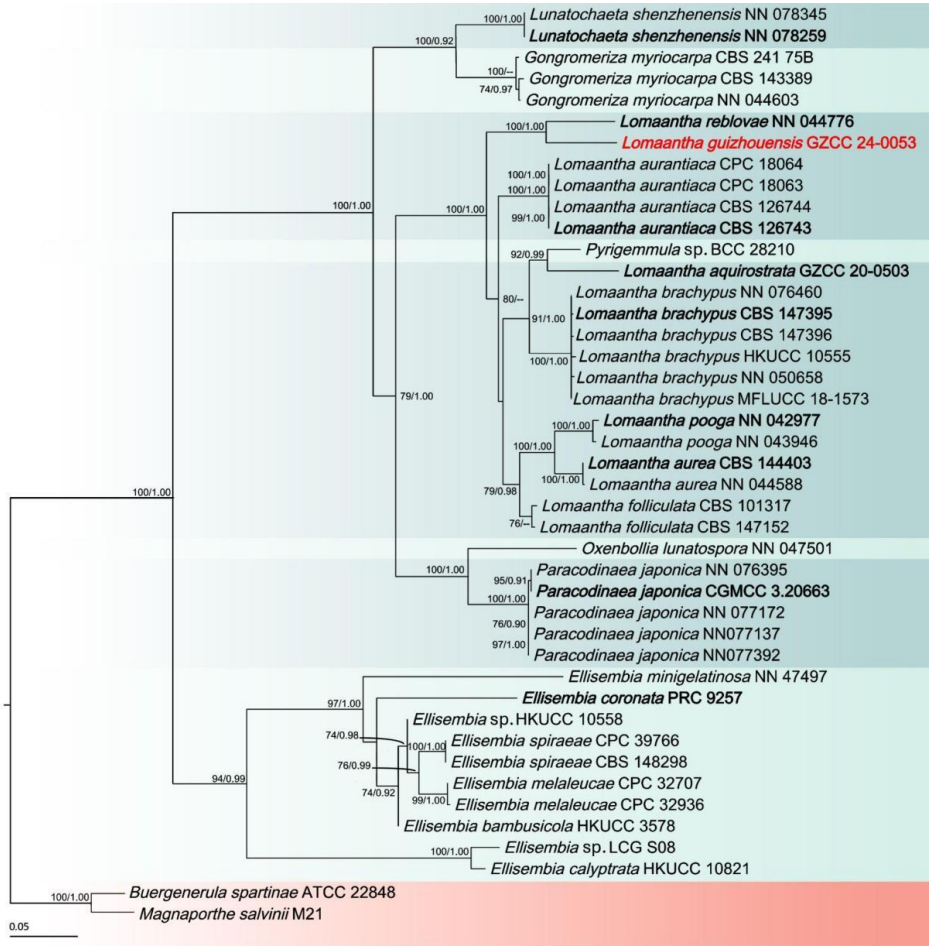


Figure 70 – The combined ITS and LSU dataset comprised 43 taxa. The aligned dataset comprised 1,317 characters, including gaps. Phylogenetic analysis based on maximum likelihood analysis was carried out using the best RAxML tree, which yielded a final likelihood value of -8183.794. The matrix contained 511 distinct alignment patterns, with 17.73% of the characters being undetermined or gaps. Estimated base frequencies were: A = 0.224, C = 0.271, G = 0.306, T = 0.199; substitution rates AC =1.250, AG =1.813, AT =1.615, CG = 0.684, CT = 6.342, GT = 1.0; gamma distribution shape parameter α = 0.251. The maximum likelihood (ML) and Bayesian inference (BI) methods for phylogenetic analyses yielded trees with similar topologies. Ex-type strains are in bold, while the new isolate is indicated in red. The tree is rooted to *Buergenerula spartinae* (ATC 22848) and *Magnaporthe salvinii* (M21).

Culture characteristics – Conidia germinated after 12 hours in the PDA culture medium, and colorless bud tubes emerged from the spores. After 20 days of culture at 28 °C, colonies on PDA medium were circular, flat, and neatly edged, the diameter is 1 cm, aerial mycelium not well-developed the color from bright yellow in the middle to dark brown at the edges, the reverse is dark brown to pale brown. The mycelium is on the surface of the medium, partially submerged, branched, septate, yellow, and smooth.

Material examined – China, Guizhou Province, Zunyi City, the Sancha River Nature Reserve in Xishui County, Longitude: 106°24′9″, latitude: 28°33′50″, on rotten wood on land, Meiyan Han, 3 October 2023, S15 (HKAS 136914, holotype), ex-type GZCC 24–0053.

GenBank numbers – GZCC 24–0053: ITS = PQ111503, LSU = PQ842538.

Notes – In the phylogenetic tree, our strain *Lomaantha guizhouensis* (GZCC 24–0053) is closely related to *L. reblovae* (NN 044776), forming a sister clade with 100% ML/1.00 BYPP support (Fig. 70). Morphologically, *L. guizhouensis* shares similar characteristics with the type specimen of *L. reblovae* (Wu & Diao 2022). However, distinct morphological differences were observed when comparing *L. guizhouensis* with *L. reblovae*. Specifically, *L. guizhouensis* exhibits

longer conidia (77–120 × 10–18 µm vs. 60–93 × 11–13 µm) (Wu & Diao 2022) and longer conidiophores (31–110 × 7–13.5 vs. 40–57 × 5.5–6.5 µm) (Wu & Diao 2022). In addition, the conidia of *L. guizhouensis* have a broader basal cell (4–7.5 µm vs. 3.5–4 µm) compared to *L. reblovae* (Wu & Diao 2022). Moreover, the conidia of *L. reblovae* are noted for their darker overall color. *Lomaantha guizhouensis* also features a unique filiform, hyaline, aseptate, and branched appendage extending from the apical cell, a characteristic not mentioned in descriptions of *L. reblovae*. Furthermore, the conidiogenous cells of *L. guizhouensis* are lageniform, while those of *L. reblovae* are cylindrical. Molecularly, *L. guizhouensis* demonstrates genetic divergence from *L. reblovae* by 7.34% (37/504 bp, without gap) in the ITS region and 3.57% (29/813 bp, without gap) in the LSU region. These genetic discrepancies, along with the morphological distinctions, provide a robust basis for classifying *L. guizhouensis* as a new species.

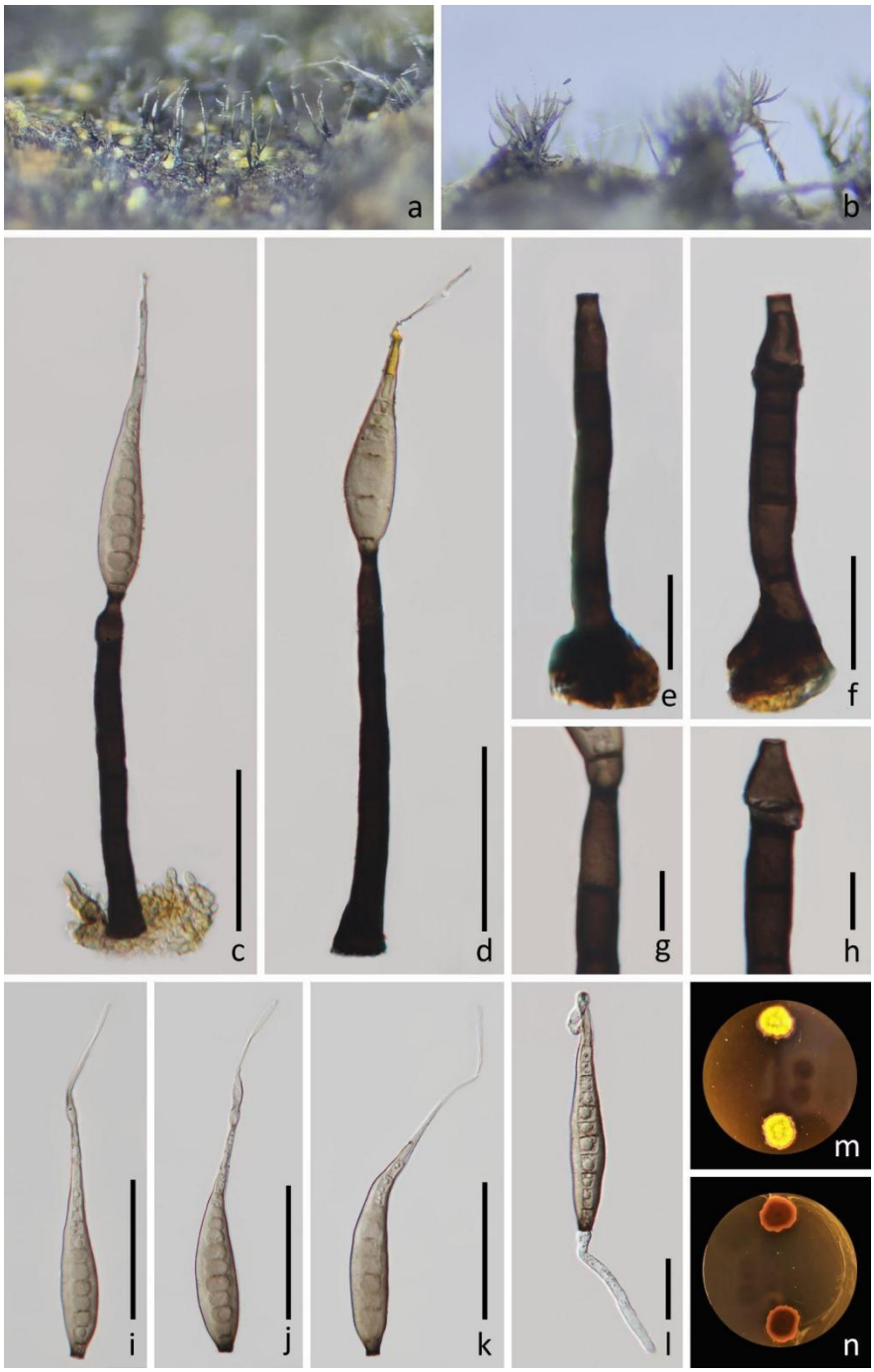


Figure 71 – *Lomaantha guizhouensis* (GZCC–24–0053). a–b Colonies on the natural substrate. c, d Conidiophores and Conidia. e, f Conidiophores and conidiogenous cells. g, h Conidiogenous

cells. i–k Conidia. l Germinated conidium. m–n Front and reverse side of pure culture. Scale bar: c–d, i–k = 50 µm, e–f, l = 20 µm, g–h = 10 µm.

Magnaporthales Thongk., Vijaykr. & K.D. Hyde
Ophioceraceae Klaubauf, E.G. LeBrun & Crous
Ophioceras Sacc., Syll. fung. (Abellini) 2: 358 (1883)

Index Fungorum number: IF3595

Ophioceras was established by Saccardo (1883) with *O. dolichostomum* as the type species. *Ophioceras* is characterized by immersed to superficial ascomata with a long neck, cylindrical or subcylindrical asci, and filiform, narrowly fusoid to cylindrical ascospores (Yang et al. 2023a, Wang et al. 2024). Only one species, *O. graminis*, has been reported in its asexual morph (Feng et al. 2024). The asexual morph is characterized by single or simple branched conidiophores, phialidic, cylindrical to lageniform conidiogenous cells, and lunate, allantoid to fusiform conidia (Feng et al. 2024). *Ceratosphaerella* has been observed to group within the *Ophioceras* clade in a multi-locus phylogenetic analysis (Perera et al. 2016, Luo et al. 2019, Jiang et al. 2021). Consequently, Jiang et al. (2021) proposed synonymizing *Ceratosphaerella* with *Ophioceras*.

Through Prof. Kevin D. Hyde's continued research, he has not only expanded our understanding of *Ophioceras*, but has also played a key role in discovering numerous new species within this genus. Of the 51 species currently listed in Index Fungorum (2025), Prof. Kevin D. Hyde and his collaborators have introduced 31 species. His work, particularly in freshwater, terrestrial ecosystems, and bambusicolous fungi, has greatly advanced the field of fungal taxonomy. In recognition of Prof. Kevin D. Hyde's outstanding contributions to mycology, herein we introduce the new species, *O. hydei*, which has been named in honor of Prof. Kevin D. Hyde. We also provide an updated phylogenetic tree for *Ophioceras* (Fig. 72).

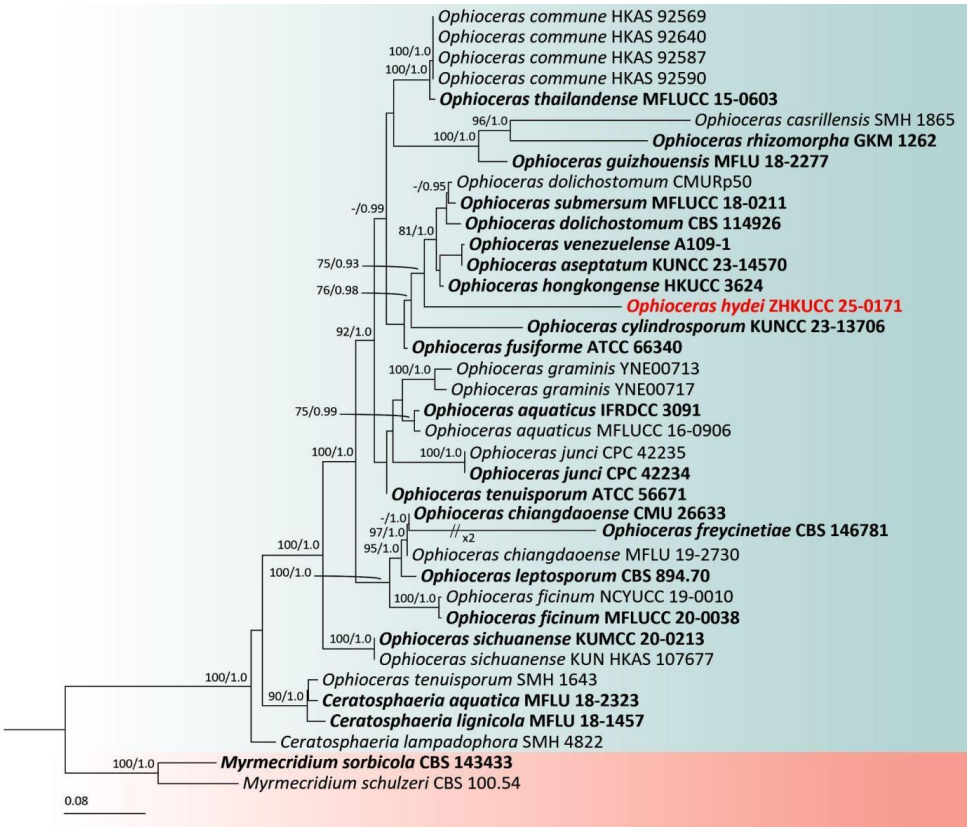


Figure 72 – Phylogram generated from maximum likelihood analysis based on combined LSU, ITS, SSU, and *tef1-α* sequence data from 38 taxa, comprising 3,581 characters. The best-scoring RAxML tree with a final likelihood value of -17422.529 is presented. The matrix contained 1,201 distinct alignment patterns, with 50.37% of the characters being undetermined or gaps. Estimated

base frequencies were as follows: A = 0.240, C = 0.262, G = 0.285, T = 0.213; substitution rates: AC = 1.022, AG = 1.689, AT = 1.195, CG = 1.275, CT = 5.214, GT = 1.0; gamma distribution shape parameter α = 0.664. Bootstrap support values for maximum likelihood (ML) equal to or greater than 70% and clade credibility values greater than 0.90 (rounded to two decimal places) from Bayesian inference analysis are labeled at each node. Ex-type strains are in bold, while the new isolate is indicated in red. The tree is rooted to *Myrmecridium sorbicola* (CBS 143433) and *M. schulzeri* (CBS 100.54).

Ophioceras hydei H.J. Zhao & W. Dong, sp. nov. Fig. 73

Index Fungorum number: IF903586; Facesoffungi number: FoF17623

Etymology – 'hydei' named in honor of the renowned mycologist Kevin D. Hyde, recognizing his significant contributions to mycology on the occasion of his 70th birthday.

Holotype – MHZU 24–1035

Saprobic on submerged decaying wood. Sexual morph: *Ascomata* 325–490 µm diam., 340–675 µm high., coriaceous, scattered, solitary, semi-immersed in the natural substratum, globose to subglobose, black, ostiolate, with a long neck. *Ostiole* 98–115 µm diam, 218–255 µm high., central, with straight upright neck at one end, black. *Necks* long, black, cylindrical, slightly tapering towards the tip, straight or slightly flexuous, mostly stand upright in the substratum. *Peridium* 29–52 µm thick, coriaceous, consisting of two layered, inner layers composed of hyaline, thin-walled cells of *textura angularis*, becoming pale brown to dark brown, cellular structure at outer layers. *Paraphyses* 4–10 µm wide, at the base, loose, tapering towards the apex, hyaline, unbranched, septate, slightly constricted at the septum. *Asci* 101–138 × 8.8–19 µm ($\overline{x}$ = 115.4 × 12.6 µm, n = 20), 8-spored, unitunicate, cylindrical, straight or slightly flexuous, short pedicellate to subsessile, rounded at the apex, with an apical ring. *Ascospores* 82–103 × 2.2–3.4 µm ($\overline{x}$ = 92.5 × 3.0 µm, n = 15), filiform to cylindrical, straight or slightly curved, hyaline to pale brown, multi-guttulate, 3-septate, smooth, thin-walled. Asexual morph: Undetermined.

Culture characteristics – Ascospores germinating on PDA within 12 hours. Colonies on PDA reaching 20 mm diam. after 4 weeks at room temperature, dry, circular, with a protrusion in the center, wavy margin, white to burlywood. Reverse circular, grey, pale brown to reddish brown, white, smooth.

Material examined – China, Guangdong Province, Meizhou City, Dapu County, Huliao Town, Shuangji Mountain (116°37′28″E, 24°20′0″N), on submerged decaying culms, 8 August 2024, H.J. Zhao, SW010 (MHZU 24–1035, holotype); ex-type ZHKUCC 25–0171.

GenBank numbers – ZHKUCC 25–0171: LSU = PV359239, SSU = PV359240, *tef1-α* = PV367584.

Notes – In the phylogenetic analysis, *Ophioceras hydei* is closely related to *O. aseptatum* (KUNCC 23–14570), *O. dolichostomum* (CMURp50, CBS 114926), *O. hongkongense* (HKUCC 3624), *O. submersum* (MFLUCC 18–0211) and *O. venezuelense* (A109-1) (Fig. 72). Morphologically, *Ophioceras hydei* resembles *O. palmae* and *O. submersum* in having globose to subglobose ascomata, cylindrical asci and filiform, septate ascospores (Tsui et al. 2001). *Ophioceras hydei* differs from *O. palmae* in that the former has semi-immersed ascomata with a long neck and pale brown ascospores. In contrast, the latter has superficial ascomata without a neck and hyaline ascospores. *Ophioceras hydei* can be distinguished from *O. submersum* by its pale brown ascospores (hyaline ascospores in *O. submersum*) and smaller ascomata (325–490 µm diam. vs. 500–600 µm diam.) (Luo et al. 2019). We have listed the dimensions of *Ophioceras hydei* and adjacent species (Table 3). The base-pair comparison between *O. hydei* (ZHKUCC 25–0171) and *O. hongkongense* (HKUCC 3624) revealed differences of 1.73% (15/869 bp) in the LSU region and 0.66% (4/603 bp) in the SSU region, while *tef1-α* sequence data are not available for *O. hongkongense* (HKUCC 3624). A comparison of the *tef1-α* sequence between *O. hydei* (ZHKUCC 25–0171) and *O. submersum* (MFLU 18-1459) revealed 4.47% (40/894 bp) differences. Based on in-depth morphological comparisons and phylogenetic analysis, we introduce *Ophioceras hydei* as a new species.



Figure 73 – *Ophioceras hydei* (MHZU 24–1035, holotype). a, b Appearance of neck on woody substrate. c Vertical section of an ascoma. d Ostiole. e Structure of the peridium. f Paraphyses. g–i Asci. j–o Ascospores. p Surface view of colony on PDA. q Reverse view of colony on PDA. Scale bars: c = 200 µm, d = 100 µm, e, g–o = 20 µm, f = 10 µm.

Table 3 Dimensions of *Ophioceras hydei* and adjacent species.

Species	Ascomata size (µm)	Asci size (µm)	Ascospores size (µm)	References
Ophioceras aseptatum	380–430 diam. × 380–430 high	140–200 × 8.8–15	62–79 × 3.3–4.6	Wang et al. (2024)
O. dolichostomum	500 diam.	100–130 × 8–12	94–110 × 2–3 (3–7)	Conway & Barr (1977)

Table 3 Continued.

Species	Ascomata size (µm)	Asci size (µm)	Ascospores size (µm)	References
O. hydei	325–490 diam. × 340–675 high	125–140 × 8–14	82–103 × 2.2–3.4	This study
O. hongkongense	700–800 diam. × 500–640 high	100–125 × 12–14	72–101 × 3.5–4.5	Tsui et al. (2001)
O. submersum	500–600 diam. × 300–400 high	115–137 × 10–11	87–109 × 3–4	Luo et al. (2019)
O. venezuelense	745–868 diam. × 730–890 high	148–180 × 11–18	130–158 × 2–4 (5)	Shearer et al. (1999)

Subclass Xylariomycetidae O.E. Erikss & Winka

Amphisphaeriales D. Hawksw. & O.E. Erikss.

Apiosporaceae K.D. Hyde, J. Fröhl., Joanne E. Taylor & M.E. Barr

Nigrospora Zimm.

Index Fungorum number: IF9124; Facesoffungi number: FoF14273

Zimmerman (1902) established *Nigrospora* to accommodate the type species *N. panici*, which was isolated as an endophyte from leaves of *Panicum amphibium* in Java, Indonesia. *Nigrospora* species occur as endophytes, saprobes, and pathogens in humans and plants (Ananya et al. 2014, Hao et al. 2020, Zhang et al. 2021, de Queiroz Brito et al. 2023). Particular species within this genus, such as *N. oryzae* and *N. sphaerica*, have notable biotechnological potential due to their ability to produce metabolites with antifungal properties against various plant pathogens, including *Fusarium* spp. and *Colletotrichum musae* (Wu et al. 2018, Dawoud et al. 2021).

Nigrospora guangdongense Y.X. Li & Doilom, sp. nov. Fig. 75

Index Fungorum number: IF903749; Facesoffungi number: FoF17672

Etymology – Refers to the type locality, Guangdong Province, China.

Holotype – MHZU 24–0242

Endophytes from asymptomatic leaves of *Wurfbainia villosa* (*Zingiberaceae*). Sexual morph: Undetermined. Asexual morph: *Mycelia* 3.0–5.5 µm wide ($\overline{x}$ = 4.0 µm, n = 30), branched, septate, hyaline. *Conidiophores* reduced to conidiogenous cells. *Conidiogenous cells* 3–11 × 4–10 µm ($\overline{x}$ = 7 × 6.5 µm, n = 30), monoblastic, determinate, solitary to aggregated in clusters on hyphae, arising from aerial hyphae, globose to subglobose to ampulliform, hyaline, smooth-walled. *Conidia* 10–15 × 4–15 µm ($\overline{x}$ = 12 × 12.5 µm, n = 30), initially pale brown to dark brown, refractive blue in water mounts, becoming black when mature, solitary, subglobose to globose in face view, ellipsoidal in the side view, shiny, aseptate, smooth-walled.

Culture characteristics – On PDA, velvety, irregular, undulate edge, reaching 2.5–3 cm diam., in 2 weeks at room temperature (25 ± 2 °C), surface: white to cream; reverse: orange-yellow patches.

Material examined – China, Guangdong Province, Yangjiang City, 23°11'39"N; 113°21'22"E, asymptomatic leaves of *Wurfbainia villosa* (*Zingiberaceae*), 1 October 2021, CF Liao, (MHZU 24–0242, holotype), ex-type ZHKUCC 24–0545; *ibid*., living culture ZHKUCC 24–0546.

GenBank numbers – ZHKUCC 24–0545: ITS = PV523285, *tef1-α* = PV536735, *tub2* = PV536733; ZHKUCC 24–0546: ITS = PV523286, *tef1-α* = PV536736, *tub2* = PV536734.

Notes – The phylogenetic analyses based on a combined ITS, *tef1-α*, and *tub2* sequence dataset (Fig. 74) revealed that our strains (ZHKUCC 24–0545 and ZHKUCC 24–0546) formed a sister branch with *Nigrospora rubi* (LC2698) with 100 % ML and 1.00 BYPP. Morphologically, *N. guangdongense* can be distinguished from *N. rubi* by its predominantly hyaline conidiogenous cells, whereas those of *N. rubi* are pale brown. Additionally, the conidiogenous cells of *N. guangdongense* are shorter than those of *N. rubi* (3–11 µm [$\overline{x}$ = 7 µm] vs. 6.5–14 µm [$\overline{x}$ = 9.94 ±

1.71 µm]). The colonies of *N. guangdongense* on PDA are velvety, with an undulate edge, and have orange-yellow patches in reverse view. In contrast, colonies of *N. rubi* are floccose, with an entire edge and have smoke-grey patches in reverse view (Wang et al. 2017). Base pair comparisons between *N. guangdongense* (ZHKUCC 24–0545, type) and *N. rubi* (LC2698, type) revealed no differences in the ITS region (0/486 bp), 1.02% differences in the *tef1-α* region (5/491 bp, including 2 gaps), and 10.43% differences in the *tub2* region (39/374 bp, including 7 gaps). Based on morphology and phylogeny, we introduce our collection, *N. guangdongense*, as a new species herein.

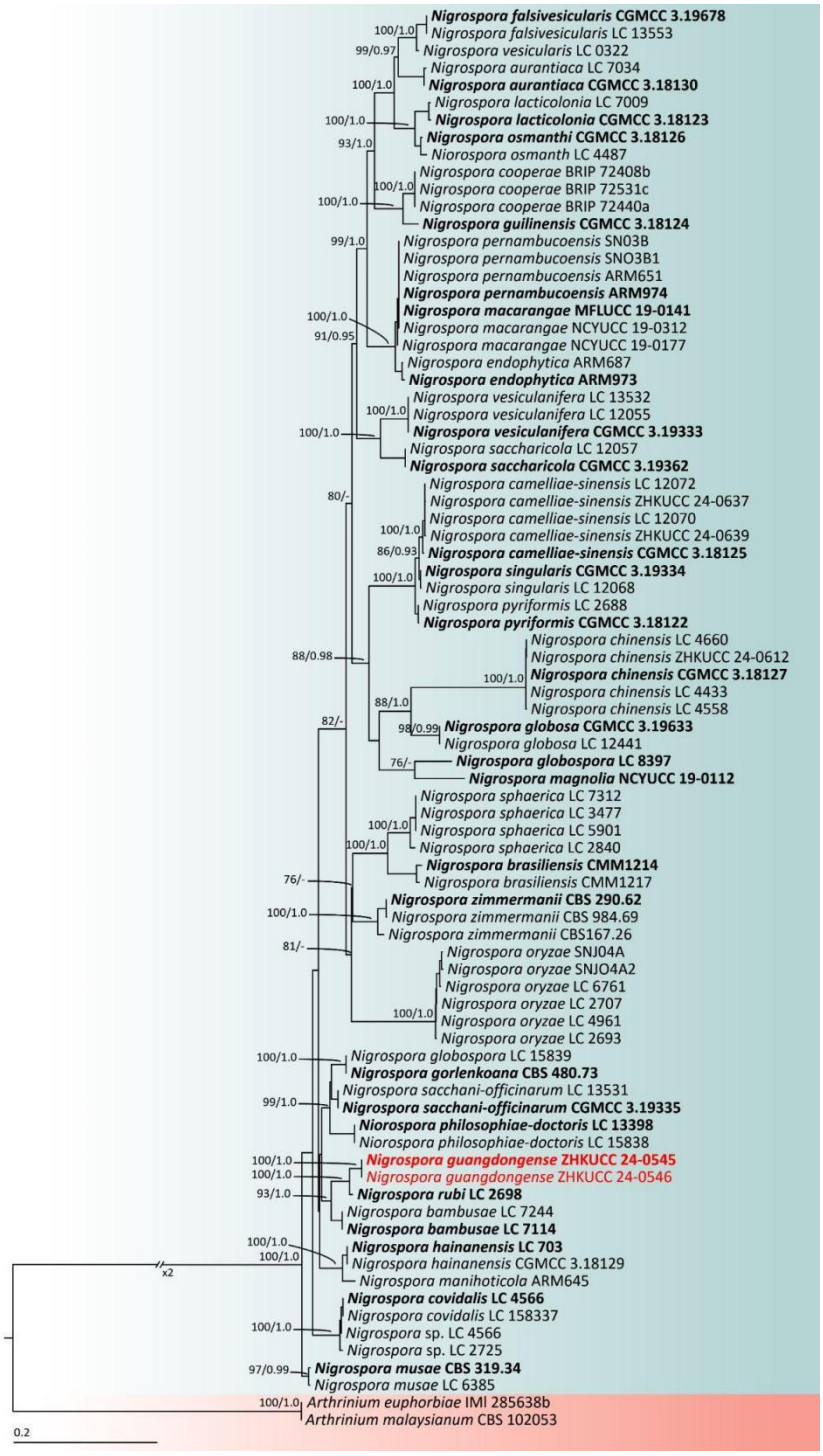


Figure 74 – Phylogram generated from maximum likelihood analysis based on combined ITS, *tef1-α*, and *tub2* sequence data from 82 taxa, comprising 1,298 characters (ITS = 502, *tef1-α* = 495, *tub2* = 299). The best-scoring RAxML tree with a final likelihood value of -10215.214 is presented. The

matrix contained 614 distinct alignment patterns, with 9.68% of the characters being undetermined or gaps. Estimated base frequencies were as follows: A = 0.217, C = 0.303, G = 0.241, T = 0.240; substitution rates: AC = 1.128, AG = 3.371, AT = 1.103, CG = 1.037, CT = 4.784, GT = 1.0; gamma distribution shape parameter α = 0.202. Bootstrap support values for maximum likelihood (ML) equal to or greater than 50% and clade credibility values greater than 0.90 (rounded to two decimal places) from Bayesian inference analysis are labeled at each node. Ex-type strains are in bold, while the new isolates are indicated in red. The tree is rooted to *Arthrinium euphorbiae* (IMl 285638b) and *A. malaysianum* (CBS 102053).

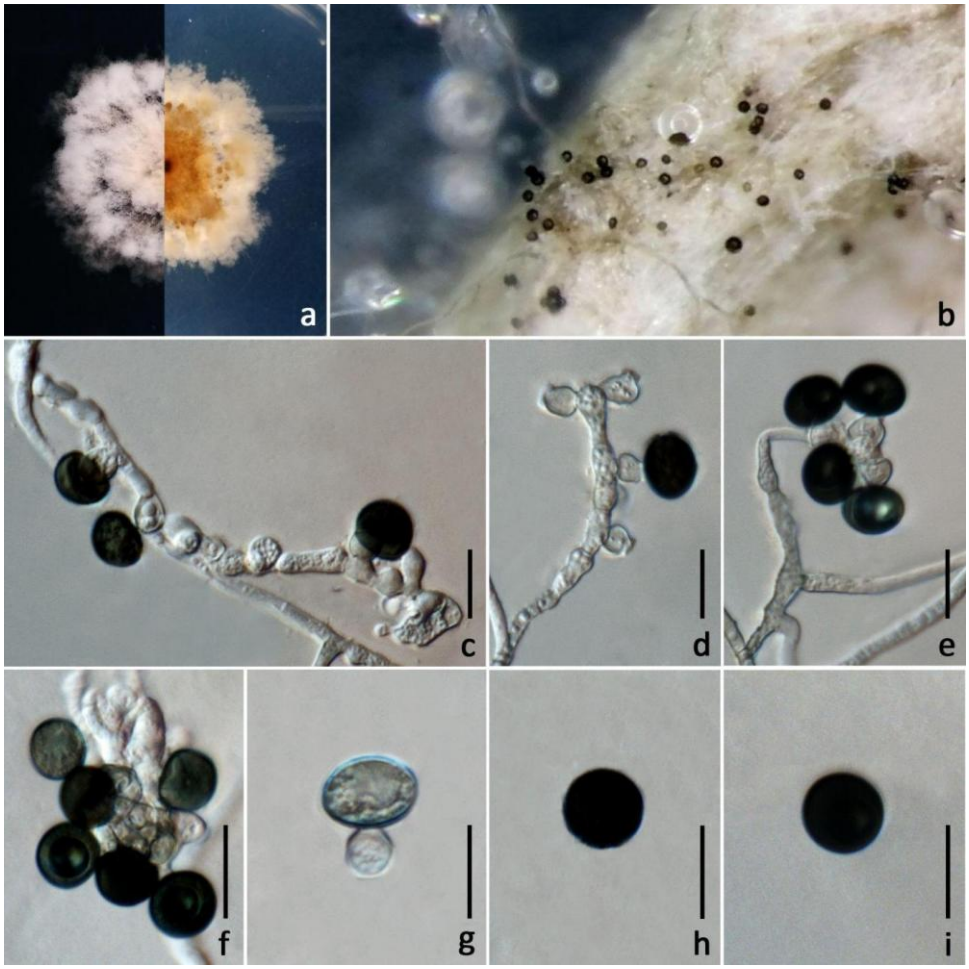


Figure 75 – *Nigrospora guangdongense* (MHZU 24–0242, holotype). a Upper and reverse views of culture on PDA. b Conidia on aerial mycelia on PDA. c–g Conidia with conidiogenous cells. h, i Conidia. Scale bars: c–i = 10 μm.

Pseudosporidesmiaceae Crous

Pseudosporidesmium K.D. Hyde & McKenzie, Fungal Diversity 80: 406 (2016)

Index Fungorum: IF551835; Facesoffungi number: FoF01758

K.D. Hyde & McKenzie established *Pseudosporidesmium* in Su et al. (2016), and typified with *P. knawiae* to accommodate *Sporidesmium knawiae*, which was introduced by Crous (2008). Currently, two species are accepted in *Pseudosporidesmium*, and both have been isolated from living leaves (Crous et al. 2008, 2017). The genus is distinguished from *Sporidesmium* and *Distoseptispora* based on strong molecular and morphological evidence. *Pseudosporidesmium* is characterized by its unique conidiophore structure and conidial morphology, particularly the percurrent rejuvenation of conidiophores, which differentiates it from *Sporidesmium* s. str.

Prof. Kevin D. Hyde's contributions to the study of *Pseudosporidesmium* have been pivotal in advancing fungal taxonomy. Together with his collaborators, Prof. Kevin D. Hyde established

the genus *Pseudosporidesmium*, designating *P. knawiae* (transferred from *Sporidesmium knawiae*) as its type species (Su et al. 2016). This addressed the polyphyly and morphological heterogeneity of *Sporidesmium*, a historically problematic genus. Prof. Kevin D. Hyde's work highlighted key distinctions, such as the percurrent rejuvenation of conidiophores in *Pseudosporidesmium*, absent in *Sporidesmium* s. str., and provided strong molecular support for the new genus.

In recognition of Prof. Kevin D. Hyde's outstanding contributions to mycology, we introduce *Pseudosporidesmium hydei* as a new species. We also provide an updated phylogenetic tree for *Pseudosporidesmium* (Fig. 76). *Pseudosporidesmium knawiae* and *P. lambertiae* were isolated from living plants in South Africa and Australia, respectively; in contrast, our newly discovered species was isolated from decaying plant material in China. This ecological diversity suggests that *Pseudosporidesmium* may have a broader habitat range than currently recognized. In the future, it is expected that more species within this genus will be described and introduced as research progresses.

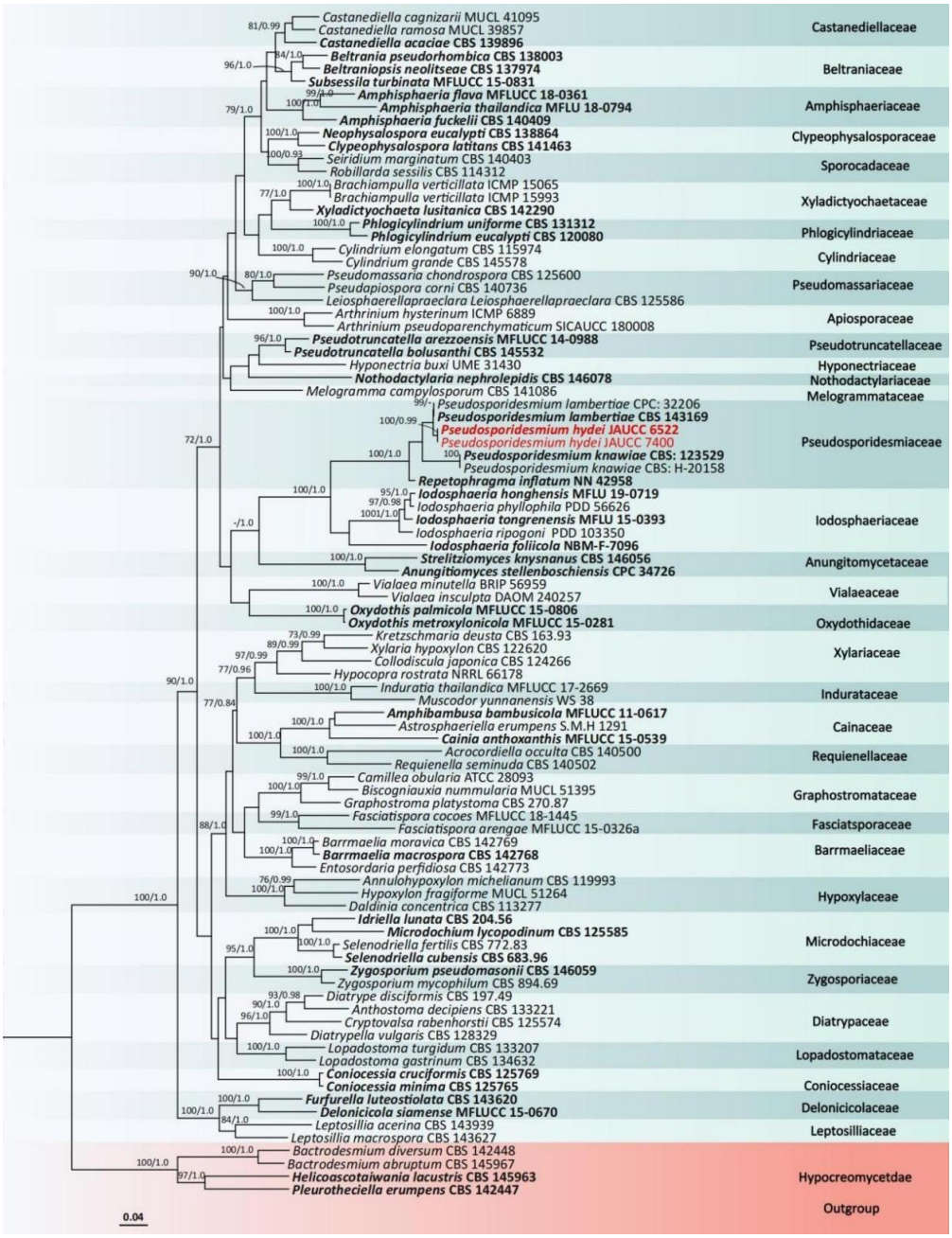


Figure 76 – Phylogram generated from maximum likelihood analysis based on combined ITS and LSU, *rpb2*, and *tef1-α* sequence data from 92 taxa, comprising 3,802 characters (ITS = 742, LSU =

890, *rpb2* = 1,119, *tef1-α* = 1,051). The best-scoring RAxML tree with a final likelihood value of -55753.608 is presented. The matrix contained 2,191 distinct alignment patterns, with 45.07% of the characters being undetermined or gaps. Estimated base frequencies were as follows: A = 0.249, C = 0.247, G = 0.271, T = 0.232; substitution rates: AC = 1.245, AG = 2.887, AT = 1.670, CG = 1.212, CT = 5.511, GT = 1.0; gamma distribution shape parameter α = 0.302. Bootstrap support values for maximum likelihood (ML) equal to or greater than 70% and clade credibility values greater than 0.90 (rounded to two decimal places) from Bayesian inference analysis are labeled at each node. Ex-type strains are in bold, while the new isolates are indicated in red. The tree is rooted to *Bactrodesmium abruptum* (CBS 145967), *B. diversum* (CBS 142448), *Helicoascotaiwania lacustris* (CBS 145963), and *Pleurotheciella erumpens* (CBS 142447).

Pseudosporidesmium hydei L.X. Mi & D.M. Hu, sp. nov. Fig. 77

Index Fungorum number: IF903727; Facesoffungi number: FoF17767

Etymology – 'hydei' named in honor of the renowned mycologist Kevin D. Hyde, recognizing his significant contributions to mycology on the occasion of his 70th birthday.

Saprobic on dried branches of *Tetradium ruticarpum* (*Rutaceae*). Sexual morph: Undetermined. Asexual morph: Hyphomycetous. *Mycelium* consisting of branched, septate, pale brown hyphae. *Conidiophores* 100–180 × 5–8 µm ($\overline{x}$ = 135 × 6.6 µm, n = 20), solitary or in some groups, flexuous or erect, somewhat repent, arising from superficial hyphae, rejuvenating percurrently, base mostly not swollen, and lacking rhizoids; stipe cylindrical, brown, smooth, thick-walled, mostly unbranched, *Conidiogenous cells* 14–35 × 5–9 µm ($\overline{x}$ = 23.8 × 6.5 µm, n = 20), terminal, cylindrical, brown; scars truncate, unthickened, 6–7 µm diam, proliferating once percurrently at apex, after which the conidiophore extends in length, before forming the next conidium; flaring collarette visible. *Conidia* 60–85 × 14–17 µm ($\overline{x}$ = 73.6 × 15 µm, n = 20), solitary, acrogenous, obclavate, smooth-walled, guttulate, base truncate (5–8 µm wide), (2–)5-euseptate, basal cell pale brown, the second cell to the last cell gradually lightens from medium brown to pale brown, forming a long beak with subobtuse apex.

Culture characteristics – Colonies erumpent and reach 25 mm diam., on PDA after 2 weeks at 25 °C, spread with abundant aerial mycelium and feathery margins, surface pale olivaceous-grey, reverse olivaceous-grey. No diffusible pigment was produced.

Material examined – China, Hunan Province, Chengzhou City, Guidong County, on dead branches of *Tetradium ruticarpum* (*Rutaceae*), 25.95 N 113.81 E, 16 September 2023, Lixue Mi, HFJAU10637, holotype, ex-type JAUCC6522; *ibid*., HFJAU10638, living culture JAUCC7400.

GenBank numbers – JAUCC 6522: ITS = PV138555, LSU = PV138437, *rpb2* = PV467636, *tef1-α* = PV467638; JAUCC 7400: ITS = PV138556, LSU = PV138438, *rpb2* = PV467637, *tef1-α* = PV467639.

Notes – Multi-locus phylogenetic analysis indicated that *Pseudosporidesmium hydei* nested within Pseudosporidesmiaceae and formed a distinct clade sister to the clade of *P. lambertiae* with 64% ML and 0.64 BYPP statistical support (Fig. 76). Morphologically, *P. hydei* differs from *P. lambertiae* in having much longer euseptate conidia (60–85 vs. 37–60 µm) (Crous et al. 2017). In addition, the conidia of *P. hydei* occasionally have 5 euseptate conidia, which have not been observed in *P. lambertiae* (Crous et al. 2017). Base pair comparison revealed 1.63% differences (8/492 bp, including 4 gaps) in the ITS region, and no differences in the LSU region. Sequence data for *rpb2* and *tef1-α* are currently unavailable for *P. lambertiae*. The PHI test revealed no significant recombination event between *Pseudosporidesmium hydei* and its closely related taxa (Φw = 1) (Fig. 78). Therefore, we propose that our isolate be classified as a new species based on both phylogenetic and morphological analyses.



Figure 77 – *Pseudosporidesmium hydei* (HFJAU10637, holotype). a–c Appearance of ascomata on woody substrate. d Conidiophores with conidia. f–h Conidiogenous cells and conidia. i–k Conidia. l Germinated conidium. m–n Colony on PDA from surface and reverse. Scale bars: d–l = 50 µm.

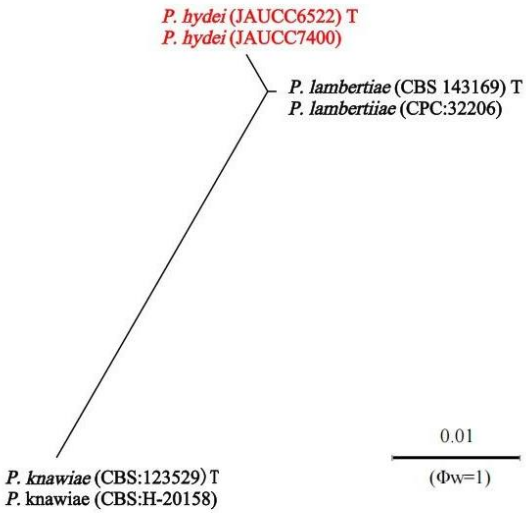


Figure 78 – PHI test results of *Pseudosporidesmium hydei* and closely related species using both LogDet transformation and splits decomposition. The PHI test results (Φw) < 0.05 indicate significant recombination within the dataset. The new taxa are in red bold type, and T indicates holotype or ex-type strains.

Xylariales Nannf.

Diatrypaceae Nitschke

Allocryptovalsa Senwanna, Phookamsak & K.D. Hyde, Mycosphere 8 (10): 1839 (2017)

Index Fungorum number: IF553857; Facesoffungi number: FoF03773

Allocryptovalsa was introduced by Senwanna et al. (2017) to accommodate *A. polyspora* as the type species, along with two new combination species: *A. cryptovalsoidea* (≡ *Eutypella cryptovalsoidea*) and *A. rabenhorstii* (≡ *Cryptovalsa rabenhorstii*). *Allocryptovalsa* is characterized by immersed stromata, polysporous or 8-spored asci, and allantoid ascospores (Senwanna et al. 2017, Hyde et al. 2020c, Maharachchikumbura et al. 2022). Currently, 11 species are listed in Index Fungorum (2025), namely *A. aceris*, *A. aquilariae*, *A. castaneae*, *A. castaneicola*, *A. cryptovalsoidea*, *A. elaeidis*, *A. polyspora*, *A. rabenhorstii*, *A. sichuanensis*, *A. truncata*, and *A. xishuangbanica*.

Prof. Kevin D. Hyde's contributions to the study of *Allocryptovalsa* have been pivotal, as he has played a key role in the discovery of new species within this genus. Of the 11 species currently listed in Index Fungorum, Prof. Kevin D. Hyde and his collaborators have introduced eight species. In recognition of his outstanding contributions to mycology, we introduce *Allocryptovalsa hydei* as a new species. We also provide an updated phylogenetic tree for *Allocryptovalsa* (Fig. 79). Since *Allocryptovalsa* has been recorded from various host species, its host specificity remains unclear; therefore, further collections from diverse hosts and geographical regions are essential to determine its host specificity (Senwanna et al. 2017, Hyde et al. 2020c, Konta et al. 2020, Zhu et al. 2021, Maharachchikumbura et al. 2022, Senanayake et al. 2023).

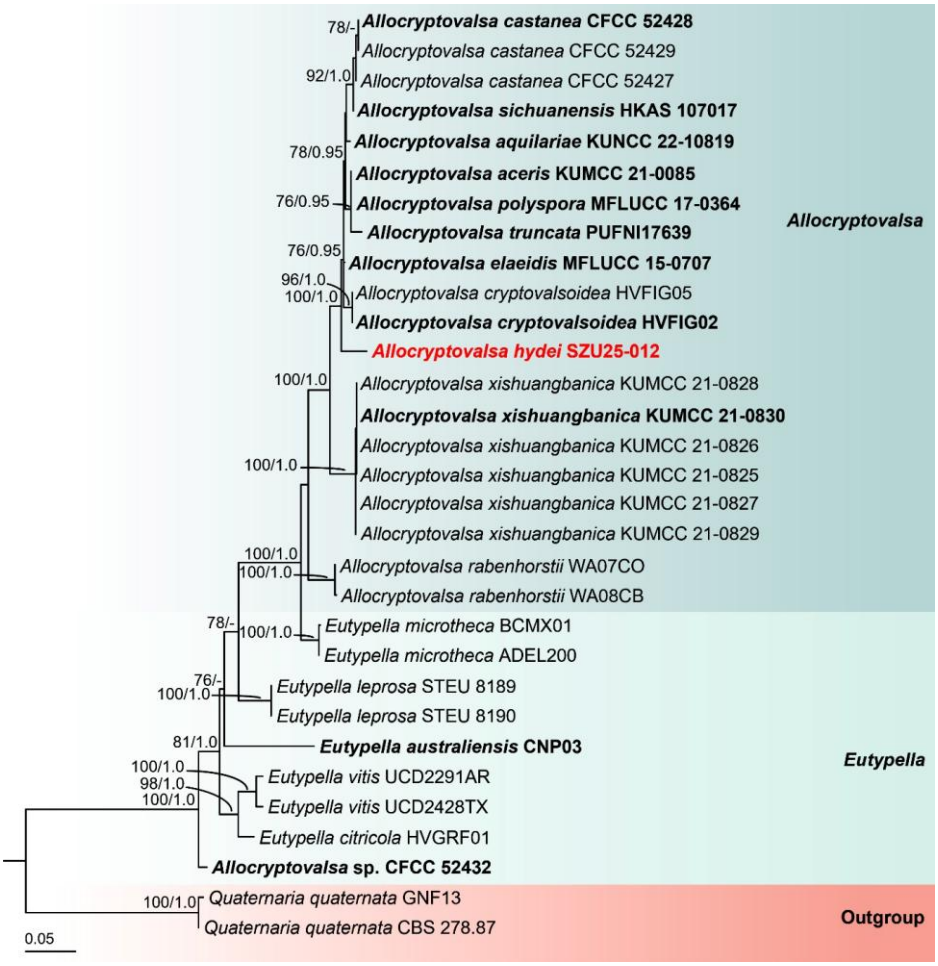


Figure 79 – Phylogram generated from maximum likelihood analysis of combined ITS and *tub2* sequence data. Related sequences of *Diatrypaceae* were obtained from Maharachchikumbura et al. (2022). The combined ITS and *tub2* sequence data from 36 taxa, comprising 1,091 characters (ITS

= 638, *tub2* = 453). The best-scoring RAxML tree with a final likelihood value of -3873.966 is presented. The matrix contained 393 distinct alignment patterns, with 27.91% of the characters being undetermined or gaps. Estimated base frequencies were as follows: A = 0.229, C = 0.268, G = 0.235, T = 0.268; substitution rates: AC = 0.976, AG = 2.913, AT = 1.336, CG = 0.875, CT = 4.687, GT = 1.0; gamma distribution shape parameter α = 1.257. Bootstrap support values for maximum likelihood (ML) equal to or greater than 75% and clade credibility values greater than 0.90 (rounded to two decimal places) from Bayesian inference analysis are labeled at each node. Ex-type strains are in bold, while the new isolate is indicated in red bold. The tree is rooted to *Quaternaria quaternate* (CBS 278.87 and GNF13).

Allocryptovalsa hydei Tennakoon & S. Hongsanan, sp. nov. Fig. 80

Index Fungorum number: IF903739; Facesoffungi number: FoF17768

Etymology – 'hydei' named in honor of the renowned mycologist Kevin D. Hyde, recognizing his significant contributions to mycology on the occasion of his 70th birthday.

Holotype – SZU25–012

Saprobic on a dead stem of an unidentified host. Sexual morph: *Ascostromata* solitary to gregarious, immersed to semi-immersed, erumpent through the surface of the bark. *Ascomata* (including neck) 500–700 × 275–400 µm ($\overline{x}$ = 674 × 315 µm, n = 10), perithecial, gregarious, immersed in the stroma, obovoid to ellipsoid, coriaceous, dark brown to black, ostiolate, papillate. *Peridium* 15–20 µm wide, composed of two sections, outer layer dark brown, thick-walled cells, arranged in *textura angularis*, inner layer hyaline, thin-walled cells of *textura prismatica*. *Hamathecium* composed of 2–4 µm wide, filiform, septate, hyaline, unbranched paraphyses. *Asci* 95–120 × 15–24 µm ($\overline{x}$ =105 × 18 µm, n = 20), clavate to elongate obovoid, polysporous, thin-walled, long pedicellate, apically rounded, narrowing towards the lower region. *Ascospores* 11.5–13 × 3.5–4.3 µm ($\overline{x}$ = 12 × 4 µm, n = 20), crowded, oblong to allantoid, pale yellowish at maturity, aseptate, slightly curved, smooth-walled, granules, without appendages and mucilaginous sheath. Asexual morph: Undetermined.

Material examined – China, Yunnan Province, Kunming, on a dead stem of an unidentified host, 12 July 2018, D. S. Tennakoon, DC23 (SZU25–012, holotype).

GenBank numbers – SZU25–012: ITS = PV053554, *tub2* = PV040714.

Notes – Morphologically, the *Allocryptovalsa* species share similar characteristics, including immersed to semi-immersed stromata, polysporous asci, and allantoid ascospores, as well as asexual morphs with hyaline, elongate allantoid conidia. However, *A. xishuangbanica* is distinct in having 8-spored asci (Trouillas et al. 2011, Senwanna et al. 2017, Zhu et al. 2021, Maharachchikumbura et al. 2022). Therefore, molecular data are crucial for distinguishing the species. According to the multi-locus phylogeny (ITS and *tub2*), our collection (SZU25-012) constitutes an independent lineage sister to a clade containing *Allocryptovalsa aceris*, *A. aquilariae*, *A. castaneae*, *A. cryptovalsoidea*, *A. polyspora*, *A. sichuanensis*, and *A. truncata* (Fig. 79). In particular, our collection shows a close phylogenetic relationship with *A. cryptovalsoidea* isolates (HVFIG02 and HVFIG02). A comparison of the 501 nucleotides across the ITS (+5.8S) gene region of our collection (SZU25-012) and *A. cryptovalsoidea* (HVFIG02) shows 2.39% differences (12 bp differences). Therefore, we introduce *A. hydei* as a new species, based on both morphological and phylogenetic evidence.

Allodiatrype Konta & K.D. Hyde, Mycosphere 11(1): 247 (2020)

Index Fungorum number: IF556641; Facesoffungi number: FoF556641

Allodiatrype was introduced by Konta et al. (2020) with the type *A. arengae*. Further, Konta et al. (2020) added *A. elaeidicola*, *A. elaeidis*, and *A.* (syn. *Diatrype*) *thailandica* to this genus. The genus currently comprises ten species (Index Fungorum 2025). Most *Allodiatrype* species are identified from dead wood in Thailand and China (Konta et al. 2020, Afshari et al. 2023). The sexual morph is characterized by 1–10-ascomata immersed in one stroma, with or without a black stromatic zone, surrounded with a ring-like, ostiolar opening, immersed, aggregated, globose to

sub-globose perithecial ascomata, unitunicate, 8-spored, cylindrical, thick walled, asci with J-, cylindrical, conspicuous apical ring, hyaline to yellowish allantoid, unicellular ascospores (Konta et al. 2020). *Allodiatrype* species closely resemble *Diatrype* species. However, *Allodiatrype* differs in having 1–10 ascomata immersed in a single stroma, with or without a black stromatic zone. In contrast, the stromata of *Diatrype* primarily spread in a large area (Konta et al. 2020). Phylogenetic relationships of *Allodiatrype* species were inferred using ITS and *tub2* sequence data (Konta et al. 2020, Afshari et al. 2023). Prof. Kevin D. Hyde's contributions to the study of *Allodiatrype* have been pivotal since the genus was first introduced in 2020. Through his continued research, Prof. Kevin D. Hyde has not only expanded our understanding of *Allodiatrype* but has also played a key role in discovering new species within this genus. Of the ten species currently listed in Index Fungorum, Prof. Kevin D. Hyde and his collaborators have introduced four species.

In recognition of Prof. Kevin D. Hyde's outstanding contributions to mycology, herein we introduce *Allodiatrype elaeidicola* as a new host and geographical record. We also provide an updated phylogenetic tree for *Allodiatrype* (Fig. 81).

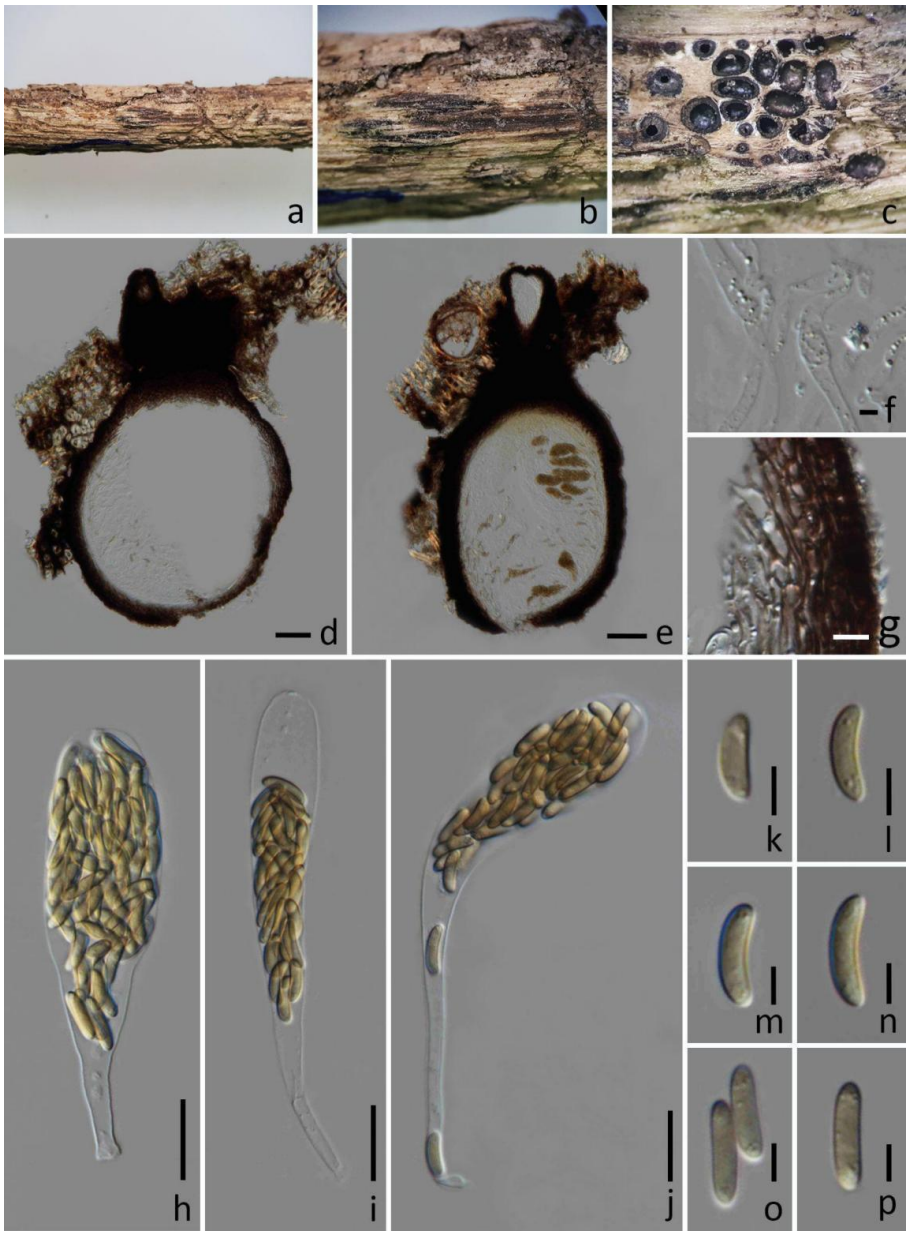


Figure 80 – *Allocryptovalsa hydei* (SZU25–012, holotype). a Dead stem. b, c Appearance of stromata on substrate. d, e Vertical sections through stromata. f Paraphyses. g Peridium. h–j Asci. k–p Ascospores. Scale bars: d, e = 50 µm, f = 2 µm, g = 10 µm, h–j = 20 µm, k–p = 5 µm.

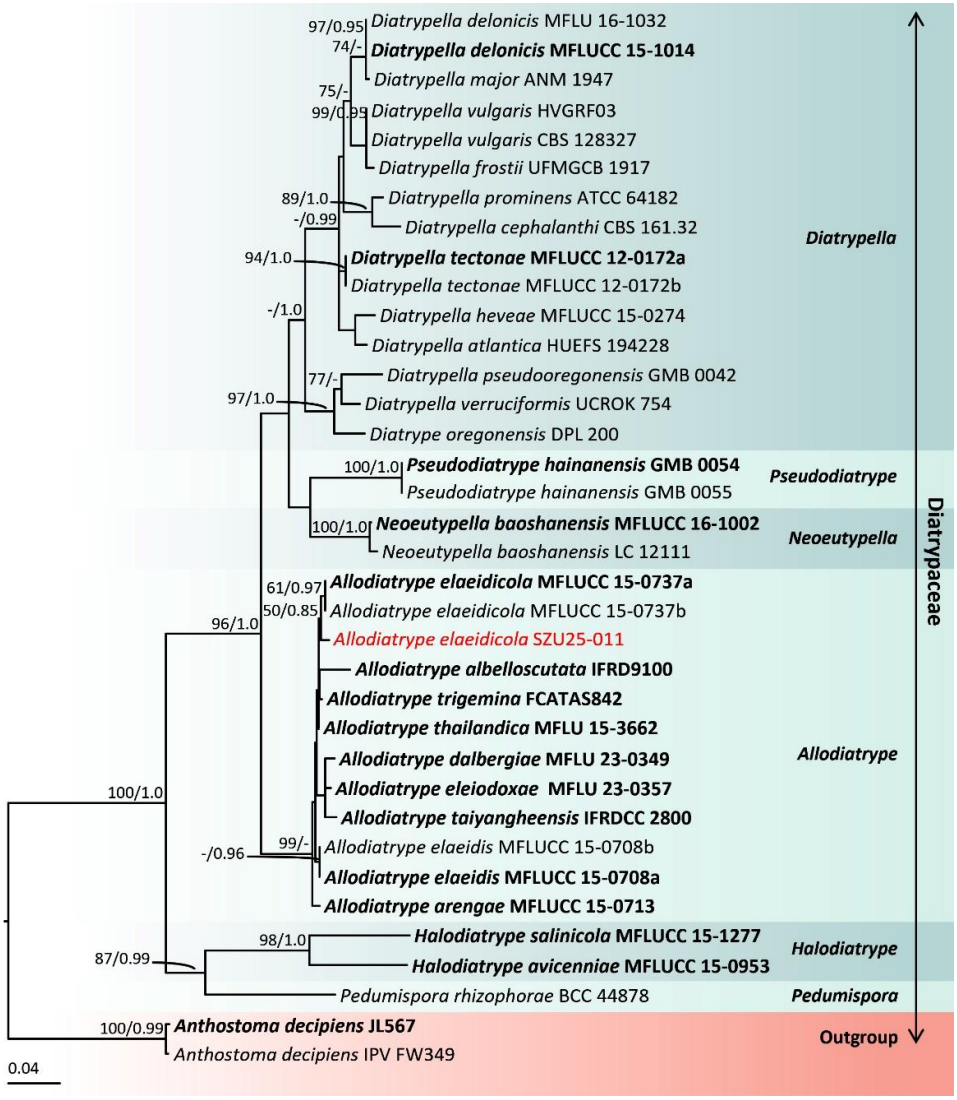


Figure 81 – Phylogram generated from maximum likelihood analysis of combined ITS and *tub2* sequence data. Related sequences of *Diatrypaceae* were obtained from Carpouron et al. (2021) and de Silva et al. (2022). The combined ITS and *tub2* sequence data from 36 taxa comprised 1,900 characters (ITS = 650, *tub2* = 1,250). The best-scoring RAxML tree with a final likelihood value of -6960.844 is presented. The matrix contained 588 distinct alignment patterns, with 60.16% of the characters being undetermined or gaps. Estimated base frequencies were as follows: A = 0.219, C = 0.274, G = 0.236, T = 0.270; substitution rates: AC = 0.855, AG = 3.512, AT = 1.158, CG = 0.659, CT = 4.256, GT = 1.0; gamma distribution shape parameter α = 0.140. Bootstrap support values for maximum likelihood (ML) equal to or greater than 70% and clade credibility values greater than 0.90 (rounded to two decimal places) from Bayesian inference analysis are labeled at each node. Ex-type strains are in bold, while the new isolate is indicated in red bold. The tree is rooted to *Anthostoma decipines* (JL567 and IPV FW349).

Allodiatrype elaeidicola S. Konta & K.D. Hyde, Mycosphere 11(1): 251 (2020) Fig. 82

Index Fungorum number: IF556930; Facesoffungi number: FoF05117

Saprobic on an unidentified dead plant branch. Sexual morph: *Stromata* 400–600 × 850–1270 µm diam. ($\bar{x}$ = 540 × 950 µm, n = 10), with well-developed interior, solitary to gregarious, erumpent, black, with black stromatic zone on host surface, glabrous, irregular in shape, pustulate, multi-ascomata, with umbilicate ostioles appearing on the surface of the stroma. *Ostiole* opening through host surface and appearing as black spots, surrounded with a ring-like structure, composed of an outer layer of dark brown, small, tightly packed, thick parenchymatous cells and an inner layer of white to light-yellow, large, loosely packed, parenchymatous cells. *Ascomata* 380–590 ×

230–260 μm diam. ($\overline{x}$ = 520 × 250 μm, n = 10), perithecial, immersed in the stroma, globose to subglobose, glabrous, individual ostioles, with a short neck. *Ostiolar canal* 160–180 × 75–120 μm diam. ($\overline{x}$ = 170 × 95 μm, n = 10), cylindrical, sulcate, with periphyses. *Peridium* 22–30 μm wide ($\overline{x}$ = 27 μm, n = 10), composed of two section layers, outer part; brown to dark brown, thick-walled cells, arranged in *textura angularis*, inner layer; hyaline, thick-walled cells of *textura angularis*. *Hamathecium* composed of 4–6 μm wide ($\overline{x}$ = 5 μm, n = 60), hyaline, filiform, septate, paraphyses. *Asci* (excluding stalks), spore-bearing part 45–60 × 9–12 μm ($\overline{x}$ = 50 × 10 μm, n = 30), 8-spored, unitunicate, clavate, apically rounded with J-apical ring, with long stalks 32–46 μm long. *Ascospores* 6–11× 2–4 μm ($\overline{x}$ = 10 × 3 μm, n = 50), overlapping, yellowish to pale-brown, ellipsoidal to cylindrical or elongate-allantoid, aseptate, smooth-walled. Asexual morph: Undetermined.

Material examined – China, Yunnan Province, Kunming, on unidentified dead plant branch, 4 November 2019, N. I. de Silva (NIM05), SZU25–011.

GenBank numbers – SZU25–011: ITS = PV053555, *tub2* = PV040715.

Notes – In the present phylogenetic analyses based on combined ITS and *tub2* sequences, the new strain (SZU25–011) clustered as a sister to *A. elaeidicola*, forming a distinct lineage with 50% ML and 0.85 BYPP statistical support (Fig. 81). The stromata of *A. elaeidicola* (1.2–2.8 mm long, 0.96–1.66 mm diam.; Konta et al. 2020) are slightly larger than those of the new strain (SZU25–011) (400–600 μm high, 850–1270 μm diam.). The asci (spore-bearing part) of *A. elaeidicola* ((17–)20–31(–43) × 4–7 μm) are slightly smaller compared to those of the new strain (SZU25–011) (45–60× 9–12 μm). Additionally, the stalk-bearing part of *A. elaeidicola* ((32–)40–60(–76) μm) is slightly longer than that of the new strain (SZU25–011) (32–46 μm). However, the ascospore size of both species shows overlapping dimensions. A comparison between *A. elaeidicola* (MFLUCC 15–0737a) and the new strain (SZU25–011) revealed a 0.37% difference (2/540 bp) in the ITS region and a 1.52% (5/328 bp) differences in the *tub2* region. *Allodiatrype elaeidicola* was identified from petioles of *Elaeis guineensis* (*Arecaceae*) in Thailand (Konta et al. 2020), while the new strain (SZU25–011) was identified from dead plant branches in China. Therefore, the new strain (SZU25–011) is described as a new host and geographical record based on multi-locus phylogeny and morphology.

Hypoxylaceae DC**.**

Annulohypoxylon Y.M. Ju, J.D. Rogers & H.M. Hsieh, in Hsieh, Ju & Rogers, Mycologia 97(4): 855 (2005)

Index Fungorum number: IF500298; Facesoffungi number: FoF02983

Annulohypoxylon was introduced by Hsieh et al. (2005) and typified with *A. truncatum.* It contains species formerly placed in the closely related *Hypoxylon*, equivalent to the *Hypoxylon* section *Annulata* sensu. The genus currently comprises 71 species (Index Fungorum 2025). They can be commonly found on dead dicotyledonous wood as saprobes (Hladki & Romero 2009, de Souza Leite et al. 2013, Fournier & Lechat 2016, Kuhnert et al. 2017), and also as endophytes on *Pandanus simplex* and *Taxus wallichiana* (Gauchan et al. 2021, Rondilla et al. 2022). *Annulohypoxylon* species are characterised by asci that are 8-spored, cylindrical, stipitate, persistent, with an apical ring that is discoid, amyloid, or infrequently inamyloid, and distinct. Ascospores are light- to dark-coloured, unicellular in both mature and immature ascospores, ellipsoid or short fusoid, inequilateral, slightly inequilateral or nearly equilateral, with acute, narrowly rounded, or broadly rounded ends, with a germ slit spore-length to much less than spore-length on the convex side or less frequently on the flattened side. Prof. Kevin D. Hyde's contributions to the study of *Annulohypoxylon* have been pivotal since the genus was first introduced in 2005. Through his continued research, Prof. Kevin D. Hyde has not only expanded our understanding of *Annulohypoxylon* but has also played a key role in discovering numerous new species within this genus. Of the 71 species currently listed in Index Fungorum, Prof. Kevin D. Hyde and his collaborators have introduced 15 species.

In recognition of his outstanding contributions to mycology, we introduce the new species, *Annulohypoxylon hydei*. We also provide an updated phylogenetic tree for *Annulohypoxylon* (Fig. 83). As some species lack molecular data, additional collections are necessary to provide a comprehensive picture of the genus.

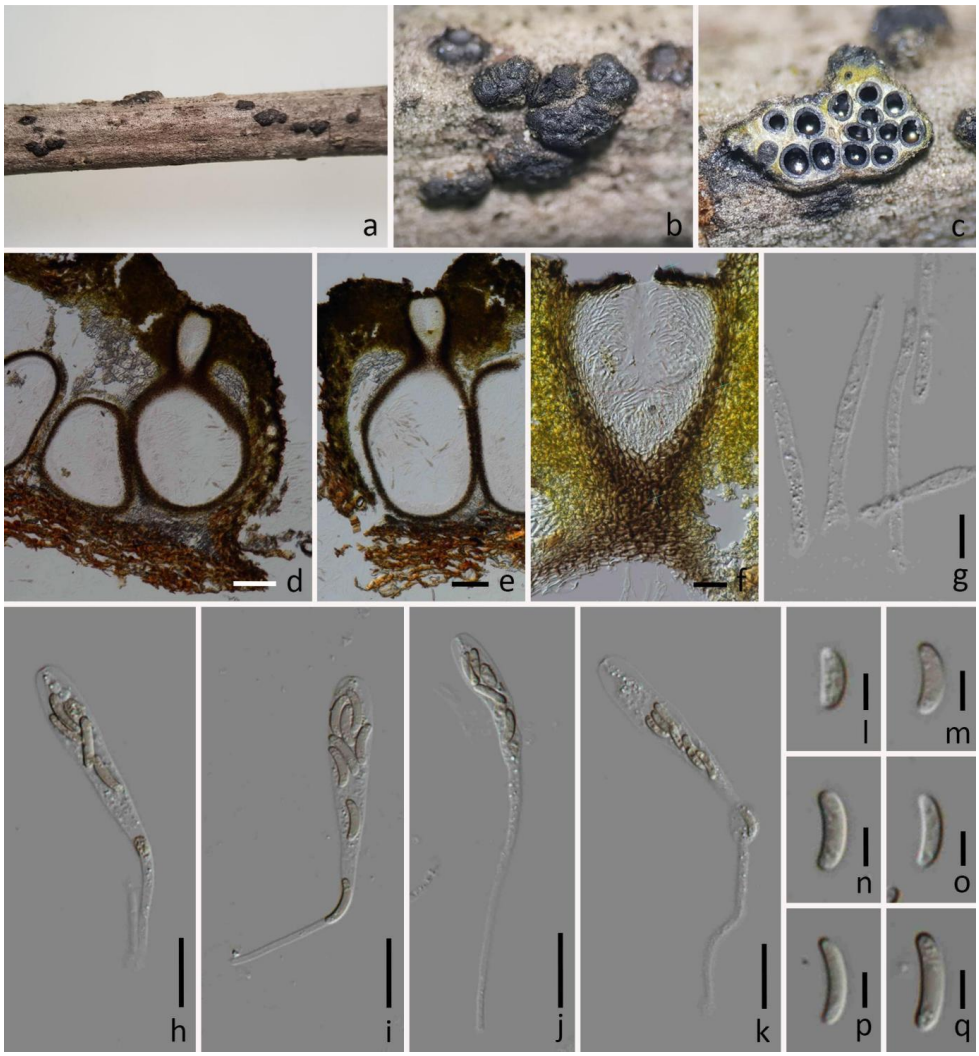


Figure 82 – *Allodiatrype elaeidicola* (SZU25–011, new host and geographical record). a The dead branch with fruiting bodies. b, c Appearance of stromata on substrate. d–f Vertical sections through stromata. g Paraphyses. h–k Asci. l–q Ascospores. Scale bars: d, e = 100 μm, f = 50 μm, g = 10 μm, h–k = 20 μm, l–q = 5 μm.

Annulohypoxylon hydei Manawas., Q.L. Tan, Y.X. Zhang, sp. nov. Fig. 84

Index Fungorum: IF901663; Facesoffungi number: FoF17674

Etymology – 'hydei' named in honor of the renowned mycologist Kevin D. Hyde, recognizing his significant contributions to mycology on the occasion of his 70th birthday

Holotype: MHZU 25–1015

Culture characteristics – Cultured on PDA for 5 days, colony diameter 62 mm (n = 5), the colony is white, circular, with regular edges, aerial hyphae dense and fluffy, brown to orange in the center of the back of the colony, forming concentric circles

Material examined – China, Guangdong Province, Guangzhou, Shaoguan City, Renhua County, Dongtang Town, Jiangtou Village, JiaYun Farm, 25°4'37" N 113°36'51" 100 m, Ishara S. Manawasinghe (MHZU 25–1015, holotype), ex-type ZHKUCC 25–0350, living culture ZHKUCC 25–0351.

GenBank numbers – ZHKUCC 25–0350: ITS = PV486813; ZHKUCC 25–0351: ITS = PV486814, *tub2* = PV494559.

Notes – In the phylogenetic analysis, *Annulohypoxylon hydei* forms a distinct lineage basal to other *Annulohypoxylon* species with 100% ML and 1.0 BYPP support (Fig. 83). *Annulohypoxylon hydei* and *A. nitens* (CBS 120705) showed 2.51% differences (23/915 bp, excluding gaps) in the ITS region, and 4.09% differences (43/1,050 bp, excluding gaps) in the *tub2* region. *Annulohypoxylon hydei* and *A. atroroseum* (EK1400) showed 3.51% differences (29/824 bp, excluding gaps) in the ITS region, and 4.59% differences (50/1,088 bp, excluding gaps) in the *tub2* region. *Annulohypoxylon hydei* and *A. stygium* (MUCL 54601) exhibit 1.79% differences (14/779 bp, excluding gaps) in the ITS region, and 2.39% differences (31/1294 bp, excluding gaps) in the *tub2* region. Following Ma et al. (2022), we attempted to induce sporulation of this isolate under various conditions; however, the species did not sporulate. The lack of sporulation, or difficulty in inducing it, is a common challenge in *Hypoxylaceae*, as similar results have also been reported in previous studies (Wibberg et al. 2021). Therefore recent studies have described new fungal species, particularly within *Hypoxylaceae* (Xylariales), based primarily on DNA sequence data and culture characteristics. Kuhnert et al. (2022) elineated cryptic lineages in *Hypoxylon* using multi-locus phylogeny (ITS-*rpb2*-*tub2*-LSU) and stromatal chemistry (HPLC-MS) when sporulation failed. Endophytic *Xylaria* taxa from asymptomatic plants were also described without conidial or ascospore observations (Ma et al. 2022), emphasizing ITS-*rpb2*-*tub2* phylogenies. However, species introducing without morphology is still and ongoing argument among mycologists. To mitigate concerns, over this approach we integrate multi-locus sequences rather than ITS and culture repositories to ensure reproducibility.

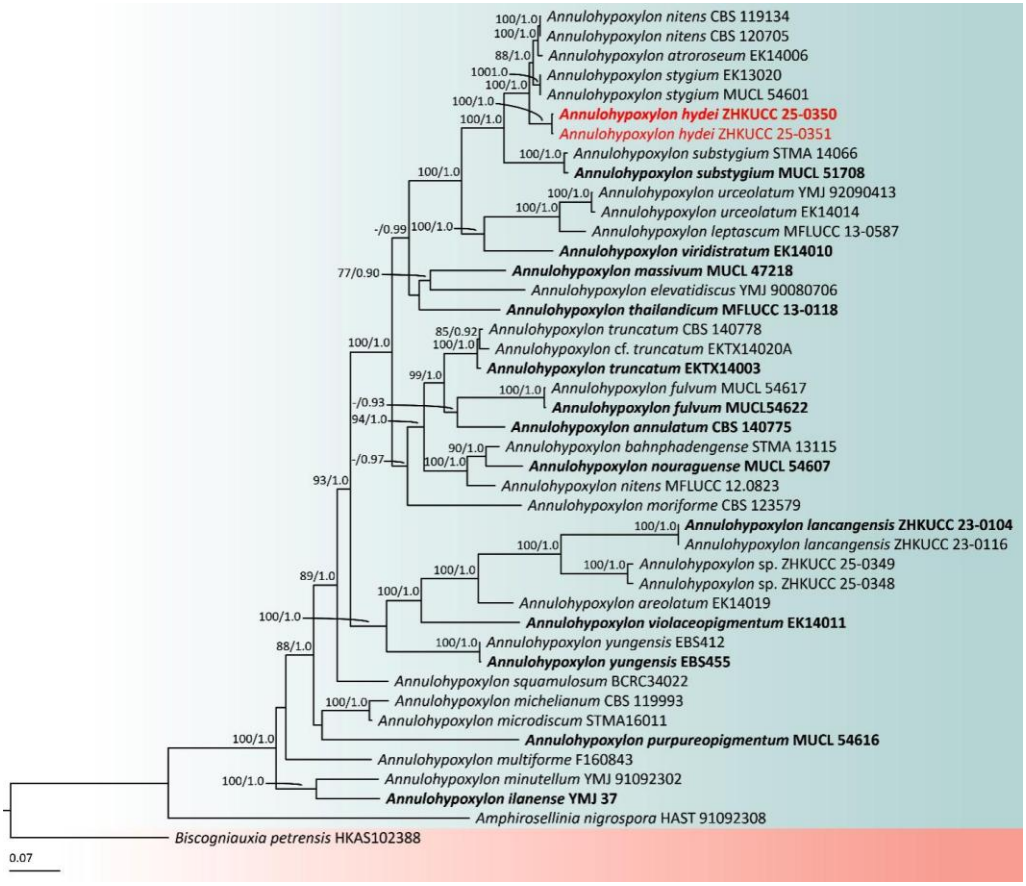


Figure 83 – Phylogram generated from maximum likelihood analysis based on combined ITS and *tub2* sequence data from 43 taxa, comprising 2,356 characters (ITS = 1,082, *tub2* = 1,454). The best-scoring RAxML tree with a final likelihood value of -24051.202 is presented. The matrix contained 1,546 distinct alignment patterns, with 29.53% of the characters being undetermined or

gaps. Estimated base frequencies were as follows: A = 0.232, C = 0.290, G = 0.228, T = 0.249; substitution rates: AC = 1.093, AG = 3.201, AT = 1.490, CG = 0.800, CT = 4.888, GT = 1.0; gamma distribution shape parameter α = 0.378. Bootstrap support values for maximum likelihood (ML) equal to or greater than 70% and clade credibility values greater than 0.90 from Bayesian inference analysis are labeled at each node. Ex-type strains are in bold, while the new isolates are indicated in red. The tree is rooted to *Biscogniauxia petrensis* (HKAS102388).

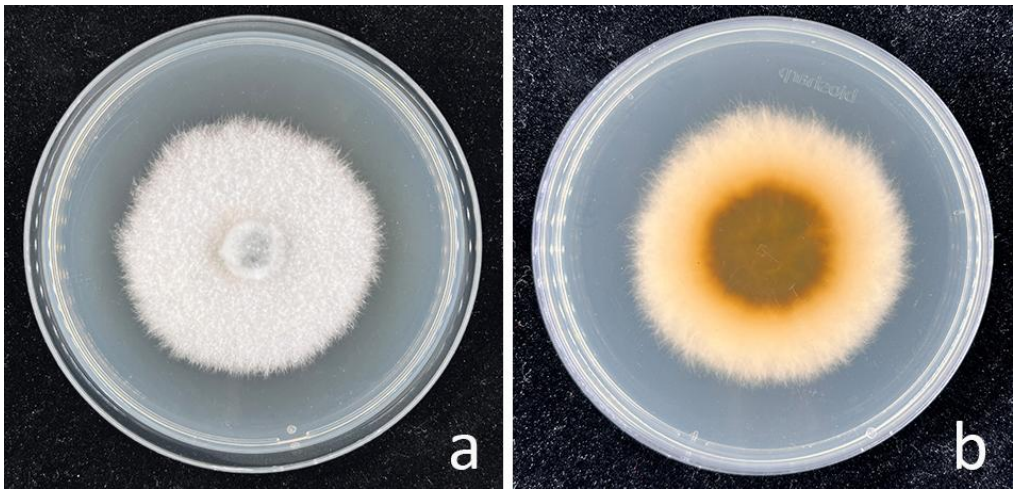


Figure 84 – *Annulohypoxylon hydei* (MHZU 25–1015). a Surface view of a colony on PDA of *Annulohypoxylon hydei*. b Reverse view of colony on PDA of *Annulohypoxylon hydei*.

Microdochiaceae Hern.-Restr., Crous & J.Z. Groenew.

Microdochium Syd. & P. Syd., Annls mycol. 22(3/6): 267 (1924)

Index Fungorum number: IF8926; Facesoffungi number: FoF02121

The genus was established by Sydow (1924), with *M. phragmitis* designated as the type species, which is found on living leaves of *Phragmites australis* in Germany. *Monographella* represents the sexual morph of this genus. Hernández-Restrepo et al. (2016) suggested using *Microdochium* over *Monographella* as *Microdochium* is more commonly used. Currently, 67 accepted species are listed in Index Fungorum (2025). *Microdochium* species are economically significant plant pathogens that impact grasses and cereals globally (Hernández-Restrepo et al. 2016, Wijayawardene et al. 2017, Farr & Rossman 2018, Hyde et al. 2020c, Yang et al. 2023b).

Microdochium guizhouensis Norph. & S.Q. Guo, sp. nov. Fig. 86

Index Fungorum number: IF903754; Facesoffungi number: FoF17769

Etymology – The name refers to the type locality, Guizhou Province, China.

Holotype – HGUP 25–0004

Saprobic on dead wood culms. Sexual morph: Undetermined. Asexual morph: On PDA medium: *Mycelium* immersed and superficial, abundant, branched, septate, thin-walled, hyaline, 2–3 µm wide. *Conidiophores* solitary, lateral, simple, rarely branched, straight, rarely bent, cylindrical, 40–13(–150) × 2.5–3.5 µm, often not clearly differentiated from the mycelium, pale brown. *Conidiogenous cells* solitary, apical, simple, ampulliform, lageniform to cylindrical, straight or bent, thin-walled, hyaline, holoblastic, sympodial to synchronous, 15–17(–40) × 2.5–3.5 µm. *Denticles* up to 8, often along the upper two-thirds of the length of the conidiogenous cell, unthickened, hyaline. *Conidia* dry, fusiform, straight, smooth with thin walls, hyaline, (0–)1-septate, (5–)7.5–10.5(–15) × (2–)2.5–3.5(–4) µm, round apex while the base is pointed and tapers to a distinct scar. Additionally, conidia can be formed directly on the denticles of hyphae.

Culture characteristics – Colonies on PDA restricted, 16–20 mm diam. after 10 days at 25 °C (room temperature), densely felted, convoluted, margin uneven, initially white to light cream. The

reverse side appears white to light gray, mycelium immersed and superficial, abundant, branched, septate, thin-walled, hyaline.

Material examined – China, Guizhou Province, Guiyang City, 8 August 2023, from soil in Chinese cabbage root in the field, S.Q. Guo, A65 (HGUP 25–0004, holotype), ex-types GUCC 25–0012, GUCC 25–0013.

GenBank numbers – GUCC 25–0012: *rpb2* = PV505431, *tub2* = PV505433; GUCC 25–0013: *rpb2* = PV505432, *tub2* = PV505434.

Notes – Phylogenetic analysis (Fig. 85) based on a multi-locus dataset (ITS, LSU, *rpb2*, and *tub2*) revealed that the newly discovered species, *M. guizhouensis*, forms a distinct and well-supported independent clade within *Microdochium*. This lineage is supported by 90% bootstrap value (Fig. 85). The phylogenetic placement indicates a close but distinct relationship to *M. sinense*, *M. nannuoshanense*, *M. phyllosaprophyticum*, and *M. salmonicolor* (Das et al. 2020, Liu et al. 2022, Zhang et al. 2023d). Morphologically, *M. guizhouensis* can be distinguished from its closest relatives by its unique conidiogenous cells, which exhibit longer holoblastic and sympodial proliferation patterns. Additionally, the conidia exhibit specific structural features that further

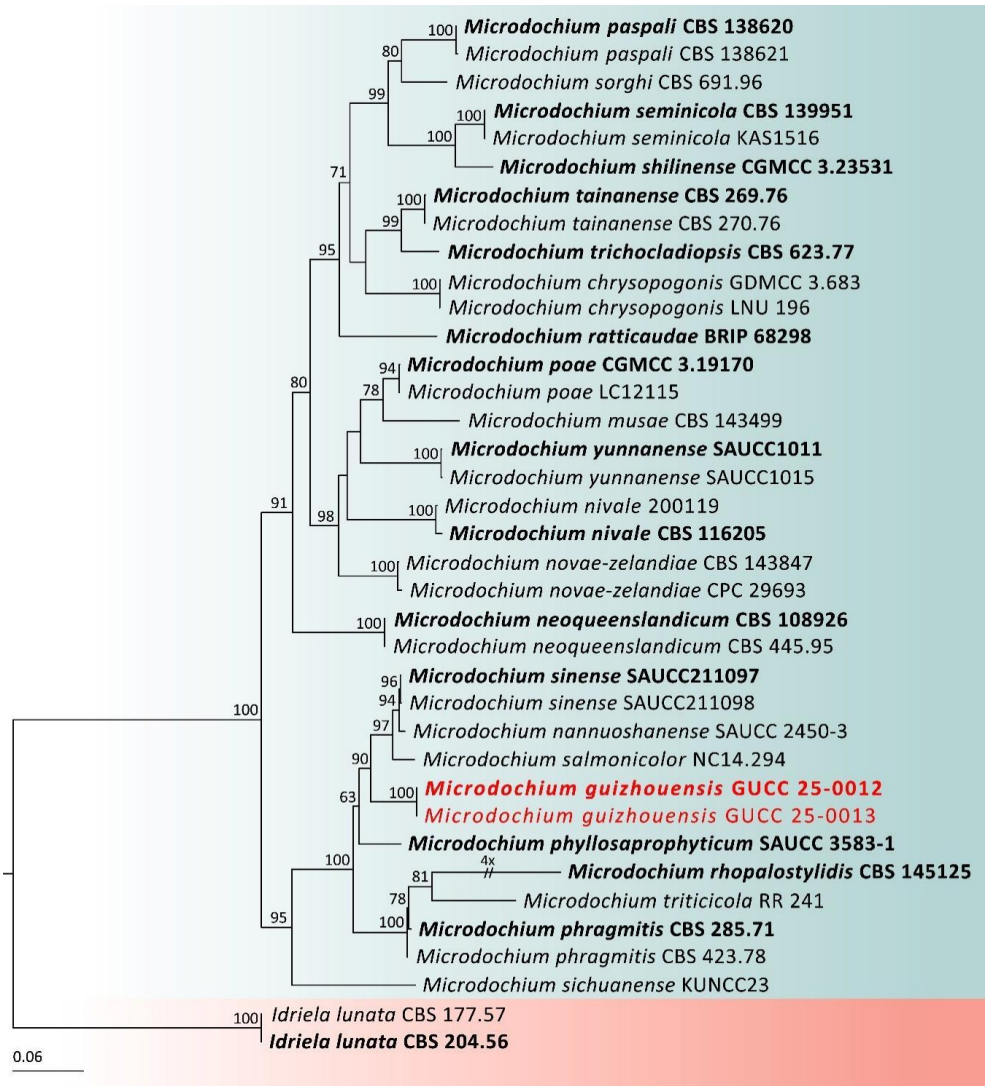


Figure 85 – Phylogram generated from maximum likelihood analysis based on combined ITS, LSU, *rpb2*, and *tub*2 sequence data from 35 strains, comprising 2,788 characters (ITS = 478, LSU = 830 *rpb2* = 839, *tub2* = 641). The best-scoring RAxML tree with a final likelihood value of -14294.011 is presented. Bootstrap support values for maximum likelihood (ML) equal to or greater than 70%

are labeled at each node. Ex-type strains are in bold, while the new isolates are indicated in red. The tree is rooted to *Idriela lunata* (strains CBS 204.56 and CBS 177.57).

differentiate *M. guizhouensis* from related taxa, as summarized in Table 4. The base-pair comparison between *M. guizhouensis* (GUCC 25–0012, type) and *M. phyllosaprophyticum* (SAUCC 3583–1, type) revealed 11.59% differences (96/828 bp, without gaps) in the *rpb2* region, and 3.90% differences (25/641 bp, without gaps) in the *tub2* region. Comparison between *M. guizhouensis* (GUCC 25–0012, type) and *M. nannuoshanense* (SAUCC 2450–3) revealed 11.96% differences (100/836 bp, without gaps) in the *rpb2* region, and 2.96% differences (19/641 bp, without gaps) in the *tub2* region. Similarly, comparison with *M. sinense* (SAUCC211097, type) revealed 11.56% differences (97/839 bp, excluding gaps) in the rpb2 region and 2.50% differences (16/641 bp, excluding gaps) in the *tub2* region. Sequence data for the *rpb2* and *tub2* are currently unavailable for *M. salmonicolor* (NC14.294), and thus could not be included in this comparison. Based on the combination of phylogenetic evidence and morphological characteristics, *M. guizhouensis* is introduced as a novel species.

Table 4. Comparison of morphological characteristics in this study.

Taxa	Conidiogenous cells		Conidia			References
	Character and shape	Size (µm)	Number of septa	Shape	Size (µm)	
M. guizhouensis	Cylindrical, straight or bent, mpulliform, lageniform, holoblastic, sympodial to synchronous solitary	15–17(–40) × 2.5–3.5	(0–)1 septate	Fusiform, straight	(5–)7.5–10.5(–15) × (2–)2.5–3.5(–4)	This study
M. nannuoshanense	Cylindrical, mono- or polyblastic, terminal, denticulate, transparent	19.0–27.0 × 2.0–3.0	aseptate	Spindle to rod-shaped, oblong to ellipsoid, straight or curved	7.0–12.0 × 2.5–4.0	Zhang et al. (2023d)
M. phyllosaprophyticum	Cylindrical and membranous, straight or slightly curved, mono- or polyblastic, terminal, denticulate	16.0–32.0 × 2.0–2.5	(0–)1 septate	Cylindrical, oblong to ellipsoid, spindle to rod-shaped, straight or curved	7.5–15.0 × 2.0–3.5	Zhang et al. (2023d)
M. salmonicolor	Subcylindrical to oval, bent in the center	4.9–8.8 × 2.0–3.2	(0–)1 septate	Fusiform, clavate	8.0–11.3 × 2.4–3.7	Das et al. (2020)
M. sinense	Cylindrical, monoblastic, terminal	16.3–22.4 × 4.1–5.7	1–3-septate	spindle-shaped or cylindrical	11.5–19.34 × 2.8–5.4	Liu et al. (2022)

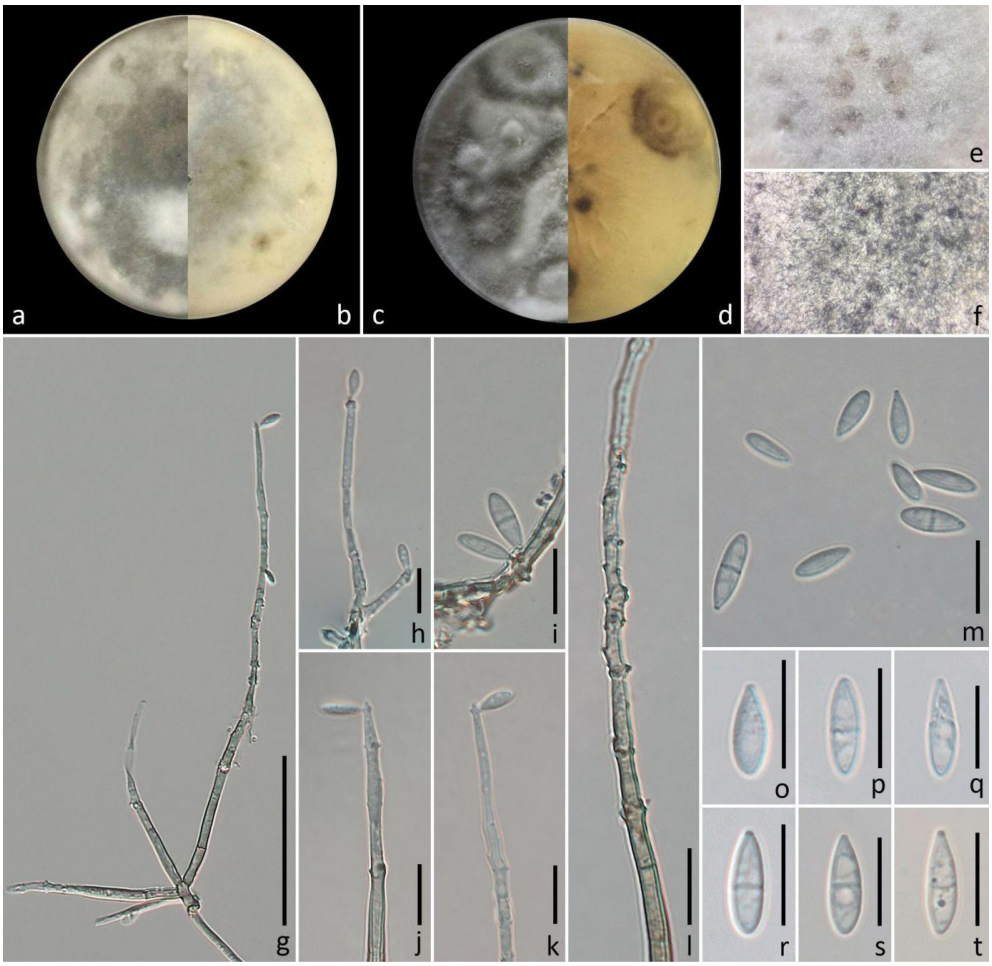


Figure 86 – *Microdochium guizhouensis* (GUCC 25–0012, ex-type). a–b Colonies on PDA at 10 days old (from above and below). c–b Colonies on CMM at 40 days old (from above and below). e Colony on PDA. f Conidiophores on CMM. g–k Conidiophores with conidiogenous cells. l Conidiogenous cells with denticles. m–t Conidia. Scale bars: g = 50 µm, h–t = 10 µm.

Phylum Basidiomycota R.T. Moore
Class Agaricomycetes Doweld
Subclass Agaricomycetidae
Agaricales Underw.
Agaricineae Fr.
Crepidotaceae (S. Imai) Singer
Crepidotus (Fr.) Staude, Schwämme Mitteldeutschl. 1: xxv, 71 (1857)

Index Fungorum number: IF17403; Facesoffungi number: FoF17770

Crepidotus was initially categorized under *Agaricus* but was later elevated to the generic rank by Staude in 1857 (Consiglio et al. 2008, Ge 2017). *Crepidotus* species are primarily found in decaying wood, characterized by small to medium-sized basidiomata with dark-colored basidiospores, and are mostly sessile or have a lateral stipe (Senn-Irlet 1995, Aime 1998, Consiglio et al. 2008, Na et al. 2022). A total of 592 *Crepidotus* records are listed in Index Fungorum (2025), encompassing 502 species (Species Fungorum 2025, accessed 18 January 2025). Since the 21st century, research on *Crepidotus* in Asia has gradually increased, and 34 species have been published, most of which are concentrated in China and India (Han et al. 2024a).

In recognition of Prof. Kevin D. Hyde's outstanding contributions to mycology, we herein introduce *Crepidotus yunnanensis* as a new species. We also provide an updated phylogenetic tree for *Crepidotus* (Fig. 87).

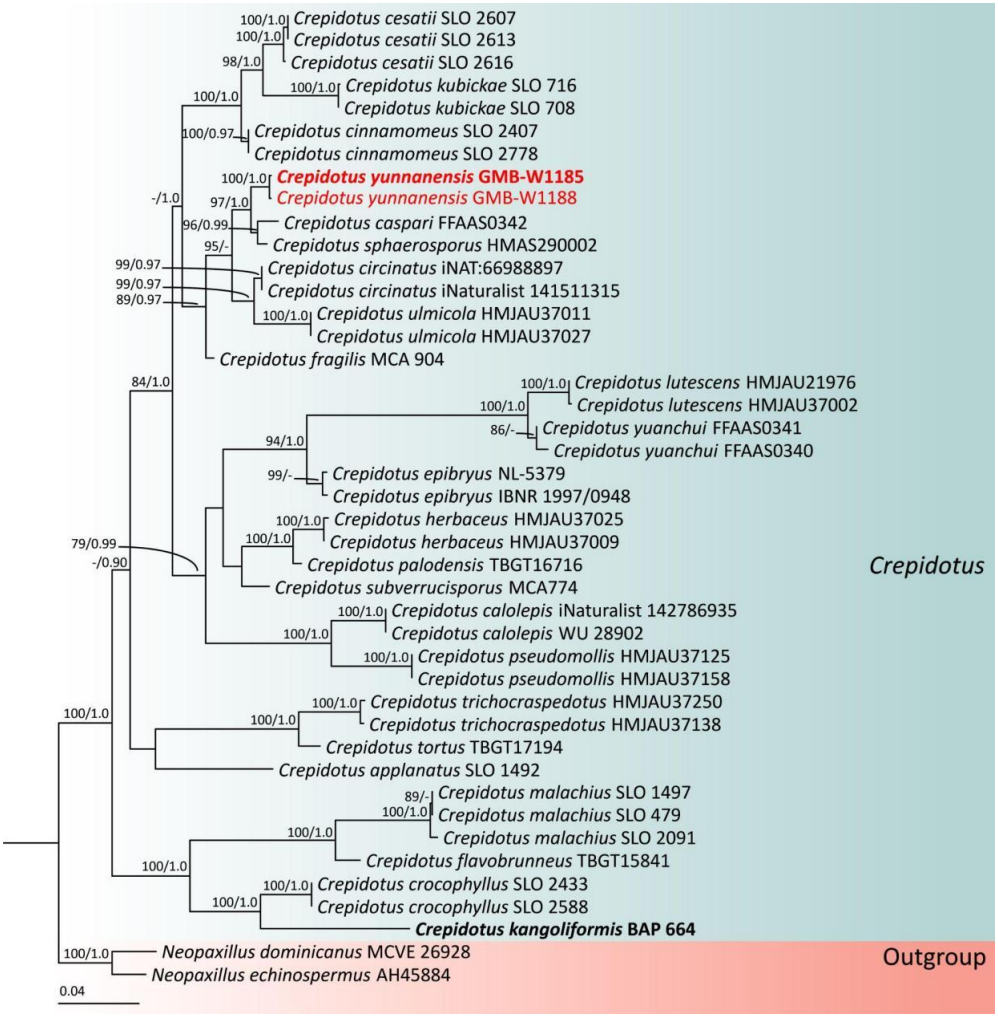


Figure 87 – Phylogram generated from maximum likelihood analysis based on combined ITS and LSU sequence data. Related sequences were obtained from Han et al. (2024a). Forty-three strains are included in the combined sequence analysis, which comprises 1,608 characters with gaps. The best-scoring RAxML tree with a final likelihood value of -13041.784 is presented. The matrix contained 836 distinct alignment patterns, with 36.21% of the characters being undetermined or gaps. Estimated base frequencies were as follows: A = 0.235, C = 0.230, G = 0.292, T = 0.243; substitution rates AC = 1.139, AG = 2.331, AT = 1.464, CG = 0.846, CT = 4.914, GT = 1.0; gamma distribution shape parameter α = 0.270. Bootstrap support values for maximum likelihood (ML) equal to or greater than 70% and clade credibility values greater than 0.90 (rounded to two decimal places) from Bayesian inference analysis are labeled at each node. Ex-type strains are in bold, while the new isolates are indicated in red. The tree is rooted to *Neopaxillus dominicanus* (MCVE26928) and *N. echinospermus* (AH45884).

Crepidotus yunnanensis D.G. Zheng & Karun., sp. nov. Fig. 88

Index Fungorum number: IF903330; Facesoffungi number: FoF17771

Etymology – "yunnanensis" refers to the type locality, "Yunnan Province", China.

Holotype – GMB-W1185

Saprobic on dead wood. Sexual morph: *Basidiomata* small, sessile, laterally attached, the lamellae to golden yellow or yellow ochre (5B7–5C7). *Pileus* 1.2–4.2 mm, in young stage spatuliform, ungulate to conchoid, margin incurved, when matured rounded flabelliform and occasionally irregularly circular, plano-convex, margin gradually straight, initially white to pearl white (C1), parts pale orange or greyish orange (5A3–5B3) when maturity, darker toward the margin, surface with pubescence, fibrillose, wavy, uneven, with tiny squama on the pileus. clear white hyphae near the point of attachment. Taste and odor indistinct. *Basidiospores* 4.8–6.6 × 3.3–

4.8 µ m, Q = 1.28–1.59, Q_m = 1.39 ± 0.21, greenish grey in 5% KOH, moderately thick-walled, finely verrucose, amygdaliform to slightly reniform in the lateral view, ovoid to ellipsoid in the dorsoventral view, sterigmata 1.7–3.3 µm long, thin-walled (<0.5 µm thick), hyaline. *Basidia* 20.5–32.4 × 5.7–10.1 µm, obtuse apex, slightly attenuated in the middle, basal contraction, hyaline, 4-spored, a few 2-spored. *Pleurocystidia* absent. *Cheilocystidia* 24.2–50.4 × 4.4–11.0 µm, clavate to narrowly, clavate, sometimes apex round or subcapitate, not forked, base contracted, flexuous, hyaline, thin-walled (<0.5 µm thick). *Clamp* connections present in all tissues. *Pileipellis* a trichoderm, with a parallel arrangement of cylindrical hyphae 3.0–6.2 µm wide, hyaline, with occasional intersecting, crooked hyphae. *Terminal cells* near pileus centre 3.7–5.8 µ m wide, cylindrical, straight or slightly flexuous, occasionally nodulose, at some places fasciculated, apically tapering; near pileus margin 3.4–5.4 µ m wide, slightly flexuous, often branched, with lateral nodes or coralloid. Asexual morph: Undetermined.

Material examined – China, Yunnan Province, Qujing City, Malong County, on the bark of a fallen decaying branch of an unidentified tree, 25°33′20″ N 103°41′43″ E, elev. 1,973 m, 21 June 2024, D. Zheng, SH41 (GMB-W1185, holotype); *ibid*., on the bark of a fallen decaying branch, 25°25′14″ N 103°29′21″ E, elev. 1,990 m, 21 June 2024, S.C. Karun., QJ342 GMB-W1188, paratype).

GenBank numbers – GMB-W1185: LSU = PQ836321, ITS = PQ809773; GMB-W1188: LSU = PQ836322, ITS = PQ809774.

Notes – In phylogenetic analyses (Fig. 87), our new collection (GMB-W1185 and GMB-W1188) forms a distinct clade and is closely related to the clade containing *Crepidotus caspari* (FFAAS0342) and *C. sphaerosporus* (HMAS290002) with statistical support of 97% ML/1.00 BYPP (Fig. 87). Based on nucleotide comparisons, *C. yunnanensis* (GMB-W1185) differs from *C. caspari* (FFAAS0342) by 3.24% (21/651 bp, without gaps) in the ITS region. Morphologically, *C. yunnanensis* is different from *C. caspari* by irregular pale orange or greyish orange (5A3–5B3) spots appear on the pileus at maturity, smaller basidiospores (4.8–6.6 × 3.3–4.8 µm vs. 6.5–7.6 × 4.6–5.5 µm), and larger basidia (20.5–32.4 × 5.7–10.1 µm vs. 19–25 × 6–8 µm). *Crepidotus yunnanensis* has verrucose, ornamented basidiospores and clamped hyphae, but the basidiospores of *C. caspari* are smooth. Thus, we identified our new collection as *Crepidotus yunnanensis* sp. nov., which should be classified in the *Crepidotus* subg. *Dochmiopus*.

Hydnangiaceae Gäum. & C.W. Dodge

Laccaria Berk. & Broome

Index Fungorum number: IF790443; Facesoffungi number: FoF13868

The genus *Laccaria* is characterized by its basidiospores, which are globose to oblong, echinulate, multinucleate, and exhibit a wide range of colors, including red, orange, brown, white, or purple (Singer 1986, Mueller 1992). The type species, *Laccaria laccata*, was initially described from Slovenia (Europe), and approximately 114 species have been documented worldwide (Tang et al. 2024). These species are recognized for their ability to form ectomycorrhizal associations with a broad range of gymnosperm and angiosperm trees, including those from the families *Betulaceae*, *Fagaceae*, *Myrtaceae*, *Pinaceae*, and *Salicaceae*, thereby playing a crucial role in nutrient cycling and forest health. Morphologically, *Laccaria* species are distinguished by their basidiomata color, basidiospore size and shape, and the number of sterigmata per mature basidia (Tang et al. 2024).

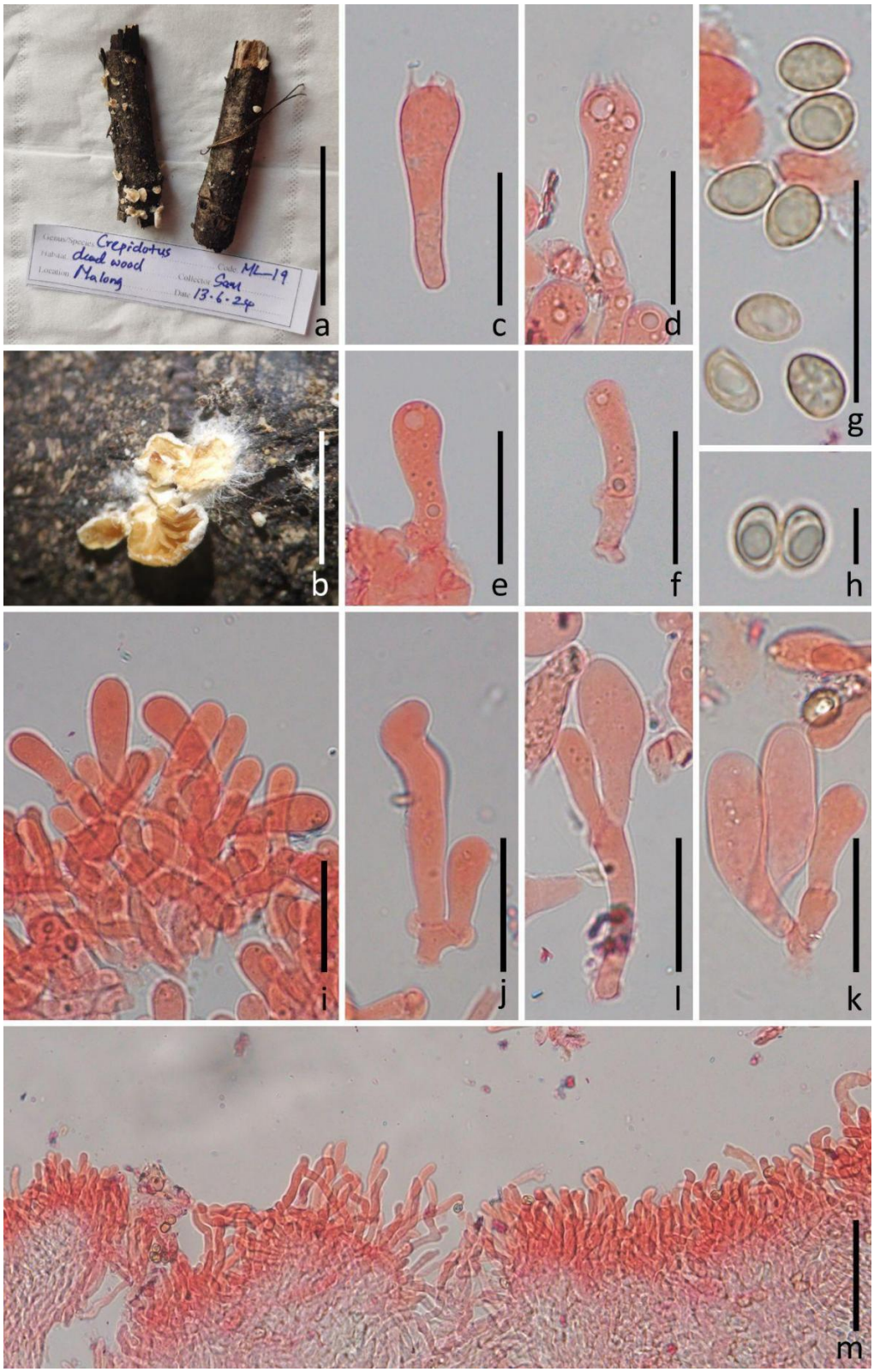


Figure 88 – *Crepidotus yunnanensis* (GMB-W1183, holotype). a Basidiomata on the decaying wood. b Dried basidiomata on the substrate. c–f Basidia. g, h Basidiospores. i–k Cheilocystidia. m Pileipellis. Scale bars: a = 1 cm, b = 20 mm, c–g, i–l = 20 µm, h = 5 µm, m = 50 µm.

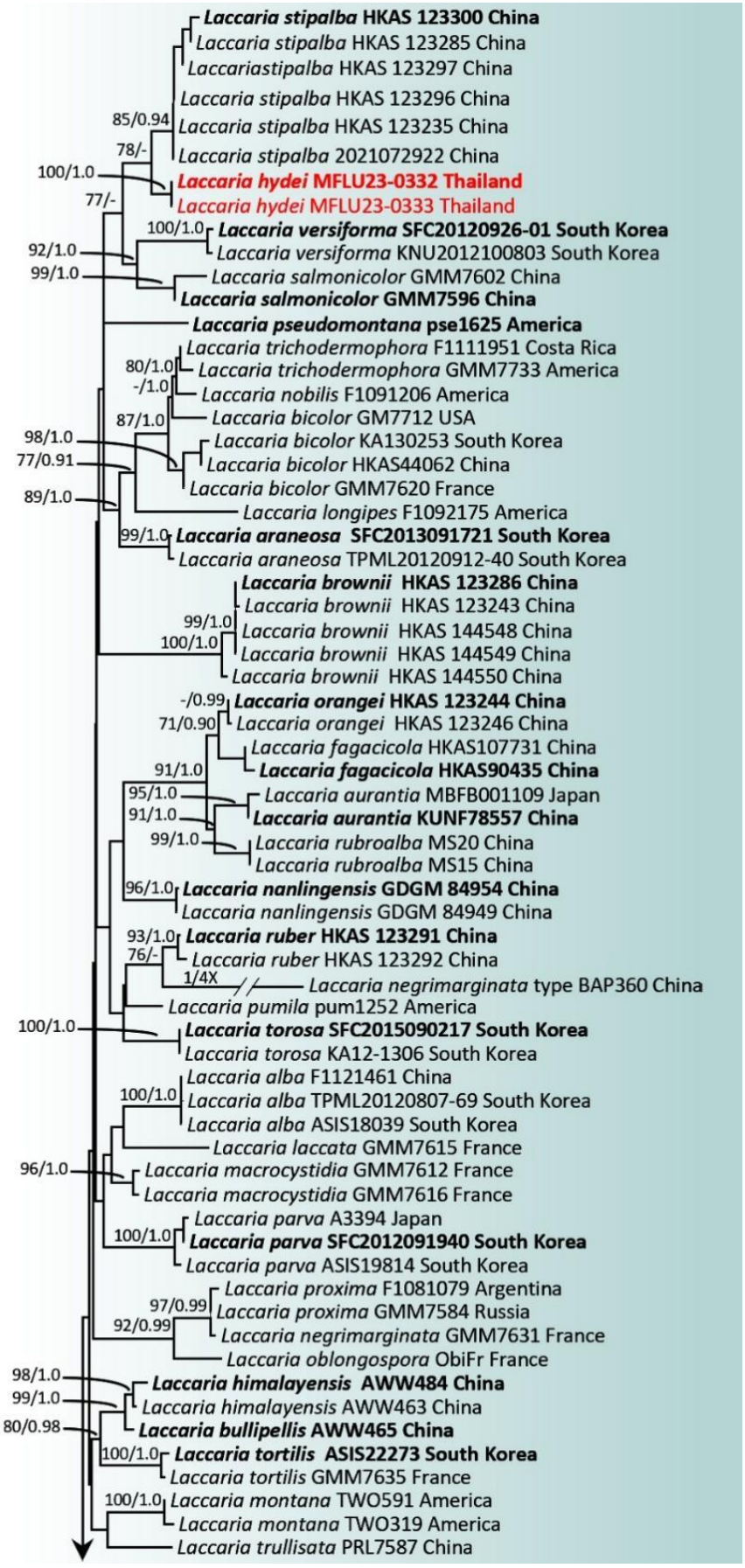


Figure 89 – Phylogram generated from maximum likelihood analysis based on combined ITS, LSU, *rpb2*, and *tef1-α* sequence data from 126 taxa, comprising 2,789 characters (ITS = 640, LSU = 869, *rpb2* = 664, *tef1-α* = 616). The best-scoring RAxML tree with a final likelihood value of -

16173.205 is presented. The matrix contained 1,112 distinct alignment patterns, with 42% of the characters being undetermined or gaps. Estimated base frequencies were as follows: A = 0.257, C = 0.211, G = 0.252, T = 0.279; substitution rates: AC = 1.490, AG = 5.858, AT = 1.561, CG = 0.912, CT = 9.019, GT = 1.0; gamma distribution shape parameter α = 0.242. Bootstrap support values for maximum likelihood (ML) equal to or greater than 70% and clade credibility values greater than 0.90 (rounded to two decimal places) from Bayesian inference analysis are labeled at each node. Type specimens are in bold, while the new isolates are indicated in red. The tree is rooted to *Mythicomyces corneipes* (ES11–10–2–A and AFTOLID972).

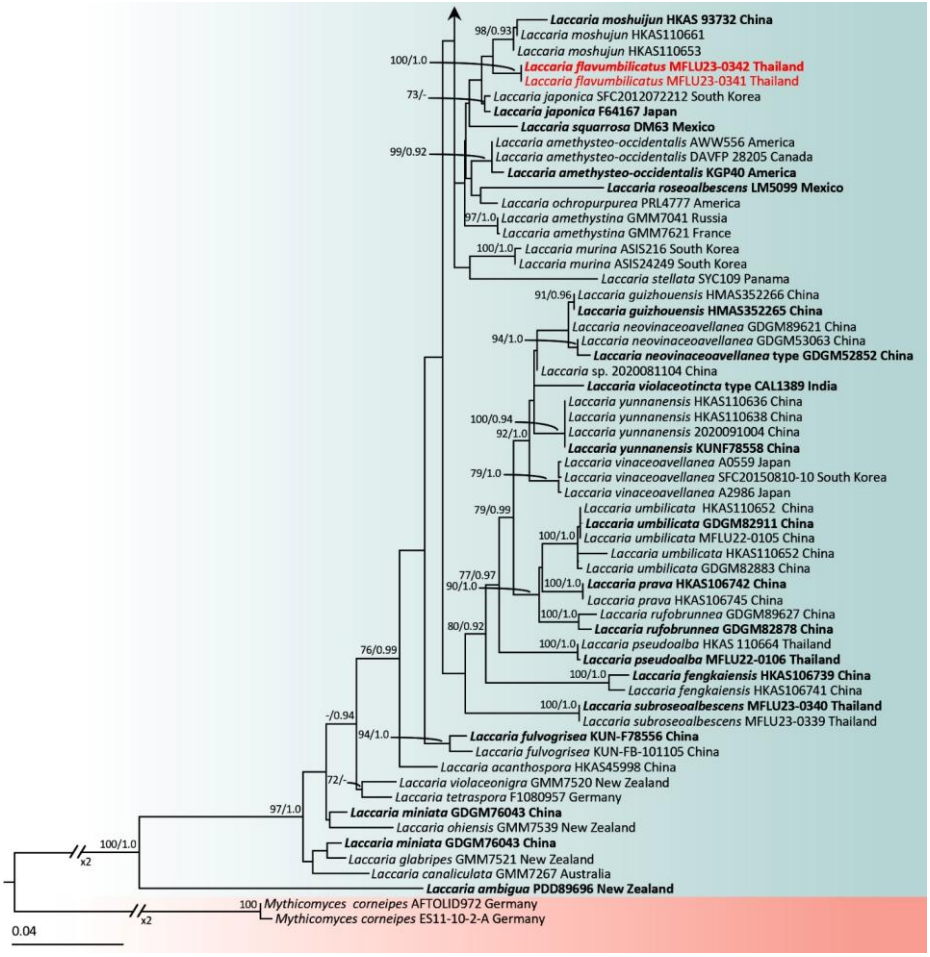


Figure 89 – Continued.

Laccaria hydei S.M. Tang & Z.L. Luo, sp. nov. Figs 90, 91

Index Fungorum number: IF903311; Facesoffungi number: FoF17301

Etymology – 'hydei' named in honor of the renowned mycologist Kevin D. Hyde, recognizing his significant contributions to mycology on the occasion of his 70th birthday.

Holotype – MFLU23–0332

Symbiotic with *Dipterocarpus*. *Basidiomata* small. *Pileus* 9–13 mm in diam., hemispherical, sometime applanate to plano-concave, dark brown (6F8) to brown (6E8) at centre, becomingreddish orange (7A6) with margin, when dry moisture loss of moisture or with age becoming whitish, clearly striate on the surface; depressed or subumbilicate on the center; margin inflexed; context thin, below 1 mm, pale orange (5A2–3), unchanging. *Lamellae* distant, arcuate, adnate with decurrent tooth, pale red (7A3), 2–3 mm in height; lamella edge even or entire, sometimes undate; lamellulae in 2–3 tiers. Stipe 48–62 × 6–7 mm, cylindrical, central, equal with an enlarged base and nearly subclavate, brown (7E8) to dark brown (7F8), smooth; stipe context stuffed, brown (7E8). *Odor and taste* not observed. *Basidia* 34–44 × 8–12 µm, av. 39 ± 4.8 × 11 ± 1.8 µm), clavate, mostly 4–spored, rarely 2–spored, sterigmata 5–8 µm × 2–4

μm, av. 6.8 ± 0.8 × 2.6 ± 0.6 μm*Basidiospores* (excluding ornamentation) [150/3/2] 6.4–10.6 × 6.7–9.4 μm, av. 7.9 ± 0.7 × 7 ± 0.6 μm, Q = 1.00–1.25, Q_m = 1.03 ± 0.09, globose to subglobose, hyaline, echinulate, spines 1–3 μm long, ca. 0.5–1.5 μm wide at the base, crowded. *Cheilocystidia* 25–35 × 6–10 μm, av. 31.2 ± 5.1 × 7.8 ± 1.0 μm, narrowly clavate, thin-walled, colorless and hyaline, abundant. *Pleurocystidia* 38–48 × 7–8 μm, av. 42.6 ± 5.5 × 7.8 ± 1.1 μm, narrowly clavate to subclavate, flexuose or mucronate, thin-walled, hyaline, abundant. *Lamellar trama* 45–51 μm thick, regular, composed of slightly thick-walled, filamentous hyphae 3–7 μm wide. *Lamellar edge* has more in number of sterile basidia. *Subhymenium* 3–6 μm thick, tightly interwoven, fusiform or irregular cells, 4–7 × 3–5 μm, av. 5.7 ± 0.5 × 3.7 ± 0.2. Pileipellis 65–95 μm thick, colourless hyaline in KOH, composed of appressed, parallel, simply septate, thin-walled, cylindrical, filamentous hyphae 8–14 μm wide, colorless and hyaline. *Stipitipellis* composed of appressed, parallel, simply septate, thick-walled, hyphae 2–5 μm wide; stipe trama composed of longitudinally arranged, pastel red in KOH, clavate terminal cells, infrequently branching, septate, thick-walled. *Caulocystidia* not seen. Clamp connections present at some septa in pileipellis, lamellae and stipitipellis.

Material examined – Thailand. Chiang Rai Province, Chiang Saen District, in association with *Dipterocarpus* sp. on the ground, scattered, gregarious, or caespitose, elevation 789 m., 21 August 2020, S. M. Tang, 2020082110 (MFLU23–0332, holotype); *ibid*., elevation 700 m., 22 August 2020, S. M. Tang, 2020082111 (MFLU23–0333).

GenBank numbers – MFLU23–0332: ITS = PV104096; MFLU23–0333: ITS = PV104097.

Notes – Phylogenetically, the new species is closely related to *L. stipalba* (Fig. 89). However, *L. stipalba* differs from *L. hydei* by having a longer and white stipe, dark orange to light grayish pink pileus, and longer sterigmata (6–13 μm; Tang et al. 2025). *Laccaria murina*, *L. anthracina*, and *L. brownii* are similar to *L. hydei* in having a grey to brown pileus. However, *L. murina* has a relatively shorter stipe and only with 2-spored basidia (Imai 1938, Cho et al. 2020). The ITS genetic distances between *L. murina* (ASIS216) and *L. hydei* (MFLU23–0332, holotype) are 3.75% (24/640 bp). *Laccaria anthracina* has relatively larger basidiomata, with pileus sizes ranging from 25 to 65 mm, and a dark surface on the stipe. The base pair differences in ITS region between *L. anthracina* (HMAS 278603) and *L. hydei* (MFLU23–0332, holotype) were 3.44% (22/640) (Wang et al. 2023).

Laccaria flavumbilicatus S.M. Tang & Z.L. Luo, sp. nov. Figs 92, 93

Index Fungorum number: IF903312; Facesoffungi number: FoF17302

Etymology – The epithet “flavumbilicatus” refers to the brownish-orange umbilicate pileus centre.

Holotype – MFLU23–0342.

Symbiotic with *Fagus* and *Dipterocarpus*. *Basidiomata* small. Pileus 13–22 mm in diam., hemispherical when young, becoming plano-convex to convex with age, brownish orange (6C5–6) at the center, light brown (5D6–8) with margin, when dry moisture loss of moisture or with age becoming whitish, clearly striate on the surface; umbilicate centre, brownish orange (6C5–6); margin straight; context thin, 1–2 mm, light brown (5D6–8), unchanging. Lamellae distant, arcuate, adnate with decurrent tooth, deep violet (15D–E8), 2–3 mm in height; lamella edge even or entire, sometimes undate; lamellulae in 3–4 tiers. Stipe 38–57 × 2.7–3.4 mm, cylindrical, central, equal with an enlarged base and nearly subclavate, yellowish white (1A2) to pale yellow (1A3), smooth; stipe context fistulose, yellowish white. Odor and taste not observed. *Basidia* 31–46 × 9–12 μm, (mean length = 37 ± 4.1, mean width = 11 ± 1.0), clavate, mostly 4–spored, rarely 2–spored, sterigmata 4–7 μm × 2–3 μm, (mean length = 6.0 ± 1.22, mean width = 2.4 ± 0.45). Basidiospores (excluding ornamentation) [102/3/2] 7.4–10.3 × 7.0–10.1 μm, (mean length = 8.6 ± 0.74, mean width = 8.6 ± 0.77), Q = 1.00–1.31, Q_m = 1.00 ± 0.09, globose to subglobose, hyaline, echinulate, spines 2–3 μm long, ca. 1–2 μm wide at the base, crowded. Cheilocystidia 14–25 × 4–6 μm, (mean length = 19 ± 3.3, mean width = 5 ± 1.0), narrowly clavate, subclavate, flexuose or mucronate, thin-walled, colorless and hyaline, abundant, not forked. Pleurocystidia absent. Lamellar trama 50–70

μm thick, regular, composed of slightly thick-walled, filamentous hyphae 3–5 μm wide. Subhymenium 11–13 μm thick, tightly interwoven, fusiform or irregular cells, 7–12 × 3–4 μm, (mean length = 9 ± 1.8, mean width = 3.6 ± 0.2). Pileipellis 60–110 μm thick, colorless hyaline in KOH, composed of appressed, parallel, simply septate, thin-walled, cylindrical, filamentous hyphae 2–4 μm wide, colorless and hyaline. Stipitipellis composed of appressed, parallel, simply septate, thick-walled, hyphae 2–5 μm wide; stipe trama composed of longitudinally arranged, colorless in KOH, clavate terminal cells, infrequently branching, septate, thick-walled, hyphae hyaline, 3–5 μm wide. Caulocystidia not seen. Clamp connections present at some septa in pileipellis, lamellae, and stipitipellis.



Figure 90 – *Laccaria hydei.* a–d Basidiomata (a, b MFLU23–0332, holotype; c–d MFLU23–0333). e–f Basidiospores of the SEM. Scale bars: a–d = 1 cm.

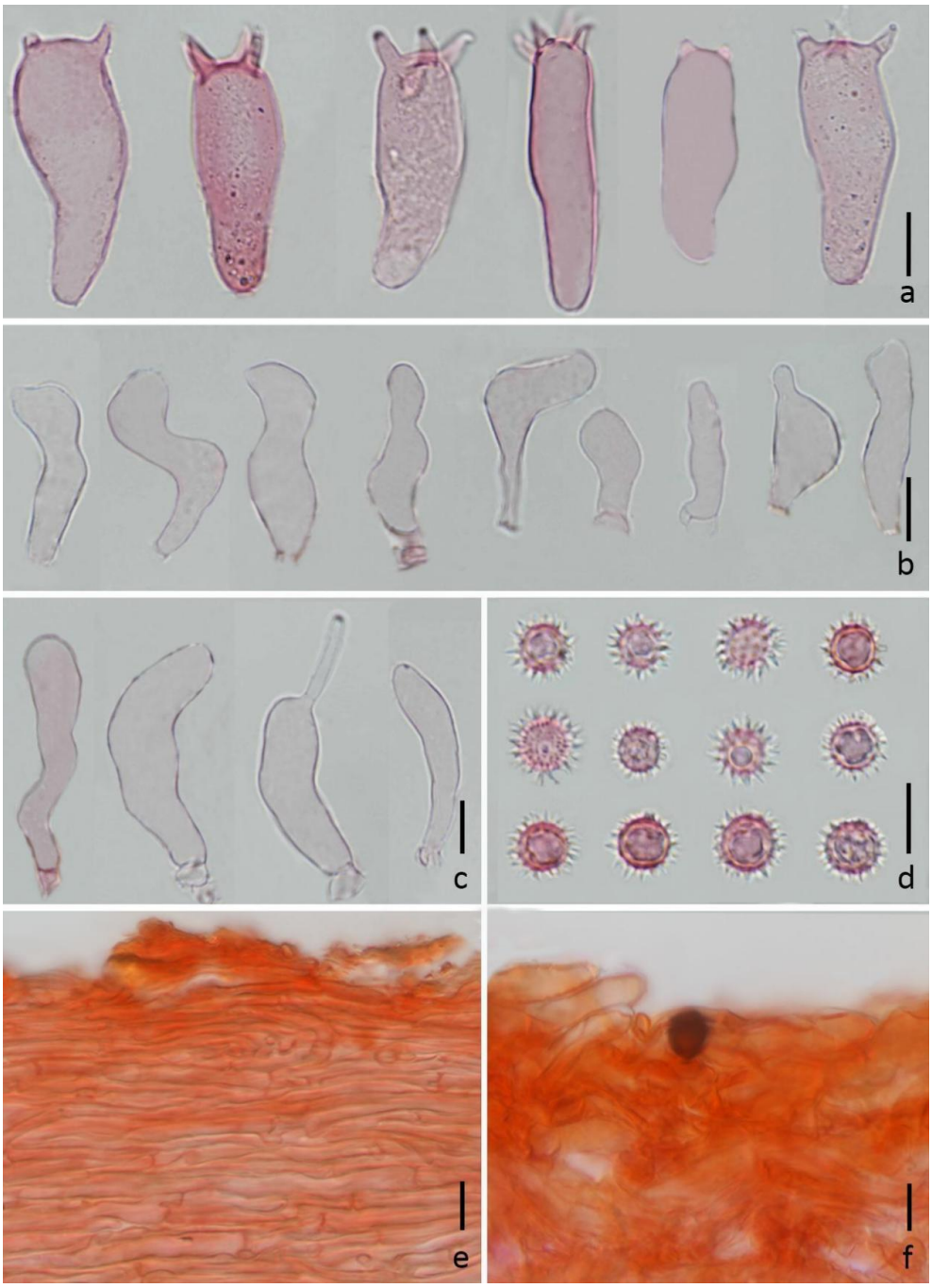


Figure 91 – *Laccaria hydei* (2020082110, MFLU23–0332, holotype). a Basidia. b Cheilocystidia. c Pleurocystidia. d Basidiospores. e Stipitipellis. f Pileipellis. Scale bars: 10 µm.

Material examined – Thailand, Chiang Mai Province, Pa Pae, Mae Taeng District, Thammikarm Monastery, elev. 589 m., symbiotic with *Fagus* and *Dipterocarpus*, 14 July 2020, S. M. Tang, 2020071423 (MFLU23–0342, holotype); *ibid*., elevation 611 m., 14 July 2020, S. M. Tang, 2020071419 (MFLU23–0341).

GenBank numbers – MFLU23–0342: ITS = PV104094, LSU = PV022781, *rpb2* = PV052241; MFLU23–0341: ITS = PV104095, LSU = PV022782, *rpb2* = PV052242.

Notes – Phylogenetically, the new species is closely related to *L. moshuijun* and *L. japonica* (Fig. 89). However, *L. moshuijun* differs from *L. flavumbilicatus* by its convex to plano-convex, violet to bluish pileus, and relatively larger pleurocystidia and cheilocystidia (Vincenot et al. 2017). *Laccaria japonica* has a convex to plano-convex, violet to purple pileus, bright violet lamellae, and cylindrical, clavate to flexuose pleurocystidia and cheilocystidia (Vincenot et al. 2017).

Laccaria amethystina and *L. amethyste-occidetalis* are morphologically similar to *L. flavumbilicatus* in having bluish lamellae. However, *L. amethystina* and *L. amethyste-occidetalis* lack cheilocystidia. ITS sequence difference between *L. amethystina* (GMM7041) and *L. flavumbilicatus* (MFLU23–0342, holotype) is 1.87% (12/640, no gaps) (Wilson et al. 2013); the ITS sequence difference between *L. amethyste-occidetalis* (AWW556) and *L. flavumbilicatus* (MFLU23–0342, holotype) is 2.5% (16/640, no gaps) (Wilson et al. 2017), thus considered them as different species.



Figure 92 – *Laccaria flavumbilicatus*. a–d Basidiomata (a from MFLU23–0342; b from MFLU23–0341; c, d from HKAS 123299). e, f Basidiospores of the SEM. Scale bars: 1 cm.

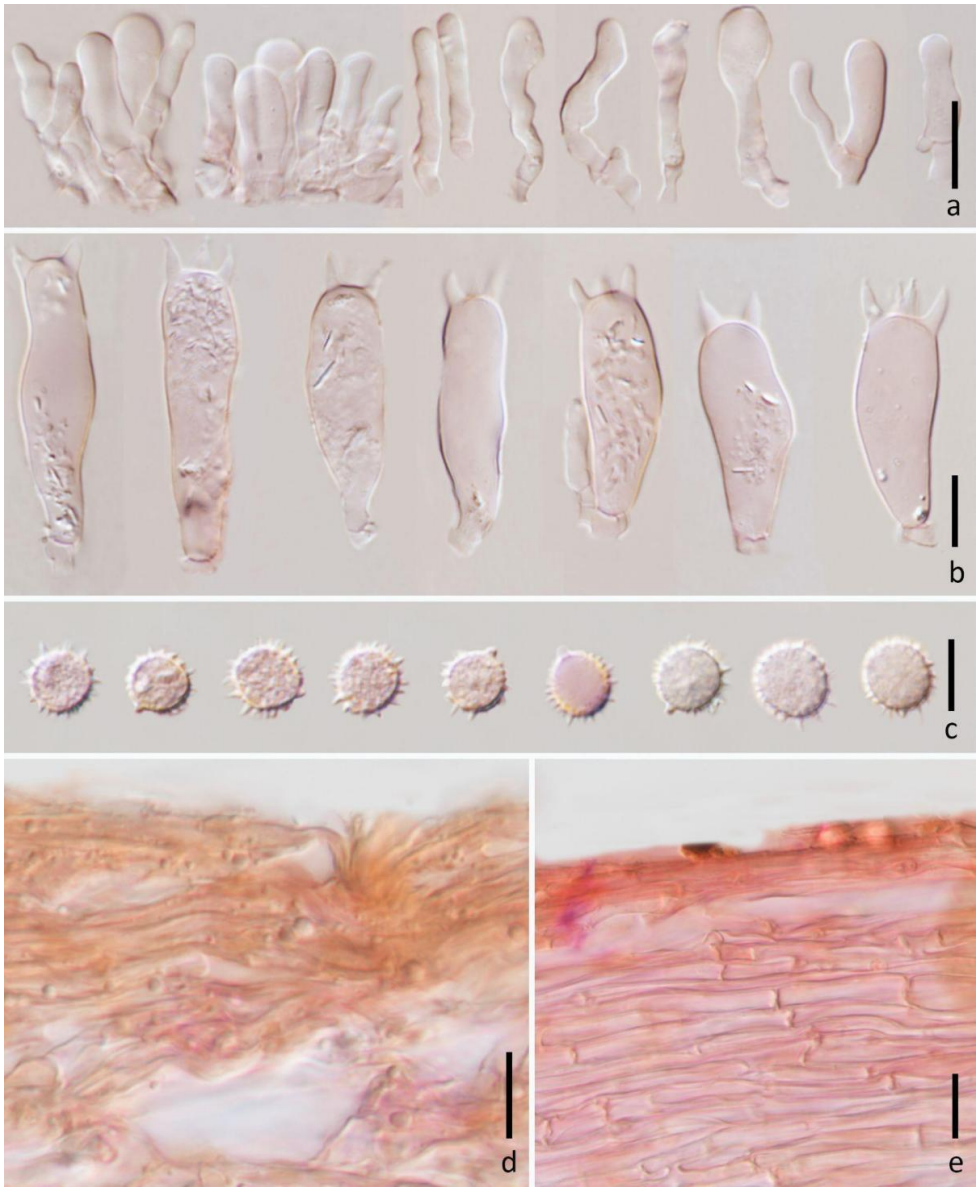


Figure 93 – *Laccaria flavumbilicatus* (MFLU23–0342). a Cheilocystidia. b Basidia. c Basidiospores. d Pileipellis. e Stipitipellis. Scale bars: 10 μm.

Psathyrellaceae Vilgalys, Moncalvo & Redhead

Candolleomyces D. Wächter & A. Melzer, Mycol. Progr. 19(11): 1228 (2020)

Index Fungorum number: IF832256; Facesoffungi number: FoF17772

Candolleomyces was introduced by Wächt & Melzer (2020) and typified with *C. candolleanus*. The genus currently comprises 53 species (Ahmad et al. 2024, Han et al. 2024b, Haqnawaz et al. 2024 a,b, Nayana & Pradeep 2024), and they inhabit terrestrial, or marine environments as lignicolous or rarely fimicolous (Wächter & Melzer 2020, Yang et al. 2023c). This genus is characterized by small to large basidiomata; veil is usually present but often fugacious, fibrillose, scaly, or granulose; spores are medium-sized, pale to medium dark, with a central germ pore; pleurocystidia are absent, and clamp connections are present (Wächter & Melzer 2020, Yang et al. 2023c). The systematic taxonomy of *Candolleomyces* has been significantly advanced in recent years due to molecular biology techniques, particularly the analysis of ITS, LSU, and *tef1-α* loci sequences (Bau & Yan 2021, Yang et al. 2023c, Han et al. 2024b).

Prof. Kevin D. Hyde's team has made contributions to the research of mushrooms, including the genus *Candolleomyces*. One species has been introduced as a result of his team's ongoing study. In recognition of his outstanding contributions to mycology, we introduce the new species,

Candolleomyces aliensis and *C. hydei*. We also provide an updated phylogenetic tree for *Candolleomyces* (Fig. 94).

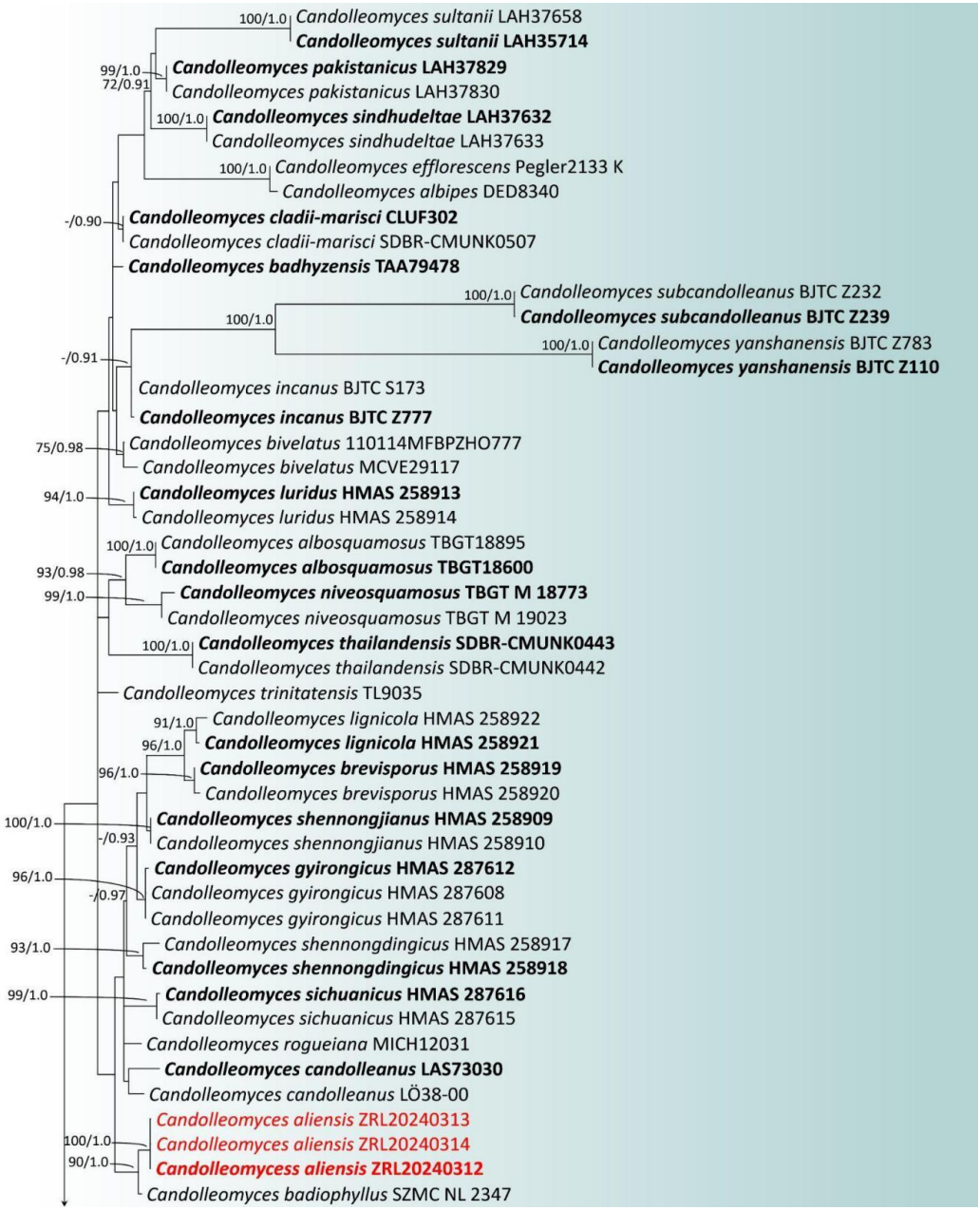


Figure 94 – Phylogram generated from maximum likelihood analysis based on combined ITS, LSU, and *tef-1α* sequence data from 58 taxa, comprising 2,586 characters (ITS = 678, LSU = 884, *tef-1α* = 1024). The best-scoring RAxML tree with a final likelihood value of -12565.995 is presented. The matrix contained 882 distinct alignment patterns, with 33.88% of the characters being undetermined or gaps. Estimated base frequencies were as follows: A = 0.244, C = 0.235, G = 0.262, T = 0.258; substitution rates: AC = 1.046, AG = 1.934, AT = 1.176, CG = 0.585, CT = 4.573, GT = 1.0; gamma distribution shape parameter α = 0.274. Bootstrap support values for maximum likelihood (ML) equal to or greater than 70% and clade credibility values equal to or greater than 0.90 (rounded to two decimal places) from Bayesian inference analysis are labeled at each node. Type specimens are in bold, while the new isolates are indicated in red. The tree is rooted to *Hausknechtia floriformis* (WU22832 and WU22833) and *H. leucosticta* (HFJAU1486 and HFJAU1526).

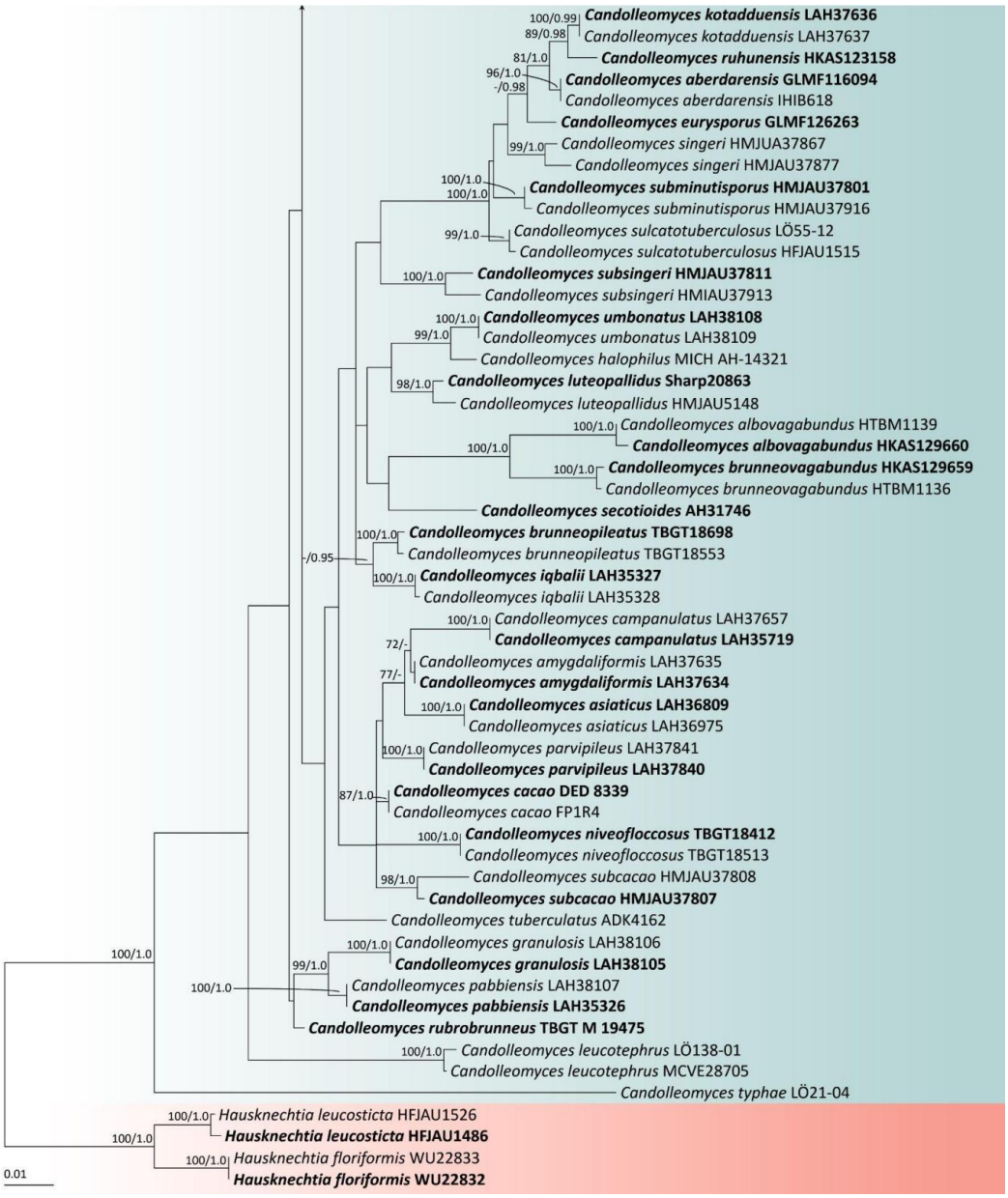


Figure 94 – Continued.

Candolleomyces aliensis R.L. Zhao & X.X. Han, sp. nov. Figs 95, 96

Index Fungorum number: IF572322; Facesoffungi number: FoF17247

Etymology – Refers to the type locality, Ali Region in China.

Under alpine meadow. *Pileus* 0.9–2.6 cm diam., fragile, paraboloid to hemispherical when young, convex to plano-convex when mature, slightly hygrophanous, presence of veil elements, striate up to 1/2 from margin at maturity, brownish orange (5C6) to yellowish brown (5F8) at the center, orange white (5A2) to brownish orange (5C5) at the edge. *Veil* is orange white (5A2), fibrillose, evanescent. *Context* thin and slightly fragile. *Lamellae* moderately crowded, narrowly adnate to adnexed, sometimes adnate with decurrent tooth, white (5A1) to orange grey (5B2) at first, brownish orange (5C4) to yellowish brown (5F8) when mature. *Stipe* 0.9–2.6 × 0.2–0.4(0.5) cm, cylindrical, hollow, slightly swollen at the base, sometimes with a bulb, with a surface covered with slight white fibrils, with slightly longitudinally striate. *Odor* and taste indistinct. *Basidiospores* (6.1)6.9–8.1(8.5) × (3.9)4.2–5.0(5.3) µm, Q = 1.53–1.74, Qm = 1.64 (±0.11), narrowly ellipsoid to oblong, with (0.6)0.8–1.2(1.4) µm germ pore, smooth, contains oil droplets, brownish orange (6C4) to light brown (6D8) in water, brown (6E5) to dark brown (6F8) in 5% KOH. *Basidia* (15.6)16.5–19.4(21.6) × (6.8)7.3–8.1(8.9) µm, clavate, hyaline, sometimes with vacuolar contents, 2 or 4-

spored. *Cheilocystidia* (24.2)26.2–31.3(34.2) × (8.5)9.4–11.3(12.3) μm, utriform to broadly utriform, claviform, rarely pyriform. *Pileipellis* a 2–3 layered irregular epithelium composed of subglobose cells, oval, (13.9)17.6–29.1(37.3) μm broad. *Trama of gills* subregularly. *Pleurocystidia* absent.

Material examined – CHINA. Xizang Autonomous Region, Ali Region, Zhada County, 565 National Road, nearby Geru Cave under alpine meadow, N 31°28′43″ E 79°40′54″, 3605 m asl, 5 August 2024, Xi-Xi Han, Lin-Hui Liu ZRL20240312 (HMAS 287998, holotype); Xizang Autonomous Region, Ali Region, Zhada County, 565 National Road, nearby Geru Cave under alpine meadow, N 31°28′43″ E 79°40′54″, 3605 m asl, 5 August 2024, Xi-Xi Han, Lin-Hui Liu ZRL20240313 (HMAS 287999); Xizang Autonomous Region, Ali Region, Zhada County, 565 National Road, nearby Geru Cave under alpine meadow, N 31°28′43″ E 79°40′54″, 3605 m asl, 5 August 2024, Xi-Xi Han, Lin-Hui Liu ZRL20240314 (HMAS 288000).

GenBank numbers – ZRL20240312: ITS = PQ862365, LSU = PQ862368, *tef1-α* = PQ857801; ZRL20240313: ITS = PQ862363, LSU = PQ862366, *tef1-α* = PQ857802; ZRL20240314: ITS = PQ862364, LSU = PQ862367, *tef1-α* = PQ857803.

Notes – Phylogenetically, *C. aliensis* is closely related to *C. badiophyllus*, the latter having synonyms such as *Psathyrella badiophylla var. neglecta* and *P. badiophylla*. *Psathyrella badiophylla var. badiophylla* can be distinguished by its longer and narrower stipe, measuring 22–50 × 0.7–1.2 mm, and tobacco-brown lamellae with a reddish hue; it also features larger spores (11.5–15.5 × 6.5–7.5 μm) (Kits van Waveren 1985). In contrast, *P. badiophylla var. neglecta* has a longer and narrower stipe (30–40 × 1.2–2 mm), dark tobacco-brown lamellae, and larger spores (10–11.5 × 5.5–6.5 μm) (Kits van Waveren 1985). The sequence divergence between *C. aliensis* and *C. badiophyllus* (SZMC-NL-2347) further supports their status as distinct species, with 1.37% differences (8/582 bp, including gaps) in the ITS region, and 0.52% (4/762 bp, including gaps) in the LSU region.

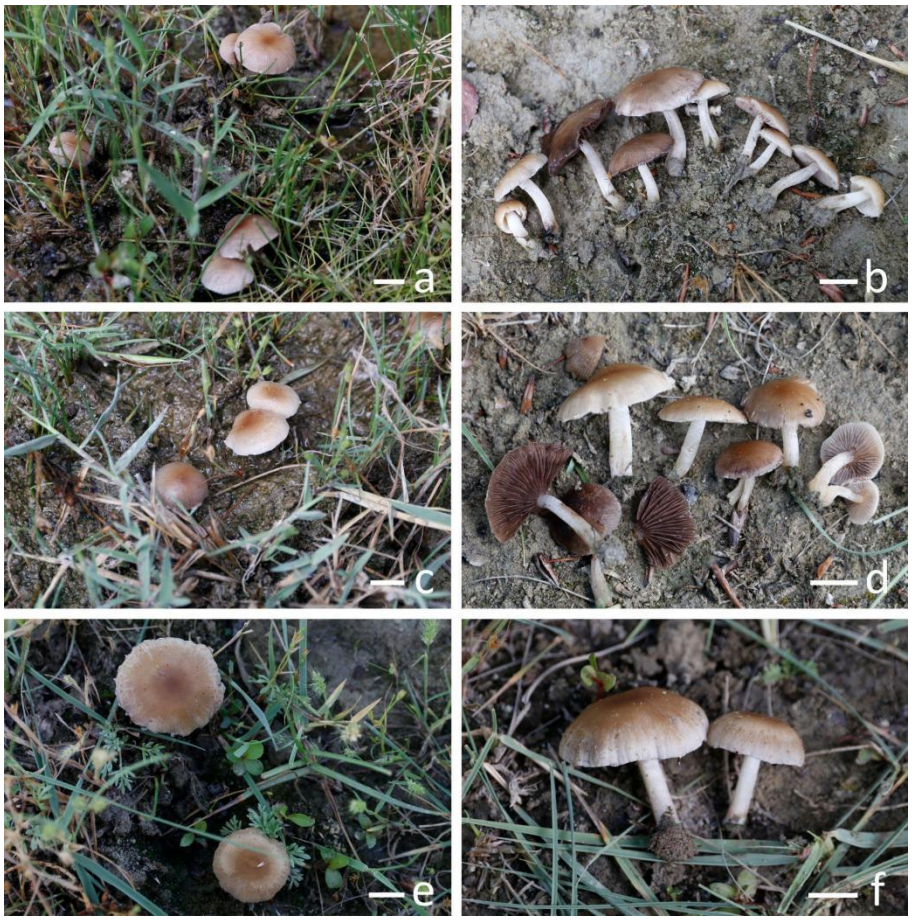


Figure 95 – Basidiomata of *Candolleomyces aliensis* in the field. a, b ZRL20240312 (holotype). c, d ZRL20240313. e, f 20240314. Scale bars: a–f = 10 mm.

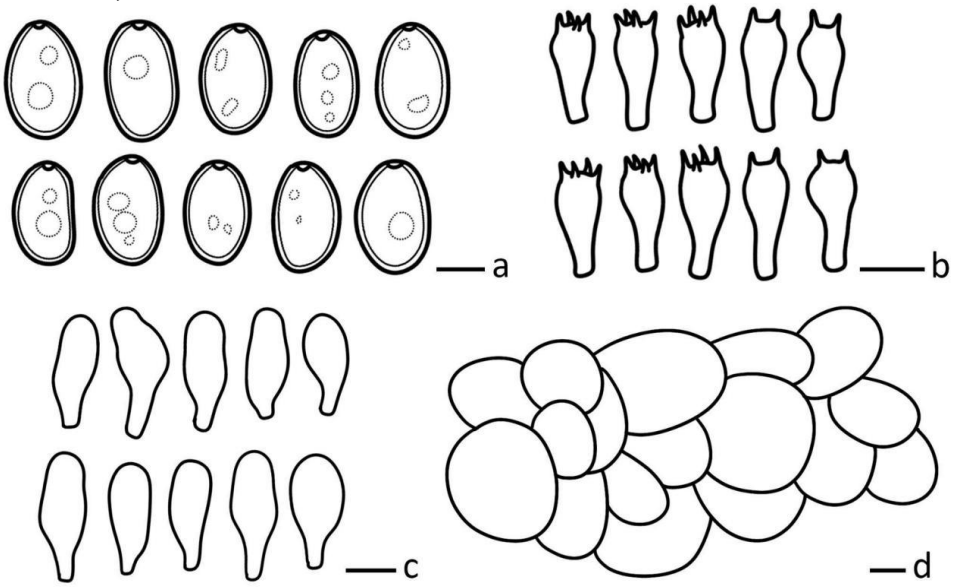


Figure 96 – Microscopic features of *Candolleomyces aliensis*. a Basidiospores. b Basidia. c Cheilocystidia. d Pileipellis. Scale bars: a = 5 mm, b–d = 10 µm.

Candolleomyces hydei W.H. Lu, Karun. & Tibpromma, sp. nov. Fig. 98

Facesoffungi number: FoF17773; MycoBank number: MB857487

Etymology – 'hydei' named in honor of the renowned mycologist Kevin D. Hyde, recognizing his significant contributions to mycology on the occasion of his 70th birthday.

Holotype – GMB-W1196

On a decaying bamboo under broadleaf mingled forest. *Basidiomata* medium. *Pileus* 10–20 mm diam., paraboloid to hemispherical when young, broadly convex to broadly convex, campanulate to the plane, and irregular, striate margins, smooth surface, orange white (5A2), pale orange (6A2), and carrot red (6B7) in the center. *Context* thin and fragile. *Lamellae* adnate to nearly free, 1–3 tiers of lamellulae, milk white to white (1A1–2), up to 2 mm wide. *Stipe* 40–80 × 1–4 mm, central, hyaline, or white (1A1), hollow, slightly flexuous, hygrophanous, tomentose at the base with longitudinal striation, annulus absent. *Odor and taste* not determined. *Basidiospores* (8.7–)9–11.5(–11.8) × 5.5–7.5(–7.8) µm, Q = 1.4–1.89, Qm = 1.61, ellipsoid to broadly ellipsoid, or subfusiform, guttulate, thick-walled, smooth, with spores exhibiting visible germ pore, light brown, greenish to yellow guttule in 1% KOH. *Basidia* (18–)20–30(–35) × (7–)8–9(–10) µm, clavate, hyaline to light yellowish brown in 1% KOH, thick-walled, smooth, and 2 or 4-spored. *Cheilocystidia* 25–40(–56) × (13–)15–18 µm, utriform, ovoid, hyaline in 1% KOH. *Pleurocystidia and Caulocystidia* absent. *Pileipellis* subglobose cells 30–41× 21–30 µm diameter, subglobose and ellipsoid, hyaline in 1% KOH. *Stipitipellis* a cutis, hyphae, septate, hyaline in 1% KOH. *Clamp connection* absent.

Material examined – China, Yunnan Province, Pu'er City, Jingdong Yi Autonomous County, 24°32'32"N 101°01'47"E, elev. 2500 m, on a decaying bamboo under broadleaf mingled forest, 30 July 2024, Wenhua Lu & Samantha C. Karunarathna, LWH165 (GMB-W1196, holotype), *ibid*., on the soil, LWH186 (GMB-W1197, isotype).

GenBank numbers – GMB-W1196: ITS = PV434833, LSU = PV434835; GMB-W1197: ITS = PV434834, LSU = PV434836.

Known distribution – Gregarious, found in bamboo wood and soil of mixed broad-leaved forests. So far, it is only known from the Yunnan Province, southwest China.

Notes – *Candolleomyces hydei* is morphologically similar to *C. candolleanus*, and *C. albosquamosus*. However, *C. albosquamosus* differs from *C. hydei* by having a larger, minute

floccose pileus, smaller basidiospores (6.0–6.4 × 3.6–4.0 µm), and basidia (14–20 × 6.0–7.2 µm),

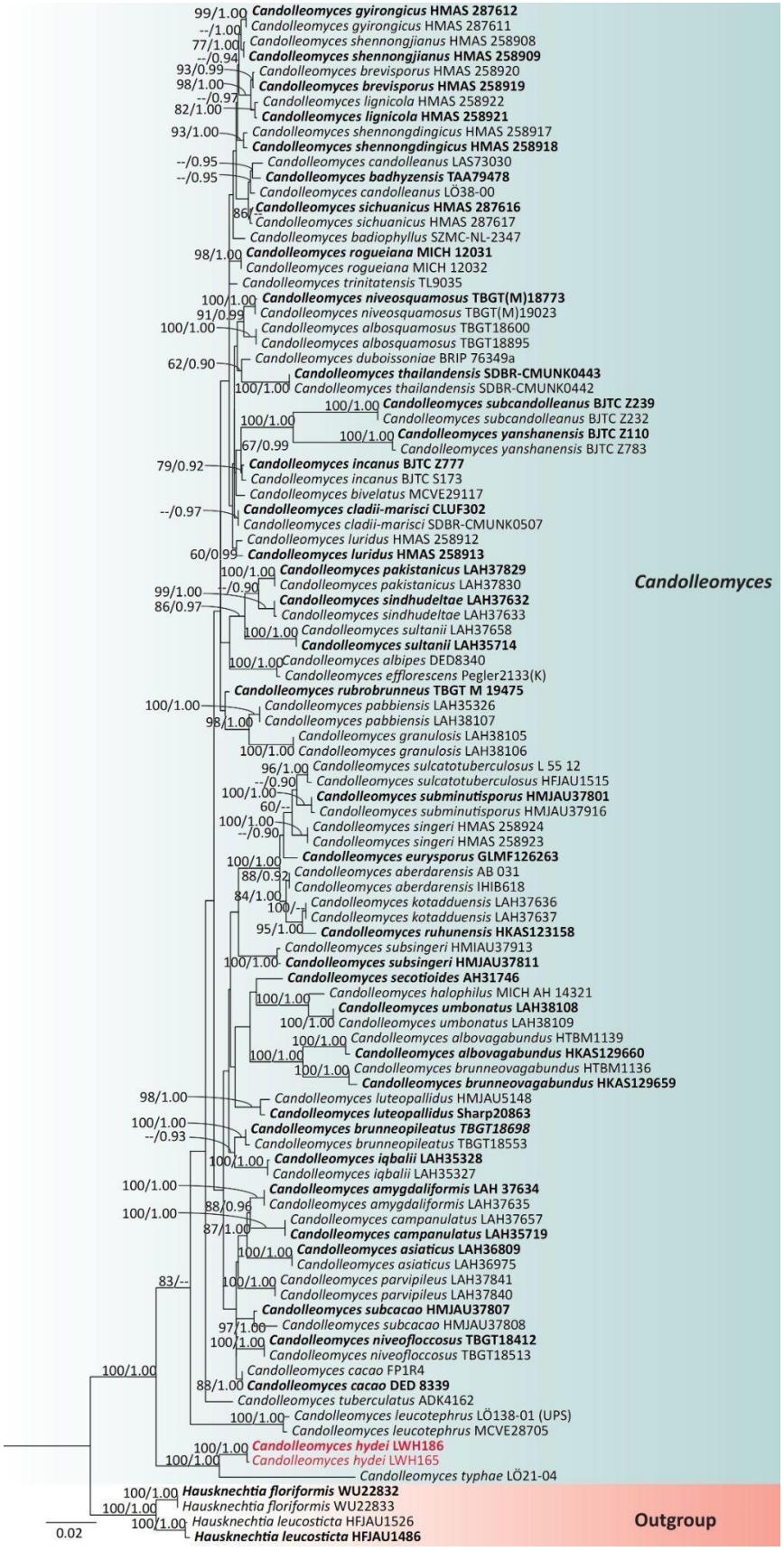


Figure 97 – Phylogram generated from maximum likelihood analysis based on combined ITS and LSU sequence data from 108 taxa, comprising 1,945 characters (ITS = 624, LSU = 1,321). The best-scoring RAxML tree with a final likelihood value of -13688.984 is presented. The matrix

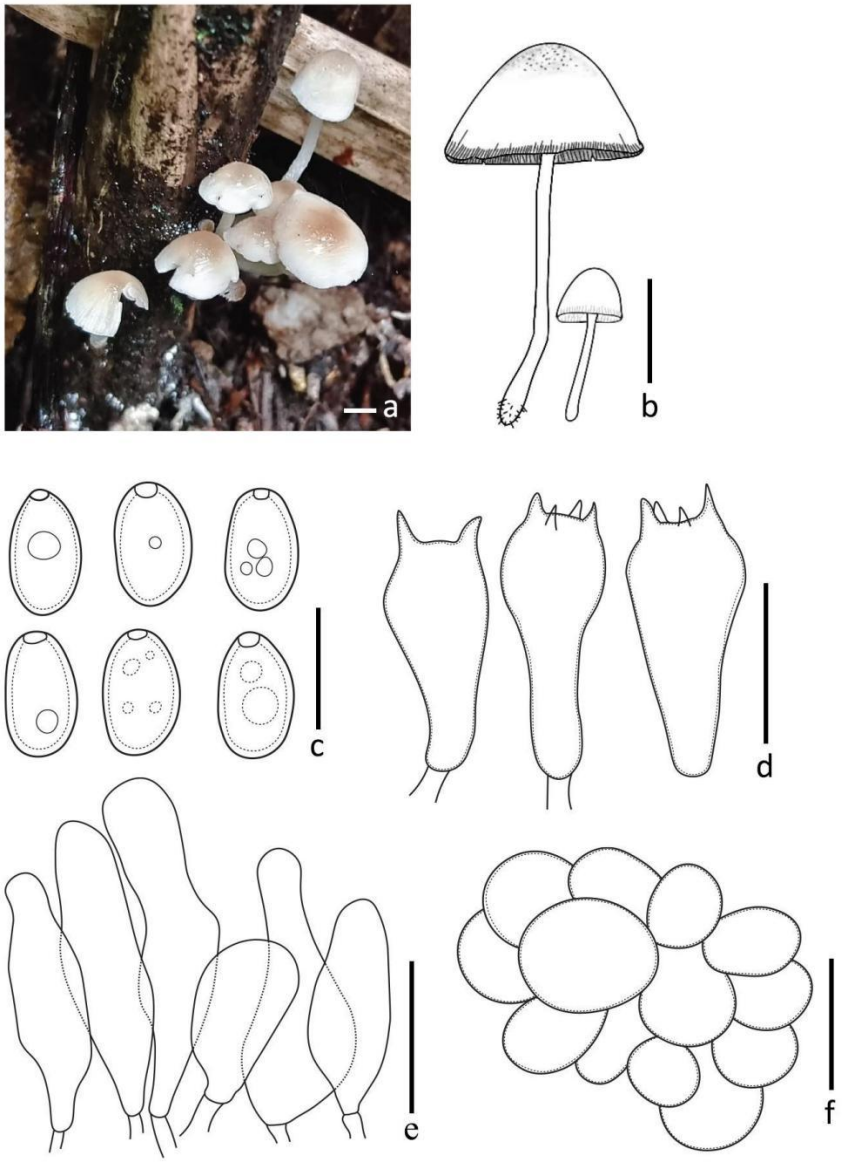


Figure 98 – *Candolleomyces hydei* (GMB-W1196, holotype). a, b Basidiomata. c Basidiospores. d Basidia. e Cheilocystidia. f Pileipellis. Scale bars: a, b = 1 cm, c = 10 µm, d–f = 20 µm

and clamp connections present in all tissues (Nayana & Pradeep 2023). *Candolleomyces candolleanus* can be distinguished as follows: difference in macroscopic morphology of basidiomata, larger pileus, smaller, elliptical purple-brown basidiospores (6.5–8 × 4–5 µm), and subcylindric, clavate, or saccate Cheilocystidia (Mifsud 2017, Wächter & Melzer 2020). According to the multigene (ITS and LSU) phylogenetic analyses (Fig. 97), *C. hydei* belongs to *Candolleomyces* and has a close phylogenetic relationship with *C. typhae* (BP 100% /1.00 PP). They form a well-supported clade cluster with other *Candolleomyces* species (BP 100% /1.00 PP) in the phylogenetic tree. In addition, the ITS sequence difference between *C. hydei* (GMB-W1196) and *C. typhae* (LÖ21–04) is 9.5% (57/599, including gaps), supporting the recognition of *C. hydei* as a distinct species. Therefore, we introduce *C. hydei* as a new species based on both morphological characteristics and, phylogenetic analyses, contained 855 distinct alignment patterns, with 36.6% of the characters being undetermined or gaps. Estimated base frequencies were as follows: A = 0.246, C = 0.232, G = 0.264, T = 0.256; substitution rates: AC = 0.960, AG = 1.852, AT = 1.201, CG = 0.705, CT = 4.544, GT = 1.0; gamma distribution shape parameter α = 0.247. Bootstrap support values for maximum likelihood (ML) equal to or greater than 60% and clade credibility values greater than 0.90 (rounded to two decimal places) from Bayesian inference

analysis are labeled at each node. Type specimens are in bold, while newly generated taxa are indicated in red. The tree is rooted to *Hausknechtia floriformis* and *H. leucosticta*.

Agaricales families *incertae sedis*

Mycenaceae Overeem

Favolaschia (Pat.) Pat., in Patouillard & Lagerheim, Bull. Soc. mycol. Fr. 8(3): 116 (1892)

Index Fungorum number: IF17578; Facesoffungi number: FoF17245

Favolaschia was established by Patouillard & Lagerheim (1892), with *F. gaillardia* as the type species (Patouillard & Lagerheim 1892). *Favolaschia* was first described in *Laschia* (= *Campanella*) (Patouillard & Lagerheim 1892). This genus is characterized by gelatinous basidiomata, poroid hymenium, a monomitic hyphal system, and the presence of gloeocystidia and acanthocystidia, which are terminal, mostly swollen hyphal tips covered with outgrowths and amyloid basidiospores (Patouillard 1900b, Singer 1945, 1974, Clémençon 1977, Gillen et al. 2012, Capelari et al. 2013, Magnago et al. 2013, Zhang & Dai 2021, Zhang et al. 2023e, 2024d). Species of *Favolaschia* are globally distributed, mainly in subtropical and tropical regions (Gillen et al. 2012, Magnago et al. 2013, Zhang et al. 2024d). This genus is mainly found in decaying parts of monocotyledonous plants and ferns (Singer 1974, Gillen et al. 2012, Zhang et al. 2024d). A total of 163 records representing 61 species (Zhang et al. 2024d, Lu et al. 2025) of *Favolaschia* are listed in Index Fungorum (http://www.indexfungorum.org; accessed on 26 May 2025). An updated phylogeny for the genus is provided in Fig. 99.

Favolaschia variistipitata W.H. Lu, Tibpromma & Karun., Phytotaxa 694(2): 148 (2025)

Fig. 100

Index Fungorum number: IF856190; Facesoffungi number: FoF17246

On decaying bamboo in a mixed deciduous forest. Basidiomata annual, gregarious, and gelatinous when fresh, becoming dry. Pilei 5−8 × 3.5−8 mm, pileal surface whitish then greyish (3B3) when fresh, turning greyish (4C4) to dirty brownish (5D4) upon drying, convex, reticulate pattern distinct matching the pores below, glabrous; margin straight, crenulated; context up to 32.1 µm, with translucent. Hymenophore concolourous with pileal surface, poroid, 60−125 pores per basidiomata; mature pores 0.5−0.9 mm diam., polygonal, size varies irregularly, larger near the base and smaller near the edge, the margin pores often incomplete; tubes up to 1.4 mm long. Stipe 1.7−3 × 1−2.2 mm, concolourous with pilei, surface gelatinous. Basidiospores 7.8−12.5 × 5.1−8.4 µm, L = 10.63 µm, W = 6.75 µm, Q = 1.49−1.54 (n = 50/3), broadly ellipsoid to subglobose hyaline, thin-walled, smooth, with one or two guttules. Basidia 40−52 × 10−13 µm, narrowly clavate with some guttles, tapered towards the base, apex broadly rounded, 2 or 4-spored, sterigmata 3.6−8 × 2.1−2.9 µm long; basidioles similar in shape to the basidia, but slightly smaller. Acanthocystidia and gloeocystidia absent. Cheilocystidia 13−20 × 4−5 µm, thin-walled, present at the dissepiment edge, irregular with small diverticulate projections on the side of the apex. Pileipellis hyphae interwoven, occasionally with some small diverticulate projections, smooth, thin-walled, 2.4−4.8 µm diam. Tramal hyphae 2.3−5.4 µm diam., thin-walled, interwoven, widely spaced in a thick gelatinous matrix, frequently branched. *Stipe hyphae* 2−6 µm, subparallel along the stipe, and some parts swollen. *Clamp connections* present in all tissues.

Culture characteristics − Colonies on PDA occurred after incubation for 5 days, reaching 7.5 cm diam., after incubating at 25°C for 20 days, from above white radiating outwards, thin, irregular, flattened with smooth surface; reverse white.

Material examined − Thailand, Chiang Rai Province, Muang, 400 m, 19°56' 27" N, 99°40'23" E, 12 May 2023, on decaying bamboo in a mixed deciduous forest, S. Khyaju, SK150 (MFLU25–0024), living culture MFLUCC 25–0026.

GenBank numbers − ITS = PQ897959, LSU = PQ899253.

Notes – Phylogenetically, our sample (MFLUCC 25–0026) forms a lineage winthin *Favolaschia variistipitata* clade (GMB1061, GMB1062, and ARFR200 Rakhe), with a strong support (99% ML, 1.00 BYPP, Fig. 99). Morphologically, our sample shares common macro- and micro-characteristics with the holotype of *F. variistipitata* (GMB1061) (Lu et al. 2025). However,

the basidiospore of our sample is slightly larger (7.8−12.5 × 5.1−8.4 µm) compared to the holotype (5–8.7 × 3.5–6.5 µm). Similarly, the basidia are also larger (40−52 × 10−13 µm) than those of the holotype (21–29 × 7–9.5 µm). Our sample exhibited 2- or 4-spored basidia, differing from the holotypic description with only 2-spored basidia. Notably, the gloeocystidia are absent in our studied sample, which is described in the holotype. Based on phylogenetic analyses (Fig. 99) and overlapping morphological characteristics, we identified our sample as *F. variistipitata.* This represents a new geographical record for Thailand.

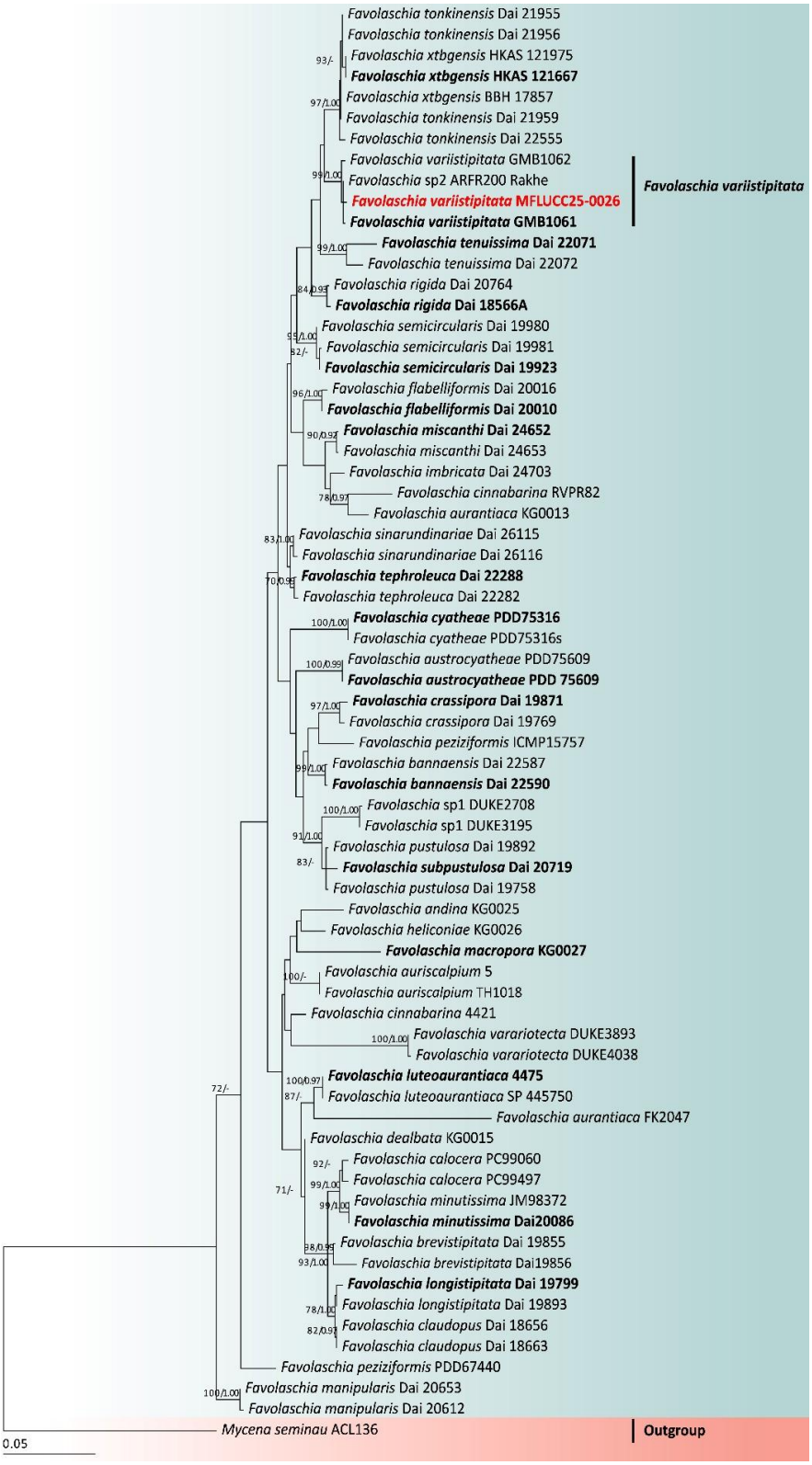


Figure 99 – Phylogram generated from maximum likelihood analysis based on combined ITS and LSU sequence data from 69 taxa, comprising 1,508 characters (ITS = 599, LSU = 909). The best-scoring RAxML tree with a final likelihood value of -6668.926 is presented. The matrix contained 476 distinct alignment patterns, with 26.77% of the characters being undetermined or gaps. Estimated base frequencies were as follows: A = 0.243, C = 0.208, G = 0.266, T = 0.282; substitution rates: AC = 1.191, AG = 2.959, AT = 1.551, CG = 0.731, CT = 5.570, GT = 1.0; gamma distribution shape parameter α = 0.219. Bootstrap support values for maximum likelihood (ML) equal to or greater than 70% and clade credibility values greater than 0.90 (rounded to two decimal places) from Bayesian inference analysis are labelled at each node. The newly generated sequence is in red bold. The tree is rooted to *Mycena seminau* (ACL136) (Zhang et al. 2024d).

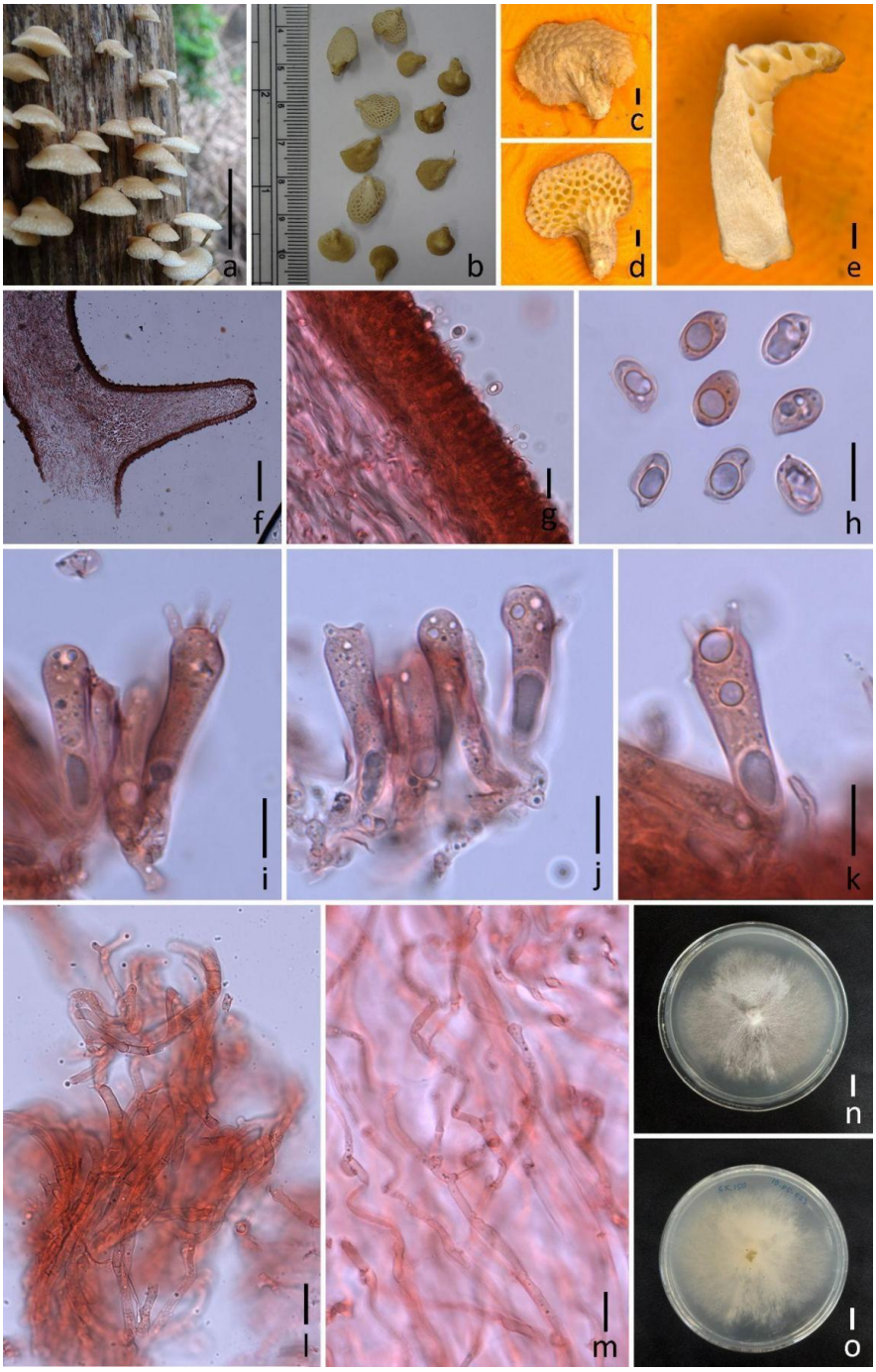


Figure 100 – *Favolaschia variistipitata* (MFLU25–0024, new geographical record). a–d Basidiomata. e Longitudinal section of basidiomata. f Vertical-section of pileus. g Vertical section of hymenium layer. h Basidiospores. i–k Basidia and basidioles. l Hyphae of pileipellis.

m Hyphae of trama. n, o Culture characteristics. Scale bars: a, n, o = 1 cm, c−e = 1 mm, f = 200 μm, g−m = 10 μm.

Class *Dacrymycetes* Doweld

Dacrymycetales Henn.

Dacrymycetaceae J. Schröt.

Dacrymyces Nees [as 'Dacryomyces'], Syst. Pilze (Würzburg): 89 (1816) [1816–17]

Index Fungorum number: IF17455

Dacrymyces is a jelly fungus genus proposed by Nees (1816), to accommodate a single species, *D. stillatus* Nees (1816). The genus is characterized by basidiomata with a soft, gelatinous to firm gelatinous consistency, exhibiting diverse forms such as pulvinate, discoid, subglobose, cerebriform, turbinate, pezizoid, or resupinate. Basidiomata are often stipitate, becoming spathulate to flabellate. *Context* gelatinized, heterogeneous or homogeneous, cortex composed of a palisade of septate hairs, septate when mature; ermination by conidia and/or germ tubes (Mendes-Alvarenga & Gibertoni 2022). Previous molecular studies showed that *Dacrymyces* is considered a polyphyletic group dispersed throughout the phylogeny of *Dacrymycetaceae* (Lian et al. 2022). Members of *Dacrymyces* typically inhabit dead trees, stumps, fallen trunks, or branches of angiosperms and gymnosperms, playing a crucial role in wood decomposition and causing brown rot (Shirouzu et al. 2009, Zamora & Ekman 2020, Mendes-Alvarenga & Gibertoni 2022). There are 235 entries for *Dacrymyces* recorded in Index Fungorum (http://www.indexfungorum.org/names/Names.asp, accessed January 9, 2025). Among these, DNA sequences for more than 30 species are available, primarily derived from ITS and LSU sequence datasets (Shirouzu et al. 2009, Zamora & Ekman 2020). These records are widely distributed across the globe, with the majority found in Europe, the Americas, Asia, and Oceania (Mcnabb 1973, Liu & Fan 1989, Shirouzu et al. 2009, 2013, Zamora & Ekman 2020, Savchenko et al. 2021). Prof. Kevin D. Hyde and his team members introduced *Dacrymyces chiangraiensis* in Tibpromma et al. (2017). This species, discovered in Thailand, enhances our understanding of jelly fungi in tropical regions and enriches the diversity and geographical distribution of *Dacrymyces* species in Thailand.

Prof. Kevin D. Hyde's team has made contributions to the research of mushrooms, including the genus *Dacrymyces*. In recognition of his outstanding contributions to mycology, we introduce the new species, *Dacrymyces undulatomarginatus*. We also provide an updated phylogenetic tree for *Dacrymyces* (Fig. 101).

Dacrymyces undulatomarginatus L. Lei & Q. Zhao, sp. nov. Fig. 102

Index Fungorum number: IF903324; Facesoffungi number: FoF17299

Etymology – The species epithet "*undulatomarginatus*" (from Latin *undulatus* = wavy and *marginatus* = margined) refers to the distinctly undulating margin of the basidiomata.

Holotype – HKAS 145921

On a fallen branch of *Abie*s sp. (*Pinaceae*). *Basidiomata* 2–5 high × 4–9 mm diam., single or gregarious, sessile or sub-stipitate; gelatinous when fresh, pustulate to pulvinate when juvenile, pulvinate or irregularly discoid when mature, and gyrose, surface yellow (2A7) to greyish yellow (2B7), pustulate to pulvinate when juvenile, pulvinate or irregularly discoid when mature, and gyrose. *Margin* irregular, wavy. *Marginal hyphae* of sterile surface hyaline, thick-walled, septate, straight or flexuous, with cylindrical, thin- to thick-walled terminal cells measuring 11.5–29 × 3.5–8 μm, without clamp connections; internal hyphae, 2.0–3.5 μm in diam., hyaline, thin-walled, septate, branched, without clamp connections. *Hymenium* limited to the superior of the basidiomata, composed of basidia and simple or branched, cylindrical hyphidia. *Basidiospores* [60/3/1] (18.5–) 20.0–23.0 (–23.5) × (11.0–) 11.5–13.0(–13.5) μm, L = 21.5 μm, W = 12.5 μm, Q = 1.62–1.86, Qm = 1.73 ± 0.12; allantoid, with an apiculum at the base, thin-walled, sub-hyaline to pale yellow, 2–8-septate, usually 6 or 7-septate when mature. *Basidia* 79–102 × 6–11 μm, cylindrical to subclavate, sub-hyaline to pale yellow, thin-walled, bifurcate. *Probasidia* 59–94 × 5–8.5 μm, cylindrical to subclavate, sub-hyaline to pale yellow, becoming bifurcate.

Material examined – China, Sichuan Province, Ganzi, Daocheng County, 30°01′48.40″ N, 100°47′25.56″ E, alt. 3,944 m, on a fallen branch of *Abie*s sp. (*Pinaceae*), 20 June 2022, Lei Lei, LEI-246 (HKAS 145921, holotype).

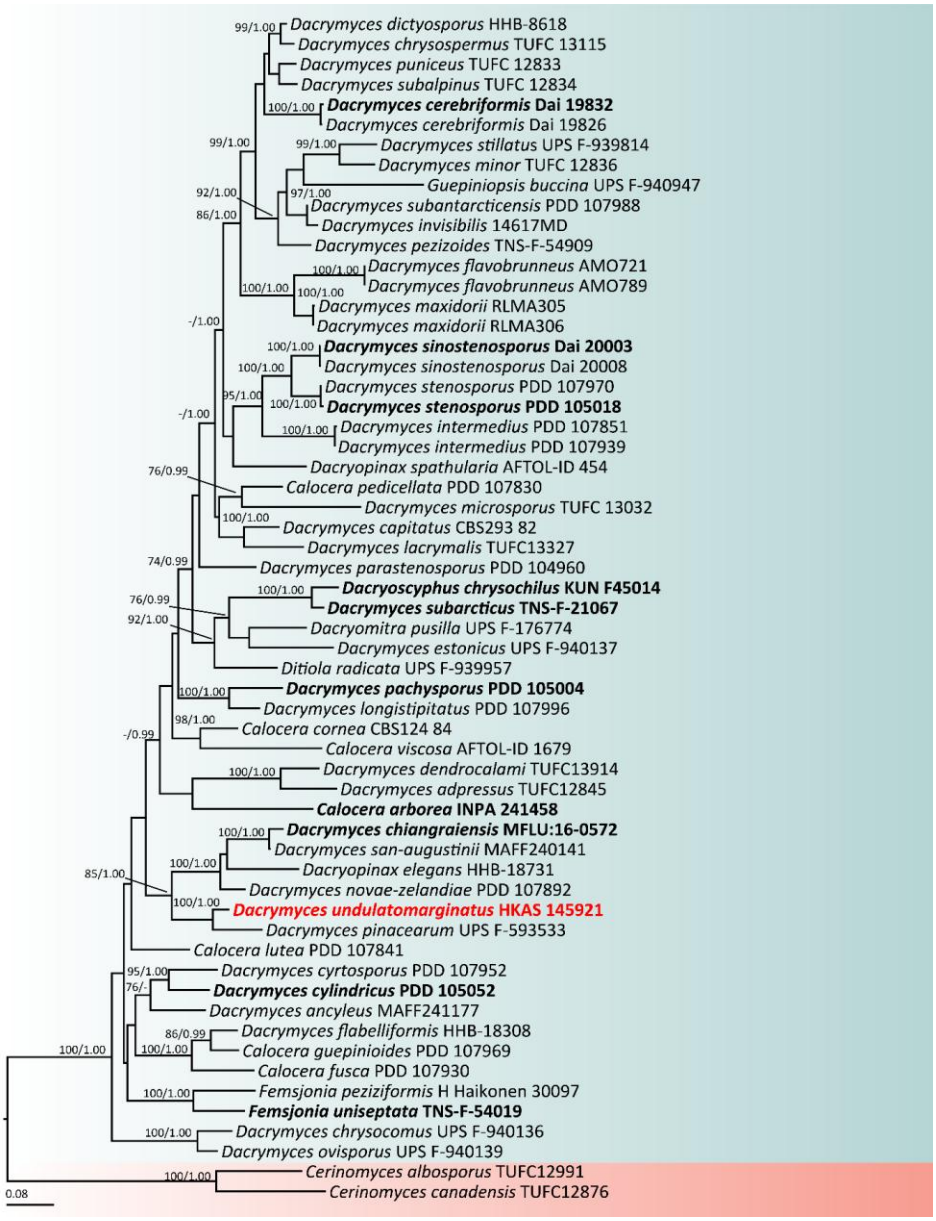


Figure 101 – Phylogram generated from maximum likelihood analysis based on combined LSU and ITS sequence data from 58 taxa, comprising 1,452 characters (ITS = 644, LSU = 808). The best-scoring RAxML tree with a final likelihood value of -18988.499 is presented. The matrix contained 867 distinct alignment patterns, with 23.85% of the characters being undetermined or gaps. Estimated base frequencies were as follows: A = 0.267, C = 0.215, G = 0.270, T = 0.248; substitution rates: AC = 1.173, AG = 2.199, AT = 1.346, CG = 0.767, CT = 4.723, GT = 1.0; gamma distribution shape parameter α = 0.585. Bootstrap support values for maximum likelihood (ML) equal to or greater than 70% and clade credibility values greater than 0.90 (rounded to two decimal places) from Bayesian inference analysis are labeled at each node. Type specimens are in bold, while the new isolate is indicated in red bold. The tree is rooted in *Cerinomyces albosporus* (TUFC12991) and *C. canadensis* (TUFC12876).

GenBank numbers – HKAS 145921: ITS = PV037615, LSU = PV037430.

Notes – In the phylogenetic analyses based on a combined ITS and LSU sequence dataset, *Dacrymyces undulatomarginatus* formed a distinct lineage as the sister clade to *D. pinacearum*, with 100% ML and 1.00 BYPP statistical support (Fig. 101). Morphologically, our collection resembles *D. novae-zelandiae* by having a gregarious habit, very small basidiomata, similar basidiospore length, and growing on coniferous wood (Mcnabb 1973). However, *D. undulatomarginatus* has wider basidiospores (20.0–23.0 × 11.5–13.0 vs. 17.5–23.0 × 4.5–7.5 µm) and larger probasidia (79–102 × 6–11 vs. 45–70 × 5–6.5 µm), and the latter has clay tones in basidiomata (Mcnabb 1973). *Dacrymyces undulatomarginatus* shares traits with *D. chiangraiensis*, such as basidiomata size and shape with a yellow surface, but the former was discovered in the subalpine region, and can be distinguished from *D. chiangraiensis* by its wider basidiospores (20.0–23.0 × 11.5–13.0 vs. 19–23 × 6.5–8 µm) and larger probasidia (79–102 × 6–11 vs. 32–53 × 7–10 µm) (Tibpromma et al. 2017). *Dacrymyces pinacerarum* was originally described in Japan based on the asexual morph. Phylogenetically, it is distinct from *D. undulatomarginatus* (Fig. 101), with notable differences in ITS (83/530 bp, 15.54%, including gaps) and LSU (19/780 bp, 2.43%) (Shirouzu et al. 2009).

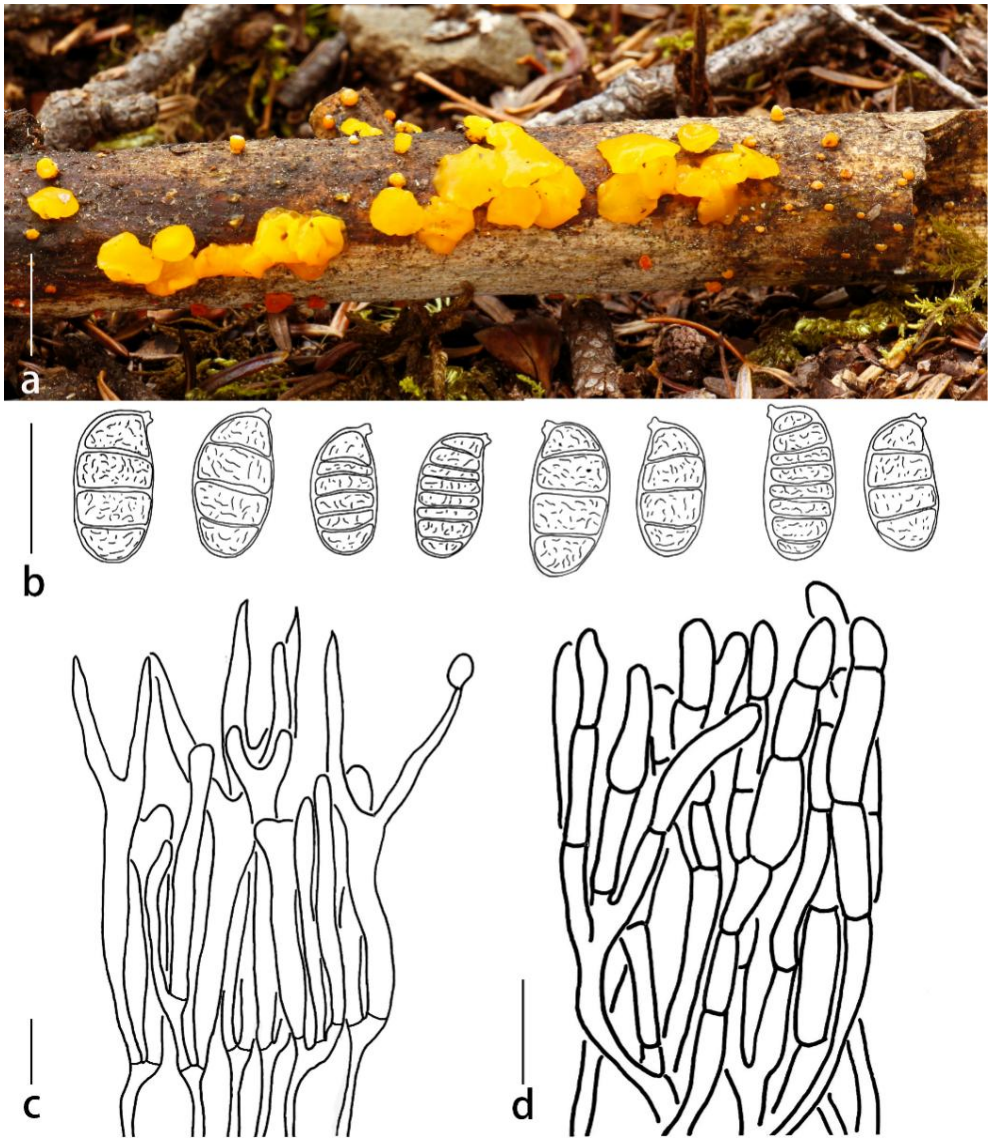


Figure 102 – *Dacrymyces undulatomarginatus* (HKAS 145921, holotype). a Basidiomata. b Basidiospores. c Probasidia and basidia. d Marginal hyphae. Scale bars: a = 10 mm, b–d = 20 µm.

ACKNOWLEDGEMENTS

Sinang Hongsanan would like to thank the National Natural Science Foundation of China (32400012), the 2023 Shenzhen Pengcheng Distinguished Positions and Scientific Research Funds for High-Tech Talents/High-Level Talents, and the Shenzhen University 2035 Program for Excellent Research (Grant No. 2024C006). Xie Ning would like to thank Natural Science Foundation of Guangdong Province (2024B1515020034), and National Key R&D Program of China (2021YFA0910800). Samantha C. Karunarathna and Saowaluck Tibpromma thank the National Natural Science Foundation of China (32260004), Yunnan Revitalization Talents Support Plan (High-End Foreign Experts Programs), and the Key Laboratory of Yunnan Provincial Department of Education of the Deep-Time Evolution on Biodiversity from the Origin of the Pearl River for their support. Yusufjon Gafforov acknowledges the support of the Agency for Innovative Development under the Ministry of Higher Education, Science, and Innovation (Project No. AL-8724052922) and the National Key R&D Program of China (Project No. 2025YFE0104500) for funding research. Raghvendra Singh thanks Science & Engineering Research Board (SERB), Department of Science & Technology (DST), Govt. of India (Scheme No. CRG/2020/006053); Incentive Grant (R/Dev./D/IoE/Incentive/2021-22/32387), Institution of Eminence, BHU, Varanasi; Bridge Grant (No. SRICC/Bridge Grant/2024-25/3151), BHU, Varanasi and Sanjay Yadav thanks Raja Jwala Prasad Post-Doctoral Fellowship (No. SRICC/RJP-PDF/2023-24/6158) under Institution of Eminence, BHU, Varanasi for providing financial support. LiLu would like to thank Mae Fah Luang University for providing her with a tuition fee scholarship for her Ph.D. Shambhu Kumar expresses gratitude to the Director of KSCSTE-Kerala Forest Research Institute for providing facilities and valuable support during the study. SK also acknowledges the Department of Biotechnology (DBT), Govt. of India, for financial support (BT/PR29521/FCB/125/15/2018). Chitrabhanu S. Bhunjun would like to thank the National Research Council of Thailand (NRCT) grant "Total fungal diversity in a given forest area with implications towards species numbers, chemical diversity and biotechnology" (grant no. N42A650547). Zaw Lin Tun would like to thank Mae Fah Luang University for providing a scholarship. Dong-Qin Dai would like to thank the Yunnan Provincial Department of Science and Technology "Zhihui Yunnan" plan (202403AM140023), the High-Level Talent Recruitment Plan of Yunnan Provinces (High-End Foreign Experts Programs and "Young Talents"), and the National Natural Science Foundation of China (No.32460002). The authors further extend their appreciation to the Meemann Chang Academician Workstation in Yunnan Province (202225AF150002) and the Yunnan Province Young and Middle-aged Academic and Technical Leaders Reserve Talents Program (202305AC350252). Li-Su Han would like to thank the Faculty of Science and Graduate School, Chiang Mai University, for supporting the tuition fee for the MSc. Thiyagaraja V would like to thank the Chinese Research Fund (project no E1644111K1) entitled "Flexible introduction of high-level expert program, Kunming Institute of Botany, Chinese Academy of Sciences, National postdoctoral special funding, Yunnan Province "Caiyun Postdoctoral Program" in 2023, Choi Wan Postdoctoral Program 2023 and National Postdoctoral funding, China. Ferreira-Sá AS, Leonardo-Silva L, and Xavier-Santos S would like to acknowledge the State University of Goiás (UEG) for logistical support, the State Secretariat for the Environment and Water Resources of Goiás (SEMARH), the management of Terra Ronca State Park (PETER) for providing the collection license, the Coordenação de Aperfeiçoamento de Pessoal de Nível Superior (CAPES) for granting a Ph.D. scholarship to ASFS (CAPES, 88887.672184/2022-00), the Fundação de Amparo à Pesquisa do Estado de Goiás (FAPEG) for granting a PDJ scholarship to LLS (FAPEG/CNPq, 202310267000437), and the Conselho Nacional de Desenvolvimento Científico e Tecnológico (CNPq) for granting a productivity scholarship to SXS (CNPq, 313260/2022-2). Rui-Fang Xu would like to thank Mae Fah Luang University for providing a tuition fee scholarship for her Ph.D. study. Yinru Xiong would like to thank the High-level Talents at Zhongkai University of Agriculture and Engineering, grant no: J2201080102 for the research fund. Wang WP and Luo ZL would like to thank the Yunnan Fundamental Research Project (202201AW070001) and

Foundation of Yunnan Province Science and Technology Department (202305AM070003) for financial support. Hai-Jun Zhao would like to thank Mae Fah Luang University for awarding a scholarship. Wei Dong thanks the National Natural Science Foundation of China (grant No. 32200015) and the foundation of the Guangzhou Bureau of Science and Technology (grant No. 2023A04J1425). We would like to thank Shaun Pennycook, Nomenclature Editor, Mycotaxon for helping with the new species name. Xing-Can Peng and Ting-Chi Wen would like to thank the funded by the National Natural Science Foundation of China (No. 31760014). ShiKe Huang acknowledges The Guizhou Basic Research Plan (Natural Science) General Project MS [2025] 071 and The Joint science and technology project between Zunyi Science and Technology Bureau and Zunyi Normal University HZ (2024) No.138. Calabon MS, Bagacay JFE, Opiña LAD, and Resurrección B. Sadaba are grateful to the UP System Balik PhD Program (OVPAA-BPhD-2022-02) entitled, 'Unraveling the hidden diversity of aquatic fungi from Panay Island, Philippines'. Xian Zhang and Ting-Chi Wen would like to thank the funded by the National Natural Science Foundation of China (No. 31760014). Tian-Ye Du extends her heartfelt gratitude to Mae Fah Luang University for granting a tuition-fee scholarship for her Ph.D. study. Shaun Pennycook is thanked for his assistance in selecting species epithets for the new species. Ishara Manawasinghe would like to acknowledge Zhongkai University of Agriculture and Engineering, talent funding (grant number KA210319288), and the Guangzhou Science and Technology Plan Project (2023A04J1427). Xi-Xi Han, Bin Cao, and Rui-Lin Zhao would like to the Survey of Wildlife Resources in Key Areas of Tibet (ZL202203601); the Projects of Science and Technology Programs of Tibet (XZ202202YD0031C). We would like to thank the Mycological Herbarium, Institute of Microbiology, Chinese Academy of Sciences (HMAS), and Shaun Pennycook (Manaaki Whenua Landcare Research, New Zealand) for his valuable suggestions on the fungal nomenclature. Sabin Khyaju thanks Thesis support grant from Mae Fah Luang University (reference no. GR ST-PS-65-22) and the Mushroom Research Foundation, Chiang Rai, Thailand. Thatsanee Luangharn would like to thank the National Research Council of Thailand (NRCT) "Total fungal diversity in a given forest area with implications towards species numbers, chemical diversity and biotechnology" (Grant no. N42A650547), and the Fundamental Fund supported by the National Science, Research and Innovation Fund "Taxonomy, phylogeny, screening of biologically active secondary metabolite and cultivation of Ganoderma species" (Grant no. 662A16005, 672A16004) and the Selecting potential mushroom strains for developing leather-sustainable materials from mushroom mycelium-base (Grant no. 682A16031). Wenhua Lu would like to thank Chiang Mai University. Mei Luo would like to thank the Key Fields of Ordinary Universities in Guangdong Province (2024ZDZX4010), the regional joint fund of Guangdong Basic and Applied Basic Research Fund - Youth Fund project (2022A1515110982), the Innovative team program of the Department of Education of Guangdong Province (2023KCXTD018), and the Guangdong Province Key Construction Discipline Scientific Research Capacity Improvement Project (2024ZDJ010). Xiang-Yu Zeng would like to thank National Natural Science Foundation of China (no. 32400013).

REFERENCES

Abeywickrama PD, Camporesi E, Jayawardena RS, Hyde KD et al. 2022 – Novel and surprising host associations of *Diaporthe* (Diaporthaceae, Diaporthales) species from Italy. Chiang Mai Journal of Science 49, 223–247.

Acar İ, Karabıyık H. 2024 – *Brunnipila calyculiformis* (Schumach.) Baral: A novel record for Türkiye. Cumhuriyet Science Journal 45(3), 486–489.

Afshari N, Karimi O, de Farias GAR, Suwannarach N et al. 2023 – Additions to *Diatrypaceae* (Xylariales): Novel taxa and new host associations. Journal of Fungi 9, 1151.

Ahmad I, Haqnawaz M, Niazi AR, Khalid AN. 2024 – A new species of *Candolleomyces* (Psathyrellaceae) from Pakistan. Phytotaxa 658(3), 280–288.

Aime MC. 1998 – Generic concepts in the Crepidotaceae as inferred from nuclear large subunit ribosomal DNA sequences, morphology, and basidiospore dormancy patterns (Doctoral dissertation, Virginia Tech).
An Y-Y, Zeng X-Y, Geng K, Hyde K et al. 2021 – One new species and one new record of *Zasmidium* in China. Biodiversity Data Journal 9, e59001.
Anand P, Isar J, Saran S, Saxena RK. 2006 – Bioaccumulation of copper by *Trichoderma viride*. Bioresource Technology 97, 1018–1025.
Ananya TS, Kindo AJ, Subramanian A, Suresh K. 2014 – *Nigrospora sphaerica* causing corneal ulcer in an immunocompetent woman: a case report. International Journal of Case Reports and Images 5(10), 675–679.
Aptroot A, Lücking R, Cáceres M. 2023 – New species and records of Graphidaceae and Gomphillaceae (lichenized fungi) from Brazil. Plant and Fungal Systematics 68(2), 249–261.
Aptroot A. 1998 – A world revision of *Massarina* (Ascomycota). Nova Hedwigia 66, 89–162.
Ariyawansa HA, Hyde KD, Jayasiri SC, Buyck B et al. 2015a – Fungal diversity notes 111–252—taxonomic and phylogenetic contributions to fungal taxa. Fungal Diversity 75, 27–274.
Ariyawansa HA, Hyde KD, Jayasiri SC, Buyck B et al. 2015b – Erratum to: Fungal diversity notes 111–252—taxonomic and phylogenetic contributions to fungal taxa. Fungal Diversity 75(1), 275–277.
Ariyawansa HA, Tsai I, Thambugala KM, Chuang WY et al. 2020 – Species diversity of Pleosporalean taxa associated with *Camellia sinensis* (L.) Kuntze in Taiwan. Scientific Reports 10(1), 12762.
Ariyawansa HA, Tsai I, Wang JY, Withee P et al. 2021 – Molecular phylogenetic diversity and biological characterization of *Diaporthe* species associated with leaf spots of *Camellia sinensis* in Taiwan. Plants 10, 1434.
Arzanlou M, Groenewald JZ, Fullerton RA, Abeln ECA et al. 2008 – Multiple gene genealogies and phenotypic characters differentiate several novel species of *Mycosphaerella* and related anamorphs on banana. Persoonia 20, 19–37.
Arzanlou M, Groenewald JZ, Gams W, Braun U et al. 2007 – Phylogenetic and morphotaxonomic revision of *Ramichloridium* and allied genera. Studies in Mycology 58, 57–93.
Awasthi N, Singh R, Kumar S. 2016 – A new species of *Pseudocercosporella* on *Andrographis paniculata* from Central India. Sydowia 68, 27–33.
Azhari A, Supratman U. 2021 – The chemistry and pharmacology of fungal genus *Periconia*: a review. Scientia Pharmaceutica 89(3), 34.
Bakhshi M, Arzanlou M, Babai-ahari A, Groenewald JZ et al. 2014 – Application of the consolidated species concept to Cercospora spp. from Iran. Persoonia 34, 65–86.
Ban S, Sakane T, Nakagiri A. 2015 – Three new species of *Ophiocordyceps* and overview of anamorph types in the genus and the family Ophiocordyceptaceae. Mycological progress 14, 1017.
Baral HO, Krieglsteiner GJ. 1985 – Bausteine zu einer Askomyzeten-Flora der BR Deutschland: In Süddeutschland gefundene inoperculate Discomyzeten mit taxonomischen, ökologischen und chorologischen Hinweisen. Beihefte zur Zeitschrift für Mykologie 6, 1–160.
Baral HO, Weber E, Gams W, Hagedorn G et al. 2018 – Generic names in the Orbiliaceae (Orbiliomycetes) and recommendations on which names should be protected or suppressed. Mycological Progress 17, 5–31.
Baral HO, Weber E, Marson G. 2020 – Monograph of Orbiliomycetes (Ascomycota) based on vital taxonomy. Part 1 and 2. Musee National d'Histoire Naturelle, Luxembourg. 1752 p.
Baral HO. 2015 – Nomenclatural novelties. Index Fungorum 252, 1–3.
Barr M. 1989 – The genus *Dothidotthia* (Botryosphaeriaceae) in North America. Mycotaxon 34, 517–526.
Barr ME. 1994 – Notes on the Amphisphaeriaceae and related families. Mycotaxon 51, 191–224.

Batista AC, Maia HS. 1956 – *Ceramothyrium*, a new genus of the family Phaeosaccardinulaceae. Atti dell'Istituto Botanico e Laboratorio Crittogamico dell'Università di Pavia 14, 23–52.
Bau T, Yan JQ. 2021 – Two new rare species of *Candolleomyces* with pale spores from China. MycoKeys 80, 149–161.
Bhunjun CS, Niskanen T, Suwannarach N, Wannathes N et al. 2022 – The numbers of fungi: are the most speciose genera truly diverse?. Fungal Diversity 114, 387–462.
Bills GF, Gloer JB. 2016 – Biologically active secondary metabolites from the fungi. Microbiology Spectrum 4(6), FUNK-0009-2016.
Bills GF, Polishook JD. 1992 – A new species of *Mycoleptodiscus* from living foliage of *Chamaecyparis thyoides*. Mycotaxon 43, 453–460.
Boehm EWA, Schoch CL, Spatafora JW. 2009 – On the evolution of the Hysteriaceae and Mytilinidiaceae (Pleosporomycetidae, Dothideomycetes, Ascomycota) using four nuclear genes. Mycological Research 113, 461–479.
Bolboli Z, Tavakolian B, Mostowfizadeh-Ghalamfarsa R, Jafari M et al. 2022 – *Stilbocrea banihashemiana* sp. nov. a new fungal pathogen causing stem cankers and twig dieback of fruit trees. Journal of Fungi 8(7), 694.
Boonmee S, Phookamsak R, Hongsanan S, Doilom M et al. 2017 – Mycosphere notes 51–101. Revision of genera in Perisporiopsidaceae and Pseudoperisporiaceae and other Ascomycota genera incertae sedis. Mycosphere 8(10), 1695–1801.
Boonmee S, Wanasinghe DN, Calabon MS, Huanraluek N et al. 2021 – Fungal diversity notes 1387–1511: taxonomic and phylogenetic contributions on genera and species of fungal taxa. Fungal Diversity 111, 1–335.
Brahmanage RS, Dayarathne MC, Wanasinghe DN, Thambugala KM et al. 2020 – Taxonomic novelties of saprobic Pleosporales from selected dicotyledons and grasses. Mycosphere 11, 2481–2541.
Braun U, Crous PW, Nakashima C. 2016 – Cercosporoid fungi (*Mycosphaerellaceae*) 5. Species on dicots (*Anacardiaceae* to *Annonaceae*). IMA Fungus 7, 161–216.
Braun U, Nakashima C, Crous PW. 2013 – Cercosporoid fungi (*Mycosphaerellaceae*) 1. Species on other fungi, Pteridophyta and Gymnospermae. IMA Fungus 4, 265–345.
Brefeld O. 1891 – AmericaUntersuchungen aus dem Gesammtgebiete der Mykologie, Ascomyceten II. Mycology 7, 50–51.
Bulliard JBF. 1789 – Herbier de la France. 9(97–108), 385–432.
Bustamante DE, Calderon MS, Leiva S, Mendoza JE, Oliva M. 2021 – Three new species of *Trichoderma* in the Harzianum and Longibrachiatum lineages from Peruvian cacao crop soils based on an integrative approach. Mycologia 113, 1056–1072.
Cai F, Druzhinina IS. 2021 – In honor of John Bissett: authoritative guidelines on molecular identification of *Trichoderma*. Fungal Diversity 107, 1–69.
Calvillo-Medina RP, Cobos-Villagran A, Raymundo T. 2020 – *Periconia citlaltepetlensis* sp. nov. (Periconiaceae, Pleosporales): A psychrotolerant fungus from high elevation volcanic glacier (Mexico). Phytotaxa 459(3), 235–247.
Cao Z, Qin W, Zhao J, Liu Y et al. 2022 – Three new *Trichoderma* species in Harzianum clade associated with the contaminated substrates of edible fungi. Journal of Fungi 8, 1154.
Capelari M, Karstedt F, de Oliveira JJS. 2013 − *Favolaschia* in remnants of the Atlantic Forest, Brazil. Mycoscience 55(1), 12–20.
Case NT, Gurr SJ, Fisher MC, Blehert DS et al. 2025 – Fungal impacts on Earth's ecosystems. Nature 638, 49–57.
Chaverri P, Branco-Rocha F, Jaklitsch W, Gazis R et al. 2015 – Systematics of the *Trichoderma harzianum* species complex and the re-identification of commercial biocontrol strains. Mycologia 107(3), 558–590.
Cheewangkoon R, Crous PW, Hyde KD, Groenewald JZ et al. 2008 – Species of *Mycosphaerella* and related anamorphs on *Eucalyptus* leaves from Thailand. Persoonia 21, 77–91.

Chen Q, Bakhshi M, Balci Y, Broders KD, et al. 2022 – Genera of phytopathogenic fungi: GOPHY 4. Studies in Mycology 101, 417–564.
Chen WH, Han YF, Liang JD, Liang ZQ. 2021–Taxonomic and phylogenetic characterizations reveal four new species of *Simplicillium* (Cordycipitaceae, Hypocreales) from Guizhou, China. Science Reports 11, 15300.
Chen XM, Suwannarach N, Du TY, Lu WH et al. 2024 – Phylogenetic and taxonomic evidence reveal *Roussoella bambusicola* sp. nov. (Pleosporales, Dothideomycetes) from Yunnan Province, China. Phytotaxa 670(2), 97–108.
Chen YJ, Jayawardena RS, Bhunjun CS, Harishchandra DL, Hyde KD. 2020 – *Pseudocercospora dypsidis* sp. nov. (*Mycosphaerellaceae*) on *Dypsis lutescens* leaves in Thailand. Phytotaxa 474(3), 218–234.
Chethana KT, Manawasinghe IS, Hurdeal VG, Bhunjun CS et al. 2021 – What are fungal species and how to delineate them?. Fungal Diversity 109(1), 1–25.
Chethana KWT, Rathnayaka AR, Samarakoon BC, Wu N et al. 2023 – AJOM new records and collections of fungi: 151-200. Asian Journal of Mycology 6(2), 89–243.
Cho HJ, Lee H, Park MS, Park KH et al. 2020 – Two new species of *Laccaria* (Agaricales, Basidiomycota) from Korea. Mycobiology 48(4), 288–295.
Chomnunti P, Ko TWK, Chukeatirote E, Hyde KD et al. 2012 – Phylogeny of Chaetothyriaceae in northern Thailand including three new species. Mycologia 104(2), 382–395.
Chouaki T, Lavarde V, Lachaud L, Raccurt CP, et al. 2002 – Invasive infections due to Trichoderma species: report of 2 cases, findings of in vitro susceptibility testing, and review of the literature. Clinical Infectious Diseases 35, 1360–1367.
Clémençon H. 1977 − Anatomie der Hymenomyceten (Anatomy of the *Hymenomycetes*); Flück Wirth Teufen, ed., Universität Lausanne, Lausanne, Switzerland.
Conner KN, Hagan AK, Zhang L. 2013 – First report of *Corynespora cassiicola*-incited target spot on cotton in Alabama. Plant Disease 97(10), 1379.
Consiglio G, Setti L, Robich G, Diaz AO, Vizzini A. 2008 – II genere *Crepidotus* in Europa. AMB Centro Studi Micologici.
Constantinescu O, Holm K, Holm L. 1989 – Teleomorph-anamorph connections in Ascomycetes. 1-3. *Stanhughesia* (Hyphomycetes) new genus, the anamorph of *Ceramothyrium*. Studies in Mycology 31, 69–84.
Conway KE, Barr ME. 1977 – Classification of *Ophioceras dolichostomum*. Mycotaxon 5, 376–380.
Correia P, Azevedo E, Caeiro MF. 2023 – Redefining the genus *Corollospora* based on morphological and phylogenetic approaches. Journal of Fungi 9(8), 841.
Crous PW, Braun U, Hunter GC, Wingfield MJ et al. 2013 – Phylogenetic lineages in *Pseudocercospora*. Studies in Mycology 75, 37–114.
Crous PW, Braun U. 2003 – Mycosphaerella and its anamorphs: 1. Names published in Cercospora and Passalora. CBS Biodiversity Series: Centraalbureau voor Schimmelcultures.
Crous PW, Cowan DA, Maggs-Kölling G, Yilmaz N et al. 2021a – Fungal Planet description sheets: 1182–1283. Persoonia: Molecular Phylogeny and Evolution of Fungi 46, 313.
Crous PW, Groenewald JZ, Wood AR. 2008 – Sporidesmium knawiae. In: Fungal Planet – A Global Initiative to promote the Study of Fungal Biodiversity. In P. W. Crous, K. A. Seifert, R. A. Samson, & D. L. Hawksworth (Eds.), *Fungal Planet no 29* (Vol. 29). Utrecht: CBS-KNAW Fungal Biodiversity Centre.
Crous PW, Groenewald JZ. 2016 – They seldom occur alone. Fungal Biology 120, 1392–1415.
Crous PW, Groenewald JZ. 2017 – The Genera of Fungi – G 4: *Camarosporium* and *Dothiora*. IMA Fungus 8, 131–152.
Crous PW, Lombard L, Sandoval-Denis M, Seifert KA et al. 2021b – *Fusarium*: more than a node or a foot-shaped basal cell. Studies in Mycology 98, 100116.
Crous PW, Wingfield MJ, Burgess TI, Carnegie AJ et al. 2017 – Fungal Planet description sheets: 625-715. Persoonia 39, 270–467.

Crous PW, Wingfield MJ, Burgess TI, Hardy GESJ et al. 2018 – Fungal Planet description sheets: 716 –784. Persoonia 40, 240–393.
Cruz LF, Menocal O, Kendra PE, Carrillo D. 2021 – Phoretic and internal transport of *Raffaelea lauricola* by different species of ambrosia beetle associated with avocado trees. Symbiosis 84(2), 151–161.
D'Souza MA, Singh SK, Bhat DJ. 2002 – New conidial fungi from Andaman Islands, India. Mycotaxon 82, 133–143.
Dai DQ, Phookamsak R, Wijayawardene NN, Li WJ et al. 2017 – Bambusicolous fungi. Fungal Diversity 82, 1–105.
Dai DQ, Wijayawardene NN, Dayarathne MC, Kumla J et al. 2022 – Taxonomic and phylogenetic characterizations reveal four new species, two new asexual morph reports, and six new country records of bambusicolous *Roussoella* from China. Journal of Fungi 8, 532.
Das K, Lee SY, Jung HY. 2020 – Molecular and morphological characterization of two novel species collected from soil in Korea. Mycobiology 48(1), 9–19.
Dawoud TM, Yassin MA, El-Samawaty ARM, Elgorban AM. 2021 – Silver nanoparticles synthesized by *Nigrospora oryzae* showed antifungal activity. Saudi Journal of Biological Sciences 28(3), 1847–1852.
Dayarathne MC, Jones EBG, Maharachchikumbura SSN, Devadatha B et al. 2020 – Morpho-molecular characterization of microfungi associated with marine based habitats. Mycosphere 11(1), 1–188.
de Queiroz Brito AC, de Mello JF, de Almeida Souza AE, dos Santos Nascimento S et al. 2023 – Richness of *Nigrospora* spp. (*Apiosporaceae*) in *Manihot esculenta* Cranz in Brazil and the description of three new species. Mycological Progress 22, 37.
De Silva DD, Rapior S, Sudarman E, Stadler M et al. 2013 – Bioactive metabolites from macrofungi: ethnopharmacology, biological activities and chemistry. Fungal Diversity 62, 1–40.
de Silva NI, Hyde KD, Lumyong S, Phillips AJL et al. 2022 – Morphology, phylogeny, host association and geography of fungi associated with plants of *Annonaceae*, *Apocynaceae* and *Magnoliaceae*. Mycosphere 13, 955–1076.
de Souza Leite T, Cnossen-Fassoni A, Pereira OL, Mizubuti ESG et al. 2013 – Novel and highly diverse fungal endophytes in soybean revealed by the consortium of two different techniques. Journal of Microbiology 51, 56–69.
Delgado G, Koukol O, Maciá-Vicente JG, Colbert W, Piepenbring M. 2024 – Redefining *Ellisembia* sensu stricto with a reassessment of related taxa in Sordariomycetes. Mycological Progress 23(1), 1–25.
Déon M, Bourré Y, Gimenez S, Berger A et al. 2012 – Characterization of a cassiicolin-encoding gene from *Corynespora cassiicola*, pathogen of rubber tree (*Hevea brasiliensis*). Plant Science 185, 227–237.
Desmazières JBHJ. 1842 – Plantes Cryptogames du Nord de la France. Fasc. 24, 1151–1200.
Desmazières JBHJ. 1845 – Onzième notice sur les plantes cryptogames récemment découvertes en France, et qui vont paraître en nature dans la collection publiée par l'auteur. Ann Sci Nat Bot. 3(Juin), 357–370.
Desmazières JBHJ. 1850 – Dix-huitième notice sur les plantes cryptogames récemment découvertes en France. Ann Sci Nat Bot. 14(2), 107–118.
Di Lecce R, Bashiri S, Masi M, Alioto D et al. 2021 – Phytotoxic metabolites from *Stilbocrea macrostoma*, a fungal pathogen of *Quercus brantii* in Iran. Natural Product Research 35, 5857–5861.
Dissanayake AJ, Bhunjun CS, Maharachchikumbura SSN, Liu JK. 2020 – Applied aspects of methods to infer phylogenetic relationships amongst fungi. Mycosphere 11, 2652–2676.
Dissanayake AJ, Phillips AJL, Hyde KD, Yan JY, Li XH. 2017 – The current status of species in *Diaporthe*. Mycosphere 8, 1106–1156.

Dissanayake AJ, Zhu JT, Chen YY, Maharachchikumbura SS et al. 2024a – A re-evaluation of *Diaporthe*: refining the boundaries of species and species complexes. Fungal Diversity 4, 1–125.
Dissanayake LS, Samarakoon MC, Maharachchikumbura SSN, Hyde KD et al. 2024b – Exploring the taxonomy and phylogeny of *Sordariomycetes* taxa emphasizing *Xylariomycetidae* in Southwestern China. Mycosphere 15(1), 1675–1793.
Doilom M, Dissanayake AJ, Wanasinghe DN, Boonmee S et al. 2017 – Microfungi on Tectona grandis (teak) in Northern Thailand. Fungal Diversity 82, 107–182.
Doilom M, Hyde KD, Phookamsak R, Dai DQ et al. 2018 – Mycosphere Notes 225–274: types and other specimens of some genera of Ascomycota. Mycosphere 9(4), 647–754.
Dong W, Hyde KD, Jeewon R, Liao CF et al. 2023 – Mycosphere notes 449–468: saprobic and endophytic fungi in China, Thailand, and Uzbekistan. Mycosphere 14(1), 2208–2262.
Dong W, Wang B, Hyde KD, McKenzie EHC et al. 2020 – Freshwater Dothideomycetes. Fungal Diversity 105(1), 319–575.
Du TY, Karunarathna SC, Tibpromma S, Hyde KD et al. 2024 – *Melomastia* (Dothideomycetes, Ascomycota) species associated with Chinese *Aquilaria* spp. MycoKeys 111, 65–86.
Ellis MB. 1971 – Dematiaceous Hyphomycetes. Commonwealth Mycological Institute, Kew, UK.
Eschweiler FG. 1824 – Systema Lichenum, Genera Exhibens rite distincta. Pluribus Novis Adaucta 25, 1–26.
Esparham N, Mohammadi H, Gramaje DA. 2020 – A survey of trunk disease pathogens within citrus trees in Iran. Plants 9(6), 754.
Fajola AO, Alasoadura SO. 1973 – *Corynespora* leaf spot, a new disease of tobacco (*Nicotiana tabacum*). Plant Disease 57, 375–378.
Farr DF, Rossman AY. 2018 – Fungal Databases, U.S. National Fungus Collections, ARS, USDA. https://fungi.ars.usda.gov/
Farr DF, Rossman AY. 2024 – Fungal Databases, U.S. National Fungus Collections, ARS, USDA. https://fungi.ars.usda.gov/
Feng JW, Chen XY, Chen KY, Druzhinina IS, Voglmayr H et al. 2024 – A reappraisal of families within the order Magnaporthales and description of new endophytic taxa associated with Poaceae plants in China. Mycosphere 15(1), 6240–6346.
Fournier J, Lechat C. 2016 – Some *Annulohypoxylon* spp. (Xylariaceae) from French Guiana, including three new species. Ascomycete.org 8, 33–53.
Fries EM. 1849 – Summa vegetabilium Scandinaviae. Sectio posterior, Uppsala.
Gao Y, Liu F, Duan W, Crous PW, Cai L. 2017 – *Diaporthe* is paraphyletic. IMA fungus 8, 153–187.
Gao Y, Thiyagaraja V, Eungwanichayapant PD, de Fariaset ARG et al. 2024 – Two new *Stictidaceae* species from grasslands in Yunnan province, China. New Zealand Journal of Botany 62, 288–302.
Gauchan DP, Vélëz H, Acharya A, Östman JR et al. 2021 – *Annulohypoxylon* sp. strain *MUS1*, an endophytic fungus isolated from *Taxus wallichiana* Zucc., produces taxol and other bioactive metabolites. 3 Biotech 11, 152.
Ge YP. 2017 – Taxonomy and phylogeny of Crepidotaceae in China. (Doctoral dissertation, PhD dissertation, Jilin Agricultural University, Changchun.
Gillen K, Laessoe T, Kirschner R, Piepenbring M. 2012 − *Favolaschia* species (*Agaricales*, *Basidiomycota*) from Ecuador and Panama. Nova Hedwigia 96(1–2), 117–165.
Goga N. 2000 – *Periconia circinata*—A new pathogen of roots and stem base of wheat in northwestern Romania. Analele Institutului de Cercetări pentru Cereale s,i Plante Tehnice Fundulea 67, 205–214.
Gomes AAM, Pinho DB, Cardeal ZDL, Menezes HC et al. 2018 – *Simplicillium coffeanum*, a new endophytic species from Brazilian coffee plants, emitting antimicrobial volatiles. Phytotaxa 333, 188–198.

Gomes RR, Glienke C, Videira SI, Lombard L et al. 2013 – *Diaporthe*: a genus of endophytic, saprobic and plant pathogenic fungi. Persoonia 31, 1–41.
Gunasekaran R, Janakiraman D, Rajapandian SG, Appavu SP et al. 2021 – *Periconia* species-An unusual fungal pathogen causing mycotic keratitis. Indian Journal of Medical Microbiology 39(1), 36–40.
Güssow HT. 1905 – Notes on a disease of cucumbers. II. Journal of the Royal Agricultural Society of England 65, 270–272.
Guu JR, Ju YM, Hsieh HJ. 2010 – Bionectriaceous fungi collected from forests in Taiwan. Botanical Studies, 51(1), 61–74.
Han MH, Na Q, Wei RX, Zeng H et al. 2024a – Phylogenetic and morphological perspectives on *Crepidotus* subg. *Dochmiopus*: exploratively unveiling hidden diversity in China. Journal of Fungi 10, 710–740.
Han SL, Wang MM, Ma ZY, Raza M et al. 2023 – *Fusarium* diversity associated with diseased cereals in China, with an updated phylogenomic assessment of the genus. Studies in Mycology 104(1), 87–148.
Han XX, Phurbu D, Ma GF, Li YZ et al. 2024b – A taxonomic study of *Candolleomyces* specimens from China revealed seven new species. Journal of Fungi 10(7), 499.
Hao Y, Aluthmuhandiram JVS, Chethana KWT, Manawasinghe IS et al. 2020 – *Nigrospora* Species Associated with Various Hosts from Shandong Peninsula, China. Mycobiology 48(3), 169–183.
Haqnawaz M, Usman M, Fatima N, Niazi AR, Khalid AN. 2024a. Three new species of the genus *Candolleomyces* (Psathyrellaceae) from Pakistan. Plant Systematics and Evolution 310(6), 42.
Haqnawaz M, Usman M, Javaid A, Ramzan F et al. 2024b. Four new species of *Candolleomyces* (Psathyrellaceae) from the Punjab Plains, Pakistan. Mycologia 116(6), 1033–1045.
Harman GE, Howell CR, Viterbo A, Chet I, Lorito M. 2004 – *Trichoderma* specie–Opportunistic, avirulent plant symbionts. Nature Reviews Microbiology 2, 43–56.
Harms H, Schlosser D, Wick LY. 2011 – Untapped potential: exploiting fungi in bioremediation of hazardous chemicals. Nature Reviews Microbiology 9, 177–192.
Hashimoto A, Matsumura M, Hirayama K, Tanaka K. 2017 – Revision of *Lophiotremataceae* (Pleosporales, Dothideomycetes): *Aquasubmersaceae*, *Cryptocoryneaceae*, and *Hermatomycetaceae* fam. nov. Persoonia 39, 51–73.
Hawksworth DL, Kirk PM, Sutton BC, Pegler DN. 1995 – Ainsworth & Bisby's dictionary of the fungi, 8th edn. CAB International, Wallingford.
Hawksworth DL, Sherwood MA. 1981 – (559)-(579) Proposals for Nomina Conservanda and Rejicienda for Ascomycete Names (Lichenized and Non-Lichenized). Taxon 30, 338–348.
Heng G, Hyde KD, Jianchu X, Valentine AJ et al. 2016 – Mycosphere Essays 4. Mycorrhizal-associated nutrient dynamics in key ecosystems and their response to a changing environment. Mycosphere 7(2), 190–203.
Hernández-Restrepo M, Bezerra JDP, Tan YP et al. 2019 – Re-evaluation of Mycoleptodiscus species and morphologically similar fungi. Persoonia, 42, 205–227.
Hernández-Restrepo M, Groenewald JZ, Crous PW. 2016 – Taxonomic and phylogenetic reevaluation of *Microdochium, Monographella* and *Idriella*. Persoonia, 36, 57–82.
Hilário S, Gonçalves MFM. 2023 – Mechanisms underlying the pathogenic and endophytic lifestyles in *Diaporthe*: an omics-based approach. Horticulturae 9, 423.
Hirooka Y, Kobayashi T, Ono T, Rossman AY, Chaverri P. 2010 – Verrucostoma, a new genus in the Bionectriaceae from the Bonin Islands, Japan. Mycologia 102(2), 418–429.
Hladki AI, Romero AI. 2009 – Taxonomic and nomenclatural aspects of *Hypoxylon* taxa from southern South America proposed by Spegazzini. Mycologia 101, 733–744.
Holz PH, Lumsden LF, Marenda MS, Browning GF, Hufschmid J. 2018 – Two subspecies of bent-winged bats (*Miniopterus orianae bassanii* and *oceanensis*) in southern Australia have diverse fungal skin flora but not Pseudogymnoascus destructans. PLoS One 13, e0204282.

Hongsanan S, Hyde KD, Phookamsak R, Wanasinghe DN et al. 2020a – Refined families of Dothideomycetes: Dothideomycetidae and Pleosporomycetidae. Mycosphere 11, 1553–2107.
Hongsanan S, Hyde KD, Phookamsak R, Wanasinghe DN et al. 2020b – Refined families of Dothideomycetes: orders and families incertae sedis in Dothideomycetes. Fungal Diversity 105, 17–318.
Hongsanan S, Maharachchikumbura SSN, Hyde KD, Samarakoon MC et al. 2017 – An updated phylogeny of Sordariomycetes based on phylogenetic and molecular clock evidence. Fungal Diversity 84, 25–41.
Hongsanan S, Norphanphoun C, Senanayake IC, Jayawardena RS et al. 2023 – Annotated notes on Diaporthe species. Mycosphere 14(1), 918–1189.
Hou LW, Giraldo A, Groenewald JZ, Rämä T et al. 2023 – Redisposition of acremonium-like fungi in Hypocreales. Studies in Mycology 105, 23–203.
Hsieh HM, Ju YM, Rogers JD. 2005 – Molecular phylogeny of *Hypoxylon* and closely related genera. Mycologia 97(4), 844–865.
Hsieh L, Tzean S, Wu WJ. 1997 – The genus *Akanthomyces* on spiders from Taiwan. Mycologia 89(2), 319–324.
Huang B, Wang S, Fan M, Li Z. 2000 – Two species of *Akanthomyces* from Dabieshan mountains. Junwu Xuebao 19, 172–174.
Huelsenbeck JP, Ronquist F. 2001 – MRBAYES: Bayesian inference of phylogenetic trees. Bioinformatics 17, 754–755.
Hyde 1992 – The effect of incubation on the occurrence of marine fungi on randomly collected lignocellulose samples. Sydowia 44(2), 131–136.
Hyde KD, Abdel-Wahab MA, Abdollahzadeh J, Abeywickrama PD et al. 2023b – Global consortium for the classification of fungi and fungus-like taxa. Mycosphere 14(1), 1960–2012.
Hyde KD, Aptroot A, Fröhlich J, Taylor JE. 1999 – Fungi from palms. XLII. *Didymosphaeria* and similar ascomycetes from palms. Nova Hedwigia 69(3–4), 449–471.
Hyde KD, Aptroot A. 1998 – Tropical freshwater species of the genera *Massarina* and *Lophiostoma* (ascomycetes). Nova Hedwigia 66, 489–502.
Hyde KD, Chaiwan N, Norphanphoun C, Boonmee S et al. 2018 – Mycosphere notes 169–224. Mycosphere 9(2), 271–430.
Hyde KD, de Silva NI, Jeewon R, Bhat DJ et al. 2020b – AJOM new records and collections of fungi: 1–100. Asian Journal of Mycology 3(1), 22–294.
Hyde KD, Dong Y, Phookamsak R, Jeewon R et al. 2020a – Fungal diversity notes 1151–1276: taxonomic and phylogenetic contributions on genera and species of fungal taxa. Fungal Diversity 100, 5–277.
Hyde KD, Hongsanan S, Jeewon R, Bhat DJ et al. 2016 – Fungal diversity notes 367–490: taxonomic and phylogenetic contributions to fungal taxa. Fungal Diversity 80, 1–270.
Hyde KD, Jones EG, Liu JK, Ariyawansa H et al. 2013 – Families of Dothideomycetes. Fungal diversity 63, 1–313.
Hyde KD, Maharachchikumbura SSN, Hongsanan S, Samarakoon MC et al. 2017a – The ranking of fungi: a tribute to David L. Hawksworth on his 70th birthday. Fungal Diversity 84, 1–23.
Hyde KD, Nilsson RH, Alias SA, Ariyawansa HA et al. 2014 – One stop shop: backbones trees for important phytopathogenic genera: I. Fungal Divers 67, 21–125.
Hyde KD, Noorabadi MT, Thiyagaraja V, He MQ et al. 2024c – The 2024 Outline of Fungi and fungus-like taxa. Mycosphere 15(1), 5146–6239.
Hyde KD, Norphanphoun C, Abreu VP, Bazzicalupo A et al. 2017b – Fungal diversity notes 603–708: taxonomic and phylogenetic notes on genera and species. Fungal Diversity 87, 1–235.
Hyde KD, Norphanphoun C, Ma J, Yang HD et al. 2023a – Mycosphere notes 387–412 – novel species of fungal taxa from around the world. Mycosphere 14(1), 663–744.

Hyde KD, Norphanphoun C, Maharachchikumbura SSN, Bhat DJ et al. 2020c – Refined families of Sordariomycetes. Mycosphere 11(1), 305–1059.
Hyde KD, Suwannarach N, Jayawardena RS, Manawasinghe IS et al. 2021 – Mycosphere notes 325-344 – Novel species and records of fungal taxa from around the world. Mycosphere 12(1), 1101–1156.
Hyde KD, Tennakoon DS, Jeewon R, Bhat DJ et al. 2019 – Fungal diversity notes 1036–1150: taxonomic and phylogenetic contributions on genera and species of fungal taxa. Fungal Diversity 96, 1–242.
Hyde KD, Wijesinghe SN, Afshari N, Aumentado HD et al. 2024a – Mycosphere Notes 469–520. Mycosphere 15(1), 1294–1454.
Hyde KD, Wijesinghe SN, Amuhenage TB, Bera I et al. 2024b – Current research in applied and environmental mycology fungal profiles 1-30. Current Research in Environmental & Applied Mycology (Journal of Fungal Biology) 14(1), 167–266.
Hyde KD, Xu J, Rapior S, Jeewon R et al. 2019a – The amazing potential of fungi: 50 ways we can exploit fungi industrially. Fungal Diversity 97, 1–136.
Hywel-Jones NL. 1996 – *Akanthomyces* on spiders in Thailand. Mycological Research 100(9), 1065–1070.
Imai S. 1938 – Studies on the Agaricaceae of Hokkaido. 1. Journal of the Faculty of Agriculture of the Hokkaido Imperial University 43, 1–378.
Index Fungorum. 2025 – Available at: http://www.indexfungorum.org (Accessed on January 2025)
Jaklitsch WM, Voglmayr H. 2015 – Biodiversity of *Trichoderma* (Hypocreaceae) in southern Europe and Macaronesia. Studies in Mycology 96, 1–87.
Jayasiri SC, Hyde KD, Ariyawansa HA, Bhat J et al. 2015 – The Faces of Fungi database: fungal names linked with morphology, phylogeny and human impacts. Fungal Diversity 74, 3–18.
Jayasiri SC, Hyde KD, Jones EBG, McKenzie EHC et al. 2019 – Diversity, morphology and molecular phylogeny of Dothideomycetes on decaying wild seed pods and fruits. Mycosphere 10, 1–186.
Jayasiri SC, Hyde KD, Jones EBG, Peršoh D et al. 2018 – Taxonomic novelties of hysteriform dothideomycetes. Mycosphere 9, 803–837.
Jayawardena RS, Hyde KD, Chethana KWT, Daranagama DA et al. 2018 – Mycosphere Notes 102–168: Saprotrophic fungi on Vitis in China, Italy, Russia and Thailand. Mycosphere 9(1), 1–114.
Jayawardena RS, Hyde KD, Wang S, Sun YR et al. 2022 – Fungal diversity notes 1512–1610: Taxonomic and phylogenetic contributions on genera and species of fungal taxa. Fungal Diversity 117, 1–272.
Jeewon R, Hyde KD. 2016 – Establishing species boundaries and new taxa among fungi: recommendations to resolve taxonomic ambiguities. Mycosphere 7(11), 1669–1677.
Jiang HB, Hyde KD, Jayawardena RS, Doilom M et al. 2019a – Taxonomic and phylogenetic characterizations reveal two new species and two new records of *Roussoella* (Roussoellaceae, Pleosporales) from Yunnan, China. Mycological Progress 18(4), 577–591.
Jiang HB, Hyde KD, Yang EF, Kakumyan P et al. 2021 – Morphological and phylogenetic appraisal of *Ophioceras* (*Ophioceraceae*, *Magnaportha*). PLoS ONE 16(8), e0253853.
Jiang N, Voglmayr H, Tian CM. 2018 – New species and records of *Coryneum* from China. Mycologia 110(6), 1172–1188.
Jiang N, Voglmayr H, Tian CM. 2019b – Morphology and phylogeny reveal two novel *Coryneum* species from China. MycoKeys 56, 67–80.
Jiang X, Xiang M, Liu X. 2016 – Nematode-trapping fungi. Microbiol Spectrum 5(1):FUNK-0022-2016.
Kalb K, Staiger B, Elix JA. 2004 – A monograph of the lichen genus *Diorygma*–a first attempt. Symbolae Botanicae Upsalienses 34(1), 133–181.
Kamal. 2010 – *Cercosporoid fungi of India*. Bishan Singh Mahendra Pal Singh Publication, Dehradun (UK), India, 351 pp.

Karimi O, Chethana KWT, de Farias ARG, Kaewchai S et al. 2024 – Morphology and multigene phylogeny reveal three new species of *Distoseptispora* (*Distoseptisporales*, *Distoseptisporaceae*) on palms (*Arecaceae*) from peatswamp areas in southern Thailand. MycoKeys 102, 55–81.
Karunarathna SC, Dong Y, Karasaki S, Tibpromma S et al. 2020 – Discovery of novel fungal species and pathogens on bat carcasses in a cave in Yunnan Province, China. Emerging Microbes & Infections 9, 1554–1566.
Kepler RM, Luangsa-Ard JJ, Hywel-Jones NL, Quandt CA et al. 2017 – A phylogenetically-based nomenclature for Cordycipitaceae (Hypocreales). IMA fungus 8, 335–353.
Khonsanit A, Luangsa-Ard JJ, Thanakitpipattana D, Kobmoo N et al. 2019 – Cryptic species within Ophiocordyceps myrmecophila complex on formicine ants from Thailand. Mycological progress 18, 147–161.
Kirk PM, Cannon PF, Minter DW, Stalpers JA et al. 2008 – Ainsworth & Bisby's Dictionary of the Fungi, 10th ed. CABI: Oxford, UK.
Kits van Waveren E. 1985 – The Dutch, French and British species of *Psathyrella*. Persoonia - Supplement 2(1), 3–300.
Kobayasi Y. 1941 – The genus Cordyceps and its allies. Report of The Tokyo Bunrika DaigakuSection B 5(84), 53–260.
Koenning SR, Creswell TC, Dunphy EJ, Sikora EJ, Mueller JD. 2006 – Increased occurrence of target spot of soybean caused by *Corynespora cassiicola* in the Southeastern United States. Plant disease 90(7), 974.
Kohlmeyer J, Kohlmeyer E. 1979 – Marine Mycology: The Higher Fungi. New York: Academic Press. 690 pp.
Kohlmeyer J, Schmidt I, Nair NB. 1967 – Eine neue *Corollospora* (Ascomycetes) aus dem Indischen Ozean und der Ostsee. Berichte der Deutschen Botanischen Gesellschaft 80, 98–102.
Kohlmeyer J, Volkmann-Kohlmeyer B, Eriksson OE. 1996 – Fungi on *Juncus roemerianus*. 8. New bitunicate ascomycetes. Canadian Journal of Botany 74, 1830–1840.
Kolomiets T, Pankratova L, Mukhina Z, Kassanelly D et al. 2008 – First report of leaf spot caused by *Periconia igniaria* on yellow starthistle in Russia. Plant Disease 92(6), 983.
Komoń-Zelazowska M, Bissett J, Zafari D, Hatvani L et al. 2007 – Genetically closely related but phenotypically divergent *Trichoderma* species cause green mold disease in Oyster mushroom farms worldwide. Appl Environ Microbiol 73, 7415–7426.
Konta S, Maharachchikumbura SSN, Senanayake IC, Mckenzie EHC et al. 2020 – A new genus *Allodiatrype*, five new species and a new host record of diatrypaceous fungi from palms (Arecaceae). Mycosphere 11, 239–268.
Konta S, Tibpromma S, Karunarathna SC, Samarakoon MC et al. 2023 – Morphology and multigene phylogeny reveal ten novel taxa in *Ascomycota* from terrestrial palm substrates (*Arecaceae*) in Thailand. Mycosphere 14(1), 107–152.
Koukol O, Delgado G, Hofmann TA, Piepenbring M. 2018 – Panama, a hot spot for *Hermatomyces* (*Hermatomycetaceae*, Pleosporales) with five new species, and a critical synopsis of the genus. International Mycological Association fungus 9, 107–141.
Kredics L, Antal Z, Dóczi I, Manczinger L et al. 2003 – Clinical importance of the genus *Trichoderma*. Acta microbiologica et immunologica Hungarica 50, 105–117.
Kredics L, Garcia Jimenez L, Naeimi S, Czifra D et al. 2010 – A challenge to mushroom growers: the green mould disease of cultivated champignons. In: Technology and education topics in applied microbiology and microbial biotechnology, pp. 295–305.
Kuhnert E, Sir EB, Lambert C, Hyde KD et al. 2017 – Phylogenetic and chemotaxonomic resolution of the genus *Annulohypoxylon* (*Xylariaceae*) including four new species. Fungal Diversity 85, 1–43.
Kularathnage ND, Tennakoon DS, Zhu X, Zhou J et al. 2023 – Reinstating *Dyfrolomyces* and introducing *Melomastia pyriformis* sp. nov. (Pleurotremataceae, Dyfrolomycetales) from

Guangdong Province, China. Current Research in Environmental & Applied Mycology 13, 426–438.
Kumar S, Singh R. 2015a – *Passalora musicola* sp. nov. a new Indian hyphomycete. Sydowia 67, 21–23.
Kumar S, Singh R. 2015b – *Pseudocercospora bischofigena*, a new cercosporoid fungus from northeastern Uttar Pradesh, India. Czech Mycology 67, 39–44.
Kumar S, Singh R. 2016 – *Passalora caesalpiniicola* sp. nov. from India on *Caesalpinia bonduc.* Mycotaxon 131, 25–30.
Kurre AK, Dewangan M, Nishad D, Mishra S. 2019 – Variability among *Corynespora cassiicola* isolates causing target leaf spot disease collected from soybean growing area of Chhattisgarh. Journal of Pharmacognosy and Phytochemistry 8(6), 603–606.
Læssøe T, Petersen JH. 2018 – Nomenclatural novelties. Index Fungorum. 369, 1.
Lechat C, Fournier J. 2019 – New insights into *Stilbocrea* (Hypocreales, Bionectriaceae): Recognition of *S. colubrensis*, a new species from Martinique (French West Indies), and observations on lifestyle and synnematous asexual morphs of *S. gracilipes* and *S. macrostoma*. Ascomycete.org 11, 183–190.
Li GJ, Hyde KD, Zhao RL, Hongsanan S et al. 2016 – Fungal diversity notes 253–366: taxonomic and phylogenetic contributions to fungal taxa. Fungal Diversity 78, 1–237.
Li J, Jia ZF. 2016 – *Diorygma fuscum* sp. nov. from China. Mycotaxon 131(3), 717–721.
Li WL, Dissanayake AJ, Luo ZL, Su HY et al. 2021 – Additions to *Distoseptispora* (*Distoseptisporaceae*) associated with submerged decaying wood in China. Phytotaxa 520, 75–86.
Li WL, Liang RR, Dissanayake AJ, Liu JK. 2023 – Mycosphere Notes 413–448: Dothideomycetes associated with woody oil plants in China. Mycosphere 14(1), 1436–1529.
Li WL, Maharachchikumbura SSN, Cheewangkoon R, Liu JK. 2022 – Reassessment of *Dyfrolomyces* and four new species of *Melomastia* from Olive (*Olea europaea*) in Sichuan Province, China. Journal of Fungi 8(1), 76.
Lian YP, Tohtirjap A, Wu F. 2022 – Two new species of *Dacrymyces* (Dacrymycetales, Basidiomycota) from Southwestern China. Diversity 14(5), 379.
Liao C, Doilom M, Bhat DJ, Chethana KWT et al. 2025 – Unveiling four new taxa and *Nigrosynnema natarajanensis* comb. nov. in Stachybotryaceae (Hypocreales) from monocotyledon plants in Guangdong Province, China. MycoKeys 114, 299–327.
Liao C, Hyde KD, Thilini Chethana KW, Dong W et al. 2024 – Three new *Periconia* species isolated from *Wurfbainia villosa* in Guangdong, China: A discussion on the doubtful taxa clustering in this genus. Diversity 16(3), 141.
Lindau. 1897 – Engler Prantl Nat Pflanzenfam Teil I (Leipzig) 1, 373.
Link HF. 1809 – Observationes in ordines plantarum naturales. Dissertatio I. Magazin der Gesellschaft Naturforschenden Freunde Berlin 3, 3–42.
Liu B, Fan L. 1989 – Two new species of *Dacrymycetaceae* from China. Acta microbiologica Sinica 8, 22–24.
Liu J, Hu Y, Luo X, Castañeda-Ruíz RF et al. 2023a – Molecular phylogeny and morphology reveal four novel species of *Corynespora* and *Kirschsteiniothelia* (Dothideomycetes, Ascomycota) from China: A checklist for *Corynespora* reported worldwide. Journal of Fungi 9(1), 107.
Liu JK, Hyde KD, Jeewon R, Phillips AJL et al. 2017a – Ranking higher taxa using divergence times: a case study in Dothideomycetes. Fungal Diversity 84, 75–99.
Liu JK, Hyde KD, Jones EBG, Ariyawansa HA et al. 2015 – Fungal diversity notes 1–110: taxonomic and phylogenetic contributions to fungal species. Fungal Diversity 72, 1–197.
Liu JK, Maharachchikumbura SSN, McKenzie EHC, Cai L et al. 2021 – Special issue: a tribute to Kevin D. Hyde on his 65th birthday. Fungal Diversity 106, 1–6.

Liu JK, Phookamsak R, Dai DQ, Tanaka K et al. 2014 – Roussoellaceae, a new pleosporalean family to accommodate the genera *Neoroussoella* gen. nov., *Roussoella* and *Roussoellopsis*. Phytotaxa 181(1), 1–33.
Liu N, Hongsanan S, Yang J, Bhat DJ et al. 2017b – *Periconia thailandica* (Periconiaceae), a new species from Thailand. Phytotaxa 323(3), 253–263.
Liu S, Liu X, Zhang Z, Xia J et al. 2022 – Three new species of *Microdochium* (*Sordariomycetes*, *Amphisphaeriales*) on *Miscanthus sinensis* and *Phragmites australis* from Hainan, China. Journal of Fungi 8(6), 577.
Liu SL, Zhao P, Cai L, Shen S et al. 2024b – Catalogue of fungi in China 1. New taxa of plant-inhabiting fungi. Mycology 16(1), 1–58.
Liu SL, Wang XW, Li GJ, Deng CY et al. 2024a – Fungal diversity notes 1717–1817: taxonomic and phylogenetic contributions on genera and species of fungal taxa. Fungal Diversity 124, 1–216.
Liu XF, Tibpromma S, Hughes AC, Chethana KWT et al. 2023b – Culturable mycota on bats in central and southern Yunnan Province, China. *Mycosphere* 14, 497–662.
Liu XZ, Zhang KQ. 1994 – Nematode-trapping species of *Monacrosporium* with special reference to two new species. Mycological Research 98, 862–868.
Lorito M, Woo SL, Harman GE, Monte E. 2010 – Translational Research on *Trichoderma*: from 'omics to the field. *Annual Review of Phytopathology* 48, 395–417.
Lu L, Tibpromma S, Karunarathna S, Thiyagaraja V et al. 2021 – Taxonomic and phylogenic appraisal of a novel species and a new record of Stictidaceae from coffee in Yunnan Province, China. Phytotaxa 528, 111–124.
Lu W, Chen X, Kumla J, Suwannarach N et al. 2025 – A new species of *Favolaschia* (Agaricales, Mycenaceae) from Yunnan Province, China. Phytotaxa 694(2), 144–160.
Lumbsch HT, Huhndorf SM. 2010 – Outline of Ascomycota – 2009. Myconet 14, 1–64.
Luo ZL, Hyde KD, Liu JK, Bhat DJ et al. 2018 – Lignicolous freshwater fungi from China II: novel *Distoseptispora* (*Distoseptisporaceae*) species from northwestern Yunnan Province and a suggested unified method for studying lignicolous freshwater fungi. Mycosphere 9, 444–461.
Luo ZL, Hyde KD, Liu JK, Maharachchikumbura SSN et al. 2019 – Freshwater *Sordariomycetes*. Fungal Diversity 99, 451–660.
Lye P, Cheng J, Lum L, Chew KL et al. 2022 – *Muyocopron laterale*: invasive human infection of a plant pathogen in an immunocompromised host. Picture of a Microorganism 28(10), 1351–1352.
Ma J, Wang Y, O'Neill NR, Zhang XG. 2011 – A revision of the genus *L.*, with the description of a new species. Mycologia 103(2), 407–410.
Ma X, Chomnunti P, Doilom M, Daranagama DA et al. 2022 – Multigene phylogeny reveals endophytic Xylariales novelties from *Dendrobium* species from Southwestern China and Northern Thailand. J Fungi 8(3), 248.
MacKenzie KJ, Sumabat LG, Xavier KV, Vallad GE. 2018 – A review of *Corynespora cassiicola* and its increasing relevance to tomato in Florida. Plant Health Progress 19(4), 303–309.
Magnago AC, Trierveiler-Pereira L, Neves MA. 2013 − Contributions towards the knowledge of *Favolaschia* (*Mycenaceae*, *Agaricomycetes*) from Brazil. Mycosphere 4(6), 1071–1078.
Maharachchikumbura SS, Wanasinghe DN, Elgorban AM, Al-Rejaie SS et al. 2022 – *Brunneosporopsis yunnanensis* gen. et sp. nov. and *Allocryptovalsa xishuangbanica* sp. nov., New Terrestrial Sordariomycetes from Southwest China. Life 12, 635.
Maharachchikumbura SSN, Hyde KD, Jones EBG, McKenzie EHC et al. 2016 – Families of Sordariomycetes. Fungal Diversity 79, 1–317.
Maharachchikumbura SSN, Hyde KD, Jones EBG, McKenzie EHC et al. 2015 – Towards a natural classification and backbone tree for Sordariomycetes. Fungal Diversity 72, 199–301.
Mains EB. 1958 – North American entomogenous species of Cordyceps. Mycologia 50(2), 169–222.

Manawasinghe IS, Calabon MS, Jones EBG, Zhang YX et al. 2022 – Mycosphere notes 345–386. Mycosphere 13(1), 454–557.
Manawasinghe IS, Hyde KD, Wanasinghe DN, Karunarathna SC et al. 2024 – Fungal diversity notes 1818–1918: taxonomic and phylogenetic contributions on genera and species of fungi. Fungal Diversity 130, 1–261.
Mapook A, Macabeo APG, Thongbai B, Hyde KD et al. 2020 – Polyketide-derived secondary metabolites from a Dothideomycetes fungus, *Pseudopalawania siamensis* gen. et sp. nov., (Muyocopronales) with antimicrobial and cytotoxic activities. Biomolecules 10, 569.
Markovskaja S, Kačergius A. 2014 – Morphological and molecular characterisation of *Periconia pseudobyssoides* sp. nov. and closely related *P. byssoides*. Mycological progress 13, 291–302.
Mazyar Y. 2010 – An in vitro study on the adsorption, absorption and uptake capacity of Zn by the bioremediator Trichoderma atroviride. Environmentasia 3, 53–59.
McKenzie EH. 2010 – Three new phragmosporous hyphomycetes on *Ripogonum* from an 'ecological island' in New Zealand. Mycotaxon 111(1), 183–196.
Mcnabb RFR. 1973 – Taxonomic studies in the *Dacrymycetaceae* VIII. Dacrymyces Nees ex Fries. New Zealand Journal of Botany 11(3), 461–524.
Mendes-Alvarenga RL, Gibertoni TB. 2022 – *Dacrymyces flavobrunneus* sp. nov. and two new combinations in *Dacrymyces* Nees based on morphological and phylogenetic data. Mycological Progress 21(12), 96.
Mifsud S. 2017 – Contribution to the Mycobiota and Myxogastria of the Maltese islands. Part I (2014-2016). Micol Veget Medit 32(1), 3–58.
Miller MA, Pfeiffer W, Schwartz T. 2012 – The CIPRES science gateway: enabling high-impact science for phylogenetics researchers with limited resources. Proceedings of the 1st Conference of the Extreme Science and Engineering Discovery Environment - Chicago, Illinois (2012.07.16–2012.07.20): Bridging from the extreme to the campus and beyond (XSEDE'12), Association for Computing Machinery, USA. pp. 1–8.
Miyamoto T, Ishii H, Seko T, Kobori S, Tomita Y. 2009 – Occurrence of *Corynespora cassiicola* isolates resistant to boscalid on cucumber in Ibaraki Prefecture, Japan. Plant Pathology 58(6), 1144–1151.
Miyazawa K, Ohmura YJP, Systematics F. 2024 – Discovery of the first lichenized fungus in the family Chaetothyriaceae (Ascomycota), *Ceramothyrium ryukyuense* sp. nov. Plant and Fungal Systematics 69(2), 167–176.
Mongkolsamrit S, Noisripoom W, Tasanathai K, Kobmoo N et al. 2022 – Comprehensive treatise of *Hevansia* and three new genera *Jenniferia*, *Parahevansia* and *Polystromomyces* on spiders in Cordycipitaceae from Thailand. MycoKeys 91, 113–149.
Mortimer PE, Jeewon R, Xu JC, Lumyong S, Wanasinghe DN. 2021 – Morpho-phylo taxonomy of novel dothideomycetous fungi associated with dead woody twigs in Yunnan Province, China. Frontiers in Microbiology 12, 654683.
Mueller GM. 1992 – Systematics of *Laccaria* (Agaricales) in the continental United States and Canada, with discussions on extralimital taxa and descriptions of extant types. Chicago, USA: Field Museum of Natural History 1992, 158p.
Mukherjee PK, Singh US, Horwitz BA, Schmoll M, Mukherjee M. 2013 – *Trichoderma*: biology and applications. Wallingford, UK: CABI. p. 344.
MycoBank. 2025 – Available at: https://www.mycobank.org/ (Accessed on January 2025)
Myoken Y, Sugata T, Fujita Y, Asaoku H et al. 2002 – Fatal necrotizing stomatitis due to *Trichoderma longibrachiatum* in a neutropenic patient with malignant lymphoma: a case report. International Journal of Oral & Maxillofacial Surgery 31, 688–691.
Na Q, Liu ZW, Zeng H, Cheng XH, Ge YP. 2022 – *Crepidotus yuanchui* sp. nov. and *C. caspari* found in subalpine areas of China. Mycoscience 63, 1–11.
Nayana P, Pradeep C. 2024 – Morphological and phylogenetic analyses reveal two new species of *Candolleomyces* (Psathyrellaceae) from India. Phytotaxa 659(3), 255–267.

Nayana PK, Pradeep CK 2023 – A new species of *Candolleomyces* (Psathyrellaceae, Agaricales) from Western Ghats, India. Phytotaxa 606(1), 63–72.
Nees von Esenbeck CG. 1816 – Das system der pilze und schwämme: Stahelschen Buchhandlung, vol. 2. Würtzburg, Germany, pp. 1–329.
Nghia NA, Kadir J, Sunderasan E, Abdullah MP et al. 2008 – Morphological and Inter Simple Sequence Repeat (ISSR) markers analyses of *Corynespora cassiicola* isolates from rubber plantations in Malaysia. Mycopathologia 166,189–201.
Niskanen T, Lücking R, Dahlberg A, Gaya E et al. 2023 – Pushing the frontiers of biodiversity research: Unveiling the global diversity, distribution, and conservation of fungi. Annual review of Environment and resources 48(1), 149–176.
Nitschke T. 1870 – *Pyrenomycetes Germanici* (2nd ed.). Eduard Trewendt, Germany, Breslau, pp 161–320.
Nograsek A, Matzer M. 1991 – Nicht-pyrenokarpe Ascomyceten auf Gefässpflanzen der Polsterseggenrasen. I. Arten auf Dryas octopetala. Nova Hedwigia 53(3–4), 445–475.
Nograsek A, Matzer M. 1994 – Nicht-pyrenokarpe Ascomyceten auf Gefäßpflanzen der Polsterseggenrasen. II. Arten auf Cyperaceae und Poaceae. Nova Hedwigia 58(1–2), 1–48.
Norphanphoun C, Gentekaki E, Hongsanan S, Jayawardena R et al. 2022 – *Diaporthe*: formalizing the species-group concept. Mycosphere 13(1), 752–819.
Norphanphoun C, Jeewon R, Mckenzie EHC, Wen TC et al. 2017 – Taxonomic position of *Melomastia italica* sp. nov. and phylogenetic reappraisal of Dyfrolomycetales. Cryptogamie Mycologie 38, 507–525.
Okane I, Nonaka K, Kurihara Y, Junichi P et al. 2020 – A new species of *Leptobacillium*, *L. symbioticum*, isolated from mites and sori of soybean rust. Mycoscience 61, 165–171.
Osorio JA, Linnakoski R, Wingfield MJ, de Beer ZW et al. 2021 – A new species in the Mycosphaerellaceae from Cecidomyiidae leaf galls on *Avicennia marina* in South Africa. Antonie van Leeuwenhoek 114, 515–526.
Patouillard N. 1900b − Essai Taxonomique sur les Families et les Genres des *Hyménomycètes*; Lucien Declume: Lons-le-Saaunier, France.
Patouillard NT, Lagerheim G. 1892 – Champignons de l'Équateur. Pugillus II. Bulletin de la Société Mycologique de France 8, 113–140.
Patouillard NT. 1900a – Champignons de la Guadeloupe. Bulletin de la Société Mycologique de France 16, 175–188.
Pem D, Hyde KD, McKenzie EHC, Hongsanan S et al. 2024 – A comprehensive overview of genera in Dothideomycetes. Mycosphere 15(1), 2175–4568.
Pem D, Jeewon R, Bhat DJ, Doilom M et al. 2019 – Mycosphere Notes 275-324: A morphotaxonomic revision and typification of obscure Dothideomycetes genera (incertae sedis). Mycosphere 10(1), 1115–1246.
Pem D, Jeewon R, Chethana KWT, Hongsanan S et al. 2021 – Species concepts of Dothideomycetes: classification, phylogenetic inconsistencies and taxonomic standardization. Fungal Diversity 109, 283–319.
Perera RH, Maharachchikumbura SSN, Ariyawansa H, Bahkali AH et al. 2016 – Two new *Pseudohalonectria* species on beech cupules (*Fagus sylvatica*) and a new genus to accommodate *P. suthepensis*. Phytotaxa 278, 115–131.
Persoon CH. 1794 – Dispositio methodica fungorum. *Romer's Neues Magazin Botanische* 1, 81–128.
Petch T. 1923 – The genus *Cladosterigma* Pat. Transactions of the British Mycological Society 8(4), 212–215.
Petch T. 1931 – Notes on entomogenous fungi. Transactions of the British Mycological Society 16(4), 209–245.
Pfister DH. 1997 – Castor, Pollux, and life histories of fungi. Micologia 89, 1–23.
Phengsintham P, Braun U, McKenzie EHC, Chukeatirote E et al. 2013a – Monograph of Cercosporoid fungi from Thailand. Plant Pathology & Quarantine 3(2), 67–138.

Phengsintham P, Chukeatirote E, McKenzie EHC, Hyde KD et al. 2013b – Monograph of Cercosporoid Fungi from Laos. Current Research in Environmental & Applied Mycology 3(1), 34–158.
Phengsintham P, Chukeatirote E, McKenzie EHC, Moslem MA et al. 2010 – Two new species and a new record of cercosporoids from Thailand. Mycosphere 1(3), 205–212.
Phookamsak R, Hyde KD, Jeewon R, Bhat DJ et al. 2019 – Fungal diversity notes 929–1035: taxonomic and phylogenetic contributions on genera and species of fungi. Fungal diversity 95, 1–273.
Phukhamsakda C, Jeewon R, McKenzie EHC, Xu JC. 2019 – Morphology and phylogeny of *Phaeoseptum mali* sp. nov. (*Phaeoseptaceae*, *Pleosporales*) on bark of *Malus halliana*. AJOM 2, 118–128.
Phukhamsakda C, McKenzie EHC, Phillips AJL, Gareth Jones EB et al. 2020 – Microfungi associated with *Clematis* (Ranunculaceae) with an integrated approach to delimiting species boundaries. Fungal Diversity 102, 1–203.
Prasher IB, Sushma Prasher SP. 2014 – *Hermatomyces indicus* sp. nov. (Hyphomycetes) from India. Nova Hedwigia 99(3–45), 51–556.
Preedanon S, Suetrong S, Srihom C, Somrithipol S et al. 2023 – Eight novel cave fungi in Thailand's Satun Geopark. Fungal Systematics and Evolution 12, 1–30.
Quaedvlieg W, Binder M, Groenewald JZ, Summerell BA et al. 2014 – Introducing the consolidated species concept to resolve species in the *Teratosphaeriaceae*. Persoonia: Molecular Phylogeny and Evolution of Fungi 33, 1–40.
Quandt CA, Kepler RM, Gams W, Araújo JP et al. 2014 – Phylogenetic-based nomenclatural proposals for Ophiocordycipitaceae (Hypocreales) with new combinations in Tolypocladium. IMA fungus 5, 121–134.
Raitviír A, Järv H. 1997 – Arcto-alpine Leotiales and Ostropales from the mountains of South Norway. Proceedings of the Estonian Academy of Sciences Biology and Ecology 46, 94–111.
Rajwar S, Singh R, Kumar S, Singh PN et al. 2025 – Morphology and phylogeny of *Pseudocercospora trifoliorum* sp. nov. (Mycosphaerellaceae) on *Grona triflora* from India. Phytotaxa 681(2), 167–185.
Réblová M, Stepanek V, Schumacher RK. 2014 – *Xylochrysis lucida* gen. et sp. nov., a new lignicolous ascomycete (Sordariomycetidae) with holoblastic conidiogenesis. Mycologia 106(3), 564–572.
Rehm H. 1893 – Rabenhorst's Kryptogamen-Flora, Pilze - Ascomyceten. 1.3(39–41), 721–912.
Ren GC, Wanasinghe DN, Monkai J, Mortimer PE et al. 2021 – Novel saprobic *Hermatomyces* species (*Hermatomycetaceae*, Pleosporales) from China (Yunnan Province) and Thailand. MycoKeys 82, 57–79.
Rodríguez HMC, Evans HC, Abreu LM, Macedo DM et al. 2021 – New species and records of *Trichoderma* isolated as mycoparasites and endophytes from cultivated and wild coffee in Africa. Scientific Reports 11, 1–30.
Rondilla RRL, dela Cruz TEE, Chang F, Nonato MG. 2022 – *Annulohypoxylon stygium*, a *Pandanus simplex*-associated fungal endophyte with *α*-glucosidase inhibitory activity. Studies in Fungi 7, 4.
Rossman AY, Adams GC, Cannon PF, Castlebury LA et al. 2015 – Recommendations of generic names in Diaporthales competing for protection or use. IMA Fungus 6, 145–154.
Saccardo PA, Paoletti G. 1888 – Mycetes Malacenses. Funghi della penisola di Malacca raccolti nel 1885 dell. Ab Benedetto Scortechini 6, 387–428.
Saccardo PA. 1875 – Conspectus generum pyrenomycetum italicorum additis speciebus fungorum Venetorum novis vel criticis, systemate carpologico dispositorum. Atti della Società Veneto-Trentina-di Istriana Scienze Naturali 4, 77–100.
Saccardo PA. 1883 – Sylloge *Pyrenomycetum*, Vol. II. Sylloge Fungorum 2, 1–813.
Saccardo PA. 1889 – Discomyceteae et Phymatosphaeriaceae. Sylloge Fungorum 8, 1–1143.

Samson RA, Brady BL. 1982 – *Akanthomyces novoguineensis sp*. nov. Transactions of the British Mycological Society 79(3), 571–572.
Samson RA, Evans HC. 1974 – Note on entomopathogenous fungi from Ghana. II. The genus *Akanthomyces*. Acta Botanica Neerlandica 23(1), 28–35.
Samuels GJ. 1996 – *Trichoderma*: A review of biology and systematics of the genus. Mycological research 100, 923–935.
Sarkar T, Chakraborty P, Karmakar A, Saha A, Saha D. 2019 – First report of *Periconia macrospinosa* causing leaf necrosis of pointed gourd in India. Journal of Plant Pathology 101, 1281.
Savchenko A, Zamora JC, Shirouzu T, Spirin V et al. 2021 – Revision of *Cerinomyces* (Dacrymycetes, Basidiomycota) with notes on morphologically and historically related taxa. Studies in Mycology 99(1), 1–72.
Scholler M, Hagedorn G, Rubner A. 1999 – A reevaluation of predatory orbiliaceous fungi. II. A new generic concept. Sydowia 51, 89–113.
Senanayake IC, Rathnayaka AR, Marasinghe DS, Calabon MS et al. 2020 – Morphological approaches in studying fungi: collection, examination, isolation, sporulation and preservation. Mycosphere 11(1), 2678–2754.
Senanayake IC, Rossi W, Leonardi M, Weir A et al. 2023 – Fungal diversity notes 1611–1716: taxonomic and phylogenetic contributions on fungal genera and species emphasis in south China. Fungal Diversity 122, 161–403.
Senn-Irlet B. 1995 – The genus *Crepidotus* (Fr.) Staude in Europe. Persoonia-Molecular Phylogeny and Evolution of Fungi 16, 1–80.
Senwanna C, Hongsanan S, Khuna S, Kumla J et al. 2024 – Insights into the molecular phylogeny and morphology of three novel *Dothiora* species, along with a worldwide checklist of *Dothiora*. Frontiers in Cellular and Infection Microbiology 14, 1367673.
Senwanna C, Phookamsak R, Doilom M, Hyde KD, Cheewangkoon R. 2017 – Novel taxa of Diatrypaceae from Para rubber (*Hevea brasiliensis*) in northern Thailand; introducing a novel genus *Allocryptovalsa*. Mycosphere 8, 1835–1855.
Senwanna, C, Hongsanan S, Phookamsak R, Tibpromma S et al. 2019 – *Muyocopron heveae* sp. nov. and *M. dipterocarpi* appears to have host-jumped to rubber. Mycological Progress 18, 741–752.
Shearer CA, Crane JL, Chen W. 1999 – Freshwater Ascomycetes: *Ophioceras* species. Mycologia 91, 145–456.
Shearer CA, Crane JL. 1971 – Fungi of the Chesapeake Bay and its Tributaries. I. Patuxent River. Mycologia 63, 237–260.
Shen HW, Bao DF, Boonmee S, Lu YZ et al. 2024b – Diversity of *Distoseptispora* (*Distoseptisporaceae*) taxa on submerged decaying wood from the Red River in Yunnan, China. MycoKeys 102, 1–28.
Shen HW, Bao DF, Boonmee S, Su XJ et al. 2023 – Lignicolous freshwater fungi from plateau lakes in China (I): Morphological and phylogenetic analyses reveal eight species of *Lentitheciaceae*, including new genus, new species and new records. Journal of Fungi 9, 962.
Shen HW, Luo ZL, Bao DF, Luan S et al. 2024a – Lignicolous freshwater fungi from China IV: Morphology and phylogeny reveal new species of Pleosporales from plateau lakes in Yunnan Province, China. Mycosphere 15, 6439–6524.
Shirouzu T, Hirose D, Oberwinkler F, Shimomura N et al. 2013 – Combined molecular and morphological data for improving phylogenetic hypothesis in *Dacrymycetes*. Mycologia 105(5), 1110–1125.
Shirouzu T, Hirose D, Tokumasu S. 2009 – Taxonomic study of the Japanese *Dacrymycetes*. Persoonia-Molecular Phylogeny and Evolution of Fungi 23(1), 16–34.

Shoemaker RA, Babcock CE. 1992 – Apllanodictyosporous Pleosporales: *Clathrospora*, *Comoclathris*, *Graphylliyum*, *Macrospora*, *Platysporoides*. Canadian Journal of Botany 70, 1617–1658.
Silvestro D, Michalak I. 2012 – raxmlGUI: a graphical front-end for RAxML. Organisms Diversity & Evolution 12, 335–337.
Singer R. 1945 − The Laschia-complex (*Basidiomycetes*). Lloydia 8, 170–230.
Singer R. 1974 − A monograph of *Favolaschia*. Beihefte zur Nova Hedwigia 50, 1–108.
Singer R. 1986 – The Agaricales in Modern Taxonomy; Koeltz Scientific Books: Koenigstein, Germany.
Singh A, Yadav S, Singh R, Dubey NK. 2022 – Taxonomy and phylogeny of a new species of *Pseudocercospora* on *Solanum nigrum* from India. Turkish Journal of Botany 46, 507–516.
Singh R, Chaurasia B, Shukla K, Upadhyaya PP. 2012 – *Passalora aseptata*, a new cercosporoid fungus from northeastern Uttar Pradesh, India. Mycotaxon 120, 461–463.
Singh R, Kumar S, Kamal. 2011 – Two new species of *Passalora* and *Pseudocercospora* from northeastern Uttar Pradesh, India. Mycotaxon 117, 137–143.
Singh R, Kumar S, Saini DC, Upadhyaya PP et al. 2013 – Diversity of *Passalora* on *Ficus*. Mycological Progress 12, 637–643.
Singh R, Verma SK, Yadav S, Bhojak P et al. 2020 – Morphology and phylogeny of *Pseudocercospora hamiltoniani*—A new species comparable to *Sirosporium* from Uttarakhand, India. Phytotaxa 458(4), 281–293.
Sivanesan A. 1984 – The bitunicate ascomycetes and their anamorphs. J. Cramer, Vaduz, p 701.
Song JY, Yang Y, Yu XD, Dissanayake AJ, Tian Q. 2023 – *Xylochrysis aquatica* sp. nov. (Woswasiaceae) from freshwater habitats in Sichuan Province, China. Phytotaxa 587(1), 31–38.
Sousa TF, Reça BNPV, Castro GS, Da Silva IJS et al. 2023 – *Trichoderma agriamazonicum* sp. nov. (Hypocreaceae), a new ally in the control of phytopathogens. Microbiological Research 275, 127469.
Spegazzini C. 1881 – Fungi argentini additis nonnullis brasiliensibus montevideensibusque. Pugillus quartus (Continuacion). Anales de la Sociedad Científica Argentina 12, 97–117.
Spegazzini C. 1910 – Mycetes Argentinenses (Series V). Anales del Museo Nacional de Historia Natural Buenos Aires 3, 329–467.
Staiger B. 2002 – Die Flechtenfamilie Graphidaceae. Bibliotheca Lichenologica 85, 1–526.
Stamatakis A. 2014 – RAxML version 8: a tool for phylogenetic analysis and post-analysis of large phylogenies. Bioinformatics 30, 1312–1313.
Su HY, Hyde KD, Maharachchikumbura SSN, Ariyawansa HA et al. 2016 – The families *Distoseptisporaceae* fam. nov., *Kirschsteiniotheliaceae*, *Sporormiaceae* and *Torulaceae*, with new species from freshwater in Yunnan Province, China. Fungal Diversity 80(1), 375–409.
Su P, Lu Z, Tian W, Chen Y, Maharachchikumbura SSN. 2023 – Six additions to the genus *Periconia* (Dothideomycetes: Periconiaceae) from *graminaceous* plants in China. Journal of Fungi 9(3), 300.
Subramanian CV. 1954 – Three new hyphomycetes. Journal of the Indian Botanical Society. 33, 28–35.
Subramanian CV. 1961 – On some species of *Cryptostictis*. Proceedings of the National Institute of Sciences of India, Part B: Biological Sciences 27, 236–245.
Subramanian CV. 1963 – *Dactylella*, *Monacrosporium* and *Dactylina*. Journal of the Indian Botanical Society 42, 291–300.
Suková M. 2005 – A revision of selected material of lignicolous species of *Brunnipila, Capitotricha, Dasyscyphella* and *Neodasyscypha* from the Czech Republic. Czech Mycology 57(1–2), 139.

Sun Y, Goonasekara ID, Thambugala KM, Jayawardena RS et al. 2020 – *Distoseptispora bambusae* sp. nov. (Distoseptisporaceae) on bamboo from China and Thailand. Biodiversity Data Journal 8, e53678.
Sung GH, Hywel-Jones NL, Sung JM, Luangsa-Ard JJ et al. 2007 – Phylogenetic classification of Cordyceps and the clavicipitaceous fungi. Studies in mycology 57, 5–59.
Sutton BC, Alcorn JL. 1974 – *Neottiosporina*. Australian Journal of Botany 22(4), 517–532.
Sutton BC, Marasas WFO. 1976 – Observations on *Neottiosporina* and *Tiarosporella*. Transactions of the British Mycological Society 67(1), 69–76.
Sutton BC, Wu WP. 1995 – *Neottiosporina sorghicola* sp. nov., associated with leaf lesions on *Sorghum vulgare* from China. Mycological Research 99(7), 831–832.
Sutton BC. 1975 – Coelomycetes. V. *Coryneum*. Mycological Papers 138, 1–224.
Swofford DL, Sullivan J. 2003 – Phylogeny inference based on parsimony and other methods using PAUP*. The phylogenetic handbook: a practical approach to DNA and protein phylogeny 1–160.
Sydow H. 1924 – Mycotheca germanic. Fasc. XLII–XLV (No. 2051–2250). Annales Mycologici 22, 257–268.
Tan YP, Bishop-Hurley SL, Shivas RG, Cowan DA et al. 2022 – Fungal Planet description sheets: 1436–1477. Persoonia 49, 261–350.
Tan YP, Shivas RG. 2022a – Index of Australian Fungi no. 3, 1–21.
Tan YP, Shivas RG. 2022b – Index of Australian Fungi no. 1, 1–18.
Tan YP, Shivas RG. 2024 – Index of Australian Fungi no. 35, 1–16.
Tanaka K, Harada Y. 2003 – *Pleosporales* in Japan (3): the genus *Massarina*. Mycoscience 44, 173–185.
Tanaka K, Hirayama K, Yonezawa H, Sato G et al. 2015 – Revision of the *massarineae* (Pleosporales, Dothideomycetes). Studies in mycology 82, 75–136.
Tang SM, Vadthanarat S, Raghoonundon B, Luo ZL et al. 2024 – New species and new records of *Laccaria* (Agaricales, Basidiomycota) from Northern Thailand. MycoKeys 107, 189–217.
Tang SM, Zhao G, Niu KY, Li RY et al. 2025 – Species diversity of edible mushrooms I – four New *Laccaria* species from Yunnan province, China. Journal of Fungi 11(3), 189.
Tedersoo L, Bahram M, Põlme S, Kõljalg U et al. 2014 – Global diversity and geography of soil fungi. Science 346, 1256688.
Teles HL, Sordi R, Silva GH, Castro-Gamboa I et al. 2006 – Aromatic compounds produced by P*ericonia atropurpurea*, an endophytic fungus associated with *Xylopia aromatica*. Phytochemistry 67(24), 2686–2690.
Tennakoon DS, Kuo CH, Maharachchikumbura SS, Thambugala KM et al. 2021 – Taxonomic and phylogenetic contributions to *Celtis formosana*, *Ficus ampelas*, *F. septica*, *Macaranga tanarius* and *Morus australis* leaf litter inhabiting microfungi. Fungal Diversity 108(1), 1–215.
Tennakoon DS, Thambugala KM, Jeewon R, Hongsanan S et al. 2019 – Additions to Chaetothyriaceae (Chaetothyriales): *Longihyalospora* gen. nov. and *Ceramothyrium longivolcaniforme*, a new host record from decaying leaves of *Ficus ampelas*. MycoKeys 61, 91–109.
Thambugala KM, Ariyawansa HA, Li YM, Boonmee S et al. 2014 – Dothideales. Fungal Diversity 68, 105–158.
Thambugala KM, Wanasinghe DN, Phillips AJL, Camporesi E et al. 2017 – Mycosphere notes 1-50: Grass (Poaceae) inhabiting Dothideomycetes. Mycosphere 8(4), 697–796.
Theissen F, Sydow H. 1915 – Die Dothideales. Kritisch-systematische riginaluntersuchungen. Annales Mycologici 13, 147–746.
Theissen F, Sydow H. 1917 – Synoptische Tafeln. Annales Mycologici 15, 389–491.
Thiyagaraja V, Lücking R, Ertz D, Karunarathna S et al. 2021 – The evolution of life modes in Stictidaceae, with three novel taxa. Journal of Fungi 7, 105.

Tibpromma S, Bhat J, Doilom M, Lumyong S et al. 2016 – Three new *Hermatomyces* species (*Lophiotremataceae*) on *Pandanus odorifer* from Southern Thailand. Phytotaxa 275, 127–139.

Tibpromma S, Hyde KD, Bhat JD, Mortimer PE et al. 2018b – Identification of endophytic fungi from leaves of Pandanaceae based on their morphotypes and DNA sequence data from southern Thailand. MycoKeys 33, 25–67.

Tibpromma S, Hyde KD, Jeewon R, Maharachchikumbura SS et al. 2017 – Fungal diversity notes 491–602: taxonomic and phylogenetic contributions to fungal taxa. Fungal Diversity 83, 1–261.

Tibpromma S, Hyde KD, McKenzie EHC, Bhat DJ et al. 2018a – Fungal diversity notes 840–928: micro-fungi associated with Pandanaceae. Fungal Diversity 93, 1–160.

Tochihara Y, Sasagawa R, Hosoya T. 2019 – Enumeration of remarkable Japanese Discomycetes (11): Notes on three species of Lachnaceae new to Japan with one new combination. Bulletin of the National Museum of Nature and Science, Series B (Botany) 45(2), 47–55.

Tode HJ. 1791 – Fungi Mecklenburgenses Selecti. Fasc. II; Generum Novorum Appendicem; Kessinger Publishing, LLC: Lüneburg, Germany Volume 2, pp. 1–67.

Treseder KK, Lennon JT. 2015 – Fungal traits that drive ecosystem dynamics on land. Microbiology and Molecular Biology Reviews 79, 243–262.

Tripathi P, Singh PC, Mishra A, Chauhan PS, et al. 2013 –*Trichoderma*: A potential bioremediator for environmental clean up. Clean Technologies and Environmental Policy 15, 541– 550.

Trouillas FP, Pitt WM, Sosnowski MR, Huang R et al. 2011 – Taxonomy and DNA phylogeny of Diatrypaceae associated with Vitis *vinifera* and other woody plants in Australia. Fungal Diversity 49, 203–223.

Tsui CKM, Leung YM, Hyde KD, Hodgkiss IJ. 2001 – Three new *Ophioceras* species (Ascomycetes) from the tropics. Mycoscience 42, 321–326.

Vanderwolf KJ, McAlpine DF, Malloch D, Forbes GJ. 2013 – Ectomycota associated with hibernating bats in eastern Canadian caves prior to the emergence of white-nose syndrome. Northeastern Naturalist 20, 115–130.

Verma SK, Yadav S, Singh G, Singh R. 2021 – *Pseudocercospora cappadocici*, a new *Stigmina*-like *Pseudocercospora* species on *Acer cappadocicum* from India. Sydowia 74, 79–91.

Videira SI, Groenewald JZ, Nakashima C, Braun U et al. 2017 – *Mycosphaerellaceae*–chaos or clarity? Studies in Mycology 87, 257–421.

Vincenot L, Popa F, Laso F, Donges K et al. 2017 – Out of Asia: Biogeography of fungal populations reveals Asian origin of diversification of the *Laccaria amethystina* complex, and two new species of violet *Laccaria*. Fungal Biology 121, 939–955.

Voglmayr H, Jaklitsch WM. 2017 – *Corynespora, Exosporium* and *Helminthosporium* revisited-new species and generic reclassification. Studies in Mycology 87(1), 43–76.

Voglmayr H, Jaklitsch WM. 2019 – *Stilbocrea walteri* sp. nov., an unusual species of Bionectriaceae. Mycological progress 18, 91–105.

Von Arx JA, Müller E. 1975 – A re-evaluation of the bitunicate ascomycetes with keys to families and genera. Studies in Mycology 9, 1–159.

Wächter D, Melzer A. 2020 – Proposal for a subdivision of the family Psathyrellaceae based on a taxon-rich phylogenetic analysis with iterative multigene guide tree. Mycological Progress 19, 1151–1265.

Wanasinghe DN, Mortimer PE, Senwanna C, Cheewangkoon R. 2020 – Saprobic Dothideomycetes in Thailand: *Phaeoseptum hydei sp. nov*., a new terrestrial ascomycete in Phaeoseptaceae. Phytotaxa. 449, 149–163.

Wanasinghe DN, Phukhamsakda C, Hyde KD, Jeewon R et al. 2018 – Fungal diversity notes 709–839: taxonomic and phylogenetic contributions to fungal taxa with an emphasis on fungi on Rosaceae. Fungal Diversity 89, 1–236.

Wang K, Liu DM, Li GJ, Liu TZ et al. 2023 – Taxonomy of *Laccaria* in China based on the specimens collected in the HMAS. Journal Fungal Research 20, 271–284.

Wang M, Liu F, Crous PW, Cai L. 2017 – Phylogenetic reassessment of *Nigrospora*: ubiquitous endophytes, plant and human pathogens. Persoonia-Molecular Phylogeny and Evolution of Fungi 39(1), 118–142.
Wang WP, Hyde KD, Bao DF, Wanasinghe DN, Lin CG et al. 2024 – Lignicolous freshwater fungi from karst landscapes in Yunnan Province, China. Mycosphere 15(1), 6525–6640.
Wei DP, Wanasinghe DN, Gentekaki E, Thiyagaraja V et al. 2021 – Morphological and phylogenetic appraisal of novel and extant taxa of Stictidaceae from northern Thailand. Journal of Fungi 7, 880.
Wei DP, Wanasinghe DN, Hyde KD, Mortimer PE, et al. 2019 – The genus *Simplicillum*. MycoKeys 60, 69–92.
Wibberg D, Stadler M, Lambert C, Bunk B et al. 2021 – High quality genome sequences of thirteen Hypoxylaceae (Ascomycota) strengthen the phylogenetic family backbone and enable the discovery of new taxa. Fungal Diversity 106, 7–28.
Wijayawardene NN, Hyde KD, Rajeshkumar KC, Hawksworth DL et al. 2017 – Notes for genera: Ascomycota. Fungal Diversity 86, 1–594.
Wijesinghe S, Dayarathne M, Maharachchikumbura S, Wanasinghe D et al. 2019 – *Ceramothyrium chiangraiense*, a novel species of Chaetothyriales (Eurotiomycetes) from *Ficus* sp. in Thailand. Asian Journal of Mycology 2(1), 269–280.
Wijesinghe SN, Zucconi L, Camporesi E, Wanasinghe DN et al. 2022 – An updated account of Fagales-inhabiting Italian Ascomycota and mycogeography, with additions to Pezizomycotina. Asian Journal of Mycology 5(2), 79–186.
Wilson AW, Hosaka K, Mueller G. 2017 – Evolution of ectomycorrhizas as a driver of diversification and biogeographic patterns in the model mycorrhizal mushroom genus *Laccaria*. New Phytologist 213, 1862–1873.
Wilson AW, Hosaka K, Perry BA, Mueller GM. 2013 – *Laccaria* (Agaricomycetes, Basidiomycota) from Tibet (Xizang Autonomous Region, China). Mycoscience 54, 406–419.
Wimalasena MK, Wijayawardene NN, Bamunuarachchige TC, Zhang GQ et al. 2025 – E*ctophoma salviniae* sp. nov., *Neottiosporina mihintaleensis* sp. nov. and four other endophytes associated with aquatic plants from Sri Lanka and their extracellular enzymatic potential. Frontiers in Cellular and Infection Microbiology 14, 1475114.
Woudenberg JHC, Groenewald JZ, Binder M, Crous PW. 2013 – *Alternaria* redefined. Studies in Mycology 75, 171–212.
Wu K, Tian W, Syed A, Elgorban AM et al. 2023 – Description of two new species of *Roussoella* (Roussoellaceae, Pleosporales) associated with bamboo from Sichuan Province, China. Phytotaxa 607(4), 235–248.
Wu W, Diao Y. 2022 – Anamorphic chaetosphaeriaceous fungi from China. Fungal Diversity 116(1), 1–546.
Wu YH, Chen GD, He RR, Wang CX et al. 2015 – Pericolactines A–C, a new class of diterpenoid alkaloids with unusual tetracyclic skeleton. Scientific Reports 5(1), 17082.
Wu Z, Xie Z, Wu M, Li X et al. 2018 – New antimicrobial cyclopentenones from *Nigrospora sphaerica* ZMT05, a fungus derived from *Oxya chinensis* Thunber. Journal of Agricultural and Food Chemistry 66(21), 5368–5372.
Xu R, Su W, Wang Y, Tian S, Li Y, Phukhamsakda C. 2024a – Morphological characteristics and phylogenetic evidence reveal two new species and the first report of *Comoclathris* (*Pleosporaceae*, Pleosporales) on dicotyledonous plants from China. MycoKeys 12, 95–112.
Xu RF, Karunarathna SC, Phukhamsakda C, Dai DQ et al. 2024b – Four new species of Dothideomycetes (Ascomycota) from Pará Rubber (*Hevea brasiliensis*) in Yunnan Province, China. MycoKeys 103, 71–95.
Xu ZH, Kuang WG, Qiu L, Zhang XG et al. 2020 – *Corynespora sinensis* sp. nov. from Jiangxi, China. Mycotaxon 135(4), 803–809.

Yadav S, Verma SK, Singh VK, Singh R et al. 2021 – Morphology and phylogeny of a new species, *Pseudocercospora haldinae* (*Mycosphaerellaceae*) on *Haldina cordifolia* from India. Phytotaxa 501(2), 281–292.
Yang EF, Phookamsak R, Jiang HB, Tibpromma S et al. 2022 – Taxonomic reappraisal of Periconiaceae with the description of three new *Periconia* species from China. Journal of Fungi 8(3), 243.
Yang J, Liu LL, Jones EBG, Hyde KD et al. 2023a – Freshwater fungi from karst landscapes in China and Thailand. Fungal Diversity 119, 1–212.
Yang J, Liu LL, Jones EBG, Li WL et al. 2021 – Morphological variety in *Distoseptispora* and introduction of six novel species. Journal of Fungi 7, 945.
Yang KL, Lin JY, Li GM, Yang ZL. 2023c – Mushrooms adapted to seawater: two new species of *Candolleomyces* (Basidiomycota, Agaricales) from China. Journal of Fungi 9, 1204.
Yang MF, Li YP, Zheng ZS, Song RQ, Zhang SF. 2023b – First report of leaf sheath disease, caused by *Microdochium seminicola*, on *Zizania latifolia* in China. Plant Disease 107, 1942.
Ye CW, Jing TT, Sha YR, Mo MH, Yu ZF. 2023 – Two new *Trichoderma* species (Hypocreales, Hypocreaceae) isolated from decaying tubers of Gastrodiaelate. MycoKeys 99, 187– 207.
Yilmaz N, Sandoval-Denis M, Lombard L, Visagie CM et al. 2021 – Redefining species limits in the *Fusarium fujikuroi* species complex. Persoonia 46, 129–162.
Yu S, Wang R, Liu HW, Zhang X, Sun JZ. 2022 – *Trichoderma bombaxalis* sp. nov, isolated from rhizosphere soils of *Lycium barbarum*. Phytotaxa 547, 147–157.
Yu XD, Zhang SN, Liang XD, Zhu JT et al. 2024 – Bambusicolous Fungi from Southwestern China. Mycosphere 15(1), 5038–5145.
Yu XD, Zhang SN, Liu JK. 2022 – Morpho-phylogenetic evidence reveals novel Pleosporalean taxa from Sichuan Province, China. Journal of Fungi 8, 720.
Zamora JC, Ekman S. 2020 – Phylogeny and character evolution in the *Dacrymycetes*, and systematics of *Unilacrymaceae* and *Dacryonaemataceae* fam. nov. Persoonia-Molecular Phylogeny and Evolution of Fungi 44(1), 161–205.
Zare R, Gams W. 2016 – More white verticillium-like anamorphs with erect conidiophores. Mycological Progress 15, 993–1030.
Zeng Q, Lv YC, Xu XL, Deng Y et al. 2022 – Morpho-molecular characterization of microfungi associated with *Phyllostachys* (Poaceae) in Sichuan, China. Journal of Fungi 8(7), 702.
Zeng XY, Tan TJ, Tian FH, Wang Y et al. 2023 – OFPT: a one-stop software for fungal phylogeny. Mycosphere 14(1), 1730–1741.
Zeng XY, Wen TC, Chomnunti P, Liu JK et al. 2016 – *Ceramothyrium longivolcaniforme* sp. nov., a new species of Chaetothyriaceae from northern Thailand. Phytotaxa 267(1), 51–60.
Zeng ZQ, Wang XH, Zhuang WY. 2024 – New species and new Chinese record of Hypocreaceae from China. Phytotaxa 650, 093–102.
Zhang F, Yang YQ, Zhou FP, Xiao W et al. 2023b – Morphological and phylogenetic characterization of five vovel nematode-trapping fungi (Orbiliomycetes) from Yunnan, China. Journal of Fungi 9(7), 735.
Zhang GJ, Li DM. 2019 – *Trichodermasis*: a review of the literature. Mycosystema 38, 1287–1297.
Zhang GQ, Wijayawardene NN, Han LH, Kumla J et al. 2024b – Three novel woody litter inhabiting fungi in *Didymosphaeriaceae*, *Phaeoseptaceae* and *Synnemasporellaceae* from Zhujiangyuan Nature Reserve, Yunnan Province, PR China. MycoKeys 106, 173– 200.
Zhang GZ, Yang HT, Zhang XJ, Zhou FY et al. 2022c –Five new species of *Trichoderma* from moist soils in China. MycoKeys 87, 133–157.
Zhang H, Zhu R, Qing Y, Yang H et al. 2022b – Polyphasic identification of *Distoseptispora* with six new species from freshwater. Journal of Fungi 8, 1063.
Zhang J, Zhang Z, Li D, Xia J, Li Z. 2023d – Three new species of *Microdochium* (*Microdochiaceae*, *Xylariales*) on *Bambusaceae* sp. and saprophytic leaves from Hainan and Yunnan, China. Journal of Fungi 9(12), 1176.

Zhang JF, Liu JK, Hyde KD, Chen YY et al. 2023a – Ascomycetes from karst landscapes of Guizhou Province, China. Fungal Diversity 122, 1–160.
Zhang JY, Hyde KD, Zhang LJ, Bai S et al. 2025 – Two novel hyphomycetes associated with ferns from China. MycoKeys 113, 101–121.
Zhang QY, Dai YC. 2021 − Taxonomy and phylogeny of the *Favolaschia calocera* complex (*Mycenaceae*) with descriptions of four new species. Forests 12(10), 1397.
Zhang QY, Liu HG, Li WY, Zhang X et al. 2024d − Three new species of *Favolaschia* (*Mycenaceae*, *Agaricales*) from South China. MycoKeys 104, 71–89.
Zhang QY, Liu HG, Papp V, Zhou M et al. 2023e − New insights into the classification and evolution of *Favolaschia* (*Agaricales*, *Basidiomycota*) and its potential distribution, with descriptions of eight new species. Mycosphere 14(1), 777–814.
Zhang S, Zhang CL, Gao ZF, Qiu CW et al. 2023c – Integrated physiological and omics analyses reveal the mechanism of beneficial fungal *Trichoderma* sp. alleviating cadmium toxicity in tobacco (*Nicotiana tabacum* L.). Ecotoxicology and Environmental Safety 267, 115631.
Zhang X, Zhang F, Jiang L, Yang YQ et al. 2022a – Two new nematode-trapping fungi (*Arthrobotrys*, Orbiliaceae) from Yunnan, China. Phytotaxa 568(3), 255–266.
Zhang Y, Fournier J, Phookamsak R, Bahkali AH et al. 2013 – *Halotthiaceae* fam. nov. (*Pleosporales*) accommodates the new genus *Phaeoseptum* and several other aquatic genera. Mycologia 105, 603–609.
Zhang Y, Koko TW, Hyde KD. 2011 – Towards a monograph of Dothideomycetes: Studies on *Diademaceae*. Cryptogamie Mycologie 32, 115–126.
Zhang Y, Qiao M, Baral H, Xu J et al. 2020 – Morphological and molecular characterization of *Orbilia pseudopolybrocha* and *O. tonghaiensis*, two new species of Orbiliaceae from China. International journal of systematic and evolutionary microbiology 70(4), 2664–2676.
Zhang Y, Wang HK, Fournier J, Crous PW et al. 2009 – Towards a phylogenetic clarification of *Lophiostoma* / *Massarina* and morphologically similar genera in the *Pleosporales*. Fungal Diversity 38, 225–251.
Zhang YX, Chen C, Nie LT, Maharachchikumbura SSN et al. 2024c – Identification and characterization of *Albonectria*, *Fusarium*, and *Neocosmospora* species associated with ornamental plants in Southern China. Mycosphere 15(1), 6641–6717.
Zhang ZF, Zhou SY, Eurwilaichitr L, Ingsriswang S et al. 2021 – Culturable mycobiota from Karst caves in China II, with descriptions of 33 new species. Fungal Diversity 106, 29–136.
Zhang ZY, Pan H, Tao G, Li X et al. 2024a – Culturable Mycobiota from Guizhou Wildlife Park in China. *Mycosphere* 15(1), 654–763.
Zhao R, Chen KY, Mao LJ, Zhang CL. 2024 – Eleven new species of *Trichoderma* (Hypocreaceae, Hypocreales) from China. Mycology 16, 180–209.
Zhao R, Mao LJ, Zhang CL. 2023 – Three new species of *Trichoderma* (Hypocreales, Hypocreaceae) from soils in China. MycoKeys 97, 21–40.
Zhao W, Hou Y, Bai J, Zhang W et al. 2016 – A new species of *Zasmidium* associated with sooty blotch and flyspeck. Phytotaxa 258(2), 190–194.
Zhaxybayeva O, Gogarten JP. 2002 – Bootstrap, Bayesian probability and maximum likelihood mapping: exploring new tools for comparative genome analyses. BMC genomics 3, 4.
Zhou DQ, Cai L, Hyde KD. 2003 – *Astrosphaeriella* and *Roussoella* species on bamboo from Hong Kong and Yunnan, China including a new species of *Roussoella*. Cryptogamie Mycologie 24, 191–197.
Zhu HY, Pan M, Wijayawardene NN, Jiang N et al. 2021 – The hidden diversity of diatrypaceous fungi in China. Frontiers in Microbiology 12, 646262.
Zhu ZX, Xu HX, Zhuang WY, Li Y. 2017 – Two new green-spored species of *Trichoderma* (Sordariomycetes, Ascomycota) and their phylogenetic positions. MycoKeys 26, 61–75.
Zimmerman A. 1902 – Ueber einige an tropischen Kulturpflanzen beobachtete Pilze III. Zentralblatt für Bakteriologie, Parasitenkunde 8, 216–221.